Numerical and Discrete Modeling of Reproductive Endocrinological Networks

Dissertation

zur Erlangung des akademischen Grades
eines Doktors der Naturwissenschaften

am Fachbereich Mathematik und Informatik
der Freien Universität Berlin

vorgelegt von

Claudia Stötzel

Berlin, Dezember 2013

Betreuer/Erstgutachter:

Prof. Dr. Dr. h. c. Peter Deuflhard
Konrad-Zuse-Zentrum für Informationstechnik und Freie Universität Berlin

Zweitgutachter:

Prof. Dr. Dres. h. c. Hans Georg Bock
Interdisziplinäres Zentrum für wissenschaftliches Rechnen und Ruprecht-Karls-Universität Heidelberg

Datum der Disputation: 3. Juli 2014

Contents

Introduction

The female endocrine system consists of several physiological components which interact to control the functioning of the reproductive system. Various organs and substances constitute to a complex network which generates a periodic development of hormones and tissues, the female hormonal cycle. The exact mechanisms behind the cycle, however, are not yet fully explored. Mathematical modeling can elucidate the complex relationships within endocrine networks on an individual subject level. On one hand, it contributes to a better understanding of the biological mechanisms behind the hormonal cycle. On the other hand, its predictive abilities, in terms of performing long-term simulations or simulating external influences, can assist with research and application in drug testing, and in the development of new therapeutic strategies.

This work joins a line of research on modeling the female hormonal cycle that started about 15 years ago with the development of dynamical models for both the ovarian and pituitary hormone production in humans by Selgrade and Schlosser [SS99, SS00]. These models were merged by Harris Clark [CSS03] to the first fully-coupled feedback model for the cycle on the whole-organism level, which was later enhanced by Pasteur [Pas08] and analyzed with respect to certain dynamical characteristics [MS11]. Reinecke and Deuflhard took this model as a basis for a more elaborate model to simulate stochastic pulse patterns of the gonadotropin-releasing hormone (GnRH) and detailed reaction kinetics in the ovaries [RD07]. The model found attention in animal sciences, where mathematical approaches are not widely spread out [WTPB$^+$11]. Since bovine fertility has been subject of extensive research, and since the functioning of the hormonal cycle is similar in humans and cows, modeling concepts were transferred to develop a model for the bovine estrous cycle. Both a new version of the model for the human menstrual cycle as well as the model for the bovine estrous cycle are a subject of this thesis.

In both humans and cows, the hormonal cycle is a result of a large feedback loop of regulations. In this thesis, as in previous work, these mechanisms are modelled as a closed system which allows to analyze how the physiological components in different parts of the whole body function together. No external stimuli are needed for the periodic behavior which results only from the developed dynamics and the parameterization of the model.

At such a high abstraction level as the whole organism, the biological knowledge comprised

in a model usually consists of only qualitative information. In particular, regulative mechanisms, i.e. stimulation or inhibition between substances, are frequently available from literature. The interest of model applicants, however, often lies rather in *quantitative output*, when concentration profiles should be predicted, or model simulations have to be fitted to measurements. One approach to generate quantitive output from qualitative biological concepts, which has been used for models on the hormonal cycle in the past, is to translate these via Hill functions into a set of *ordinary differential equations* (ODEs). Each of the ODEs then represents the time dependent change of an involved substance, and the model is thus a system of often highly nonlinear ODEs. A variety of established tools from numerical analysis can be used for the simulation, parameter identification, and analysis of the model dynamics.

Sometimes, however, it might be useful to take a step back and see the bigger picture, the regulatory concepts behind the model. If one concentrates on the simulation of *qualitative behavior*, where the interaction of components does not continuously depend on the value of the variables, *discrete models* offer a variety of possibilities. Whether one takes as input quantitative details or only qualitive information, given the output as a set of consecutive events always leads to a finite state space that can be explored more systematically. In this thesis, an new approach to model the hormonal cycle with a discrete model is presented.

Outline

After a short overview of numerical modeling techniques that are useful for modeling the hormonal cycle, this thesis describes the development of a numerical model for the bovine estrous cycle, and in comparison to this presents a new version of the numerical model for the human menstrual cycle. It describes the use of several analysis techniques to investigate the continuous dynamics, as well as the derivation of a discrete model for the bovine estrous cycle.

Chapter 1 begins with the description of existing numerical models on the hormonal cycle, and then presents the *numerical modeling concepts* that are used in this thesis. The established algorithms that are applied are described. The simulation of the system does not cause any difficulties, while the inverse problem arising from the high number of unknown parameters is rather difficult and is discussed in detail.

In Chapter 2, the development of an ODE model for the *bovine estrous cycle* is described in detail. The model describes growth and decay of the *follicles* (Foll) and *corpus luteum* in the ovaries, together with the development of the key hormones in other parts of the organism that regulate and result from these processes. Biological background and modeling concepts will be presented that lead to a system of 15 ODEs with 60 unknown parameters. This model is then validated with results from synchronization studies, where administratrion of prostaglandin $F_{2\alpha}$ ($PGF_{2\alpha}$) leads to a restart of the cycle and thus to

a synchronization of the estrus of multiple individuals. A new ODE model for follicular development is presented that accounts for new observations from measurements.

Chapter 3 presents a new version of a differential equation model for the *human menstrual cycle*, based on previous work. Special emphasis is put on the comparison with the bovine model. The new human model incorporates processes that take place on a cellular level, in particular a detailed GnRH receptor model, in order to simulate GnRH agonist and antagonist treatments. The model consists of 33 ODEs and 114 parameters. Differences to the ODE model for the bovine estrous cycle are described in detail. A need for a similar modeling approach for follicular waves as in the estrous cycle is discussed.

Chapter 4 applies *continuous analysis tools* to the model of the bovine estrous cycle, and important characteristics of the model are presented and discussed. In particular, the Floquet multipliers of the system are calculated. Moreover, the difference in the number of follicular waves depending on the parameter configuration are explored with the help of spectral analysis. A model reduction technique taking into account the qualitative structure of the network is presented that reduces the system from 15 ODEs and 60 unknown parameters to 10 ODEs and 38 parameters.

In contrast to the advancing level of detail in Chapter 3, Chapter 5 takes a step in the opposite direction, and investigates the regulatory concepts behind the cycle. A *piecewise-linear model* is presented as a first discrete modeling approach. Parameter constraints necessary for periodic solutions are derived which are also valid for the ODE model. Since the state space is too large to analyze in a straightforward manner, a purely *discrete model* of the bovine estrous cycle, derived from the Jacobian of the ODE model with respect to the variables, is presented. Herein, state variables as well as the time variable take only discrete values. In the finite state space, global stability can be analyzed. Specific reduction techniques are developed that lead to smaller models that can be validated with qualitative knowledge. In particular, relations to the simulation of the ODE model are discussed, and certain dynamics of the ODE model can be reproduced with the derived core models.

Chapter 1

Numerical Modeling Tools for Endocrinological Networks

Endocrinological networks regulate the functioning of the mammalian hormonal cycle. A complex system of substances and chemical mechanisms generates the periodic development of hormones and tissues within the cycle. In higher primates, where menstruation occurs, the term *menstrual cycle* is used, while in other mammals, where the endometrium plays a more important role for the functioning of the cycle, the term *estrous cycle* is used. Throughout this thesis, the notation *menstrual cycle* will always refer to the human, and *estrous cycle* will usually refer to the bovine hormonal cycle. Note that the often read word *estrus* refers to a certain phase of the estrous cycle right before ovulation. Among species, the involved mechanisms as well as the duration of the cycle vary, but many endocrine functions are identical among mammals.

Numerical modeling is a quantitative approach to describe these mechanisms in a system that, usually with the help of computer simulations, can reproduce and predict time courses of the involved substances. In contrast to pure qualitative models, numerical models take into account numerical values from the underlying biology, such as chemical reaction rates or concentration thresholds for certain regulations. This enables a quantitative interpretation of simulation results, which can be compared to - and in future ideally replace - *in vivo* experiments.

In this chapter, an overview of existing numerical models of endocrine mechanisms is given, followed by a presentation of the modeling concepts used in this thesis, and an explanation of the applied numerical routines.

1.1 Existing Models on Endocrinological Mechanisms

Modeling of the entire female hormonal cycle is still at its beginnings. In the past decades, several mathematical models have been developed for parts of the hormonal interplay in the menstrual cycle. Particular endocrine mechanisms behind certain observations have been reproduced by computer simulations, but also the interplay of different developments in the whole body have become of interest to modelers. In animal sciences, mathematical models in general have received relatively little attention, but this is currently changing. A selection of mathematical models on the mammalian and, in particular, the human hormonal cycle will briefly be described in the following.

1.1.1 Models on the Menstrual Cycle

Much work has been done on developing mathematical models for certain aspects of the human menstrual cycle, e.g. the modeling of follicular selection [CMTC02] and the GnRH pulses [CF07]. These models are built on a cellular level and provide a possible extension for a whole-body-model in the future. Until now, however, only parts of the cycle are taken for studies, and the various feedback loops resulting from certain mechanisms are not considered.

In [ZWG03], a model for the surge of the *luteinizing hormone* (LH) is developed, that reproduces pulse patterns on a small time scale. It is assumed that there exist two oscillators, in the hypothalamus and the pituitary, that are both influenced by *estradiol* (E2). These two oscillators interact to generate pulses of LH. Model simulations match data for LH serum concentrations over a time span of a whole cycle. However, there is no feedback of LH on the rest of the cycle, and the oscillators are forced by external frequencies.

In contrast to this, the model developed in [RPP$^+$03] incorporates the feedback occurring between GnRH, LH, the *follicle-stimulating hormone* (FSH), E2, and *progesterone* (P4) for certain phases of the cycle. It includes a GnRH pulse pattern that results in rapid oscillatory behavior of the other substances. The model distinguishes between early follicular stages and mid-luteal stages, which describe the direct influence of the gonadotropins LH and FSH on the ovarian substances P4 and E2. The oscillations are results of a large feedback loop and do not need external stimuli. This model is capable of reproducing measured 24 h records of estradiol and LH pulse profiles. However, it does not investigate developments on a larger time scale as several cycles. Moreover, processes in the ovarian tissues are not modeled explicitly, but treated as black boxes.

A model describing the production of the steroid hormones P4, E2, and *inhibin* (Inh) by the ovaries has been presented in [SS99]. In this model, nine ODEs describe the development of follicular and luteal stages that represent different capacities to synthesize hormones. The development of the stages is regulated by explicit time dependent functions for LH

and FSH. Algebraic equations for the development of the steroid hormones are derived as linear combinations of the ovarian stages. In [SS00], a four-dimensional ODE model for the synthesis and release of FSH and LH as function of E2, P4, and Inh is presented. In [Har01], these two models of the ovarian function and of the hypothalamic-gonadal axis were merged together, and a closed feedback loop was presented. Processes in the two main compartments pituitary and ovaries were coupled such that they now influence each other. This approach considers the cycle on a whole-organism level, taking into account the most important feedback mechanisms. This model oscillates without external stimuli, and the periodic behavior results from the interplay of the developed mechanisms. It consists of 13 differential equations, of which 2 are delay differential equations, plus 3 algebraic equations, and 45 parameters.

This work of Harris [Har01] also investigates multiple stable solutions of the merged ODE model. It is observed that there exist different limit cycles which correspond to different pathological situations. In particular, a certain limit cycle can be interpreted as the PCO syndrome. Pasteur [Pas08] enhances this model towards the study of multiple inhibin influences. Margolskee [MS13] extends this model by incorporating the anti mullerian hormone (AMH). Long-term simulations with the latter model show the decrease of cyclicity for a healthy woman over the time span from 20 years to 55 years.

In [Rei09], the model of Harris is taken as a basis for a more elaborate model, a system of 50 delay differential equations and 208 parameters. Mechanisms among steroids in the ovaries and a more detailed description of GnRH are included, and simulations for the administration of hormonal contraceptives are performed successfully. More details of this model will be presented and discussed in Chapter 3.

1.1.2 Models on the Estrous Cycle

There are several studies that deal with certain parts of the estrous cycle. Soboleva ([SPP$^+$00]) develops a mathematical model for follicular selection in cattle and sheep. Apart from mathematical modelers, there are also experimentalists who look at the course of several hormone concentrations in different physiological compartments throughout the cycle [Per04, MFD$^+$13], and aim at relating experimental data in a non-mechanistic way.

For bovine, apart from the reproductive system, there exist several mathematical models that deal with nutrition and digestion. As pioneering for mathematical modeling in animal sciences can the work of Baldwin [Bal95] be considered, who presented an elaborate model for bovine nutrition, as well as Dijkstra ([DNBF92]), who developed a model of the rumen function. In [MS07], a dynamic model is developed with several subsystems of differential equations for metabolisms in different parts of the bovine body. Integrating nutritional and reproductive models to improve reproductive efficiency in dairy cattle is one scientific research goal for the future.

A similar approach on modeling the bovine estrous cycle, as presented in this thesis, has been taken by [POK+12]. It builds upon the work of Schlosser and Selgrade, and develops a model for the estrous cycle that, in contrast to this thesis, contains different follicular stages. In fact, modeling this part of the estrous cycle is one of the most critical factors, as will be discussed in Section 2.4.

1.2 Modeling Concepts

In this thesis, ordinary differential equations (ODEs) are chosen for modeling the hormonal cycles numerically. Each ODE in such a system describes the time-dependent change of an involved substance. The right hand sides are built from the chemical mechanisms and regulations among each other. The number of substances one aims to include in the model constitutes the minimum number of variables and thus the minimum dimension of the ODE system that is developed. But initially, before producing a system of ODEs, a qualitative representation of the model has to be derived.

The first step in building a model for a biological phenomenon is to draw a rough *flowchart* of the biological concepts one aims to reflect. This flowchart will be updated throughout the modeling process. Although it seems to be a preliminary step, deriving a flowchart is probably one of the most challenging tasks in modeling. Usually, this highly interdisciplinary task is performed by mathematicians and biologists, who together need to take many decisions to find a formal description of the complex phenomenons. The level of detail needs to be decided on, such that the model on the one hand stays close to reality in order to be reliable. On the other hand, reducing the number of included mechanisms is desirable not only due to computational costs but also for reasons of clarity. Multiple choices need to be made about what is important and what is negligible for the moment. In other words, the key mechanisms of a highly complex biological system need to be identified that build up a realistic and reliable abstraction level.

In this thesis, a *compartmental approach* is chosen for the modeling of endocrinological networks on the whole-organism level, in order to reduce complexity. *Physiologically based compartments*, i.e. parts of the organism that play an important role in the regulation of the cycle, are depicted. For the menstrual cycle, these are the hypothalamus, the pituitary, and the ovaries. For the estrous cycle, additionally, the uterus plays a role. The compartments are connected by the blood stream, which constitutes another compartment. Each substance that is decided to be a key substance and thus part of the model occurs in at least one physiological compartment. However, some of the substances occur in two physiological compartments. In the latter case, two variables are defined for this substance, each for its evolution in a separate compartment. If a substance occurs only in one physiological compartment, only one variable in the system of ODEs is needed to describe its evolution.

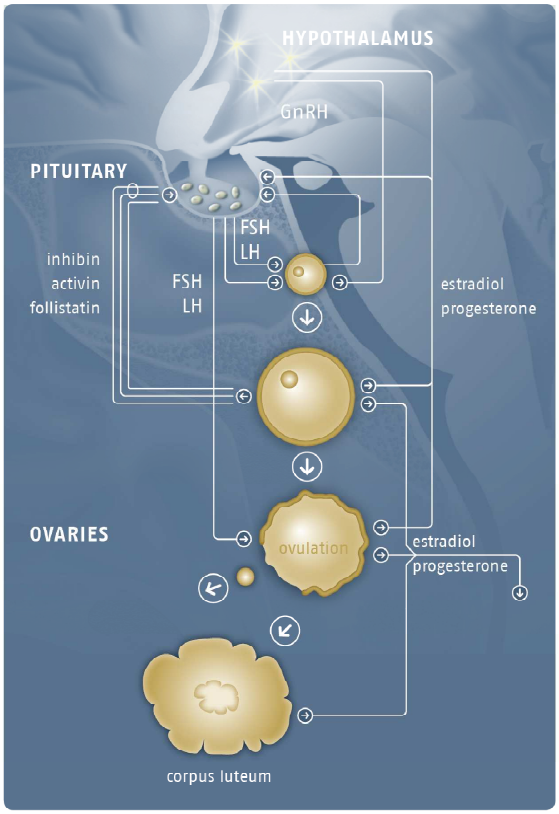

Figure 1.1: Rough flowchart of the model for the human menstrual cycle. This first step in the modeling procedure is the basis for more elaborate flowcharts that will be described in detail in the corresponding chapters. Source: [DRm10]

Throughout the modeling process, the decisions on the flowchart are usually revised, mechanisms are added or deleted. In Figure 1.1, the mechanisms behind the model for the human menstrual cycle are depicted in a first draft. The relevant more elaborate flowcharts for the models in this thesis will be presented in the corresponding chapters. For the bovine model, the derivation of the flowchart will be described in detail in Section 2.1. The final flowchart of the human model is mainly based on previous work [RmD$^+$12], as will be described in Section 3.2. Finally, every variable will be represented by a vertex, and the relations between the variables will be represented by edges between the corresponding vertices. The flowchart thus illustrates the considered mechanisms between the depicted substances, and hence represents the qualitative description of the model.

Having developed a flowchart of the variables and their relations, several techniques are helpful to translate this information into a corresponding system of differential equations. Essentially, only a few mathematical concepts are necessary to derive a set of ODEs that describes the model that is, until here, derived only in graphical notation. These concepts will be described in the following.

Biochemical Reaction Systems

When processes on the molecular level, e.g. receptor binding mechanisms or biochemical reactions, should be incorporated into the model, this can be done via a quantitative approach, which takes into account specific chemical reaction rates. The translation of biochemical reaction systems to ordinary differential equations has been described in [DB02].

Ideally, a quantitative model of a biological phenomenon would consist of only biochemical reactions. However, many mechanisms in the mammalian organism are only partly explored, the level of detail of a model is thus limited by the available information. As a consequence, the question arises, on which level of detail the whole model should be built. Both the benefit for the modeling question and the computational costs have to be considered. For models that include mechanisms on the whole-organism level, many details can be neglected, as they still comprise several unknowns or are simply too complex for the modeling purpose.

The endocrinological models treated in this thesis have a very high abstraction level. In the model of the bovine estrous cycle, there was no interest to go into the molecular level of detail, thus biochemical reaction systems are not yet used in the present bovine model. However, the level of detail can be adjusted according to the application, as has been performed with the human model GynCycle that will be presented in Chapter 3. In GynCycle, reactions that take place on the single-cell level are an important part of the model. The model is able to reproduce experimental results after the administration of substances that are known to have different receptor binding mechanisms. These re-

ceptor binding mechanisms are implemented in the model as will be explained in Chapter 3.

The basic idea when modeling biochemical reaction systems is the law of mass action kinetics, which states that the rate of the reaction is proportional to the product of reactant concentrations. A simple reaction

$$\mathrm{A} \xrightarrow{k} \mathrm{B},$$

where a substance B is produced from a substance A, with a reaction rate constant $k \geq 0$, translates to the two ODEs

$$\frac{d}{dt} y_{\mathrm{A}} = -k \cdot y_{\mathrm{A}}, \quad \frac{d}{dt} y_{\mathrm{B}} = +k \cdot y_{\mathrm{A}},$$

where y_{A} and y_{B} are quantities, e.g. concentrations or number of molecules, of the substances A and B, respectively.

A typical reversible receptor binding mechanism, where a ligand binds to its receptor forming a complex, follows the same principle: The reaction scheme

$$\mathrm{L} + \mathrm{Rec} \underset{k_2}{\overset{k_1}{\rightleftharpoons}} (\mathrm{L\text{-}Rec})$$

translates to ODEs for the corresponding quantities

$$\begin{aligned} y'_{\mathrm{L}} &= k_2 \cdot y_{\mathrm{L\text{-}Rec}} - k_1 \cdot y_{\mathrm{L}} \cdot y_{\mathrm{Rec}}, \\ y'_{\mathrm{Rec}} &= k_2 \cdot y_{\mathrm{L\text{-}Rec}} - k_1 \cdot y_{\mathrm{L}} \cdot y_{\mathrm{Rec}}, \\ y'_{(\mathrm{L\text{-}Rec})} &= k_1 \cdot y_{\mathrm{L}} \cdot y_{\mathrm{Rec}} - k_2 \cdot y_{(\mathrm{L\text{-}Rec})}. \end{aligned}$$

These concepts are used in a variety of mathematical models of biological phenomena. They represent a modeling approach close to biological reality. Often, reaction rate constants k can be estimated from experiments, and the number of unknown constants in the model can thus be reduced. Also, there exist multiple databases, e.g. the KEGG database [Dat06], that collect knowledge on molecular interactions and reaction networks. Using these databases, new models can be built based on existing models, which allows to upgrade a model at low cost if needed.

In this thesis, it is always assumed that there are enough molecules of the reactants, ligands and receptors, such that the law of mass action kinetics holds and the reaction rate is linearly dependent on the substrate concentrations. If only few molecules are present, a possibility to model the reaction is via Michaelis-Menten kinetics, where the reaction rate sigmoidally depends on the present concentrations. This leads to another important modeling concept, considering that the reactants act as threshold-dependent regulators of the reaction. If one even includes the binding affinity of the molecules, the "speed" of the reaction can be incorporated in a model via the Hill equation

$$\frac{y_{(\mathrm{L\text{-}Rec})}}{y_{\mathrm{Rec}} + y_{(\mathrm{L\text{-}Rec})}} = \frac{y_{\mathrm{L}}^n}{T_{0.5}^n + y_{\mathrm{L}}^n},$$

where $T_{0.5}$ is the concentration when half of the receptors are bound. The idea of the Hill equation, introduced by A.V. Hill in 1910 [Wei97], therefore provides a possibility to include regulatory functions with different "speeds" into a model. This leads to an important modeling concept.

Hill Functions

Developing the right hand sides of the ODEs is often not as straightforward as above. Often, quantitative biological mechanisms are unknown, whereas information about qualitative regulation between substances is available. In other cases, the exact biological information is more specific than necessary, and can be abbreviated.

In both cases, qualitative regulations, i.e. stimulations or inhibitions between the involved substances, can be included into a model via *Hill functions*. Hill functions represent black boxes that might reflect a variety of biochemical reactions. They allow one to translate regulatory information into differential equations. The regulatory information, a discontinuous switch, is written as a continuous function, such that it can be included in the right hand side of an ODE.

An unscaled Hill function is a sigmoidal function between zero and one, which switches at a specified threshold from one level to the other with a specified steepness. Stimulatory Hill functions are used for positive effects and are defined as

$$h^+(y_S(t); T, n) := \frac{y_S(t)^n}{T^n + y_S(t)^n}.$$

$y_S(t)$ represents the effector, T the threshold for change of behavior, and n controls the steepness of the curve. Inhibitory Hill functions are used for the decelerated effects and are defined as

$$h^-(y_S(t); T, n) := \frac{T^n}{T^n + y_S(t)^n}.$$

Here, the value of the Hill function has its maximum at the lowest value of the initiating substrate $S(t)$, and switches to zero if this substrate passes the threshold T.

In general, the steepness coefficient n has an unknown value which reflects the speed, or smoothness, of the regulation. It could be estimated by parameter estimation, but results are usually highly dependent on other parameters. Thus, in this thesis, these values are fixed in the parameter estimation procedure. Usually, the steepness coefficient $n = 2$ is chosen, but, when appropriate, $n = 1, 5$, or 10 is set to capture slower or steeper effects.

Whenever a Hill function is used, it is provided with another parameter m, which controls the height of the switch. This parameter serves as maximum stimulatory respectively inhibitory effect. For abbreviation of notation, the scaled Hill functions are introduced as

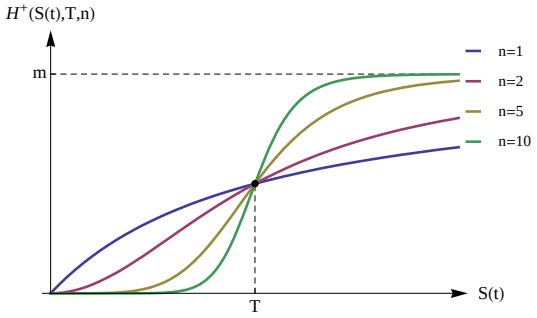

Figure 1.2: Scaled positive Hill functions with different steepness coefficients. A higher coefficient n leads to a steeper switch of the regulation.

$$\boxed{\begin{aligned} H^{+}_{\mathrm{S1,S2}}(y_{\mathrm{S1}}(t)) &:= m^{\mathrm{S2}}_{\mathrm{S1}} \cdot h^{+}(y_{\mathrm{S1}}(t); T^{\mathrm{S2}}_{\mathrm{S1}}, n^{\mathrm{S2}}_{\mathrm{S1}}), \\ H^{-}_{\mathrm{S1,S2}}(y_{\mathrm{S1}}(t)) &:= m^{\mathrm{S2}}_{\mathrm{S1}} \cdot h^{-}(y_{\mathrm{S1}}(t); T^{\mathrm{S2}}_{\mathrm{S1}}, n^{\mathrm{S2}}_{\mathrm{S1}}). \end{aligned}}$$

S1 denotes the initiating substance, and S2 the substance that is being regulated by the Hill function, i.e. the substance where the Hill function occurs in the corresponding right hand side in the ODE system.

The described Hill functions regulate the mechanisms between two substances. In particular, a substance regulates the course of another substance, and a corresponding Hill function thus appears on the right hand side of the ODE system. The exact regulations are specified in the following.

Production-Clearance and Synthesis-Release Relationships

Recall that a physiologically-based compartmental approach has been chosen for the models in this thesis, i.e. some substances occur in one physiological compartment, and others in two. In the latter case, two variables are needed to describe the evolution of the substance. In this thesis, the rate of change of a variable is usually the result of a positive and a negative term, its production, synthesis, or release from another compartment, and its clearance or release into another compartment.

Whenever a substance occurs only in one compartment, the following ODE is chosen,

$$\frac{d}{dt} y_{\mathrm{S}}(t) = \mathit{Prod}_{\mathrm{S}}(t) - \mathit{Clear}_{\mathrm{S}}(t),$$

where $\mathit{Prod}_{\mathrm{S}}(t)$ and $\mathit{Clear}_{\mathrm{S}}(t)$ are nonnegative functions that need to be specified. Often, they depend on other substances via Hill functions. In many cases, $\mathit{Clear}_{\mathrm{S}}(t)$ is simply

a linear term which depends only on a clearance rate constant and the current concentration of S. This leads then to an exponential decay, which preserves the variable from becoming negative. Whenever $Clear_{\mathrm{S}}(t)$ is modeled as nonlinear, it still depends on the current concentration of S. This guarantees that the solutions of all ODEs are nonnegative.

Whenever a substance occurs in two compartments, it is assumed that it is synthesized in a source compartment, and fully released into a sink compartment, where it is cleared. The release from one compartment to another, as well as the synthesis in the source location are usually regulated by other substances via Hill functions. The change of a substance $y_S(t)$ appearing in two compartments over time is modeled as

$$\begin{aligned} \frac{d}{dt} y_{\mathrm{S}_{Source}}(t) &= Syn_{\mathrm{S}}(t) - Rel_{\mathrm{S}}(t), \\ \frac{d}{dt} y_{\mathrm{S}_{Sink}}(t) &= Rel_{\mathrm{S}}(t) - Clear_{\mathrm{S}}(t), \end{aligned}$$

where $Syn_{\mathrm{S}}(t)$ and $Rel_{\mathrm{S}}(t)$ are nonnegative functions. These functions often comprise Hill functions via simple arithmetic operations. The function $Rel_{\mathrm{S}}(t)$ describes the amount of the substance S that is transported from one compartment to another.

By this concept of variables in two compartments, in the human and the bovine model, the substances GnRH, LH and FSH are modeled, which occur in the physiological compartments hypothalamus, pituitary, and blood. Analogously, it is also used for follicles and corpus luteum in the bovine model, and for the transition of follicular stages in the human model. More details will be given in Sections 2.2 and 3.2.

Thus, the time-dependent change of a substance is always the result of the difference of two terms. Production, clearance, synthesis and release usually depend on other components. To model these regulations as differentiable functions, Hill-functions are used as described above.

The preceding concepts lead to a system of differential equations which possibly includes delays. Especially in the beginning of a modeling processes, delays can be used to connect different parts of the model and bridge arising gaps. Every delay stands for a lack of knowledge in the model. There are some shortcomings in the usage of delays, therefore, their avoidance is desirable.

Omitting Delay Differential Equations

In many biological models, delay differential equations (DDEs) are used to account for intermediate steps as e.g. transport processes or possibly multiple reactions that occur between the synthesis of a substance and its action. DDEs are of the form

$$\frac{dy(t)}{dt} = f(y(t), y(t-\tau)).$$

In [Rei09, BmR+11], several delay differential equations are used. As the precise numerical values for the delays are usually not known, they are treated as unknown parameters. However, as the values of delays have a large impact on the cycle length and thus on the residual, the delay is typically the most sensitive parameter. Numerical experiments suggest that the large impact of the delay may not represent the possibly lower impact of the multiple reactions that are comprised by the delay.

There exist elaborate algorithms for solving DDEs (e.g. RADAR [GH01]) that use *dense output methods*, but the choice of solvers is larger in the case of ordinary differential equations. This and the distortion by the highly sensitive delays makes it desirable to omit delays in a model.

Several techniques can be applied to transform systems of delay differential equations into ODE systems without delay.

- Adjusting parameters: If the delay is not too large, an adjustment of parameters values is often possible. For example, two ODEs could be rewritten as follows

$$\left.\begin{array}{rcl} y_i'(t) &=& m_i \cdot \frac{y_j(t-\tau)}{y_j(t-\tau)+T_i} - c_i \cdot y_i(t) \\ y_j'(t) &=& m_j \cdot f(y) - c_j \cdot y_j(t) \end{array}\right\} \rightarrow \left\{\begin{array}{rcl} y_i'(t) &=& m_i \cdot \frac{y_j(t)}{y_j(t)+\widetilde{T_i}} - c_i \cdot y_j(t) \\ y_j'(t) &=& \widetilde{m_j} \cdot f(y) - \widetilde{c_j} \cdot y_j(t) \end{array}\right.$$

  The parameters m_j, c_j, and T_i can be adjusted according to their interpretation:

  - In regulatory mechanisms, the thresholds of the Hill functions control the timing of certain events. Increasing the value of the threshold T_i implies a later regulation in case of a rising regulating substance, and can therefore replace the effect of a delay.
  - The adaption of reaction rates m_j and c_j is another possibility to delay a certain event. When lowering growth and clearance rate constants by the same linear factor, the peak of the variable occurs at a later time.

- If adaption of parameters does not lead to the desired effects, introduction of delay compartments can be pursued. This implies the integration of a new equation which can be interpreted as the designated substance in an effect compartment. The idea stems from non-physiological compartmental modeling in pharmacokinetics. The same substance is regarded as being present in two compartments, of which one is the downstream of the other. As a result, instead of having a delay for a certain substance, this substance is transformed into another substance, which then accomplishes the mechanism without delay.

Whenever delays are larger and cannot be omitted by the above described procedures, mechanisms in a model need to be adjusted in order to obtain a system without delays.

Having derived a system of ordinary differential equations, this system can now be simulated and fitted to measurements with the help of established elaborate numerical algorithms.

1.3 Numerical Algorithms

In this section, the numerical routines that have been used will be explained. Mainly two algorithms are used for the development and simulation of an ODE model, a solver for the system of differential equations, and a parameter identification algorithm.

1.3.1 Solver

As many biological models, the hormonal cycle models are highly nonlinear. Although the ODEs without the capability of capturing drug administration in this thesis are not stiff, the administration of drugs can lead to steep slopes, which immediately change the model behavior. The system could become stiff, therefore, a solver for stiff differential equations is used. This ensures an appropriate approximation of the solution in any case. During model development, it is sometimes necessary to include delay differential equations to incorporate black boxes. As long as delays are in the model, the solver RADAR5 [GH01], especially designed for stiff delay differential equations, is used. As modeling improves, these delay differential equations can often be replaced by ordinary differential equations, as described in the previous section. A delay differential solver is no longer needed.

There exists a variety of solvers for stiff ordinary differential equations. For the simulation of the hormonal cycle, the solver LIMEX is used. LIMEX is a *L*inearly *IM*plicit *E*uler scheme with e*X*trapolation, especially suited for stiff differential equations [ENOD99]. The solver LIMEX includes an adaptive step size control, which uses an appropriate interpolation scheme in order to compute solutions with prescribed accuracy at any designated time points. This is often not possible with other ODE solvers [DRWD13].

1.3.2 Parameter Identification

A particular difficulty in modeling complex biological systems is the identification of unknown parameters. At such a high abstraction level as the whole-organism, parameters can often not be measured from experiments. Some parameters even do not have a unique biochemical counterpart, e.g. a threshold of a Hill function in the biological context could refer to a borderline level above which a certain reaction can take place. This value could be influenced by one or more saturation concentrations of substances that have not been modeled explicitly; a clearance rate might be the result of deactivation, internalization

and elimination of a bound compound. The values of the model parameters may thus represent the interplay of multiple biological processes. However, for other parameters, measurements or information from literature can give at least starting values for further identification.

What is measured often and is taken here as reference for model validation are time courses of concentrations of substances in the blood. For the hormonal cycle, these often include LH, FSH, progesterone and estradiol. These substances appear as variables in the models. Parameters are thus determined by fitting the solution curves of the ODEs to measured concentration profiles.

The numerical tools used for parameter identification have been described in detail in [Deu11]. For a better comprehension, the Gauss-Newton algorithm and the sensitivity analysis that are used here are described in the following. This Gauss-Newton algorithm, implemented in [DRWD13], has the advantage that it only needs single shooting, as opposed to multiple shooting in [Boc87, Boc81]. It thus requires less memory capacity. Although multiple shooting has better convergence properties, this can be compensated for large systems by applying the transformation $p \rightsquigarrow \exp(\widetilde{p})$ which is based on the *Arrhenius* equation [DB02]. Moreover, in the case of stiff ODE systems, numerical difficulties that might result from the choice of the intermediate steps in the multiple shooting case are omitted.

Affine-covariant Gauss-Newton Method

Fitting a model simulation to measurements, i.e. identifying parameter values that result in the observed behavior, is an inverse problem. If it is known how the outcome of a simulation should ideally look like, the underlying system needs to be found. In the previous section, an n-dimensional autonomous system of ordinary differential equations $y'(t,p) = f(p, y(t,p))$ has been derived, where p is a vector of unknown parameters that need to be identified.

Now, assume that m measurements are given which the simulation $y(t,p)$ should match. The information of the measurements is written as a quadruple $(t_j, k_j, z_j, \delta z_j)$, $j = 1, \ldots, m$, where t_j are the measurement time points, k_j indicate the then measured substances, $1 \leq k_j \leq n$, and $z_j \in \mathbb{R}$ the measured values for the substance y_{k_j} at time t_j. δz_j are the corresponding measurement tolerances. Note that, often, at one time point, several substances have measured, which leads to several t_j's being equal. Also, the measurements for a particular substance usually consist of a series of measurements, and thus many of the k_j's are equal.

The inverse problem is to find the values for p such that the solution of the system for the components k_j at the m measurement time points equals the corresponding measurements values, i.e. $y_{k_j}(t_j, p) = z_j$, $j = 1, \ldots, m$. As equality is unlikely to be fulfilled, the differ-

ence of the values is minimized, taking into account the measurement tolerances δz_j. An affine-invariant Gauss-Newton method as described in [Deu11] is used to solve this problem.

Briefly, the idea is to apply Newton's method to a reformulation of the least squares approach

$$\|F(p)\|_2^2 := \sum_{j=1}^{m} \left(\frac{y_{k_j}(t_j; p) - z_j}{\delta z_j} \right)^2 = \min \text{ w.r.t. } p$$

which is usually credited to Gauss. Since $\|F(p)\|_2^2 = F(p)^T F(p)$ is continuous, a necessary condition for a minimum at p is that its derivative equals zero. It can be shown that $(F(p)^T F(p))' = 2F'(p)^T F(p)$. Thus, the root of $G(p) := F'(p)^T F(p)$ is searched. This is done with Newton's method which is derived from Taylor expansion of G around a starting guess p^0, $G(p) = G(p^0) + G'(p^0)(p - p^0) + O(p - p^0)$, as p tends to p^0. Thus, the problem becomes to find the root of $G(p)+G'(p)\Delta p$. Calculating $G'(p) = F'(p)^T F'(p)+F''(p)^T F(p)$, and assuming that the second derivative is omittable around the starting guess, the problem is transferred to finding the root of $F'(p)^T F'(p)\Delta p + F'(p)^T F(p)$. This leads to the normal equation for the linear problem $\|F'(p)\Delta p + F(p)\|_2 = \min$ w.r.t. p, which has the formal solution

$$\Delta p = -F'(p)^+ F(p). \qquad (*)$$

$F'(p)^+$ denotes the pseudo-inverse of the matrix $F'(p)$, which in case of $m \geq q$ and full rank of $F'(p)$ can be calculated as $F'(p)^+ = (F'(p)^T F'(p))^{-1} F'(p)$, and in case of rank-deficiency can be determined e.g. via QR decomposition and shortest Least Squares solution as described in Algorithm 3.20 in [DB02]. In general, any decomposition $A = BC$, $B \in \mathbb{R}^{m \times r}$ $C \in \mathbb{R}^{r \times q}$ with $r = rank(A) < q \leq m$ leads to the pseudo-inverse $A^+ = C^T(CC^T)^{-1}(B^T B)B^T)$.

The term $(*)$ is called Gauss-Newton update, and is calculated in every iteration beginning from a starting guess $p^{(0)}$. Step size correction factors and rank reduction techniques lead to an adapted strategy. For simplicity, we describe the undamped update strategy first. As long as the Gauss-Newton update is not too small, the algorithm calculates

$$p^{(k+1)} = p^{(k)} + \Delta p^{(k)} = p^{(k)} - F'(p^{(k)})^+ F(p^{(k)}).$$

In every iteration, during the calculation of $F'(p^{(k)})^+$, a QR-decomposition of the Jacobian $F'(p^{(k)})$ is performed via Householder transformations. This QR-decomposition stops if the matrix R is almost singular, i.e. if $\delta \cdot R_{11} < R_{rr}$, δ reflecting the accuracy in $F'(p^k)$. As a side product, this also delivers the numerical rank r of the matrix F' at the current parameter values $p^{(k)}$, which plays an important role in the identifiability of the parameters that will referred to in the next subsection.

The *ordinary Gauss-Newton update* is set as $\Delta p^{(k)} = -F'(p^{(k)})^+ F(p^{(k)})$. Before proceeding to the next iteration step, a *simplified Gauss-Newton update* is also calculated with the help of the current Jacobian, $\overline{\Delta p^{(k+1)}} = -F'(p^{(k)})^+ F(p^{(k+1)})$. Unless a maximum number

of iterations is reached earlier, the algorithm terminates if this simplified update falls under a specified tolerance. Since the update and thus this stopping criterion depends on the rank of the Jacobian, potentially a rank-reduction is performed, which offers a possibility to proceed to another iteration.

The affine-invariant Gauss-Newton method has been implemented in the code NLSCON (Nonlinear Least-Squares problems with CONstraints) [NW00]. Several adaptive controls regarding the step size and rank reduction of the Jacobian are included in this algorithm, which proceeds as follows: First, the parameters are scaled such that are all in the same range. This is possible because the algorithm is invariant under scaling in the full rank case. Then, the least squares functional is calculated for the starting guess $p^{(0)}$ of the parameters. Since in the convergent phase, the simplified GN update is always smaller than the ordinary GN-update, it is checked throughout the algorithm whether it holds

$$\|\overline{\Delta p^{(k+1)}}\|_2 < \|\Delta p^{(k)}\|_2.$$

If this monotonicity test fails, the update $\Delta p^{(k)}$ is damped based on a theoretical prediction. For details see [Deu11]. If the automatically determined damping factor is too small, a rank reduction of the Jacobian is performed, until the monotonicity test holds true.

Sometimes, model and data do not fit together and the GN-algorithm fails to converge. In order to obtain convergence to an existing solution, Theorem 4.7 in [Deu11] gives sufficient conditions. Besides starting with a good initial guess $p^{(0)}$, amongst others the Jacobian must satisfy a certain Lipschitz condition. Additionally, the compatibility of the current parameterization of the model to the data needs to be fulfilled. This can be measured by

$$\kappa(p^{(k)}) = \frac{|\Delta p^k|}{|\Delta p^{k-1}|}.$$

As $k \to \infty$, $\kappa(p^{(k)})$ approaches the asymptotic convergence rate $\kappa(p^*)$ of the Gauss-Newton algorithm. $\kappa(p^*)$ can be interpreted as *incompatibility factor*. If $\kappa(p^*) < 1$, the problem is called *adequate*. The Gauss-Newton algorithm converges locally linearly for adequate problems and locally quadratically for compatible nonlinear least-squares problems, i.e. if $\kappa(p^*) = 0$, to a solution that is unique within the subspace of identifiable parameters [Deu11].

The described Gauss-Newton method monitors the rank of the Jacobian throughout the iterations and thus splits the parameter space into one part which can be identified by the given data, and another part which cannot. If the rank of the Jacobian is maximal and the algorithm still fails to converge, even after trying multiple $p^{(0)}$, the model equations need to be improved. In the rank-deficient case, inclusion of more data can possibly enlarge the set of estimatable parameters. During the development of the models in this thesis, parameter identification has been used as a tool throughout the iterative process of successive model extension, reduction and refinement. Some parameters could be identified

in smaller sub-models, but became unidentifiable after being embedded into a larger model.

As long as not all unknown parameters can be identified from given data, a choice needs to be made which parameters to vary in the identification procedure. Typically, multiple parameters are set fixed, and hence the dimension of the inverse problem is possibly much lower than the actual number of unknown parameters. Sensitivities and subconditions can be consulted to decide which parameters to keep fixed and which to determine in the next identification run.

Sensitivities and Subconditions

During a run of NLSCON, sensitivities and subconditions are calculated. Here, we use these calculations to derive two real-valued numbers for each parameter: the column norms of the sensitivity matrix (belonging to a parameter) and the *subcondition of a parameter*.

A change of value of a parameter with a high *sensitivity* (a large corresponding column norm) has - locally - a larger impact on the solution of an ODE model than a parameter that is less sensitive. Therefore, it is convenient to concentrate on the most sensitive parameters first, i.e. the parameters associated with a high column norm of the sensitivity matrix and to leave out the insensitive parameters as they - locally - do not influence the simulation much.

The *subcondition of a parameter* is the subcondition of the matrix that would be the sensitivity matrix if a certain reduced problem which will be explained later in this section would be considered. It provides information about identifiability of the reduced parameter set. By ordering the matrix R during the QR-decomposition of the Jacobian - derived from the current parameterization - an order for the inclusion of parameters into the reduced set of parameters to be identified is suggested.

One has to keep in mind that both the sensitivity analysis and the calculation of the subconditions is performed with a current set of parameters values, and thus does not provide reliable information for a different set of values. Therefore, the most meaningful information for the final model would actually be after the successful identification run. An a posteriori sensitivity analysis can nevertheless be consulted before the next run, assuming that sensitivities do not differ greatly in a set of parameter values close to the current one. Treating the absolute numbers of the sensitivity analysis with caution, a sensitivity analysis nevertheless gives insight into parameter dependencies, and can thus help explore the structure of the model.

In the following, the calculations, as performed in NLSCON, and the resulting derivation of the two numbers consulted for the decision which parameters to identify are described. Both calculations are based on the *sensitivity matrix*.

The sensitivity matrix of the ODE system with respect to the parameters is described via the Jacobian $J(t) = \frac{d}{dp}y(t, p = \tilde{p})$. Since y is not known explicitly, this matrix is obtained by numerically solving the variational equation

$$\frac{d}{dt}J(t) = f_y(\tilde{y}, \tilde{p}) \cdot J(t) + f_p(\tilde{y}, \tilde{p}), \quad J(0) = 0,$$

where $f_y = \frac{\delta f}{\delta y}$ and $f_p = \frac{\delta f}{\delta p}$ are preferably computed analytically by symbolic differentiation, or can be obtained by numerical differentiation. It is also possible to approximate $J(t)$ via numerical differentiation, calculating $(y(t, \tilde{p} + \delta\tilde{p}) - y(t, \tilde{p}))/\delta\tilde{p}$, $\delta\tilde{p}$ being a small step size. However, the solver LIMEX used in this thesis efficiently solves the variational equation in every step [SMEN04].

Evaluating $J(t)$ at specified time points of interest t_i, e.g. measurement time points, and scaling the entries of the matrix to make the values comparable, potentially making use of specified thresholds ϑ_j and ϑ_{y_i}, leads to the sensitivity matrix

$$S := \begin{bmatrix} \tilde{J}(t_1) \\ \vdots \\ \tilde{J}(t_m) \end{bmatrix}, \; \tilde{J}_{ij}(t_k) := J_{ij}(t_k) \cdot \frac{\max\{|p_j|, \vartheta_j\}}{\max_i(\max\{|y_i|, \vartheta_{y_i}\})}.$$

Each entry of the matrix S represents the sensitivity of one solution component with respect to one parameter at a specified time point. To obtain comparable values for the decision about inclusion in the identification, the 2-norms of each column of S are taken. These column norms represent the sensitivities of all measured components at all measured time points with respect to one parameter. Column norms as used during the modeling procedure are displayed in Figure 1.3. Parameters that are associated with a low column norm are likely to play a minor role at the measured time points, and are thus candidates to keep fixed in the next identification run.

The other value that gives a suggestion about inclusion of parameters in the identification procedure is the *subcondition of the parameters* that is derived from the subconditions of reduced sensitivity matrices. These terms are closely related to the numerical rank of the sensitivity matrix.

Due to the column pivoting during the QR-decomposition of S via a permutation matrix P, $S = QRP$, the upper triangular matrix R is sorted such that the absolute values of the diagonal entries are in descending order, $|R_{11}| \geq |R_{22}| \geq \ldots \geq |R_{nn}|$.

Recall that the numerical rank r of S is defined via the inequality $|R_{r+1,r+1}| < \delta|R_{11}| \leq |R_{rr}|$, where δ reflects the accuracy in S. The numerical rank gives the number of parameters that can be identified from the given data: If a diagonal entry of R would be

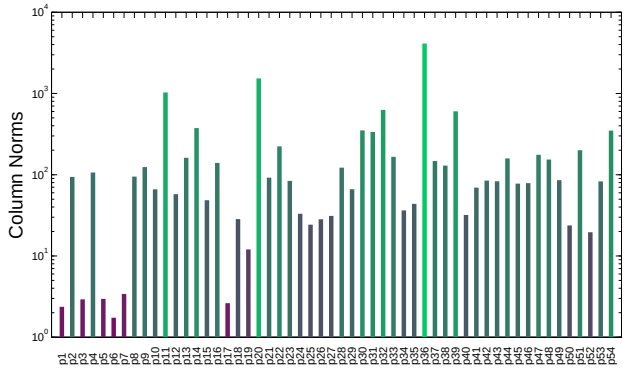

Figure 1.3: Column norms of a sensitivity matrix, as presented in [BmR+10]. A high column norm indicates a parameter that plays an important role for the measured substances at all measurement time points, a low value corresponds to a parameter that does not influence the solution much at these time points.

numerically zero, this would lead to linear dependencies in the columns of S. The parameters associated with these columns in S would have the same influence on the solution. Therefore, these parameters would not be identifiable simultaneously.

As each column of R corresponds to a column of S and thus to a particular parameter, the sorting of R implicitly states which parameters are among the r most identifiable parameters.

Instead of only looking at the rank and the sorting of R, one can go further and calculate the subcondition of S to decide which parameters to identify in a next run. The subcondition of a matrix S, as defined in [Deu11], results from its QR-decomposition with column pivoting. For $R_{nn} \neq 0$, it is defined as the ratio of the smallest and the largest entry of the diagonal of R,

$$sc(S) := \frac{|R_{11}|}{|R_{nn}|}.$$

For $R_{nn} = 0$, $sc(S) := \infty$ which is equivalent to S being singular. Note that, by construction, it always holds $sc(S) \geq 1$.

The numerical rank and the subcondition are closely related. If $\delta sc(S) \geq 1$, then the inequality $\delta|R_{11}| < |R_{nn}|$ is violated. It follows that the numerical rank of S is smaller than the number of unknown parameters n. On the other hand, if the numerical rank r of S is smaller than n, then $\frac{|R_{11}|}{|R_{nn}|} \geq \frac{1}{\delta}$. The relation $\delta sc(S) \geq 1$ is thus equivalent to the rank of the S being not full.

In order to define subconditions for parameters, a reduced sensitivity matrix is introduced that would be the sensitivity matrix if only the first i parameters, according to the sorting

of R, were to identify,

$$S|_i := \begin{bmatrix} S_{11} & \dots & S_{1i} \\ \vdots & \ddots & \vdots \\ \vdots & \ddots & \vdots \\ S_{m1} & \dots & S_{mi} \end{bmatrix} = Q \begin{bmatrix} R_{11} & \dots & R_{1i} \\ 0 & \ddots & \vdots \\ \vdots & 0 & R_{ii} \\ 0 & \dots & 0 \end{bmatrix}.$$

The *subcondition of a parameter* p_i is now defined as the subcondition of the reduced sensitivity matrix,

$$sc(p_i) := sc(S|_i) = \frac{|R_{11}|}{|R_{ii}|}.$$

Then, the numerical rank of S being r is equivalent to $sc(S|_r) \leq \frac{1}{\delta} < sc(S|_{r+1})$.

If the subcondition of a parameter is small (close to 1), the sensitivity matrix of the reduced problem is well-scaled, i.e. the orders of magnitude are not too different, and there are no linear dependencies in the columns of S. The further away the subcondition is from $\frac{1}{\delta}$, the easier the handling of the inverse problem becomes.

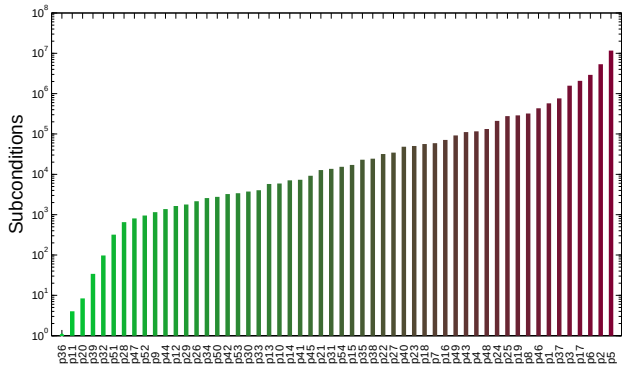

Figure 1.4: Subconditions of all parameters of a model, as presented in [BmR+10]. Given the Jacobian for the current parameterization, the subcondition numbers for the parameters give a hint to identifiability of parameter sets.

Subconditions of parameters, as used during the modeling procedure, are displayed in Figure 1.4. The leftmost parameter is associated with the smallest diagonal value of R. The sorting of the parameters according to the entries of R, i.e. according to growing subcondition, suggests in which order to include the parameters into the identification run.

The predictability of parameter values decreases with increasing subcondition. Typically, a kink in the subcondition figure occurs when the numerical rank of S has been reached. It therefore indicates that the following parameters cannot be identified from the given data,

at least not simultaneously with the previous parameters.

After the parameters suggested by the subconditions have been identified, the procedure is repeated with the remaining parameters. Setting some of the parameters from the preceding run as fixed usually leads to a different sorting of the remaining ones and completely different subconditions. For the decision about which parameters to set fixed in the following run, sensitivities can be consulted. However, as these values only provide local information, the decision is not definitive, and can be varied in the following runs to enlarge the set of parameters included in the identification procedure.

Chapter 2

Modeling of the Bovine Estrous Cycle

Bovine fertility is the subject of extensive research in animal sciences, especially because, concurrent with increased milk yield, fertility of dairy cows has declined during the last decades. Subfertility has negative implications for dairy farm profitability, sustainability of animal production and animal welfare, as it takes more time and effort to get cows to be pregnant. The decline in fertility is manifested in alterations in hormone patterns, reduced expression of estrous behavior, and lower conception rates. However, the mechanisms by which selection for higher milk yield can result in poorer fertility are not fully explored. A mathematical model of the bovine estrous cycle can help to increase the understanding of the complex interplay of factors involved in the reproductive cycle. In this chapter, the concepts presented in Section 1.2 are used to derive an ODE model of the bovine estrous cycle (BovCycle).

Although the endocrine and physiologic regulation of the bovine estrous cycle has been studied extensively, mathematical models of cycle regulation are scarce and of limited scope, e.g. [MRKB09] and [SPP$^+$00]. A number of models have been developed for other ruminant species, especially ewes, e.g. [CMTC02] and [HKM98], but these models also do not contain all the key players that are required to simulate follicle development and the accompanying hormone levels throughout consecutive cycles.

The model presented in this thesis has been inspired by a model of the human menstrual cycle [Rei09]. The endocrine mechanisms that regulate the bovine estrous cycle and the human menstrual cycle are very similar. In both species, the interplay of various organs and substances results in the periodic hormonal changes and tissue development. In successive periods, the female is preparing for reproduction by producing a fertilizable oocyte. During the reproductive life time in healthy individuals, if fertilization does not take place, the oocyte undergoes atresia, and the periodic hormonal interplay continues as before.

In both humans and cows, the female endocrine system consists of several glands and regulates the periodic changes of multiple substances necessary for reproduction. In every cycle, hormones are secreted from the hypothalamic-pituitary-gonadal axis into the blood-

stream, where they distribute and influence several functions in the body. Their most important task in reproduction is to regulate processes in the ovaries, where follicles and corpus luteum develop. These produce steroids that are released into the blood and from therein regulate the processes in the hypothalamic-pituitary-gonadal axis. The hormonal cycle is thus a result of a large feedback loop, whose self-regulation is a complex interplay of multiple components. In order to model the cycle as one closed system that generates the cyclic hormonal changes without external stimuli, and to analyze how the multiple components in different parts of the body function together, a whole-organism approach is chosen.

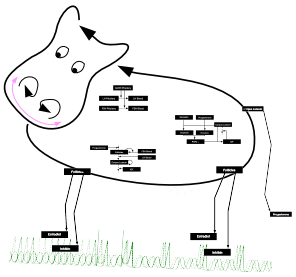

Figure 2.1: A modelers view on a cow, the underlying mechanisms are to be explored

With a closed model of the hormonal interactions, it is expected to learn more about the functioning of the bovine estrous cycle as a result of the interplay of various substances in different parts of the body. Apart from the investigation of the interplay of the involved substances, a computer model of the estrous cycle can also be used to perform *in silico* trials. Drug treatments can be simulated at low cost, and the effect of long term therapeutic strategies can be accessed at low risk. Finally, model simulations allow to investigate the course of substances for which experimental data is not available.

As the models of the bovine and the human cycle in this thesis are very similar, another motivation for developing a model of the reproductive cycle for the bovine was to transfer results to the model of the human menstrual cycle. At the beginning of this work, it was expected to have an easier access to experimental data relating to the bovine estrous cycle, but this turned out to be not as simple. However, a model for the bovine estrous cycle that describes the key features has been developed. A variety of possibilities exploiting the characteristics of this model have been applied, that could also be used to understand more about the dynamics in the human menstrual cycle. The development of the bovine cycle model will be described in this chapter.

2.1 Biological Background

Though discrete and numerical models lead to different output information, in this thesis the input information for both model types is similar, since the numerical models are mainly based on regulatory, i.e. qualitative, information. As described in Section 1.2, deriving a flowchart is the first and most essential step.

Independent of the decision on the model type (e.g. discrete or continuous), which leads to different output information, the decision on the level of detail of the model is crucial. One has to find reliable abstraction levels that display the most important mechanisms. In order to analyze the dynamic relations between the system components, rather than only focusing on individual parts, it should be incorporated how the multiple components function together to generate periodic solutions. In case of the hormonal cycle, components in many different parts of the body are involved. Therefore, in order to see the cycle as one closed system that generates the cyclic changes without external stimuli, a whole-body-approach is convenient. To include a preferably large amount of biological information from literature, a physiologically-based pharmacokinetic approach, in which the components, respectively variables, refer to substances in different physiological compartments, is suitable.

Before designing a model on the whole-organism level it is important to decide on the physiological compartments to be considered. For this it is crucial to decide on the key substances that have to be included in the model. Starting from scratch, the first step is to study the substances for which measurements are available, and that are known to play a role in the hormonal cycle. Typically, in bovine and in humans, among the measured substances are P4, E2, LH, and FSH. The least thing one wants to capture in the model is a relation between the measured substances. However, several other substances are known to be involved in their regulation. Initially, all available information about biological mechanisms behind the regulation of the measured substances is represented in a diagram. Subsequently, more substances and regulations are added to the diagram, which consist of nodes that represent substances, and arcs, which represent the interactions between the substances. This graphical representation of the considered variables and their interaction is called network, thus a system whose underlying structure is mathematically a graph. As the measured substances occur in ovaries, blood and pituitary, these compartments are the first ones included in a first sketch. It will turn out when considering the mechanisms that drive the production, synthesis, release, or clearance of these four substances, the hypothalamus as well as the uterus will become important. Besides GnRH, the follicles and the corpus luteum, five more substances will be introduced in the mentioned physiological compartments.

On one hand, the model becomes more flexible when integrating more mechanisms and substances into the model. One the other hand, one wants to answer the modeling question with the least possible computational costs, thus dispensable information regarding the modeling objective is left out in the model. Of course, the choice of the included com-

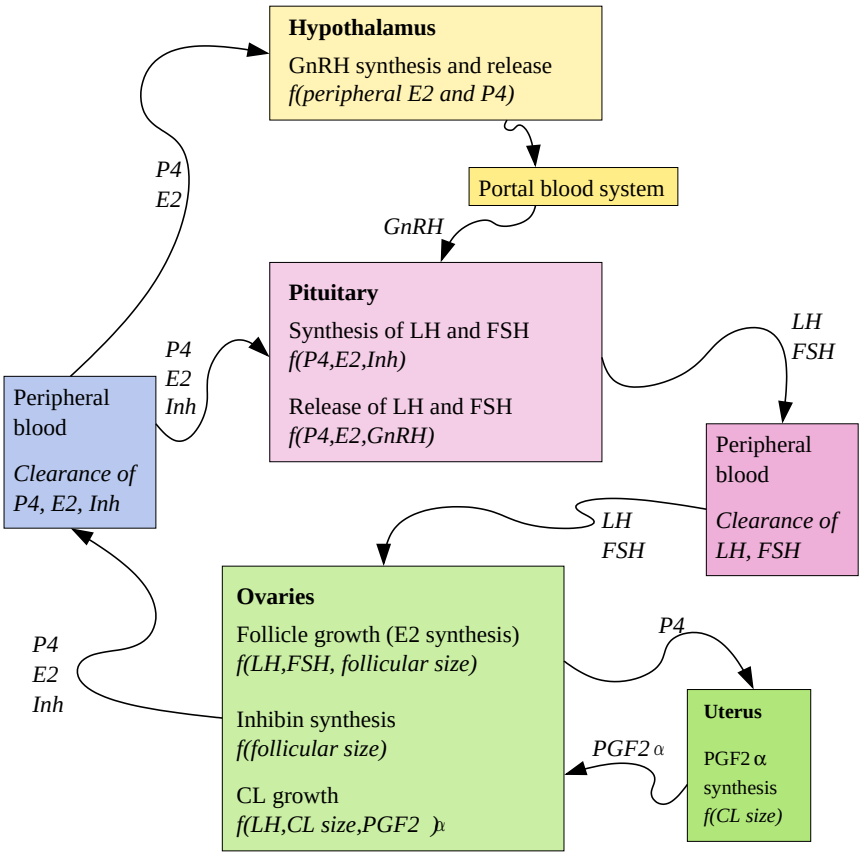

Figure 2.2: Schematic representation of the compartments in the model of the bovine estrous cycle

partments and substances is still depending on the modeler. An extensive literature search needs to be performed, and among the most difficult tasks is to decide which information not to include.

For the model of the bovine estrous cycle, orientation in the existing human models ([Har01, Rei09]) is also helpful. Therein, processes are included that take place in several parts of the organisms, the different compartments. Namely, these are the hypothalamus, the pituitary, the ovaries, and the blood stream, which also connects the other compartments. As in bovine, in [Har01] the gonadotropins are synthesized in the pituitary and released into the blood, from where they influence follicular development, ovulation, and luteal development in the ovaries. In the ovarian compartment, the steroid hormones E2, P4, and Inh are produced, released into the blood stream, from where they influence the processes in the hypothalamus and the pituitary.

In Figure 2.2, a first sketch of the model for the bovine estrous cycle is illustrated. It comprises a schematic representation of the compartments in the model, and is based on the biological knowledge described in the following. A detailed flowchart, together with the mathematical formulas for a continuous model, is derived in the subsequent section.

2.1.1 Processes in the Ovaries and the Uterus

A normal bovine estrous cycle includes two or three wave-like patterns of *follicle development*, in which a cohort of follicles start to grow [For94]. Each follicular wave is initiated by an increase of follicle stimulating hormone (FSH) release from the anterior pituitary [GBBK02]. In the first one or two waves, a dominant follicle deviates from the cohort of growing follicles that subsequently does not ovulate, but undergoes regression under influence of progesterone produced by the corpus luteum.

The *corpus luteum* (CL) develops within 2-3 days after ovulation, starting the synthesis and release of *progesterone* (P4), which maintains the readiness of the endometrium for receiving the embryo. In absence of a conceptus, the CL will regress at day 17-18 of the cycle [MSS09, TR91]. If the CL reaches a certain size, it continues to grow without further stimulation by LH [SJO01].

Dominant follicles secrete increasing amounts of *inhibin* (Inh) which, released into peripheral blood, suppresses FSH synthesis and thus reduces FSH release[GBB$^+$01]. Hence, the growth of subordinate follicles is suppressed. Ovulation or regression of the dominant follicle eliminates this suppression, allowing the onset of the next follicular wave [BGF$^+$01, GBB$^+$01].

The growing follicles also produce *estradiol* (E2), which is released into peripheral blood. E2 affects LH synthesis and release [GKHP$^+$07] and FSH release [BBKG02, LPRC05].

When the CL is regressed under influence of $PGF_{2\alpha}$ from the uterus, the concentration of progesterone decreases [NJS+00]. The dominant follicle present at that moment develops and matures, and ovulation can then take place, triggered by a peak of the luteinizing hormone. Once an oocyte is successfully ovulated, the remains of the follicle form a new P4-producing CL. If conception has failed, the CL regresses, P4 levels decrease, and the cycle restarts (reviewed in [BVBW10]).

Substances Involved in Luteolysis

Pulsatile $PGF_{2\alpha}$ release from the uterus induces CL regression. The rise of P4 early in the cycle initiates a series of events or mechanisms that eventually lead to the rise of PGF2α, followed by a decline of PGF2α a few days later. P4 first prevents a too early release of $PGF_{2\alpha}$ pulses, but simultaneously stimulates synthesis of enzymes required for $PGF_{2\alpha}$ production.

Among the regulators of $PGF_{2\alpha}$ are also oxytocin (OT), and E2 [SLM+91]. In the later luteal phase, changed expression of P4 and OT receptors results in a gradual decrease in the suppression of $PGF_{2\alpha}$ [SGF+09], leading to an OT induced pulsatile release of $PGF_{2\alpha}$ [AGF+09, Poy95].

The mechanisms involved in luteolysis are complex, a more detailed description will be given with the detailed presentation of the modeled mechanisms in Section 2.2.

2.1.2 Processes in the Hypothalamus and the Pituitary

The processes in hypothalamus, pituitary gland, and gonads are influenced by the steroid hormones E2, Inh, and P4, which are produced in the ovaries and released into the blood.

Elevated E2 levels increase the secretion of the *gonadotropin releasing hormone* (GnRH), which triggers the LH surge and thereby induces ovulation. Pulsatile signaling of GnRH regulates LH and FSH secretion [PM05]. Since GnRH induces the LH surge, it indirectly induces ovulation [TK84]. The GnRH pulse generator is located in the hypothalamus and is modulated by P4 and E2 [Goo88]. During the luteal phase, both P4 and E2 suppress the activity of the GnRH pulse generator. During pro-estrus however, elevated E2 levels change estrogen receptor signaling, which induces a GnRH surge [GKHP+07, Goo88]. GnRH is released into the portal circulation of the pituitary and binds to GnRH receptors of the anterior pituitary [VWB+97].

The LH surge at the day before ovulation induces ovulation of the ovulatory follicle and formation of the CL. The LH surge shuts down E2 and Inh production capacity of the

ovulatory follicle [CTK+75, WIR+04]. High P4 levels suppress the release of LH via the inhibition of the GnRH pulse generator [BKC+96]. Additionally, high P4 levels decrease pituitary sensitivity to E2, thereby increasing the amount of E2 required to induce the LH surge necessary for ovulation [Goo88]. Ovulation can take place because the inhibiting effect of P4 on the surge of luteinizing hormone (LH) is removed [ML95]. Peak LH levels are about five times as high as basal levels or higher [BGF+01, EH73, KW82, DBTW86].

FSH synthesis is inhibited by Inh [BBKG02]. P4 and E2 modulate FSH release via effects on the anterior pituitary and on the GnRH pulse generator in the hypothalamus. Peak FSH serum levels are about three times higher than basal levels [BGF+01, EKWF97].

2.2 Numerical Model

From the first scheme of the relations between the substances in different physiological compartments, depicted in Figure 2.2, a mathematical model is derived. Detailed regulations as well as ODE formulations of these mechanisms are described in the following.[1]

In the figures in this section, green arrows mark stimulatory effects, stump red arrows represent inhibitory effects, and dashed arrows indicate transformations. Each box represents one ODE, and '$*$' marks a degraded substance.

2.2.1 The ODEs for GnRH, FSH, and LH

GnRH stimulates LH release, resulting in an LH surge concurrent with the GnRH surge. GnRH synthesis is taken constant as long as the amount of GnRH in the hypothalamus is below a threshold. On the one hand, GnRH release is inhibited when P4 levels are above a threshold and when both P4 and E2 levels are above a threshold. On the other hand, GnRH release is stimulated when P4 levels are low and E2 reaches a threshold, resulting in a surge of GnRH. GnRH concentration in the pituitary depends on GnRH amount released from the hypothalamus, and is further increased by high E2 levels. This represents that E2 up-regulates the expression of GnRH receptors in the pituitary, which means that the sensitivity of the pituitary for GnRH increases [Goo88, VWB+97].

The mechanisms regulating GnRH in the model are illustrated in Figure 2.3. In the system of ODEs, the amount of GnRH in the hypothalamus is a result of synthesis in the

[1] Note that the notation in comparison to [mPHR12] has changed. Here, the variables, i.e. the solutions of the ODE system, are denoted as $y_{\text{Substance}}$, for a better comparison to the corresponding discrete variables $x_{\text{Substance}}$ in Chapter 5.

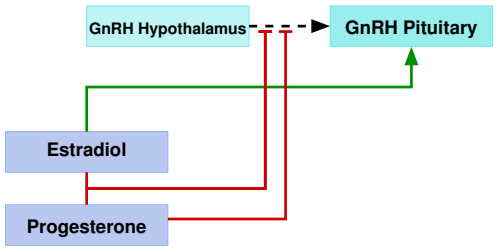

Figure 2.3: Mechanisms regulating GnRH in the bovine model. GnRH is transported, i.e. released, from the hypothalamus to the pituitary (marked with a black dashed arrow). P4 inhibits GnRH release, itself and together with E2 (marked with a red stump arrow). E2 also exerts a positive effect (marked with a green arrow) on GnRH in the pituitary due to its stimulatory effect on GnRH receptors.

hypothalamus and release into the pituitary,

$$\frac{d}{dt}y_{\mathrm{Gh}}(t) = Syn_{\mathrm{G}}(t) - Rel_{\mathrm{G}}(t). \tag{B1}$$

GnRH synthesis depends on its current level in the hypothalamus. If this level approaches a specified threshold, synthesis decreases until zero. This effect is modeled as logistic growth,

$$Syn_{\mathrm{G}}(t) = c_{\mathrm{G},1} \cdot \left(1 - \frac{y_{\mathrm{Gh}}(t)}{\mathrm{G}^{\max}_{Hypo}}\right). \tag{1}$$

As long as GnRH in the hypothalamus is far below its maximum, the factor $1 - \frac{y_{\mathrm{Gh}}(t)}{\mathrm{G}^{\max}_{Hypo}}$ has only a small impact.

The release of GnRH from the hypothalamus to the pituitary is dependent on its current level in the hypothalamus. Furthermore, E2 inhibits GnRH release during the luteal phase, i.e. if P4 and E2 are high at the same time, which is comprised in the function

$$\begin{aligned} &H^{-}_{P_4\&E_2,G}(y_{\mathrm{P4}}(t), y_{\mathrm{E2}}(t)) = \\ &m_{\mathrm{P4\&E2}}\Big(h^{-}(y_{\mathrm{P4}}(t); T^{\mathrm{G},1}_{\mathrm{P4}}, 2) + h^{-}(y_{\mathrm{E2}}(t), T^{\mathrm{G},1}_{\mathrm{E2}}, 2) - h^{-}(y_{\mathrm{P4}}(t); T^{\mathrm{G},1}_{\mathrm{P4}}, 2)h^{-}(y_{\mathrm{E2}}(t); T^{\mathrm{G},1}_{\mathrm{E2}}, 2)\Big) \\ &\qquad = m_{\mathrm{P4\&E2}}\Big(1 - h^{+}(y_{\mathrm{P4}}(t); T^{\mathrm{G},1}_{\mathrm{P4}}, 2)h^{+}(y_{\mathrm{E2}}(t); T^{\mathrm{G},1}_{\mathrm{E2}}, 2)\Big). \end{aligned}$$

This function inhibits GnRH release only if both substrates are above their threshold. Additionally, the release of GnRH is inhibited by P4 only,

$$Rel_{\mathrm{G}}(t) = \left(H^{-}_{\mathrm{P4\&E2,G}}(y_{\mathrm{P4}}(t), y_{\mathrm{E2}}(t)) + H^{-}_{\mathrm{P4,G}}(y_{\mathrm{P4}}(t))\right) \cdot y_{\mathrm{Gh}}(t). \tag{1}$$

Changes in GnRH amount in the pituitary are dependent on the released amount from the hypothalamus, but also on the presence of E2. E2 increases the number of GnRH receptors

in the pituitary. This effect is included in the equation as a positive Hill function. GnRH clearance from pituitary portal blood is proportional to the GnRH level in the pituitary, i.e. GnRH clearance is represented by $c_{G,2} \cdot y_G(t)$, in which $c_{G,2}$ is a constant,

$$\frac{d}{dt} y_G(t) = Rel_G(t) \cdot H^+_{E2,G}(y_{E2}(t)) - c_{G,2} \cdot y_G(t). \tag{B2}$$

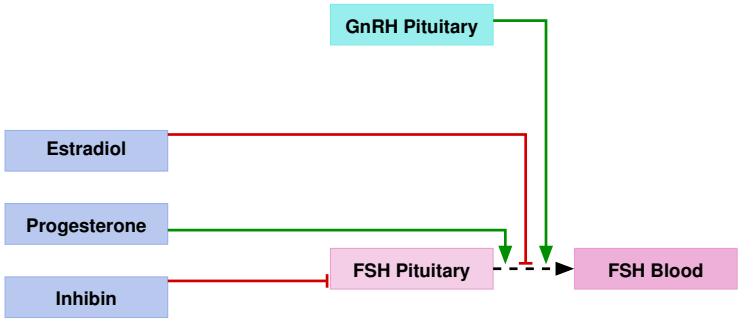

Figure 2.4: Mechanisms regulating FSH. FSH synthesis in the pituitary is inhibited by inhibin, and its release from the pituitary into the blood is regulated by P4, E2, and GnRH.

FSH is synthesized in the pituitary and released into the blood,

$$\frac{d}{dt} y_{FSHp}(t) = Syn_{FSH}(t) - Rel_{FSH}(t). \tag{B3}$$

The FSH synthesis rate in the pituitary is dependent on Inh. The former delay of inhibin on FSH in the model [BmR+11], as also used in the model of [Har01], could be omitted by adjusting the threshold in the corresponding Hill function. FSH is synthesized when the Inh level is low, i.e. high Inh levels inhibit FSH synthesis, which is included as a negative Hill function,

$$Syn_{FSH}(t) = H^-_{Inh,FSH}(y_{Inh}(t)).$$

Besides a basal FSH release from the pituitary to the blood, the release is also stimulated by P4 and GnRH, and inhibited by E2,

$$Rel_{FSH}(t) = \left(b_{FSH} + H^+_{P4,FSH}(y_{P4}(t)) + H^-_{E2,FSH}(y_{E2}(t) + H^+_{G,FSH}(y_G(t)\right) \cdot y_{FSHp}(t).$$

Concluding, FSH serum level is a result of the difference between the released amount from the pituitary and clearance in the blood,

$$\frac{d}{dt} y_{FSH}(t) = Rel_{FSH}(t) - c_{FSH} \cdot y_{FSH}(t), \tag{B4}$$

where c_{FSH} is the FSH clearance rate constant.

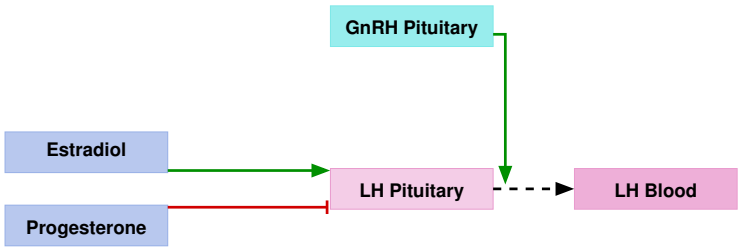

Figure 2.5: Mechanisms regulating LH

As depicted in Figure 2.5, LH synthesis is stimulated by E2 and inhibited by P4. Besides a small basal LH release, there is a surge of LH when GnRH in the pituitary reaches a threshold. Like FSH, the LH serum level depends on synthesis in the pituitary, release into the blood and clearance thereof,

$$\frac{d}{dt}y_{\mathrm{LH_P}}(t) = Syn_{\mathrm{LH}}(t) - Rel_{\mathrm{LH}}(t). \tag{B5}$$

LH synthesis in the pituitary is stimulated by E2 and inhibited by P4,

$$Syn_{\mathrm{LH}}(t) = H^{+}_{\mathrm{E2,LH}}(y_{\mathrm{E2}}(t)) + H^{-}_{\mathrm{P4,LH}}(y_{\mathrm{P4}}(t))$$

We assume a low constant basal LH release b_{LH} from the pituitary into the blood. On top of that, LH release is stimulated by GnRH,

$$Rel_{\mathrm{LH}}(t) = \left(b_{\mathrm{LH}} + H^{+}_{\mathrm{G,LH}}(y_{\mathrm{G}}(t))\right) \cdot y_{\mathrm{LH_P}}(t).$$

Summarizing, LH in the blood is obtained as

$$\frac{d}{dt}y_{\mathrm{LH}}(t) = Rel_{\mathrm{LH}}(t) - c_{\mathrm{LH}} \cdot y_{\mathrm{LH}}(t), \tag{B6}$$

where c_{LH} is the LH clearance rate constant.

2.2.2 The ODEs for Follicles and Corpus Luteum, and for the Hormones E2, Inh, and P4

The ovaries contain a pool of small *follicles* with immature oocytes. Under the influence of FSH, a cohort of 8-41 growing follicles emerge [AJSM08]. Approximately two days after cohort recruitment, one follicle is selected to become the dominant follicle, and continues to grow [BG98]. This deviation of the dominant follicle is associated with increased FSH and LH receptor binding, activating the enzymes that catalyze steroidogenesis, resulting in increased E2 production and higher E2 serum levels [BG98]. Small follicles of an emerging cohort of follicles release each very small amounts of E2 and Inh per follicle, and taken together this amount is not negligible. Furthermore, there is always a medium-size or large

follicle present [IMA+00, Wis87, WIR+04], which results in a basal hormone production throughout the cycle. Different follicles are recruited, grow, and regress in each wave. However, total E2 and Inh production capacity is modeled as a continuous function throughout subsequent waves and cycles, representing the total amount of hormone production of the follicles present at any moment. The capacity of follicles to produce E2 and Inh is denoted as *follicular function* in the rest of this work.

The dominant follicle expresses more FSH receptors, and it can therefore continue to grow even when FSH serum levels are low [BBKG02]. In the model, the emergence of a follicular wave is induced when FSH exceeds a threshold which becomes lower when follicles become larger, representing that larger follicles are more sensitive to FSH. Follicle regression is promoted by high P4 levels and by the LH surge, the stimulus for ovulation. The differential equation for follicular function y_{Foll} is

$$\frac{d}{dt}y_{\text{Foll}}(t) = \widetilde{H^+}_{\text{FSH,Foll}}\big(y_{\text{FSH}}(t)\big) - \Big(H^+_{\text{P4,Foll}}(y_{\text{P4}}(t)) + H^+_{\text{LH,Foll}}(y_{\text{LH}}(t))\Big) \cdot y_{\text{Foll}}(t) \tag{B7}$$

where

$$\widetilde{H^+}_{\text{FSH,Foll}}\left(y_{\text{FSH}}(t)\right) := m^{\text{Foll}}_{\text{FSH}} \cdot h^+\Big(y_{\text{FSH}}(t), T^{\text{Foll}}_{\text{FSH}} \cdot h^+\big(y_{\text{Foll}}(t), T^{\text{Foll}}_{\text{Foll}}, n^{\text{Foll}}_{\text{Foll}}\big), n^{\text{Foll}}_{\text{FSH}}\Big).$$

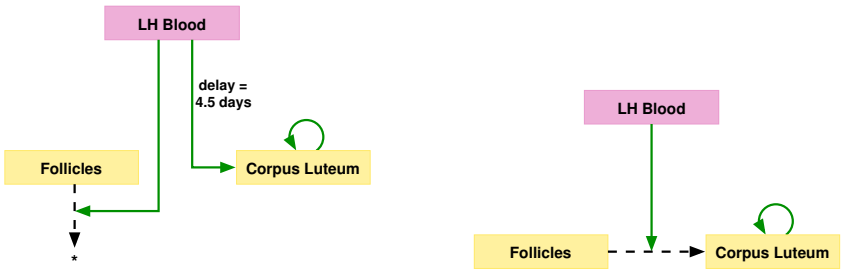

(a) Former mechanisms as in [BmR+11]

(b) Advanced mechanisms

Figure 2.6: An example of how parts of the model changed throughout the model development. The regulation of ovulation formerly needed a delay, and Foll and CL size were independent of each other. Since it is known that remainings of the ruptured follicle transform to the rising CL [RKF+01], the ovulatory follicle now directly transforms into the CL.

The development of the *corpus luteum* is induced by the LH surge. During the first modeling approaches [BmR+11], a delay was incorporated in the effect of LH on the CL, to account for the time required for the process of transition from follicle to CL [NJS+00] and the shift from E2 to P4 production [DBTW86, DB85]. LH, as the initiator of ovulation, was responsible for decay of the dominant follicle, and at the same time the initiator of

the rise of the CL 4.5 days after the LH peak. A delay differential equation was needed to model this effect. The atretic follicles disappeared from the system, and the CL emerged independently of the size of the just ovulated dominant follicle. However, it is known that thecal and granulosa cells of the ruptured follicle transform to small and large luteal cells which form the rising CL ([RKF+01]). Therefore, to make the model more realistic and to be able to account for different sizes of the dominant follicle ([RIR10]), the involved mechanisms were changed. The ovulatory follicle now directly influences the initiation of CL growth, and no further delay differential equation is needed. The old and new mechanisms are illustrated in Figure 2.6.

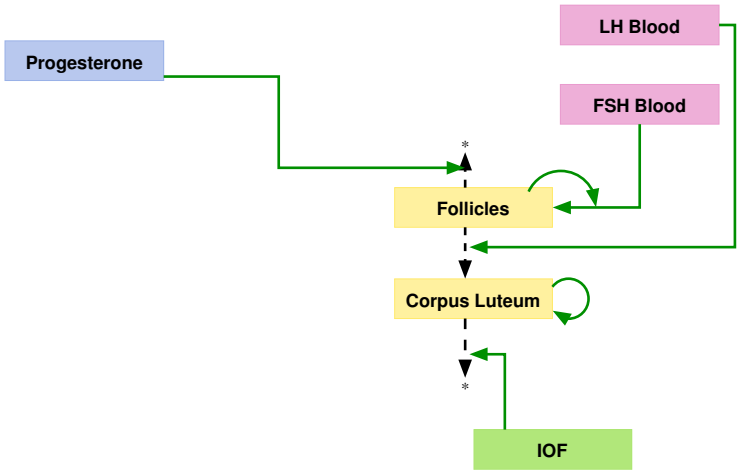

Figure 2.7: Mechanisms regulating the processes in the ovaries

In each cycle a new CL develops, but CL development is modeled as a continuous function of P4 producing tissue, denoted as *CL function* in this work. The differential equation describing CL function is

$$\begin{aligned}\frac{d}{dt}y_{\mathrm{CL}}(t) = \mathrm{SF} \cdot H^{+}_{\mathrm{LH,CL}}\big(y_{\mathrm{LH}}(t)\big) \cdot y_{\mathrm{Foll}}(t) \\ + H^{+}_{\mathrm{CL,CL}}\big(y_{\mathrm{CL}}(t)\big) - H^{+}_{\mathrm{IOF,CL}}\big(y_{\mathrm{IOF}}(t)\big) \cdot y_{\mathrm{CL}}(t).\end{aligned} \tag{B8}$$

In the model, the part of the follicles decaying due to LH, i.e. the ovulated follicle, is now preserved in the system, forming the rising CL. The scaling factor SF is included to keep the relative levels of the substances between 0 and 1. Further growth of the CL is modeled by a self-growth, i.e. a positive influence of the CL on its own size from a certain size on.

Having derived the ODEs for the tissues in the ovaries, the production of the hormones produced by these tissues can be modeled. These hormones are the steroids estradiol (E2) and progesterone (P4), and inhibin (Inh).

E2 serum levels are higher in ovulatory than in non-ovulatory waves [BGF+01, EH73] and reach peak levels around estrus [BGF+01, EH73, EKWF97, GEBP81, KDWF76, Wis87]. This suggests that the preovulatory follicle has the largest capacity to produce and release E2, although its maximum size is not significantly different from the maximum size of non-ovulatory dominant follicles. Considering the results in [Aco07, AOK+00], where a better vascularity of the ovulatory follicle is reported, it is reasonable that the ovulatory follicle can secrete more E2 than non-ovulatory follicles and, consequently, E2 serum levels are highest at estrus. In the model, the rate of E2 production and release to the blood is directly dependent on follicular function.

Inhibin exists in two different forms, inhibin A and inhibin B, but only inhibin A is considered in the bovine model, as it is the predominant form in bovine follicular fluid [BBKG02]. Compared to basal Inh serum levels, peak levels are almost doubled in non-ovulatory waves and increase further in ovulatory waves [PRGM03]. In the model, Inh production rate is, as E2, directly dependent on follicular function.

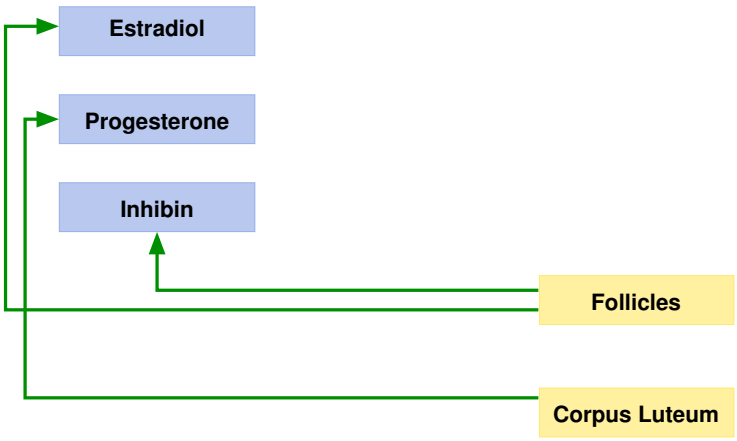

Figure 2.8: Mechanisms regulating the production of the hormones E2, Inh, and P4. These substances are directly dependent on follicular and CL function. The green arrows describe the positive effect of the Foll and CL level on hormone production.

The CL is the main source of *progesterone* (P4). Serum P4 concentration is near to zero around estrus and high during the luteal phase [AMG92, DMT+86, EH73, KKW+95, SEM69]. A high correlation between CL diameter and P4 output was reported in [PCK+91, SKBR88, WIR+04].

In Figure 2.8, the production of the hormones estradiol, inhibin, and progesterone, is illustrated. The production of substances do not comprise regulations in form of Hill functions, but can be modeled directly. Since it is known that P4 production of the CL is not absolutely proportional to the CL size ([KBG90]), P4 production is modeled to be lower at

start of CL growth compared to later luteal stages. It is assumed that production of P4 depends on the surface size and thus quadratically on CL. Also, a quadratic relationship between the follicles and E2, as well as between the follicles and Inh, is assumed.

The equations for P4, E2, and Inh do not contain any Hill functions,

$$\frac{d}{dt}y_{\mathrm{P4}}(t) = c_{\mathrm{CL}}^{\mathrm{P4}} \cdot y_{\mathrm{CL}}(t)^2 - c_{\mathrm{P4}} \cdot y_{\mathrm{P4}}(t), \tag{B9}$$

$$\frac{d}{dt}y_{\mathrm{E2}}(t) = c_{\mathrm{Foll}}^{\mathrm{E2}} \cdot y_{\mathrm{Foll}}(t)^2 - c_{\mathrm{E2}} \cdot y_{\mathrm{E2}}(t), \tag{B10}$$

$$\frac{d}{dt}y_{\mathrm{Inh}}(t) = c_{\mathrm{Foll}}^{\mathrm{Inh}} \cdot y_{\mathrm{Foll}}(t)^2 - c_{\mathrm{Inh}} \cdot y_{\mathrm{Inh}}(t). \tag{B11}$$

The parameters c_{P4}, c_{E2} and c_{Inh} denote the respective clearance rate constants.

2.2.3 The ODEs for Oxytocin, Enzymes, Intra-Ovarian Factors, and $PGF_{2\alpha}$

In [BmR+11], the rise of $PGF_{2\alpha}$ triggering the decay of the CL was modeled as a black box, depending with large delays on P4 only. In [BRm+11], this was improved as enzymes were introduced that stimulate $PGF_{2\alpha}$, and the model became more robust. These enzymes required for the production and release of $PGF_{2\alpha}$ are stimulated by P4 [SLM+91, SGF+09]. The ODE for the development of the enzymes is now

$$\frac{d}{dt}y_{\mathrm{Enz}}(t) = H^{+}_{\mathrm{P4,Enz}}\big(y_{\mathrm{P4}}(t)\big) - c_{\mathrm{Enz}} \cdot y_{\mathrm{Enz}}(t). \tag{B12}$$

In [BRm+11], the enzymes were the only predecessors of $PGF_{2\alpha}$. However, simulating the administration of $PGF_{2\alpha}$ it turned out that the modeling of luteolysis still had some deficits. It is known that after the administration of $PGF_{2\alpha}$ the responsive CL decays immediately [HH74]. In the original model, the CL did not decay fast enough after administration of PGF_{syn}, and neither after rise of the regular $PGF_{2\alpha}$. But since P4 levels, which fall with the CL, should stay on a high level for the duration of the first two follicular waves, the CL needed to decay later. That means the initiator of luteolysis, $PGF_{2\alpha}$, needed to appear a couple of days later compared to the original model. To account for this effect, the mechanisms that lead to a rise in $PGF_{2\alpha}$ were modeled more precisely. The development of the model regarding luteolysis is illustrated in Figure 2.9.

Instead of leaving only the enzymes (Enz) being responsible for $PGF_{2\alpha}$ levels as in [BRm+11], OT is introduced as another initiator of $PGF_{2\alpha}$ [KSM+99]. E2 stimulates OT synthesis in the granulosa cells [VF93] and within this the effect of OT on $PGF_{2\alpha}$ [AGBF96]. It is assumed that OT production quadratically depends on CL size, and that it is cleared with constant rate c_{OT}. The equation for the rise and fall of OT is now

$$\frac{d}{dt}y_{\mathrm{OT}}(t) = H^{+}_{\mathrm{E2,OT}}\big(y_{\mathrm{E2}}(t)\big) \cdot y_{\mathrm{CL}}(t)^2 - c_{\mathrm{OT}} \cdot y_{\mathrm{OT}}(t). \tag{B13}$$

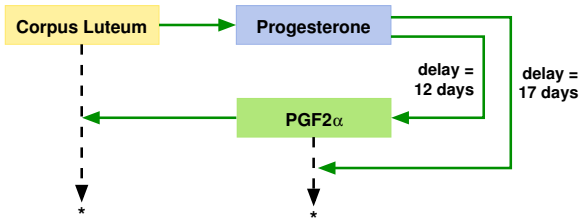

(a) Mechanisms in the first model([BmR$^+$11])

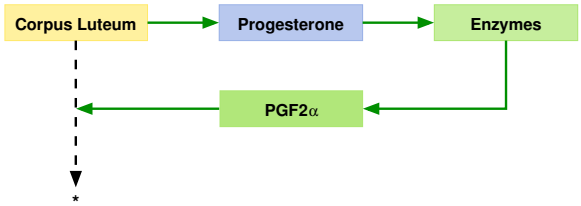

(b) Mechanisms in a modified model ([BRm$^+$11])

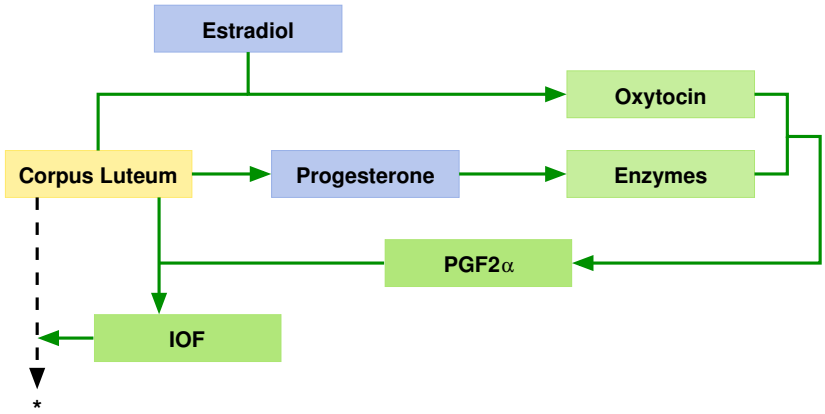

(c) Advanced mechanisms within the current model

Figure 2.9: Changes in the mechanisms involved in luteolysis. In (a), P4 was driving luteolysis with large time delays. In (b), enzymes were responsible for the rise of $PGF_{2\alpha}$. In the advanced model, oxytocin and inter-ovarian factors were added to the drivers of luteolysis.

OT together with Enz are now responsible for the rise of $PGF_{2\alpha}$. The function $H^+_{E2,OT}(y_{E2}(t))$ represents a stimulatory effect if the levels of Enz and OT are both high. With the constant clearance rate c_{PGF}, the equation for $PGF_{2\alpha}$ becomes

$$\frac{d}{dt}y_{PGF}(t) = H^+_{Enz\&OT,PGF}\big(y_{Enz}(t), y_{OT}(t)\big) - c_{PGF} \cdot y_{PGF}(t). \tag{B14}$$

In former models, $PGF_{2\alpha}$ triggered luteolysis directly, independent of estrous stage. However, it is known that the CL is not sensitive to the action of $PGF_{2\alpha}$ at early luteal stage. Therefore, the action of $PGF_{2\alpha}$ on the CL is remodeled. According to [SFDO08], the direct action of $PGF_{2\alpha}$ on the CL is mediated by local factors: endothelin-1-system, cytokines, and nitric oxide. The expression of these inter-ovarian substances is upregulated by $PGF_{2\alpha}$, and strictly depends on the stage of the CL. A new component to the model is introduced, and named *inter-ovarian factors* (IOF). IOF is stimulated by $PGF_{2\alpha}$ only if the CL has reached a certain size, and cleared with the constant rate c_{IOF},

$$\frac{d}{dt}y_{IOF}(t) = H^+_{PGF\&CL,IOF}\big(y_{PGF}(t), y_{CL}(t)\big) - c_{IOF} \cdot y_{IOF}(t). \tag{B15}$$

The rise of the inter-ovarian factors now induces luteolysis.

The complete model for the bovine estrous cycle can be found in Table A.4 in the Appendix. The list of identified parameter values is provided in Table A.5, and the initial values in Table A.6.

The model of the bovine estrous cycle is dimensionless in the sense of [LS88], i.e. the numerical values of the components are independent of the standard of measurement. Simulated hormone levels and ovarian components have been scaled to be between 0 and 1 by dividing the equation by its maximum output level. Once measurement data is available, the functions can be scaled to the corresponding quantities by scaling the involved parameters. This can be done because, until now, none of the parameters has a fixed value verified by experiments. The simulated dimensionless output functions are referred to as *relative level*.

2.2.4 Sensitivity Analysis and Parameter Identification

Parameter estimation is performed with an affin-covariant Gauss-Newton method as described in Chapter 3. To get good initial values, several feedback mechanisms are neglected at first, and the model is successively built with the help of Gaussian input curves.

To get good experimental data for parameter estimation is difficult. In figure 2.11, data profiles for the most important hormones are depicted. Based on this, artificial measurement points are created.

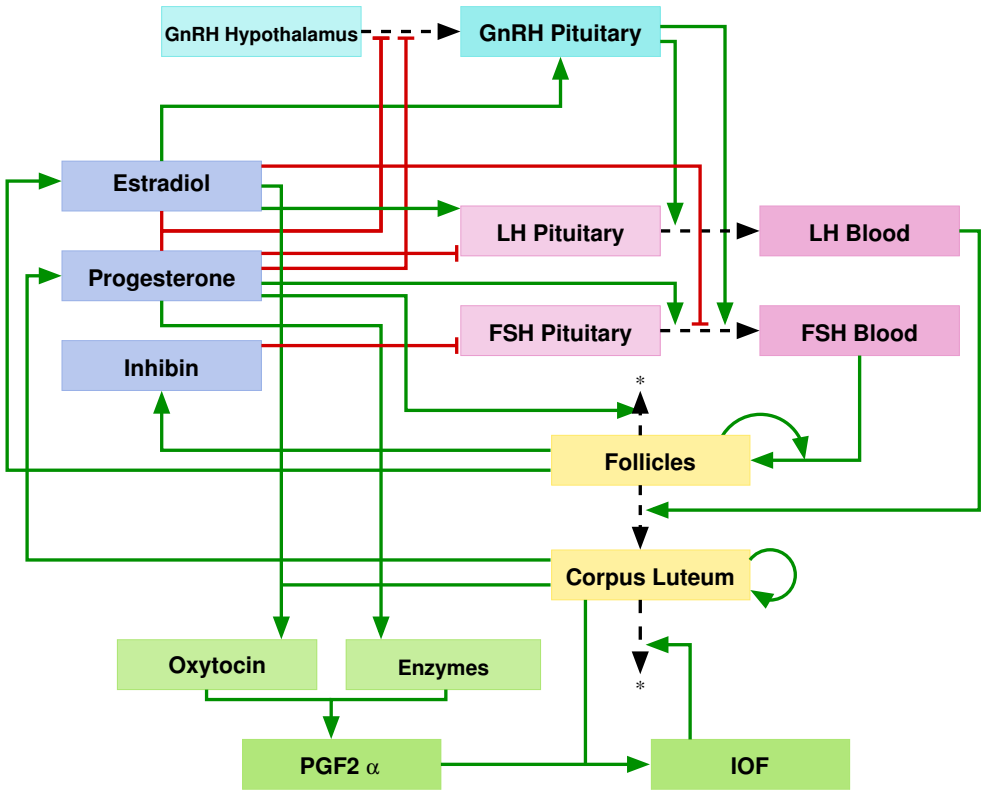

Figure 2.10: Flowchart for the model of the bovine estrous cycle. A green arrow marks a stimulatory effect, a red stump arrow an inhibitory influence. A black dashed arrow means a transition, and '$*$' marks a degraded substance.

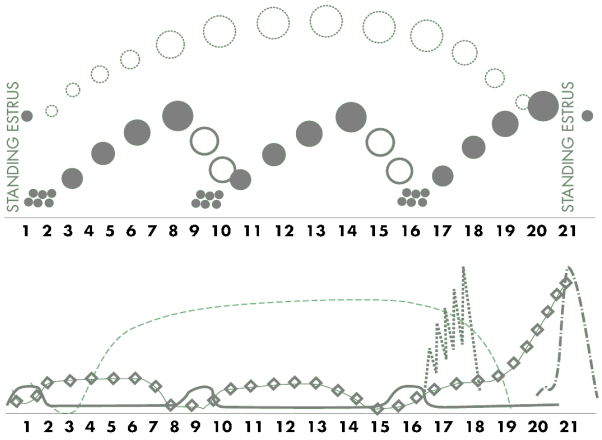

Figure 2.11: Typical qualitative profiles as published in e.g. [Per04]. The upper figure shows the development of three follicular waves together with the growth and regression of the corpus luteum during one estrous cycle. The lower figure demonstrates the changes in concentrations of different hormones that regulate the cycle. Depicted are FSH (solid line), P4 (dashed line), E2 (diamond line), LH (dashed dotted line, rise around day 20), and $PGF_{2\alpha}$ (dotted line, rise around day 16). Ovulation is caused by the LH peak and occurs around day 21.

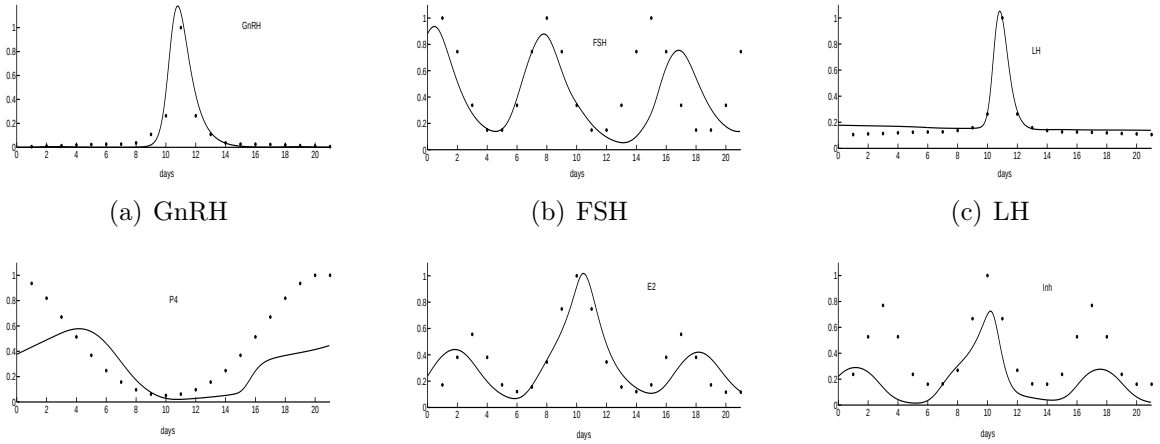

(a) GnRH (b) FSH (c) LH

(d) P4 (e) E2 (f) Inh

Figure 2.12: Simulations with BovCycle together with artificial data points, created based on profiles published in literature.

Obtaining Initial Values for the Parameter Estimation

Many of the parameters are not measurable, sometimes the range of values is known, and some are completely unknown. Estimating all model parameters simultaneously under those circumstances is impossible. For local convergence of the Gauss-Newton algorithm, it is crucial to start the identification routine with a good initial guess for the parameters. For this, the closed feedback loop of mechanisms is cut up, and the time courses of the substances are fitted.

Following [Har01], as a first step input curves are defined that describe the development for the plasma hormones E2, P4 and Inh over time. Composition of these input curves is based on published data for endocrine profiles of cows with a normal estrous cycle, see for example [Per04], depicted in Figure 2.11. As input curves, sums of Gaussian functions are taken, where height, width, and time point of the peak are identified with the Gauss-Newton algorithm, using artificial data points.

$$y_{\mathrm{E2}}(t) = p_1 + p_2 \cdot e^{\frac{-(t+p_3)^2}{p_4}} + p_5 \cdot e^{\frac{-(t+p6)^2}{p_7}} + p_8 \cdot e^{\frac{-(t-p9)^2}{p_{10}}} + p_{11} \cdot e^{\frac{-(t+p_{12})^2}{p_{13}}},$$
$$y_{\mathrm{P4}}(t) = p_{14} + p_{15} \cdot e^{\frac{-(t-p_{16})^2}{p_{17}}} + p_{18} \cdot e^{\frac{-(t+p_{19})^2}{p_{20}}},$$
$$\mathrm{Inh}(t) = p_{21} + p_{22} \cdot e^{\frac{-(t+p_{23})^2}{p_{24}}} + p_{25} \cdot e^{\frac{-(t+p_{26})^2}{p_{27}}} + p_{28} \cdot e^{\frac{-(t-p_{29})^2}{p_{30}}} + p_{31} \cdot e^{\frac{-(t+p_{32})^2}{p_{g33}}}.$$

These Gaussian functions with the identified parameters p_1-p_{33} then are used to identify the parameters involved in the regulation of the other hormones, by fitting the simulation curves to measurements reported in literature. Step by step, more parameters are identified, until the input curves are replaced by the corresponding ODE formulations. The set of then 60 parameter values for the parameters are used in the Gauss-Newton algorithm as starting values for identifying all parameters simultaneously. These first steps are visualized in Figure 2.13.

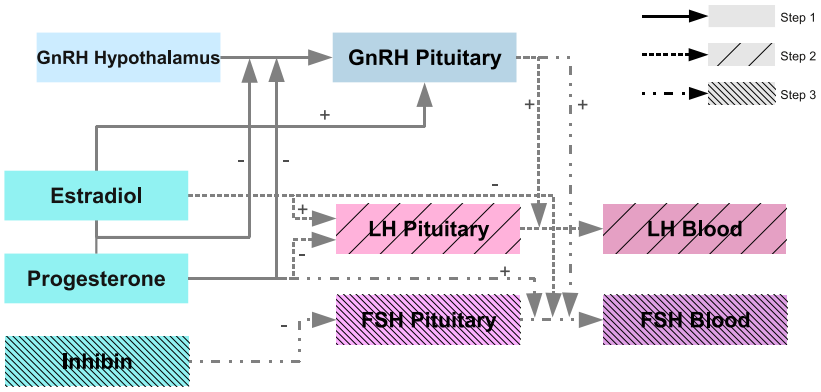

Figure 2.13: The first steps in generating successively good initial guesses for parameter optimization and enlarging the set of estimated parameters.

Afterwards, the profiles of follicular function, PGF2α and CL function are fitted to be in line with empirical knowledge. Finally, the input curves for P4, E2, and Inh are replaced by their original ODE description to obtain a closed network, and the number of estimated parameters increases.

Parameter estimation is done subsequently while generating the components of the model and enlarging the set of parameters. A parameter value obtained by the optimization procedure can be overwritten throughout the modeling process; the previous value then serves as starting value for the optimization procedure in the next modeling step. The final set of parameters leads to simulation results that are, together with the artificial data, illustrated in Figure 2.12.

2.3 Simulation and Model Validation

Validation of the model consists of investigation how adequately the model simulations match given information. Experimental data required for model validation would for example consist of measured hormonal concentrations of healthy, untreated, individual cows at different stages of estrous cycle. Unfortunately, measurements published in literature are rare and do often not meet the requirements for validation; observed time scales are often too small or too coarse, or too few substances are measured. Only recently, data-derived profiles for LH, FSH, E2, and P4 were published in [MFD$^+$13] which are useful for validating the model with respect to the course of the reproductive hormones in healthy cows.

Another possibility to validate the model is to check the correctness of the model for a specific scenario where the system answer is known.

2.3.1 Administration of PGF2α

An example of a scenario where the response of the estrous cycle is known are synchronization protocols ([SDS$^+$08]) with prostaglandin $F_{2\alpha}$ ($PGF_{2\alpha}$). Simulation of this scenario with the model will serve as its validation in the following. In veterinary medicine, $PGF_{2\alpha}$ and its analogues are administered to cows mainly to make use of their luteolytic action, e.g. in estrus synchronization protocols. It is known that the sudden rise of this substance at certain stages of the estrous cycle results in an immediate decay of the responsive CL, and an immediate fall of progesterone levels in plasma.

$PGF_{2\alpha}$ is responsible for the onset of luteolysis in the cow. With luteolysis the luteal phase of the cycle ends and a new estrous can take place. $PGF_{2\alpha}$ induces functional luteolysis by reducing progesterone production followed by structural luteolysis with tissue degeneration and cell death [MCL99, SFDO08]. $PGF_{2\alpha}$ is synthesized in the endometrium and released in

pulses, regulated by E2, P4 and OT during the estrous cycle [SLM+91, AGBF96, XLSG98]. In veterinary medicine, administration of synthetical analogues of $PGF_{2\alpha}$ (e.g. Cloprostenol, Luprostiol, Tiaprost) or original $PGF_{2\alpha}$ (e.g. Dinoprost) is used for various purposes in the cow such as induction of estrous or synchronization protocols. The effect of the treatment depends on the stage of estrous cycle which determines the responsiveness of the CL on the luteolytic action of $PGF_{2\alpha}$ [SFDO08]. At midluteal stage of the estrous cycle administration of $PGF_{2\alpha}$ leads to luteolysis within a few hours. This results in a decrease of P4 concentration, increase of E2, a peak of the Luteinizing Hormone (LH) and ovulation [SSW84].

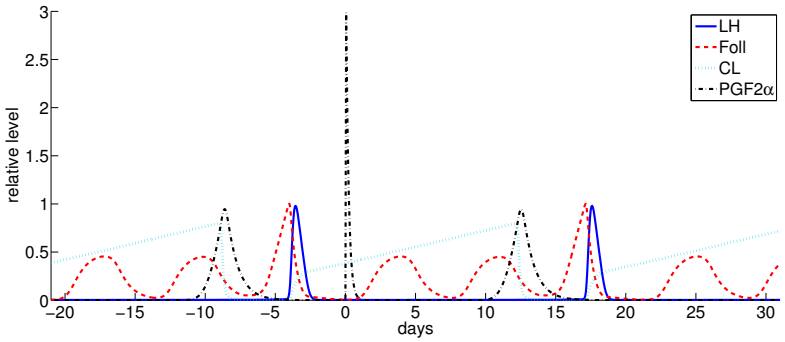

(a) $PGF_{2\alpha}$ administration in early luteal phase

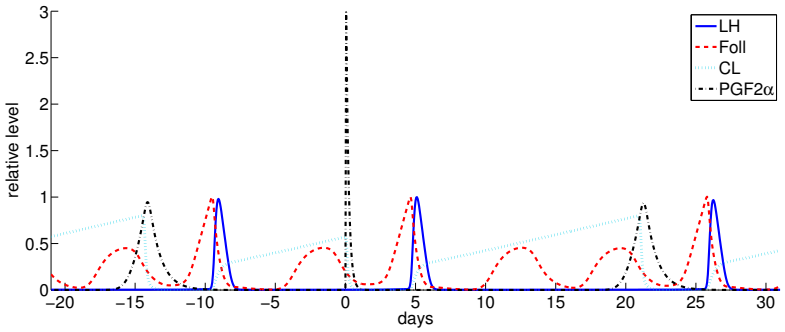

(b) $PGF_{2\alpha}$ administration in mid-luteal phase

Figure 2.14: Simulation results with the advanced model for Foll, CL, and LH, and total $PGF_{2\alpha}$ after administration of PGF_{syn} on different stages of the cycle. A high peak of Foll indicates ovulation. In (a) it is shown that there is no response if ovulation has occurred only four days before administration, in (b) it can be observed that giving PGF_{syn} ten days after ovulation leads to a decay in CL, an LH peak and ovulation within five days after administration.

It is known that $PGF_{2\alpha}$ and its analogues have a very short half-life [SLHS75, Kro03]. Therefore, an additional component was needed in the model that falls rapidly. Analogues of $PGF_{2\alpha}$, denoted PGF_{syn} in the following, have an up to three times higher biological

activity than original $PGF_{2\alpha}$ [Kro03]. Even low doses of PGF_{syn} caused a peak in $PGF_{2\alpha}$ that exceeded the natural level [GAP+09]. Due to this high potency of PGF_{syn} , parameters were identified that lead to a three times higher relative level of PGF_{syn} compared to normal $PGF_{2\alpha}$ levels. The effect of the synthetical analogue is modeled by summing the level of PGF_{syn} to the normal $PGF_{2\alpha}$ level.

To model the rise of PGF_{syn} in the system, a function is taken which is zero before dosing time (t_D), and has a sharp left-skewed peak with maximum shortly after t_D. This leads to a slight delay in the effect of the injection. As suggested in [Rei09], based on techniques described in [KV98], the probability density function of the Gamma-distribution is chosen with fixed shape parameter $\alpha = 2$, and inverse scale parameter β leading to a left-skewed curve which has its maximum at $t = \frac{1}{\beta}$. The change of concentration of synthetic $PGF_{2\alpha}$ is calculated as

$$\frac{d}{dt} y_{\mathrm{PGF}}(t) = D \cdot \beta^2 \cdot t_{mod}(t) \cdot \exp\left(-\beta \cdot t_{mod}(t)\right) - c_{PGF_{syn}} \cdot y_{\mathrm{PGF}}(t).$$

The parameter D represents the amount of administered drug scaled to obtain the designated height of the relative level of PGF_{syn}. The parameter $c_{PGF_{syn}}$ denotes the clearance rate constant of PGF_{syn}. The modified time function t_{mod} is given as

$$t_{mod}(t) = \max(0, t - t_D).$$

The rise of PGF_{syn} is large right after dosing time and approaches zero quickly thereafter, leading to a rapid decay of the function $y_{\mathrm{PGF}}(t)$.

In Figure 2.14 it can be observe that virtual administration of $PGF_{2\alpha}$ in the early luteal stage does not lead to a decay of the CL, while at later time points of the cycle it results in an immediate decay of the responsive CL, an LH peak, and ovulation during the following follicular wave.

Figure 2.15 shows the simulation results for the follicles of six different cows during virtual administration of $PGF_{2\alpha}$. At the day of first administration (day zero), when the cows are each in a different stage of their estrous cycle, the high peaks of the curves denoting the time points of ovulation. In (a), a single dose of $PGF_{2\alpha}$ is given, which impacts the cycle of at least two cows (cow3 and cow4). In (b), a second dose is given seven days after the first dosage, now influencing the cycle of two other cows (cow1 and cow2). In (c), the second dose is given 14 days after the first dose, now influencing four cows (cow3, cow4, cow5 and cow6).

In a study performed at the institute of animal reproduction, faculty of veterinary medicine of Freie Universität Berlin, a single dose of 5 mg $PGF_{2\alpha}$ has been injected to seven cows, and plasma progesterone concentrations have been measured before and after the administration. In particular, blood has been collected every morning (8:00h) and evening (17:00h)

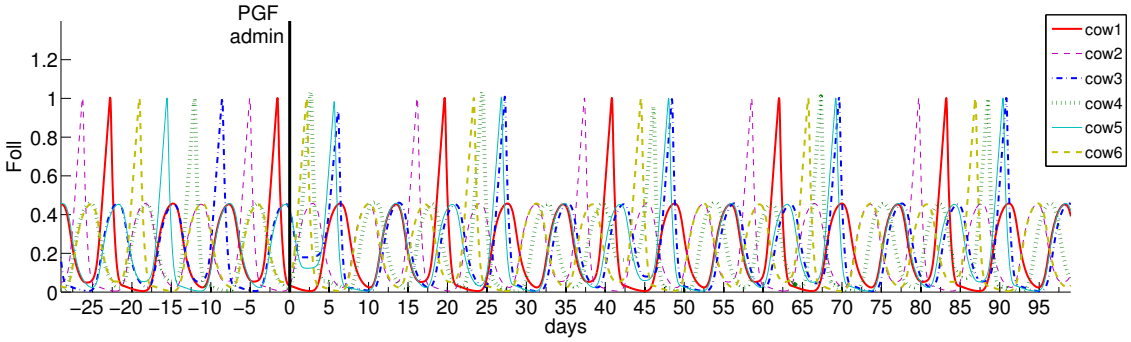

(a) Single dose application of PGF2α

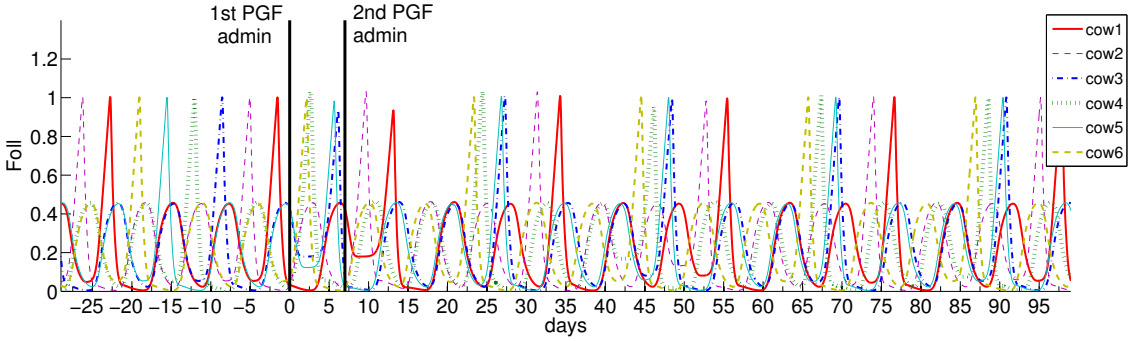

(b) Second dosage after seven days

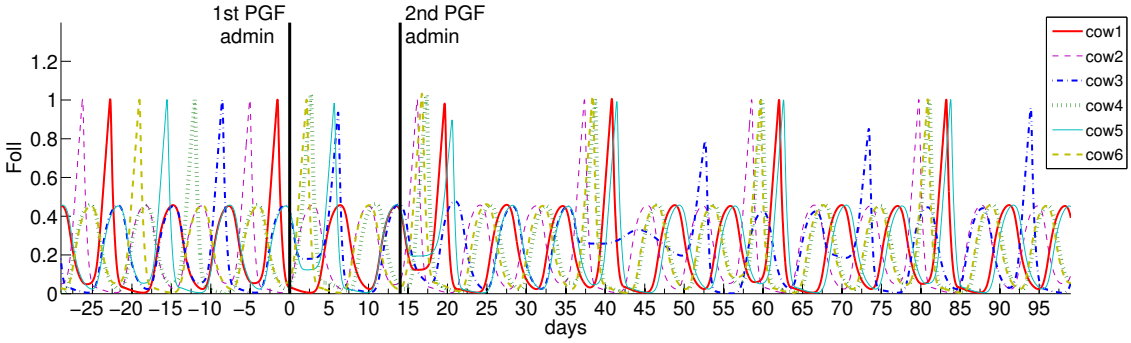

(c) Second dosage after 14 days

Figure 2.15: Simulation results for the follicles of six different cows during virtual administration of $PGF_{2\alpha}$. Day zero denotes the day of first administration.

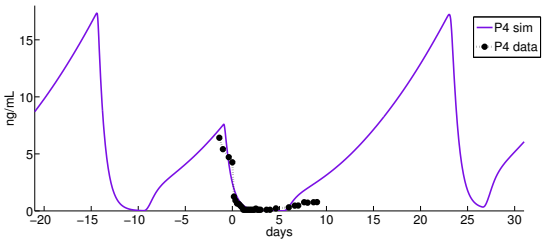

(a) Progesterone concentration

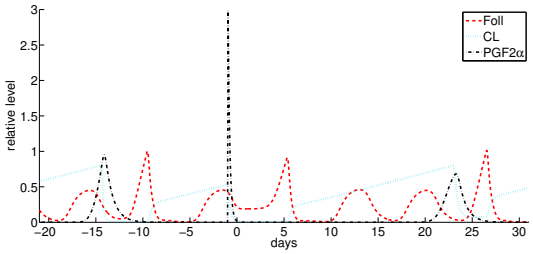

(b) Relative levels of $PGF_{2\alpha}$ and processes in the ovaries

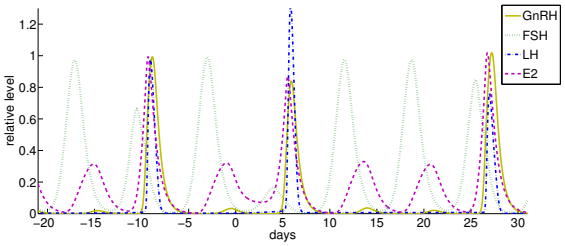

(c) Relative levels of selected other hormones

Figure 2.16: Simulation of a single dose of $PGF_{2\alpha}$ and its impact on other components of the model. Parameters have been fitted such that the simulated P4 levels match the given experimental P4 data. With the set of identified parameters, we can investigate the course of the other model components. In particular, we can observe that ovulation occurs six days after injection.

before the injection, every four hours after the injection, and twice a day after ovulation (detected by ultrasound).

Parameters have been identified so that the simulated P4 level matches the given data. Note that, here, simulated concentrations instead of relative levels for progesterone are observed. Certain parameter units therefore have to be adapted adequately. In Figure 2.16(a) an example of measured P4 concentrations for one of the examined cows is shown, together with the simulated P4 concentration. Ovulation has been detected by ultrasound a couple of days after the PG injection. This is well captured in the simulation. Not only does this approve the model of the bovine estrous cycle, the simulation also provides insight about the development of substrates that are not measured after a single $PGF_{2\alpha}$ injection. For example, in Figure 2.16(c) a GnRH peak after administration of $PGF_{2\alpha}$ can be observed, which can be understood as an increase in pulse frequency and is in the scope of expected observations.

2.4 Improved Modeling of Follicular Development

In bovine, development of follicles to ovulatory or near-ovulatory size occurs throughout the entire cycle, see [For94]. Two or three times per cycle, a cohort of primordial follicles start to grow and mature. In non-ovulatory waves, all follicles undergo atresia one after another. At which point a new cohort of follicles emerge is not clear. In BovCycle, where follicles are incorporated as follicular capacity, a new wave does not start until the previous one decayed. There is, however, evidence that a next wave already starts to grow when the previous one is still high.

In several other models on the hormonal cycle ([Har01, POK+12]), follicles are modeled as masses that pass through discrete stages of maturation. In the bovine model in this thesis, only one differential equation describes the follicular development, interpreted as follicular capacity to produce the hormones estradiol and inhibin. Simulation with the model lead to several distinct follicular waves per cycle. This is in line with data profiles from [PCK+91]. In contrast to this, more recent measurements for follicular size rather show an overlapping of the different waves ([CLEB12]). A next wave already starts to develop when the preceding one is not yet decayed. This motivates to modify the model towards the ability to simulate overlapping waves.

A dataset is available [1] that includes, amongst others, daily ultrasound measurements of the follicular diameters in 31 cows. Follicular waves can be clearly visible from the data. In every cow, several follicular waves start to grow within one cycle, mostly while other waves is still high. Examples of these follicular measurements are depicted in Figure 2.17.

[1] The dataset was kindly provided by Stephen Butler, Animal & Grassland Research and Innovation Centre, Teagasc, Moorepark, Fermoy, Co. Cork, Ireland

Consideration of only the total follicle size would not lead to conclusions regarding wave patterns, as the development of the sum of all follicular measurements over time does not significantly oscillate.

In [Boe12], parameters were fitted to a large dataset of measurements for cows. It turned out though that the model was not capable of reflecting all of the data, in particular, the measurements for follicular development. The added up follicular measurements do not match the corresponding simulation output of BovCycle, which has a distinct wave-like pattern. When adding up the waves in the dataset, they smooth out. Thus, here, an approach to modify this part of the model is presented. This modification especially captures the measurements for overlapping follicular waves.

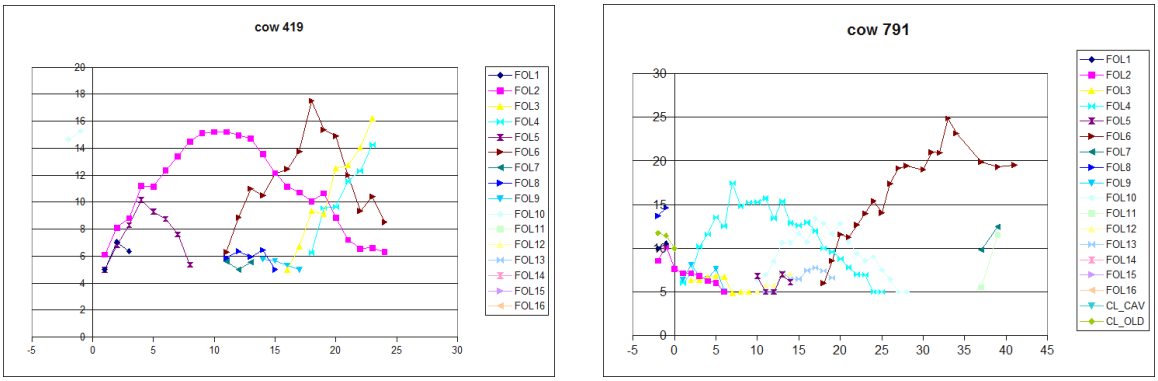

Figure 2.17: Examples of measurements for follicular diameter (mm) of two individual cows. Time units are days. When the dominant follicle of the first follicular wave is high, the next wave starts to rise.

In the new approach, a periodic solution should be obtained for each different follicular wave, which starts to decay as soon as another wave starts to emerge. As the solutions for the different waves should interact, the use of more than one ODE is an obvious possibility. This way, each wave is represented by an extra ODE. To begin with, a three wave pattern is modeled. As a new wave grows, the old wave decays, which is interpreted here as a predator-prey relationship, also named Lotka-Volterra approach. This approach originally consist of two ODEs which interact competitively, as for example described in [LS88].

The ODEs for a two-dimensional Lotka-Volterra approach are of the form

$$\begin{aligned}\frac{d}{dt}y_{\text{predator}}(t) &= \tilde{k}_1 \cdot y_{\text{predator}} - \tilde{k}_2 \cdot y_{\text{predator}} \cdot y_{\text{prey}},\\ \frac{d}{dt}y_{\text{prey}}(t) &= \tilde{k}_3 \cdot y_{\text{predator}} \cdot y_{\text{prey}} - \tilde{k}_4 \cdot y_{\text{prey}}.\end{aligned}$$

This can be extended to a three-dimensional system. Another ODE is coupled to the previous ones,

$$\begin{aligned}
\frac{d}{dt}y_{\text{Wave1}}(t) &= k_1 \cdot y_{\text{Wave1}} \cdot y_{\text{Wave3}} - k_2 \cdot y_{\text{Wave1}} \cdot y_{\text{Wave2}},\\
\frac{d}{dt}y_{\text{Wave2}}(t) &= k_3 \cdot y_{\text{Wave1}} \cdot y_{\text{Wave2}} - k_4 \cdot y_{\text{Wave2}} \cdot y_{\text{Wave3}},\\
\frac{d}{dt}y_{\text{Wave3}}(t) &= k_5 \cdot y_{\text{Wave2}} \cdot y_{\text{Wave3}} - k_6 \cdot y_{\text{Wave1}} \cdot y_{\text{Wave3}}.
\end{aligned}$$

Linking this to the rest of the model is obtained by using the model output of FSH, LH, and P4. The same mechanisms as for follicular production capacity are now used for every follicular wave. In particular, FSH stimulates the growth of the follicular waves, and P4 and LH stimulate follicular decay. Recall that the ODE describing follicular capacity was

$$\begin{aligned}
\frac{d}{dt}y_{\text{Foll}}(t) = m^{\text{Foll}}_{\text{FSH}} \cdot h^{+}\Big(y_{\text{FSH}}(t), T^{\text{Foll}}_{\text{FSH}} \cdot h^{+}\big(y_{\text{Foll}}(t), T^{\text{Foll}}_{\text{Foll}}, n^{\text{Foll}}_{\text{Foll}}\big), n^{\text{Foll}}_{\text{FSH}}\Big)\\
- \Big(H^{+}_{\text{P4,Foll}}(y_{\text{P4}}(t)) + H^{+}_{\text{LH,Foll}}(y_{\text{LH}}(t))\Big) \cdot y_{\text{Foll}}(t)
\end{aligned}$$

Follicular function had a positive self-influence on itself, included as growing FSH sensitivity as follicles rise. In the new approach, the follicular waves are interacting with each other, and another follicular self-influence is not incorporated. Instead, FSH is directly stimulating each emerging wave. This is incorporated by multiplying a stimulatory Hill function to the growth term of each wave.

In the new approach, the influence of P4 and LH is modeled as before, i.e. by multiplying positive Hill functions to the decay of each follicular wave.

The corresponding Hill functions are

$$\begin{aligned}
H^{+}_{\text{FSH,Foll}}(y_{\text{FSH}}(t)) &= m^{\text{Foll}}_{\text{FSH}} \frac{y_{\text{FSH}}(t)^2}{(T^{\text{Foll}}_{\text{FSH}})^2 + y_{\text{FSH}}(t)^2},\\
H^{+}_{\text{P4,Foll}}(y_{\text{P4}}(t)) &= m^{\text{Foll}}_{\text{P4}} \frac{y_{\text{P4}}(t)^2}{(T^{\text{Foll}}_{\text{P4}})^2 + y_{\text{P4}}(t)^2},\\
H^{+}_{\text{LH,Foll}}(y_{\text{LH}}(t)) &= m^{\text{Foll}}_{\text{LH}} \frac{y_{\text{LH}}(t)^2}{(T^{Foll}_{\text{LH}})^2 + y_{\text{LH}}(t)^2}.
\end{aligned}$$

These Hill functions are now multiplied to the growth and decay rates of the follicular waves. The ODEs for the three follicular waves become

$$\begin{aligned}
\frac{d}{dt}y_{\text{Wave1}}(t) &= H^{+}_{\text{FSH,Foll}}\big(y_{\text{FSH}}(t)\big) \cdot k_1 \cdot y_{\text{Wave1}} \cdot y_{\text{Wave3}} \\
&\quad - \Big(H^{+}_{\text{P4,Foll}}\big(y_{\text{P4}}(t)\big) + H^{+}_{\text{LH,Foll}}\big(y_{\text{LH}}(t)\big)\Big) \cdot k_2 \cdot y_{\text{Wave1}} \cdot y_{\text{Wave2}} \\
\frac{d}{dt}y_{\text{Wave2}}(t) &= H^{+}_{\text{FSH,Foll}}\big(y_{\text{FSH}}(t)\big) \cdot k_3 \cdot y_{\text{Wave1}} \cdot y_{\text{Wave2}} \\
&\quad - \Big(H^{+}_{\text{P4,Foll}}\big(y_{\text{P4}}(t)\big) + H^{+}_{\text{LH,Foll}}\big(y_{\text{LH}}(t)\big)\Big) \cdot k_4 \cdot y_{\text{Wave2}} \cdot y_{\text{Wave3}} \\
\frac{d}{dt}y_{\text{Wave3}}(t) &= H^{+}_{\text{FSH,Foll}}\big(y_{\text{FSH}}(t)\big) \cdot k_5 \cdot y_{\text{Wave2}} \cdot y_{\text{Wave3}} \\
&\quad - \Big(H^{+}_{\text{P4,Foll}}\big(y_{\text{P4}}(t)\big) + H^{+}_{\text{LH,Foll}}\big(y_{\text{LH}}(t)\big)\Big) \cdot k_6 \cdot y_{\text{Wave1}} \cdot y_{\text{Wave3}}
\end{aligned}$$

In this way, the system of three overlapping waves is regulated by the ODE model for the bovine cycle, described in equations (B1)-(B15). For the time being, the influence of the follicular waves on the rest of the system, in particular on y_{E2} and y_{Inh}, is not implemented yet.

The following parameters have been used to obtain the simulation results in Figure 2.18,

No.	Symbol	Value	Unit
p_{fw1}	k_1	1.186	1/([t][Foll])
p_{fw2}	k_2	1	1/([t][Foll])
p_{fw3}	k_3	1.056	1/([t][Foll])
p_{fw4}	k_4	1	1/([t][Foll])
p_{fw5}	k_5	0.9622	1/([t][Foll])
p_{fw6}	k_6	1	1/([t][Foll])
p_{fw7}	$T^{\text{Foll}}_{\text{FSH}}$	0.03	[FSH]
p_{fw8}	$m^{\text{Foll}}_{\text{P4}}$	1.17	[-]
p_{fw9}	$T^{\text{Foll}}_{\text{P4}}$	0.1	[P4]
p_{fw10}	$m^{\text{Foll}}_{\text{LH}}$	0.298	[-]
p_{fw11}	$T^{\text{Foll}}_{\text{LH}}$	0.02	[LH]

Prospectively, when coupling this approach to the rest of the model to fit data for the other hormones as well, different parameter values will be identified. In particular, the parameters k_2, k_4, and k_6 could have different values, as the follicular waves will probably have different decay rates.

The presented approach still needs to be coupled to the rest of the model in the way that y_{E2} and y_{Inh} will become directly dependent on the follicular waves. With the presented approach, the amplitude of the sum of the follicular waves is not always sufficiently large

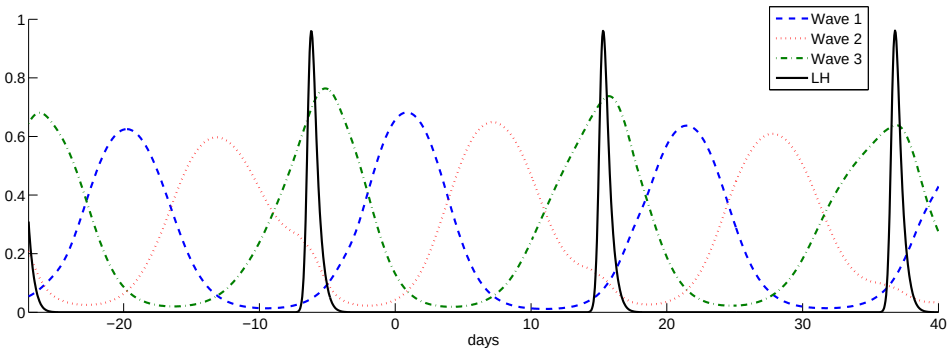

Figure 2.18: Simulation of overlapping follicular waves, influenced by FSH, LH, and P4.

for a qualitative interpretation. A possibility to make a qualitative difference of follicular function throughout the cycle would be to provide the waves with different maturation levels. Also, to validate a coupling of the follicular waves to E2 and Inh, detailed measurements for E2 and Inh will be necessary. This remodeling of the processes in the ovaries could be a task for the future, because the modeling of ovarian tissues is still raw in BovCycle. Also, the CL would then need to become directly dependent on the last follicular wave which leads to ovulation.

The next step to include more biological details into the model would be to explicitly model follicular tissue as composed of thecal and granulosa cells. These cells have different properties regarding steroid production. After ovulation, they transform to small and large luteal cells, respectively, which also have different production capacities [Goo88]. With these steps, the production of E2, Inh and P4 in the model could also become more detailed.

Chapter 3

Comparison with a Model for the Human Menstrual Cycle

In this chapter, a model that integrates the dynamics of the major substances involved in the menstrual cycle will be presented and compared to the bovine model (BovCycle). The human model, denoted as GynCycle similarly describes the development of several hormones, receptors, and follicular and luteal tissues throughout the cycle in a system of ordinary differential equations.

The physiologic and endocrine mechanisms that regulate the human menstrual cycle and the bovine estrous cycle are similar. In both humans and cows, the female endocrine system consists of several glands and regulates the periodic changes of multiple substances necessary for reproduction. In every cycle, GnRH released from the hypothalamus regulates the secretion of the hormones LH and FSH from the pituitary into the bloodstream, where they distribute and influence several functions in the body. They regulate processes in the ovaries, where follicles and corpus luteum develop. These produce steroids that are released into the blood and from therein regulate the processes in the hypothalamic-pituitary-gonadal axis.

Unlike in bovine, in humans the uterus does not play a role for the functioning of the cycle. Even in the absence of the uterus, cyclicity can proceed [MCL99]. Luteolysis, the decay of the corpus luteum, thus happens in a different way than in bovine. The hormone $PGF_{2\alpha}$, released in pulses from the uterus, is not needed for CL regression in humans.

Two different patterns of follicle development are identified in mammals. In humans (and rats and pigs), the development of follicles to ovulatory size occurs only during the *follicular phase*, which denotes the time span between luteolysis and ovulation. In contrast, in cattle (and sheep and horses), development of follicles to ovulatory or near-ovulatory size occurs throughout the cycle [For94]. The hormonal cycle of the human has a longer follicular phase, compared to the cycle of cows (and pigs, sheep and horses) ([Joh07]). In contrast, the *luteal phase*, which denotes the time span between ovulation and luteolysis, is

about 14 days in human ([Joh07]) and 17-18 days in bovine ([MSS09, TR91]). An average human menstrual cycle is about 28 days long ([Joh07]), while an average bovine cycle lasts about 21 days ([AJSM08]).

3.1 Model Background

In contrast to BovCycle, the model for the human menstrual cycle presented in this thesis is chosen not to be dimensionless. Since measurements are available from experimental studies, variables and thus parameters have been provided with physical units.

The here presented model of the human menstrual cycle is an enhancement of the model in [Rei09], which will be called *Reinecke model* in the following. The Reinecke model is based on models by Selgrade, Schlosser, and Harris ([SS99, Har01]), which will here be called the *Selgrade model*. As these models, in order to analyze the dynamic relations between the system components, it is incorporated how the multiple components function together to generate periodic solutions. Along the presentation of the model, the special emphasis in this chapter is on the differences to the bovine model.

The Reinecke model consists of 50 differential equations, three of them delay differential equations, and 201 parameters. The model describes the large feedback loop that captures the main hormonal developments within the monthly cycle in females. The feedback loop includes processes in hypothalamus, pituitary, and ovaries, connected by the blood stream. GnRH (gonadotropin releasing hormone) is generated in the hypothalamus, from where it is released in pulses into the pituitary. In the pituitary, the gonadotropins LH (luteinizing hormone) and FSH (follicle stimulating hormone) are synthesized, controlled by the hormones estradiol (E2), progesterone (P4), inhibin A and inhibin B. The latter four ones belong to the hormones that are often measured in blood. The release of the gonadotropins into the blood stream is additionally controlled by the GnRH pulses. Several publications also assume a pulse like pattern of LH and FSH, but this is not considered in the Reinecke model and will not be in this work. Once the gonadotropins LH and FSH, which complete the group of often measured substances in plasma, are in the blood, they control processes in the ovaries. In particular, they regulate the development of the folliculogenesis and luteal development. As in the preceding models of Selgrade, Schlosser, and Harris, a model was chosen for the follicles that considers several successive follicular stages that transform into one another. The follicles and luteal tissue produce steroids in the ovaries. These steroids transform into the already introduced hormones estradiol, progesterone, inhibin A, and inhibin B, which regulate synthesis and release of GnRH and the gonadotropins along the hypothalamic-pituitary-axis. A rough overview of this large feedback system is already illustrated in Figure 1.1 in Chapter 1, detailed representations will be given in the following.

For the model in this thesis, several adjustments to the Reinecke model have been made

that will be presented here. The two major changes regard the steroidogenesis in the ovaries, and the GnRH pulse generation in the hypothalamus. Both parts of the Reinecke model have been considered as too detailed for the moment. However, they still could be reintegrated if necessary, depending on the interest of model applicants.

Steroid hormones are generated from cholesterol in the thecal and granulosa cells in the follicles, as well as in the luteal cells after ovulation ([JL06]). This process, called steroidogenesis, is catalyzed by several enzymes that are activated in the follicular and luteal cells. The enzyme activation and the biosynthesis of steroid hormones in the ovaries have been modeled in detail in [Rei09]. The underlying reactions are known quite precisely from the KEGG database ([Dat06]). This large database is an approach to bundle knowledge from a large amount of experiments in a coherent way, and provides a great tool for modelers. Information from this database can be considered as validated. However, steroidogenesis is only a small element within the hormonal cycle. It describes in detail the production of the often measured steroid hormones estradiol, progesterone, and inhibin. In the Reinecke model, the activation of the enzymes, i.e. the model part before steroidogenesis, is not yet validated and potentially imprecise. It is thus the critical factor with regard to reliability and preciseness of the model. For this reason, the whole steroidogenesis is replaced by a simpler model part for the production of the steroid hormones.

In the Reinecke model, the integration of the information from the KEGG database is performed with the help of linear combinations of the different follicular and luteal stages. In contrast, in [SS99, Har01], linear combinations of these stages directly describe the development of the steroid hormones. In both the Reinecke and the Selgrade model, the coefficients within the linear combinations, i.e. the hormone production or enzyme activation rates, are not known from literature, but have in both cases been identified by parameter identification algorithms, using measurements for the steroid hormones. The numerical values for these coefficients, interpreted as production rates, stand for a black box, since several chemical reactions are not considered. In comparison with the Selgrade model, the Reinecke model reduces the black box of the ovarian hormone production. However, certain black box aspects are still present in the Reinecke model, and a similar number of coefficients is only estimated from algorithms. In this work, steroidogenesis was not a focus, and therefore an approach based on [SS99, Har01] is chosen.

The gonadotropin releasing hormone (GnRH) controls the release of the gonadotropins LH and FSH from the pituitary into the blood. It is known that a pulse-like pattern is crucial for the functioning of GnRH, and elaborate models exist to model GnRH pulse generation ([CF07, TAS$^+$07]). In the Reinecke model, a stochastic pulse generator is implemented in a sophisticated way. Pulses of stochastic GnRH masses are generated according to a known frequency, which leads to a pulsatile GnRH concentration that changes on a time scale of minutes. However, the gonadotropins LH and FSH, the only direct successors of GnRH, have not been implemented in a pulse-like manner. In contrary, in the model these substances only respond to average levels of GnRH in the pituitary, such that the pulse-like

pattern of GnRH is not necessary. Although it is known that pulses of GnRH are required in reality, taking into account the high abstraction level of the model, an elaborate pulse model does not lead to great benefit for the rest of the model. Instead, it significantly increases the simulation time. Considered as an overapproximation for the moment, the modeling approach of stochastic GnRH pulses is omitted. Instead, only pulse frequency and amount of released GnRH are computed. In the future, implementing LH and FSH also in pulses, and integrating them into the whole-body feedback loop, could require the reimplementation of an elaborate GnRH pulse generator.

Model development and extension largely depend on the application and the interest of users. Crucial for the model development is the availability of experimental data. In [RmD$^+$12], the purpose was to develop a model for GnRH receptor binding that can capture the responses after agonist and antagonist treatment. GnRH receptor binding mechanisms, as well as similar LH and FSH receptor mechanisms were included. Also, the development of follicular and luteal stages were modified. The resulting model from [RmD$^+$12] will be described in the next Section.

3.2 Numerical Model

The above described considerations led to a new model of the female menstrual cycle that will be described in the following. The model consists of 33 ODEs and 114 unknown parameters. Also, an extension of the model, a pharmacokinetic submodel, will be presented. The aim of the pharmacokinetic submodel is to capture effects that are observed after the administration of GnRH agonists and antagonists. [1]

While GnRH *agonists* act just like natural GnRH itself, GnRH *antagonists* compete with natural GnRH for receptor binding without having a direct effect on the gonadotropins. Agonists have an initial stimulating action, followed by a prolonged suppression effect on the receptors (called desensitization), while antagonists only suppress the effect of natural GnRH. Agonists are used for treatment of cancer and endometriosis, and antagonists mainly in in vitro fertilization treatments. In order to be able to simulate both agonist and antagonist treatments, developing a detailed model for the GnRH receptor mechanisms is crucial. This leads to a deeper level of detail in comparison with the BovCycle. It is assumed that the main interaction of the agonists and antagonists with the rest of the model occurs by binding to the free, unbound GnRH receptors. Before binding to the receptors, however, the agonists and antagonists are processed through the body as will be explained in the following.

[1] Note that the notation in comparison to [RmD$^+$12] has changed. Here, in line with the notation in Chapter 2, the variables, i.e., the solutions of the ODE system, are denoted as $y_{Substance}$.

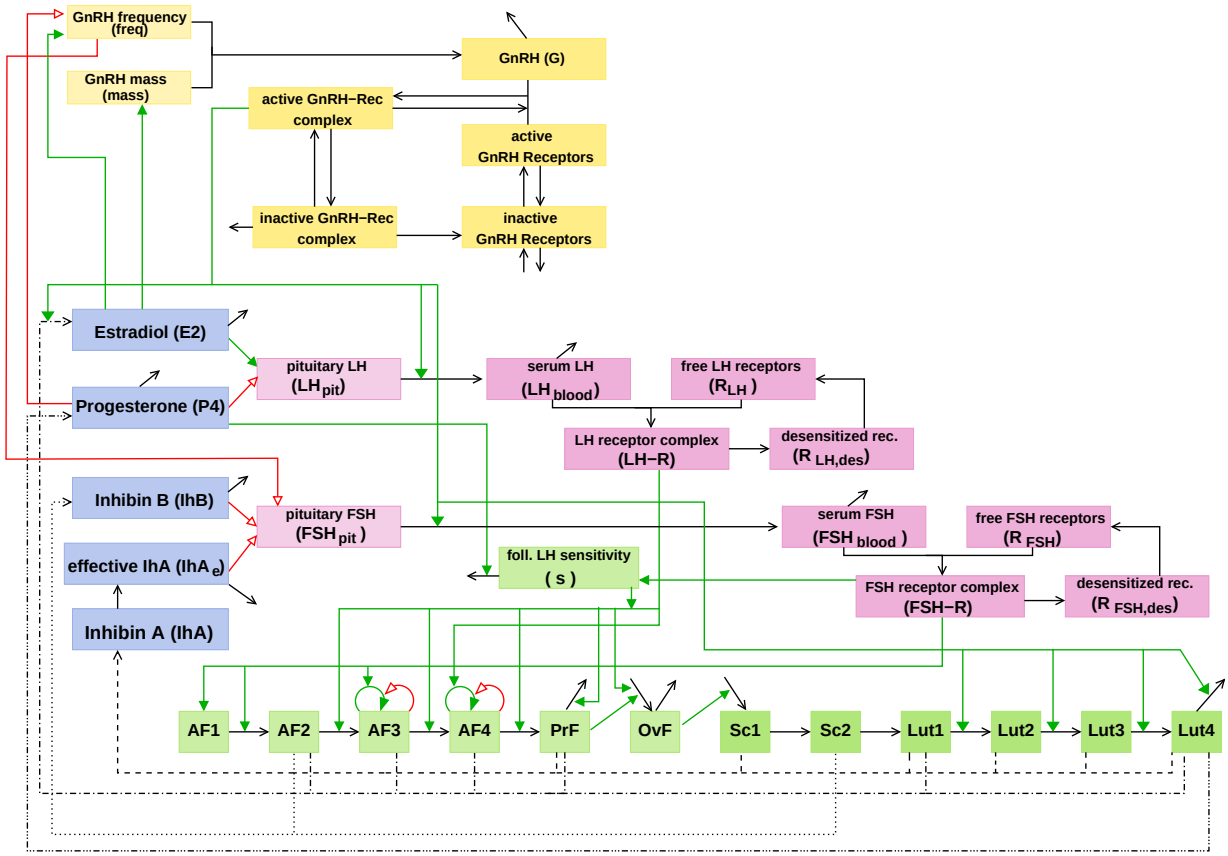

Figure 3.1: The flowchart for the model of the female menstrual cycle as presented in [RmD+12]. Each box represents a variable that is described by a differential equation, the arrows mark the mechanisms between the variables. Red and green arrows stand for inhibitory and stimulatory mechanisms, respectively, and black arrows mark transformations.

3.2.1 A Pharmacokinetic Submodel for Drug Administration

Administration of substances or drugs can be modeled via a classical pharmacokinetic compartment model, as for example described in [DGS02]. Depending on the development of the drug in the blood after dosing, a certain number of compartments are assumed which the drug passes through. These compartments do not necessarily have a direct physiological interpretation, but are used as black boxes that potentially comprise several organs or tissues. If the measured amount of the drug decreases in two phases, a distribution phase and an elimination phase, two non-physiological compartments are assumed for the drug to pass through before reaching the blood. If no such phases can be identified, one compartment is chosen to be sufficient for the drug before it reaches the blood.

For the human model GynCycle, data for the GnRH antagonist Cetrorelix is available that suggests the use of a two-compartment model, thus, additionally to a dosing compartment, the use of a central and a peripheral compartment. In the model, the drug is administered directly into a dosing compartment, from where it is transported into a central compartment. The drug in the central compartment binds to free GnRH receptors. A certain rate of the drug is always reaching a peripheral compartment, and from there transported back into the central compartment. Regarding the data of the GnRH agonist Nafarelin, the decrease of drug concentration occurs in only one phase, such that a one-compartment approach is sufficient.

The amount of antagonist in the dosing compartment is denoted as $\mathrm{Ant_D}$, in the central compartment as $\mathrm{Ant_C}$, and in the peripheral compartment as $\mathrm{Ant_P}$. Likewise, $\mathrm{Ago_D}$ denotes the amount of agonist in the dosing compartment, and $\mathrm{Ago_C}$ its amount in the central compartment. The reaction scheme for the two-compartment pharmacokinetik (PK) model for the dosing of the antagonist is

$$\mathrm{Ant_D} \xrightarrow{k_A^{\mathrm{Ant}}} \mathrm{Ant_C} \underset{k_{PC}^{\mathrm{Ant}}}{\overset{k_{CP}^{\mathrm{Ant}}}{\rightleftharpoons}} \mathrm{Ant_P} \quad , \qquad \mathrm{Ant_C} \xrightarrow{cl_{\mathrm{Ant,C}}} *,$$

and the reaction scheme via a one-compartment PK model for the agonist is

$$\mathrm{Ago_D} \xrightarrow{k_A^{\mathrm{Ago}}} \mathrm{Ago_C} \xrightarrow{k_{cl}^{\mathrm{Ago,C}}} *.$$

The $*$ represents a component without feedback to the rest of the system, which is neglected during the simulation. At the time points of dosing, the drug is administered directly into the dosing compartment, from where it is absorbed linearly into the central compartment. From the central compartment, the drug binds reversibly to free, active GnRH receptors (denoted RG), building a ligand-receptor complex (denoted (Ago-RG) and (Ant-RG)),

$$\mathrm{Ago_C} + \mathrm{RG} \underset{k_{off}^{\mathrm{Ago}}}{\overset{k_{on}^{\mathrm{Ago}}}{\rightleftharpoons}} \text{(Ago-RG)}, \quad \mathrm{Ant_C} + \mathrm{RG} \underset{k_{off}^{\mathrm{Ant}}}{\overset{k_{on}^{\mathrm{Ant}}}{\rightleftharpoons}} \text{(Ant-RG)}.$$

It is assumed that only a part of the drug in the central compartment is available for protein binding. Thus, the amount of agonist (and accordingly antagonist) that is reaching the central compartment from the dosing compartment is multiplied with the fraction unbound in plasma, f_u^{Ago} and f_u^{Ant}, respectively, known from literature for the administered drug. The amount of drug in every compartment is described in an ODE, which leads to the ODEs:

$$\frac{d}{dt}y_{\text{Ant,D}}(t) = -k_A^{\text{Ant}} \cdot y_{\text{Ant,D}}(t) \tag{PK1}$$

$$\begin{aligned}\frac{d}{dt}y_{\text{Ant,C}}(t) = {} & k_A^{\text{Ant}} \cdot y_{\text{Ant,D}}(t) \cdot f_u^{\text{Ant}} - k_{cl}^{\text{Ant,C}} \cdot y_{\text{Ant,C}}(t) \\ & - k_{CP}^{\text{Ant}} \cdot y_{\text{Ant,C}}(t) + k_{PC}^{\text{Ant}} \cdot y_{\text{Ant,P}}(t) \\ & - k_{on}^{\text{Ant}} \cdot y_{\text{RG}}(t) \cdot y_{\text{Ant,C}}(t) + k_{off}^{\text{Ant}} \cdot y_{\text{(Ant-RG)}}(t)\end{aligned} \tag{PK2}$$

$$\frac{d}{dt}y_{\text{Ant,P}}(t) = k_{CP}^{\text{Ant}} \cdot y_{\text{Ant,C}}(t) - k_{PC}^{\text{Ant}} \cdot y_{\text{Ant,P}}(t) \tag{PK3}$$

$$\frac{d}{dt}y_{\text{Ago,D}}(t) = -k_A^{\text{Ago}} \cdot y_{\text{Ago,D}}(t) \tag{PK4}$$

$$\begin{aligned}\frac{d}{dt}y_{\text{Ago,C}}(t) = {} & k_A^{\text{Ago}} \cdot y_{\text{Ago,D}}(t) \cdot f_u^{\text{Ago}} - k_{cl}^{\text{Ago,C}} \cdot y_{\text{Ago,C}}(t) \\ & - k_{on}^{\text{Ago}} \cdot y_{\text{RG}}(t) \cdot y_{\text{Ago,C}}(t) + k_{off}^{\text{Ago}} \cdot y_{\text{(Ago-RG)}}(t)\end{aligned} \tag{PK5}$$

With these ODEs, drug administration can be simulated by adding the dosing amount to $y_{\text{Ago,D}}$ or $y_{\text{Ant,D}}$, respectively. For identification of the unknown parameters that occur in the ODEs (PK1)-(PK5), a possibility to get good starting values is to first fit the uncoupled equations (PK1)-(PK5) to measured agonist and antagonist concentrations. Afterwards, after connecting the above equations to the rest of the model, parameters need to be reestimated with the help of measurements for other substances, that are taken after the dosing time.

3.2.2 GnRH and its Receptor Binding Mechanisms

The coupling of the PK submodel to the rest of the model occurs via reaction-rate equations, as described in Section 1.2. The drug in the central compartment reversibly binds to free, active GnRH receptors. A model of these mechanisms thus requires an elaborate receptor model for GnRH. This implies a new level of detail that has not yet been considered in BovCycle. The receptor binding mechanisms take place on a cellular level, the coupling to the rest of the model on a whole-organism level needs to be done accurately.

Before going into the cellular level, an ODE for the amount of GnRH in the pituitary, representing unbound GnRH proteins, is derived.

Elaborate models for GnRH pulsatility are available, but as in the BovCycle, such detailed mechanisms are not considered for the moment. As GnRH pulses act on a much smaller time scale than the rest of the model, including them would significantly increase the simulation time without great benefit. However, for humans there exists more knowledge on GnRH pulse frequency and pulse sizes. As in bovine, GnRH is synthesized in the hypothalamus and released in pulses into the pituitary. GnRH in the hypothalamus is not explicitly modeled with an ODE as in the bovine model. Instead, two continuous functions are derived: The function $freq : t \to \mathbb{R}$ represents the pulse frequency and another function $mass : t \to \mathbb{R}$ accounts for the amount of released GnRH mass. Both functions are defined via the mechanisms of E2 and P4 on GnRH which are derived as follows: GnRH frequency is inhibited by P4 and stimulated by E2 [CBB02, SJO72, Hal09]. While the GnRH pulse mass is inhibited at low E2 concentrations [EDGK94], it is assumed that E2 is stimulatory at high concentrations, when it induces the GnRH surge [CM10]. This leads to the following functions *freq* and *mass*,

$$\begin{aligned} freq(t) &= H^{-}_{\mathrm{P4},freq}(y_{\mathrm{P4}}(t)) \cdot (1 + H^{+}_{\mathrm{E2},freq}(y_{\mathrm{E2}}(t))), \\ mass(t) &= H^{+}_{E2,mass}(y_{\mathrm{E2}}(t)). \end{aligned}$$

These functions represent an average pulse behavior that changes on a time scale of days. Together, they account for the release of GnRH into the pituitary: The rate of unbound GnRH reaching the pituitary is $k_G \cdot mass(t) \cdot freq(t)$.

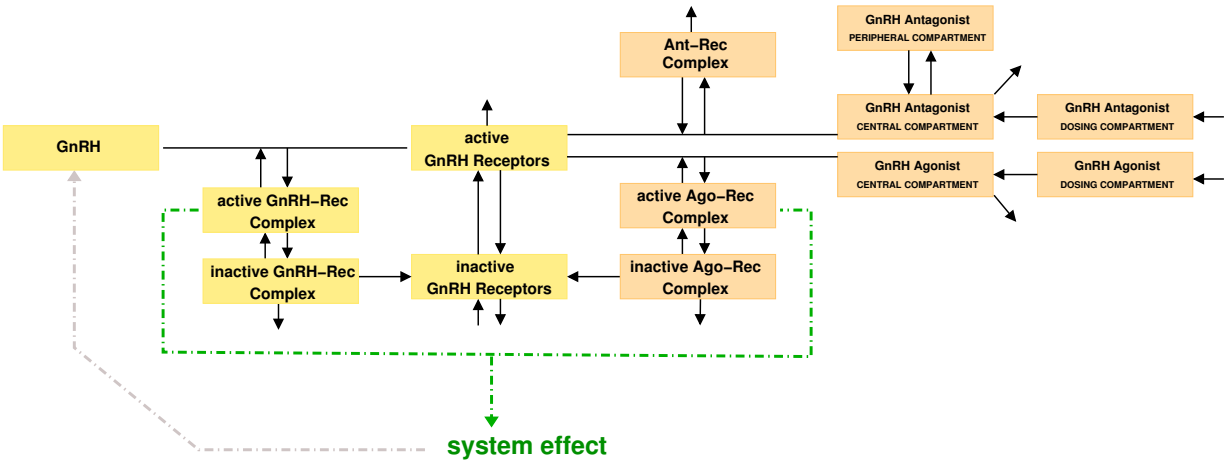

Figure 3.2: GnRH receptor mechanisms with coupled PK model for GnRH agonist and antagonist administration

GnRH receptor binding is described via the following mechanisms: In the pituitary, the GnRH receptors available for binding, denoted RG, are assumed to be on the cell surface.

A pool of inactive GnRH receptors RG$*$ is assumed to be inside the cell, not available for binding. Deactivation of active receptors, i.e. internalization into the cell, and recycling of inactive receptors to become active, occurs permanently with rates k_{inter}^{RG} and k_{recy}^{RG}, respectively. The amount of GnRH released from the hypothalamus binds via a reversible reaction to its free receptors on the cell surface, forming an active GnRH-receptor-complex (G-RG), which also lies on the cell surface. As the free receptors, the bound complex is also permanently inactivated and activated, with rates $k_{act}^{(\mathrm{G\text{-}RG})}$ and $k_{inact}^{(\mathrm{G\text{-}RG})}$, respectively. Inside the cell, a certain amount of the inactive complex (G-RG)* is degraded, another part irreversibly dissociates into the cell, forming new inactive GnRH receptors, RG$*$, in the pool. Apart from the mentioned recycling to become active, inactive receptors degrade with rate k_{degr}^{RG}. New inactive receptors are not only formed from the mentioned internalization of RG, but are also permanently synthesized in the cell with rate k_{syn}^{RG}.

The model is a reduced version of the EGFR system as presented in [KKKH09], merging the there supposed three components for the ligand-receptor-complex inside the cell, the degraded ligand-receptor-complex and the degraded ligand (here: GnRH) into one term in our model: the degradation of the GnRH-receptor-complex.

The above described reaction scheme is:

$$\mathrm{G} + \mathrm{RG} \underset{k_{off}^{G}}{\overset{k_{on}^{G}}{\rightleftharpoons}} (\mathrm{G\text{-}RG}) \quad , \qquad \mathrm{G} \xrightarrow{k_{degr}^{G}} * \quad ,$$

$$(\mathrm{G\text{-}RG}) \underset{k_{inact}^{(\mathrm{G\text{-}RG})}}{\overset{k_{act}^{(\mathrm{G\text{-}RG})}}{\rightleftharpoons}} (\mathrm{G\text{-}RG})^* \quad , \qquad (\mathrm{G\text{-}RG})^* \xrightarrow{k_{degr}^{(\mathrm{G\text{-}RG})}} * \quad ,$$

$$\mathrm{RG} \underset{k_{inter}^{\mathrm{RG}}}{\overset{k_{recy}^{\mathrm{RG}}}{\rightleftharpoons}} \mathrm{RG}* \quad , \qquad \mathrm{RG}* \underset{k_{syn}^{\mathrm{RG}}}{\overset{k_{degr}^{\mathrm{RG}}}{\rightleftharpoons}} * \quad ,$$

$$(\mathrm{G\text{-}RG})^* \xrightarrow{k_{diss}^{(\mathrm{G\text{-}RG})}} \mathrm{RG}* \quad .$$

The corresponding differential equations are:

$$\begin{aligned}
\frac{d}{dt}y_{\mathrm{G}}(t) &= k_G \cdot mass(t) \cdot freq(t) - k_{on}^{G} \cdot y_{\mathrm{G}}(t) \cdot y_{\mathrm{RG}}(t) \\
&\quad + k_{off}^{G} \cdot y_{(\text{G-RG})}(t) - k_{degr}^{G} \cdot y_{\mathrm{G}}(t) && \text{(H1)} \\
\frac{d}{dt}y_{\mathrm{RG}}(t) &= k_{off}^{G} \cdot y_{(\text{G-RG})}(t) - k_{on}^{G} \cdot y_{\mathrm{G}}(t) \cdot y_{\mathrm{RG}}(t) \\
&\quad - k_{inter}^{\mathrm{RG}} \cdot y_{\mathrm{RG}}(t) + k_{recy}^{\mathrm{RG}} \cdot y_{\mathrm{RG}^*}(t) && \text{(H2)} \\
\frac{d}{dt}y_{\mathrm{RG}^*}(t) &= k_{diss}^{(\text{G-RG})} \cdot y_{(\text{G-RG})^*}(t) + k_{inter}^{\mathrm{RG}} \cdot y_{\mathrm{RG}}(t) - k_{recy}^{\mathrm{RG}} \cdot y_{\mathrm{RG}^*}(t) \\
&\quad + k_{syn}^{\mathrm{RG}} - k_{degr}^{\mathrm{RG}} \cdot y_{\mathrm{RG}^*}(t) && \text{(H3)} \\
\frac{d}{dt}y_{(\text{G-RG})}(t) &= k_{on}^{G} \cdot y_{\mathrm{G}}(t) \cdot y_{\mathrm{RG}}(t) - k_{off}^{G} \cdot y_{(\text{G-RG})}(t) \\
&\quad - k_{inact}^{(\text{G-RG})} \cdot y_{(\text{G-RG})}(t) + k_{act}^{(\text{G-RG})} \cdot y_{(\text{G-RG})^*}(t) && \text{(H4)} \\
\frac{d}{dt}y_{(\text{G-RG})^*}(t) &= k_{inact}^{(\text{G-RG})} \cdot y_{(\text{G-RG})}(t) - k_{act}^{(\text{G-RG})} \cdot y_{(\text{G-RG})^*}(t) \\
&\quad - k_{degr}^{\mathrm{RG}} \cdot y_{(\text{G-RG})^*} - k_{diss}^{\mathrm{RG}} \cdot y_{\mathrm{RG}^*}(t) && \text{(H5)}
\end{aligned}$$

Having derived a detailed GnRH receptor binding scheme, the agonist and antagonist mechanisms can now be coupled to the model. Both substances bind via a reversible reaction to the free GnRH receptors on the cell surface, RG, and form a complex, (Ago-RG) or (Ant-RG), respectively. The difference between agonists and antagonists is in the function of the bound complex:

- The bound antagonists (Ant-RG) have no effect on the rest of the model, they only block the free GnRH receptors and partly degrade. In the model, no difference is made concerning the activeness of the complex.

- In contrast, the bound agonists (Ago-RG) act in the same way on the on the rest of the model as the GnRH-Receptor complex itself. Also, the receptor mechanisms are chosen to be the same as for GnRH. This means that there is a permanent inactivation and activation between the complex on the inside and on the surface of the cell with the rates $k_{act}^{(\text{Ago-RG})}$ and $k_{inact}^{(\text{Ago-RG})}$, respectively. As with (G-RG)*, a certain amount of the inactive complex (Ago-RG)* is degraded, and another part dissociates to form new inactive GnRH receptors, RG$*$, in the pool.

The reaction scheme is:

$$\begin{aligned}
&\mathrm{Ant_C} + \mathrm{RG} \underset{k_{off}^{\mathrm{Ant}}}{\overset{k_{on}^{\mathrm{Ant}}}{\rightleftharpoons}} \text{(Ant-RG)} \quad , \quad \text{(Ant-RG)} \xrightarrow{k_{degr}^{\mathrm{Ant}}} * \quad , \\
&\mathrm{Ago_C} + \mathrm{RG} \underset{k_{off}^{\mathrm{Ago}}}{\overset{k_{on}^{\mathrm{Ago}}}{\rightleftharpoons}} \text{(Ago-RG)} \quad , \\
&\text{(Ago-RG)} \underset{k_{inact}^{\text{(G-RG)}}}{\overset{k_{act}^{\text{(G-RG)}}}{\rightleftharpoons}} \text{(Ago-RG)*} \quad , \quad \text{(Ago-RG)*} \xrightarrow{k_{degr}^{\text{(Ago-RG)}}} * \quad , \\
&\text{(Ago-RG)*} \xrightarrow{k_{diss}^{\text{(Ago-RG)}}} \mathrm{RG}* \quad .
\end{aligned}$$

The development of the bound antagonist, as well as of the active and inactive agonist-receptor complexes are thus calculated as:

$$\begin{aligned}
\frac{d}{dt} y_{\text{(Ant-RG)}}(t) &= k_{on}^{\mathrm{Ant}} \cdot y_{\mathrm{RG}}(t) \cdot y_{\mathrm{Ant,C}}(t) \\
&\quad - k_{off}^{\mathrm{Ant}} \cdot y_{\text{(Ant-RG)}}(t) - k_{degr}^{\mathrm{Ant}} \cdot y_{\text{(Ant-RG)}}(t) \qquad \text{(PK6)} \\
\frac{d}{dt} y_{\text{(Ago-RG)}}(t) &= k_{on}^{\mathrm{Ago}} \cdot y_{\mathrm{RG}}(t) \cdot y_{\mathrm{Ago,C}}(t) - k_{off}^{\mathrm{Ago}} \cdot y_{\text{(Ago-RG)}}(t) \\
&\quad + k_{act}^{\mathrm{Ago}} \cdot y_{\text{(Ago-RG)*}}(t) - k_{inact}^{\mathrm{Ago}} \cdot y_{\text{(Ago-RG)}}(t) \qquad \text{(PK7)} \\
\frac{d}{dt} y_{\text{(Ago-RG)*}}(t) &= -k_{act}^{\mathrm{Ago}} \cdot y_{\text{(Ago-RG)*}}(t) + k_{inact}^{\mathrm{Ago}} \cdot y_{\text{(Ago-RG)}}(t) \\
&\quad - k_{diss}^{\mathrm{Ago}} \cdot y_{\text{(Ago-RG)*}}(t) - k_{degr}^{\mathrm{Ago}} \cdot y_{\text{(Ago-RG)*}}(t) \qquad \text{(PK8)}
\end{aligned}$$

The agonist and antagonist reversibly bind to free GnRH receptors on the cell surface, and inactive GnRH receptors are formed from the agonist-receptor complex inside the cell. Therefore, equations $(H2)$ and $(H3)$ have to be adjusted. They become

$$\begin{aligned}
\frac{d}{dt} y_{\mathrm{RG}}(t) &= k_{off}^{G} \cdot y_{\text{(G-RG)}}(t) - k_{on}^{G} \cdot y_{\mathrm{G}}(t) \cdot y_{\mathrm{RG}}(t) \\
&\quad - k_{inter}^{\mathrm{RG}} \cdot y_{\mathrm{RG}}(t) + k_{recy}^{\mathrm{RG}} y_{\mathrm{RG*}}(t) \\
&\quad - k_{on}^{\mathrm{Ago}} \cdot y_{\mathrm{Ago,C}}(t) \cdot y_{\mathrm{RG}}(t) + k_{off}^{\mathrm{Ago}} \cdot y_{\text{(Ago-RG)}}(t) \\
&\quad - k_{degr}^{\mathrm{Ago}} \cdot y_{\mathrm{Ant,C}}(t) \cdot y_{\mathrm{RG}}(t) + k_{off}^{\mathrm{Ant}} \cdot y_{\text{(Ant-RG)}}(t), \qquad \text{(H2a)} \\
\frac{d}{dt} y_{\mathrm{RG*}}(t) &= k_{diss}^{\text{(G-RG)}} \cdot y_{\text{(G-RG)*}}(t) - k_{back}^{\text{(G-RG)}} y_{\mathrm{RG*}}(t) \\
&\quad + k_{inter}^{\mathrm{RG}} \cdot y_{\mathrm{RG}}(t) - k_{recy}^{\mathrm{RG}} y_{\mathrm{RG*}}(t) \\
&\quad + k_{syn}^{\mathrm{RG}} - k_{degr}^{\mathrm{RG}} \cdot y_{\mathrm{RG*}}(t) + k_{diss}^{\mathrm{Ago}} \cdot y_{\text{(Ago-RG)*}}(t). \qquad \text{(H3a)}
\end{aligned}$$

The effect of the agonist-receptor-complex is added to the effect GnRH-receptor complex wherever it appears. In particular, the release of the gonadotropins Rel_{LH}, Rel_{FSH}, and the

development of the corpus luteum are directly affected by GnRH agonist administration. All other components of the system are indirectly influenced.

These GnRH mechanisms are validated with experimental data from agonist and antagonists studies as will be presented in the next section. The same GnRH mechanisms could also be used for BovCycle, as soon as detailed GnRH mechanisms become interesting for modelers.

3.2.3 The Gonadotropins LH and FSH

As GnRH, the gonadotropins LH and FSH also occur in a pulsatile manner, but pulsatility, as e.g. modeled in [ZWG03], is not included in the model for the moment. Instead, average levels of the gonadotropins are considered.

The development of LH and FSH is regulated by similar mechanisms as in the bovine model. In the same manner as in BovCycle, LH and FSH in GynCycle occur in the two compartments pituitary and blood. They are synthesized in the pituitary and released into the blood. In the model, the ODEs describing their development over time are - also as in BovCycle - specified via synthesis-release relationships as described in Section 1.2. In contrast to BovCycle, receptor binding mechanisms are included for both LH and FSH in the blood.

As in BovCycle, LH synthesis in the pituitary is stimulated by E2 and inhibited by P4 [SS99]. However, there are differences regarding the interaction of the P4 and E2 mechanisms with each other, and that there is a constant LH synthesis assumed. The release of LH from the pituitary into the blood is identical to the bovine model: LH release is mainly stimulated by GnRH, i.e. by the active bound GnRH-receptor complex, and additionally, if present, by the active bound agonist-receptor complex. Inspired by [HKM98], there is a also small constant release rate of LH into the blood ($b_{\mathrm{LH}_{Rel}}$). In contrast to the dimensionless bovine model, a parameter V_{blood} is used here that corresponds to the blood volume. From the blood, unbound LH is on the one hand cleared constantly with rate constant cl_{LH}, and on the other hand binds to free LH receptors with rate constant k_{on}^{LH}. This leads to the ODEs:

$$
\begin{aligned}
Syn_{\mathrm{LH}}(t) &= \left(b_{Syn}^{\mathrm{LH}} + H^{+}_{\mathrm{E2,LH}}(y_{\mathrm{E2}}(t)\right) \cdot H^{-}_{\mathrm{P4,LH}}(y_{\mathrm{P4}}(t)) \\
Rel_{\mathrm{LH}}(t) &= \left(b_{Rel}^{\mathrm{LH}} + H^{+}_{\mathrm{(G\text{-}RG),LH}}\left(y_{\mathrm{(G\text{-}RG)}}(t) + y_{\mathrm{(Ago\text{-}RG)}}(t)\right)\right) \cdot y_{\mathrm{LHp}}(t) \\
\frac{d}{dt} y_{\mathrm{LHp}}(t) &= Syn_{\mathrm{LH}}(t) - Rel_{\mathrm{LH}}(t) \qquad \text{(H6)} \\
\frac{d}{dt} y_{\mathrm{LH}}(t) &= \frac{1}{V_{\mathrm{blood}}} \cdot Rel_{\mathrm{LH}}(t) - \left(k_{on}^{\mathrm{LH}} \cdot y_{\mathrm{RL}}(t) + cl_{\mathrm{LH}}\right) \cdot y_{\mathrm{LH}}(t) \qquad \text{(H7)}
\end{aligned}
$$

FSH mechanisms in the human model differ from the ones in the cow model, though, in both models, FSH synthesis is inhibited by inhibin and its release is stimulated by GnRH. However, the human model GynCycle does not have additional influences of P4 and E2 on FSH release as the bovine model, and it takes into account GnRH influences on FSH synthesis. Another difference between the two models comes from the modeling of inhibin.

In the human model in this thesis, in contrast to the bovine model, a difference is made between inhibin A and inhibin B In BovCycle, only inhibin A is considered as it is the predominant form in bovine follicular fluid. In the former models for the human menstrual cycle, [Har01] and [Rei09], only one inhibin is included. Later, in [Pas08], a multiple inhibin model is presented. This serves as a basis for the modeling of inhibin in this thesis which will be described further down. FSH synthesis (Syn_{FSH}) is inhibited by inhibin A and B ([GIO^{+}96, HHBC98, MCD^{+}90, SJA^{+}00]), and stimulated by low GnRH frequencies.

In [Pas08], the effects of both inhibin A and inhibin B are included with delays into the FSH mechanism. The delay of inhibin A is 2.5 days, while the delay of inhibin B is only 1 day. These delays are free parameters in the model of [Pas08], and sensitivity analysis therein shows a low sensitivity of the delay of inhibin B on the rest of the model. With the help of techniques described in Section 1.2, the delay of inhibin B can be omitted. For inhibin A, an effect compartment is introduced. Inhibin A in the effect compartment is regarded as being the downstream of inhibin A produced in the ovaries. As a result, to omit an explicit delay for a y_{IhA}, it is transformed into y_{IhAe}, which then goes into the equation for FSH without delay. This accounts for the former explicitly modeled delayed effect of inhibin A.

As in BovCycle, there is a small constant release rate of FSH into the blood (b_{FSH}), but the release is mainly stimulated by the GnRH-receptor complex and additionally - if present - by the agonist-receptor complex. From the blood, unbound FSH is cleared constantly with rate constant cl_{FSH} or binds to free FSH receptors with rate constant k_{on}^{FSH}. The ODEs for FSH are thus:

$$Syn_{\mathrm{FSH}}(t) = \frac{1}{1 + \left(\frac{y_{\mathrm{IhAe}}(t)}{T_{\mathrm{IhAe}}}\right)^{n_{\mathrm{IhAe}}} + \left(\frac{y_{\mathrm{IhB}}(t)}{T_{\mathrm{IhB}}}\right)^{n_{\mathrm{IhB}}}} \cdot H^{-}_{freq,\mathrm{P4}}(freq(t))$$

$$Rel_{\mathrm{FSH}}(t) = \left(b_{\mathrm{FSH}_{Rel}} + H^{+}_{(\mathrm{G\text{-}RG}),\mathrm{FSH}}(y_{(\mathrm{G\text{-}RG})}(t) + y_{(\mathrm{Ago\text{-}RG})}(t))\right) \cdot y_{\mathrm{FSHp}}(t)$$

$$\frac{d}{dt}y_{\mathrm{FSHp}}(t) = Syn_{\mathrm{FSH}}(t) - Rel_{\mathrm{FSH}}(t) \tag{H8}$$

$$\frac{d}{dt}y_{\mathrm{FSH}}(t) = \frac{1}{V_{\mathrm{blood}}} \cdot Rel_{\mathrm{FSH}}(t) - \left(k^{\mathrm{FSH}}_{on} \cdot y_{\mathrm{RF}}(t) + cl_{\mathrm{FSH}}\right) \cdot y_{\mathrm{FSH}}(t) \tag{H9}$$

LH and FSH receptor binding mechanisms are assumed to be similar. The FSH receptor recycling as modeled in [CMS+01] is taken and incorporated into the model for both substances. The mechanisms are described by the chemical reaction kinetics

$$\begin{aligned}
\mathrm{LH} + \mathrm{RL} &\xrightarrow{k^{\mathrm{LH}}_{on}} (\mathrm{LH\text{-}RL}) \quad , \quad \mathrm{FSH} + \mathrm{RF} \xrightarrow{k^{\mathrm{FSH}}_{on}} (\mathrm{FSH\text{-}RF}),\\
(\mathrm{LH\text{-}RL}) &\xrightarrow{k^{\mathrm{LH}}_{des}} \mathrm{RL_{des}} \quad , \quad (\mathrm{FSH\text{-}RF}) \xrightarrow{k^{\mathrm{FSH}}_{des}} \mathrm{RF_{des}},\\
\mathrm{RL_{des}} &\xrightarrow{k^{\mathrm{LH}}_{recy}} \mathrm{RL} \quad , \quad \mathrm{RF_{des}} \xrightarrow{k^{\mathrm{FSH}}_{recy}} \mathrm{RF}.
\end{aligned}$$

The corresponding differential equations for LH and FSH receptor binding are:

$$\frac{d}{dt}y_{\mathrm{RL}}(t) = k^{\mathrm{LH}}_{recy} \cdot y_{\mathrm{RLdes}}(t) - k^{\mathrm{LH}}_{on} \cdot y_{\mathrm{LH}}(t) \cdot y_{\mathrm{RL}}(t) \tag{H10}$$

$$\frac{d}{dt}y_{(\mathrm{LH\text{-}RL})}(t) = k^{\mathrm{LH}}_{on} \cdot y_{\mathrm{LH}}(t) \cdot y_{\mathrm{RL}}(t) - k^{\mathrm{LH}}_{des} \cdot y_{(\mathrm{LH\text{-}RL})}(t) \tag{H11}$$

$$\frac{d}{dt}y_{\mathrm{RLdes}}(t) = k^{\mathrm{LH}}_{des} \cdot y_{(\mathrm{LH\text{-}RL})}(t) - k^{\mathrm{LH}}_{recy}(t) \cdot y_{\mathrm{RLdes}}(t) \tag{H12}$$

$$\frac{d}{dt}y_{\mathrm{RF}}(t) = k^{\mathrm{FSH}}_{recy} \cdot y_{\mathrm{RFdes}}(t) - k^{\mathrm{FSH}}_{on} \cdot y_{\mathrm{FSH}}(t) \cdot y_{\mathrm{RF}}(t) \tag{H13}$$

$$\frac{d}{dt}y_{(\mathrm{FSH\text{-}RF})}(t) = k^{\mathrm{FSH}}_{on} \cdot y_{\mathrm{FSH}}(t) \cdot y_{\mathrm{RF}}(t) - k^{\mathrm{FSH}}_{des} \cdot y_{(\mathrm{FSH\text{-}RF})}(t) \tag{H14}$$

$$\frac{d}{dt}y_{\mathrm{RFdes}}(t) = k^{\mathrm{FSH}}_{des} \cdot y_{(\mathrm{FSH\text{-}RF})}(t) - k^{\mathrm{FSH}}_{recy} \cdot y_{\mathrm{RFdes}}(t) \tag{H15}$$

3.2.4 The Processes in the Ovaries: Follicular and Luteal Development

The processes in the ovaries are modeled in a different approach than in the bovine model. In BovCycle, follicular and luteal function are modeled each in one ODE. Thus, two ODEs - representing the capacity of the follicles and the corpus luteum to produce ovarian hormones - comprise all considered effects in the ovaries. A variety of other approaches have been used in the past to model follicles and corpus luteum, as has been discussed in [Rei09].

In GynCycle, follicular and luteal functions are modeled in several discrete stages, each of them described by a differential equation. This approach is adopted from [Rei09, Pas08]. Every stage has both its characteristic development and its hormone production. In the first stage, follicular growth is initiated by bound FSH. Then, transition from one follicular stage to the next is stimulated by bound LH and/or FSH.

With increasing size, stimulated by FSH, the follicles evolve LH-receptors on the granulosa cells, thus becoming more sensitive to LH, which stimulates their decay. The LH receptors disappear with the development of the corpus luteum. A new component $y_{\mathrm{s}}(t)$ is introduced that represents the LH sensitivity of the follicles,

$$\frac{d}{dt}y_{\mathrm{s}}(t) = H^{+}_{\mathrm{FSH,s}}\left(y_{(\mathrm{FSH\text{-}RF})}(t)\right) - H^{+}_{\mathrm{P4,s}}\left(y_{\mathrm{P4}}(t)\right) \cdot y_{\mathrm{s}}(t). \tag{H16}$$

All LH dependent transition rates between different follicular stages are now multiplied with the LH sensitivity $y_{\mathrm{s}}(t)$.

The corpus luteum starts to develop under the condition that there is an LH peak and the follicles are already large enough for ovulation. Therefore an ovulatory follicle OvF only develops when the preovulatory follicle PrF is large enough. To make the ovulatory scar Sc1 independent from the size of the ovulatory follicle OvF, its growth only depends on OvF via a Hill function. Furthermore, the transitions between different luteal stages are stimulated by the GnRH-receptor complex and the agonist-receptor complex, respectively. This modification became necessary to account for a truncated luteal phase after agonist administration in the late luteal phase.

Summarizing, the equations for the twelve follicular and luteal stages are:

$$\frac{d}{dt}y_{\mathrm{AF1}}(t) = H^{+}_{\mathrm{FSH,AF1}}\left(y_{(\text{FSH-RF})}(t)\right) - k^{\mathrm{AF2}}_{\mathrm{AF1}} \cdot y_{(\text{FSH-RF})}(t) \cdot y_{\mathrm{AF1}}(t) \tag{H17}$$

$$\frac{d}{dt}y_{\mathrm{AF2}}(t) = k^{\mathrm{AF2}}_{\mathrm{AF1}} \cdot y_{(\text{FSH-RF})}(t) \cdot y_{\mathrm{AF1}}(t) - k^{\mathrm{AF3}}_{\mathrm{AF2}} \cdot \left(\frac{y_{(\text{LH-RL})}(t)}{\mathrm{SF}_{(\text{LH-RL})}}\right)^{n^{\mathrm{AF3}}_{\mathrm{AF2}}} \cdot y_{\mathrm{s}}(t) \cdot y_{\mathrm{AF2}}(t) \tag{H18}$$

$$\begin{aligned}\frac{d}{dt}y_{\mathrm{AF3}}(t) = {} & k^{\mathrm{AF3}}_{\mathrm{AF2}} \cdot \left(\frac{y_{(\text{LH-RL})}(t)}{\mathrm{SF}_{(\text{LH-RL})}}\right)^{n^{\mathrm{AF3}}_{\mathrm{AF2}}} \cdot y_{\mathrm{s}}(t) \cdot y_{\mathrm{AF2}}(t) \\ & + k^{\mathrm{AF3}}_{\mathrm{AF3}} \cdot y_{(\text{FSH-RF})}(t) \cdot y_{\mathrm{AF3}}(t) \cdot \left(1 - \frac{y_{\mathrm{AF3}}(t)}{\mathrm{AF}_{\max}}\right) \\ & - k^{\mathrm{AF4}}_{\mathrm{AF3}} \cdot \left(\frac{y_{(\text{LH-RL})}(t)}{\mathrm{SF}_{(\text{LH-RL})}}\right)^{n^{\mathrm{AF4}}_{\mathrm{AF3}}} \cdot y_{\mathrm{s}}(t) \cdot y_{\mathrm{AF3}}(t)\end{aligned} \tag{H19}$$

$$\begin{aligned}\frac{d}{dt}y_{\mathrm{AF4}}(t) = {} & k^{\mathrm{AF4}}_{\mathrm{AF3}} \cdot \left(\frac{y_{(\text{LH-RL})}(t)}{\mathrm{SF}_{(\text{LH-RL})}}\right)^{n^{\mathrm{AF4}}_{\mathrm{AF3}}} \cdot y_{\mathrm{s}}(t) \cdot y_{\mathrm{AF3}}(t) \\ & + k^{\mathrm{AF4}}_{\mathrm{AF4}} \cdot \left(\frac{y_{(\text{LH-RL})}(t)}{\mathrm{SF}_{(\text{LH-RL})}}\right)^{n_{\mathrm{AF4}}} \cdot y_{\mathrm{AF4}}(t) \cdot \left(1 - \frac{y_{\mathrm{AF4}}(t)}{\mathrm{AF}_{\max}}\right) \\ & - k^{\mathrm{PrF}}_{\mathrm{AF4}} \cdot \left(\frac{y_{(\text{LH-RL})}(t)}{\mathrm{SF}_{(\text{LH-RL})}}\right) \cdot y_{\mathrm{s}}(t) \cdot y_{\mathrm{AF4}}(t)\end{aligned} \tag{H20}$$

$$\begin{aligned}\frac{d}{dt}y_{\mathrm{PrF}}(t) = {} & k^{\mathrm{PrF}}_{\mathrm{AF4}} \cdot \left(\frac{y_{(\text{LH-RL})}(t)}{\mathrm{SF}_{(\text{LH-RL})}}\right) \cdot y_{\mathrm{s}}(t) \cdot y_{\mathrm{AF4}}(t) \\ & - k^{\mathrm{PrF}}_{cl} \cdot \left(\frac{y_{(\text{LH-RL})}(t)}{\mathrm{SF}_{(\text{LH-RL})}}\right)^{n^{\mathrm{OvF}}_{\mathrm{PrF}}} \cdot y_{\mathrm{s}}(t) \cdot y_{\mathrm{PrF}}(t)\end{aligned} \tag{H21}$$

$$\frac{d}{dt}y_{\mathrm{OvF}}(t) = k^{\mathrm{OvF}} \cdot \left(\frac{y_{(\text{LH-RL})}(t)}{\mathrm{SF}_{(\text{LH-RL})}}\right)^{n^{\mathrm{OvF}}_{\mathrm{PrF}}} \cdot y_{\mathrm{s}}(t) \cdot H^{+}_{\mathrm{PrF,OvF}}(y_{\mathrm{PrF}}(t)) - k^{\mathrm{OvF}}_{cl} \cdot y_{\mathrm{OvF}}(t) \tag{H22}$$

$$\frac{d}{dt}y_{\mathrm{Sc1}}(t) = H^{+}_{\mathrm{OvF,Sc1}}\left(y_{\mathrm{OvF}}(t)\right) - k^{\mathrm{Sc2}}_{\mathrm{Sc1}} \cdot y_{\mathrm{Sc1}}(t) \tag{H23}$$

$$\frac{d}{dt}y_{\mathrm{Sc2}}(t) = k^{\mathrm{Sc2}}_{\mathrm{Sc1}} \cdot y_{\mathrm{Sc1}}(t) - k^{\mathrm{Lut1}}_{\mathrm{Sc2}} \cdot y_{\mathrm{Sc2}}(t) \tag{H24}$$

$$\begin{aligned}\frac{d}{dt}y_{\mathrm{Lut1}}(t) = {} & k^{\mathrm{Lut1}}_{\mathrm{Sc2}} \cdot y_{\mathrm{Sc2}}(t) \\ & - k^{\mathrm{Lut2}}_{\mathrm{Lut1}} \cdot \left(1 + H^{+}_{(\text{G-RG}),\mathrm{Lut}}\left(y_{(\text{G-RG})}(t) + y_{(\text{Ago-RG})}(t)\right)\right) \cdot y_{\mathrm{Lut1}}(t)\end{aligned} \tag{H25}$$

$$\begin{aligned}\frac{d}{dt}y_{\mathrm{Lut2}}(t) = {} & k^{\mathrm{Lut2}}_{\mathrm{Lut1}} \cdot \left(1 + H^{+}_{(\text{G-RG}),\mathrm{Lut}}\left(y_{(\text{G-RG})}(t) + y_{(\text{Ago-RG})}(t)\right)\right) \cdot y_{\mathrm{Lut1}}(t) \\ & - k^{\mathrm{Lut3}}_{\mathrm{Lut2}} \cdot \left(1 + H^{+}_{(\text{G-RG}),\mathrm{Lut}}\left(y_{(\text{G-RG})}(t) + y_{(\text{Ago-RG})}(t)\right)\right) \cdot y_{\mathrm{Lut2}}(t)\end{aligned} \tag{H26}$$

$$\begin{aligned}\frac{d}{dt}y_{\mathrm{Lut3}}(t) = {} & k^{\mathrm{Lut3}}_{\mathrm{Lut2}} \left(1 + H^{+}_{(\text{G-RG}),\mathrm{Lut}}\left(y_{(\text{G-RG})}(t) + y_{(\text{Ago-RG})}(t)\right)\right) \cdot y_{\mathrm{Lut2}}(t) \\ & - k^{\mathrm{Lut4}}_{\mathrm{Lut3}} \cdot \left(1 + H^{+}_{(\text{G-RG}),\mathrm{Lut}}\left(y_{(\text{G-RG})}(t) + y_{(\text{Ago-RG})}(t)\right)\right) \cdot y_{\mathrm{Lut3}}(t)\end{aligned} \tag{H27}$$

$$\begin{aligned}\frac{d}{dt}y_{\mathrm{Lut4}}(t) = {} & k^{\mathrm{Lut4}}_{\mathrm{Lut3}} \left(1 + H^{+}_{(\text{G-RG}),\mathrm{Lut}}\left(y_{(\text{G-RG})}(t) + y_{(\text{Ago-RG})}(t)\right)\right) \cdot y_{\mathrm{Lut3}}(t) \\ & - k^{\mathrm{Lut4}}_{cl} \cdot \left(1 + H^{+}_{(\text{G-RG}),\mathrm{Lut}}\left(y_{(\text{G-RG})}(t) + y_{(\text{Ago-RG})}(t)\right)\right) \cdot y_{\mathrm{Lut4}}(t)\end{aligned} \tag{H28}$$

On the basis of these equations, the production of the ovarian hormones can be modeled, as will be described in the following.

3.2.5 Ovarian Hormones in the Blood

As in bovine, the ovarian hormones estradiol, progesterone, and inhibin A and B are produced by the follicles and the corpus luteum. In both the bovine and the human model, linear dependencies hold between ovarian tissue and hormone concentration in the blood. In bovine, a single equation for follicular production capacity leads to similar profiles for estradiol and inhibin. Also, only one equation for luteal tissue in the bovine results in a similar course of corpus luteum and progesterone. In both humans and cows, E2 is only produced by the follicles, and P4 only by luteal tissue. However, inhibin in bovine is only produced by the follicular tissue, but in humans by both follicles and corpus luteum. In humans, the multiple stages of ovarian development allow for a more precise hormone production calculation throughout the cycle.

In humans, the ability of the follicles to produce estradiol is stimulated by LH since LH induces androgen synthesis. As described above, an effect compartment for inhibin A is introduced in order to account for a delayed effect of this substance which has been reported in [RPM+98, SS99], and to avoid delay differential equations. Instead of being cleared, inhibin A is first transferred into another compartment. The ODEs for the ovarian hormones are:

$$\begin{aligned}\frac{d}{dt}y_{\mathrm{E2}}(t) &= b_{\mathrm{E2}} + k^{\mathrm{E2}}_{\mathrm{AF2}} \cdot y_{\mathrm{AF2}}(t) + k^{\mathrm{E2}}_{\mathrm{AF3}} \cdot y_{\mathrm{LH}}(t) \cdot y_{\mathrm{AF3}}(t) \\ &\quad + k^{\mathrm{E2}}_{\mathrm{AF4}} \cdot y_{\mathrm{AF4}}(t) + k^{\mathrm{E2}}_{\mathrm{PrF}} \cdot y_{\mathrm{LH}}(t) \cdot y_{\mathrm{PrF}} \\ &\quad + k^{\mathrm{E2}}_{\mathrm{Lut1}} \cdot y_{\mathrm{Lut1}}(t) + k^{\mathrm{E2}}_{\mathrm{Lut4}} \cdot y_{\mathrm{Lut4}}(t) - k^{\mathrm{E2}}_{cl} \cdot y_{\mathrm{E2}}(t) \qquad \text{(H29)}\\ \frac{d}{dt}y_{\mathrm{P4}}(t) &= b_{\mathrm{P4}} + k^{\mathrm{P4}}_{\mathrm{Lut4}} \cdot y_{\mathrm{Lut4}}(t) - k^{\mathrm{P4}}_{cl} \cdot y_{\mathrm{P4}}(t) \qquad \text{(H30)}\\ \frac{d}{dt}y_{\mathrm{IhA}}(t) &= b_{\mathrm{IhA}} + k^{\mathrm{IhA}}_{\mathrm{PrF}} \cdot y_{\mathrm{PrF}}(t) + k^{\mathrm{IhA}}_{\mathrm{Sc1}} \cdot y_{\mathrm{Sc1}}(t) + k^{\mathrm{IhA}}_{\mathrm{Lut1}} \cdot y_{\mathrm{Lut1}}(t) + k^{\mathrm{IhA}}_{\mathrm{Lut2}} \cdot y_{\mathrm{Lut2}}(t) \\ &\quad + k^{\mathrm{IhA}}_{\mathrm{Lut3}} \cdot y_{\mathrm{Lut3}}(t) + k^{\mathrm{IhA}}_{\mathrm{Lut4}} \cdot y_{\mathrm{Lut4}}(t) - k^{\mathrm{IhA}} \cdot y_{\mathrm{IhA}}(t) \qquad \text{(H31)}\\ \frac{d}{dt}y_{\mathrm{IhAe}}(t) &= k^{\mathrm{IhA}} \cdot y_{\mathrm{IhA}}(t) - k^{\mathrm{IhAe}}_{cl} \cdot y_{\mathrm{IhAe}}(t) \qquad \text{(H32)}\\ \frac{d}{dt}y_{\mathrm{IhB}}(t) &= b_{\mathrm{IhB}}(t) + k^{\mathrm{IhB}}_{\mathrm{AF2}} \cdot y_{\mathrm{AF2}}(t) + k^{\mathrm{IhB}}_{\mathrm{Sc2}} \cdot y_{\mathrm{Sc2}}(t) - k^{\mathrm{IhB}}_{cl} \cdot y_{\mathrm{IhB}}(t) \qquad \text{(H33)}\end{aligned}$$

The model for the human menstrual cycle consists of 33 ODEs and 114 unknown parameters. Identified parameter values and initial values can be found in the appendix. In [RmD+12], more detailed simulation results can be found. A selection of the most impor-

tant results will be presented in the following.

3.3 Simulation and Model Validation

The simulation of the above derived model for the human menstrual cycle leads to quasi-periodic solutions for all 33 variables. The period, i.e. the cycle length, of the simulation is 28 days. In figure 3.3, one cycle of the simulation of the four most often measured hormones (LH, FSH, estradiol and progesterone) is depicted, together with measured data of 12 healthy individuals, pulled from a Pfizer database. The simulation shows that the model captures the average course of the four substances well, and is thus consistent with experimental data.

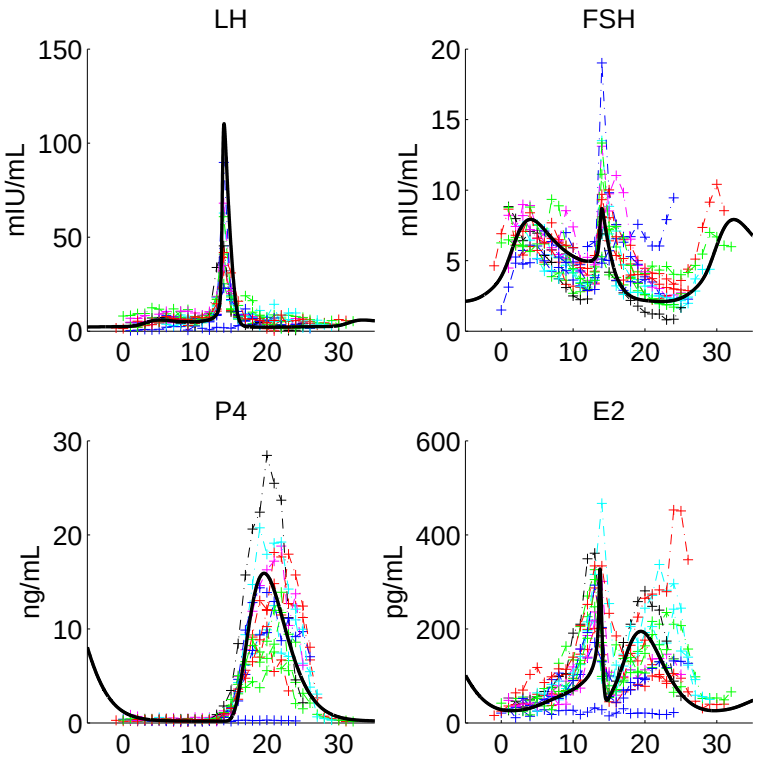

Figure 3.3: Simulation with GynCycle together with measurements from healthy individuals. Time units are days.

In Figure 3.4, the effect of virtual single doses of 100μg GnRH Agonist is shown, together with experimental data for LH from three individuals after single subcutaneous doses of 100μg GnRH Agonist Nafarelin at different times in the cycle. The administration of

Nafarelin in the early follicular phase postpones ovulation. In the late follicular phase, agonist administration triggers ovulation, the following cycles are shorter and return to their original length within the next three cycles. Administered in the luteal phase, Nafarelin shortens the luteal phase. These findings are in line with literature [MHM+85, FJO+02], and thus emphasize the predictive ability of the model.

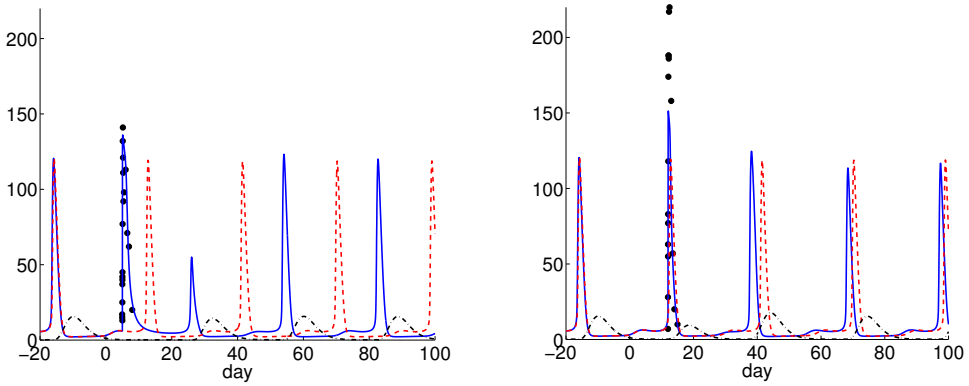

(a) Administration in the early follicular phase leads to a delayed ovulation

(b) Administration in the late follicular phase leads to immediate ovulation

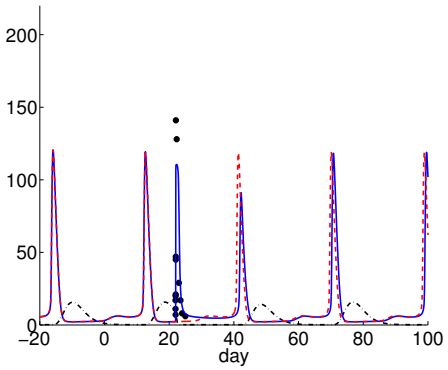

(c) Administration in the luteal phase results in truncated luteal phase

Figure 3.4: Profiles of LH after administration of a single dose of 100μg GnRH Agonist Nafarelin at different phases within the cycle (blue), together with experimental data of a corresponding study (black dots), and the simulation for LH without administration (dashed red)

In Figure 3.5, simulation results together with data from an experimental multiple dose study with the GnRH agonist Nafarelin are shown. After an initial stimulatory phase, LH levels are suppressed but acute responses to Nafarelin are maintained, whereas P4 is suppressed constantly. This is in line with findings from [MBA+86].

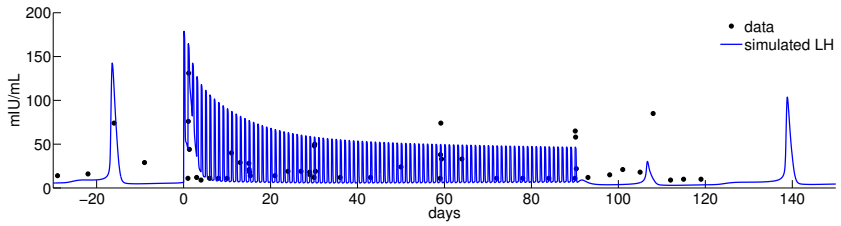

(a) LH

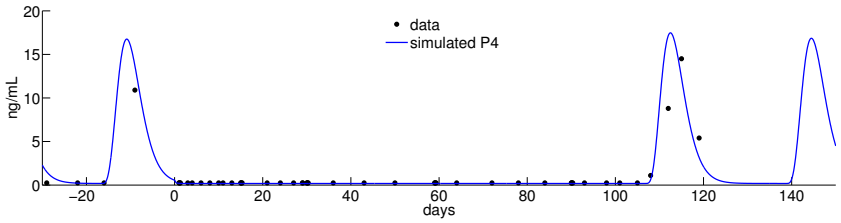

(b) P4

Figure 3.5: Profiles of LH and P4 during administration of multiple doses of 250μg GnRH Agonist Nafarelin

Simulation results from GnRH antagonist administration can be found in [RmD+12]. Several studies with different dosing amounts and different dosing time points can be well captured with the current model.

The model for the human menstrual cycle can be found in Table A.1 in the Appendix, together with the list of parameter values (Table A.2) and initial values (Table A.3).

Summarizing, the modifications of the Reinecke model still lead to good results concerning the data of healthy individuals. The elimination of time delays, as well as the omittment of the detailed steroidogenesis in the ovaries and the no longer stochastic pulse pattern have not lead to disadvantages regarding the simulation for healthy individuals. In addition, the ability of the new model to capture the effects of GnRH agonist and antagonist is a great advancement, and a step towards reliable predictions with the model of the human menstrual cycle.

Of course, there are large differences between the simulations results with the human and the bovine model. However, some similarities can be observed. The course of the four most often measured hormones is depicted in Figure 3.6. One can observe that in both BovCycle and GynCycle, the course of LH over the cycle has a peak-like shape, the peak marks the time point of ovulation. P4 starts to grow shortly afterwards, but grows much longer in bovine, having its maximum level shortly before luteolysis. E2 and FSH both have several waves per cycle. As discussed in Chapter 2, adjustments to BovCycle need to be made to make the curves less wave-like, and more smooth. Regarding the experimental

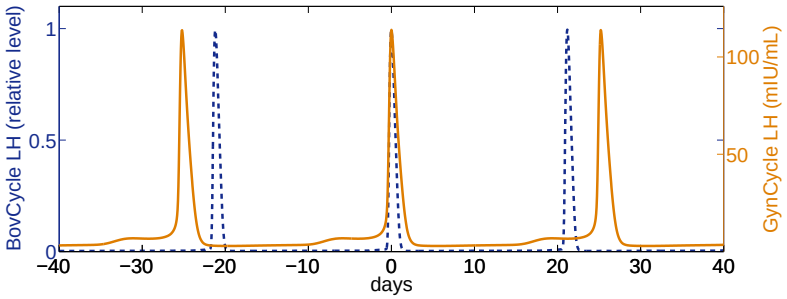

(a) LH

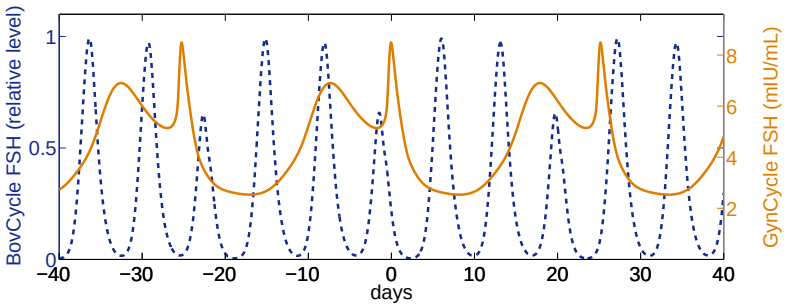

(b) FSH

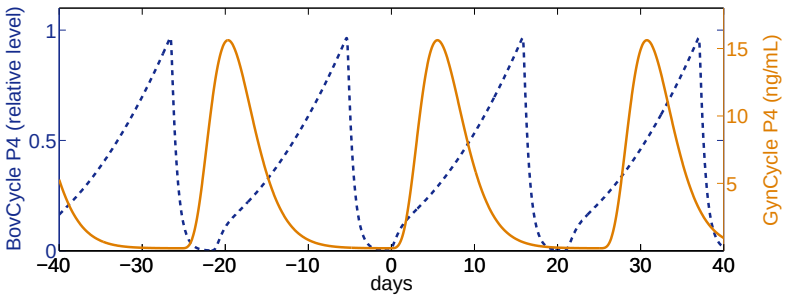

(c) P4

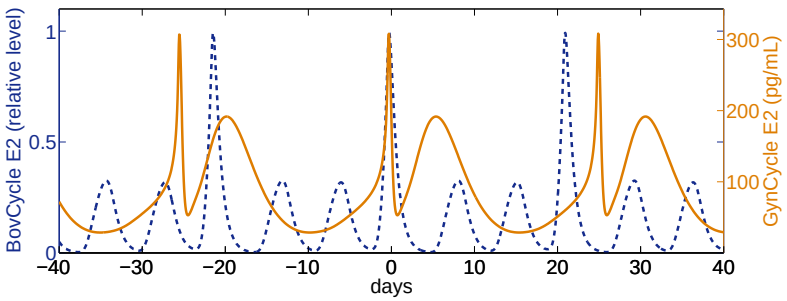

(d) E2

Figure 3.6: Simulation with GynCycle together with simulation with BovCycle, centered around the LH peak at day zero. The orange line shows the course of the hormones as simulated with the human model, the blue dashed line shows simulations with the bovine model.

data, the model of the human menstrual cycle already captures the course of FSH and E2 well.

3.4 Discussion of Follicular Waves

In the model GynCycle, the existence of several follicular waves per cycle has not been taken into consideration. There is, however, evidence, that also in humans, follicles grow and decay in a wave-like pattern. This approach has been discussed in Chapter 2.4.

Follicular development consists of several successive stages of maturation that a cohort of follicles passes through. In humans, as in the above presented model, it is often assumed that this follicular development occurs exclusively between the decay of the corpus luteum and ovulation, called the follicular phase. With ovulation, the follicular phase ends, and the remainings of the follicle form the corpus luteum. During the luteal phase, follicular growth is suppressed by progesterone, and it is commonly expected that the follicles do not significantly start to grow during this phase.

Typical simulation results for follicles with GynCycle are depicted in Figure 3.7. One can observe in the figure, that the follicles start to rise only once in every cycle.

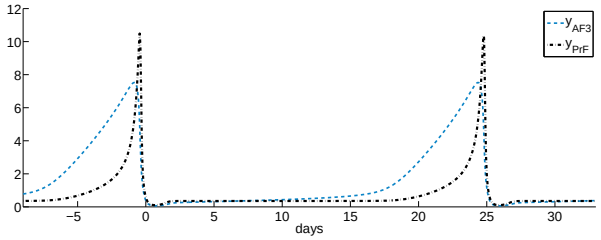

Figure 3.7: Simulation results with GynCycle for antral follicles and preovulatory follicles. Ovulation in the model takes place at day 0.

However, there is a lot of evidence that also in humans, follicular development occurs in waves. In [For94] it is stated that follicular development occurs only in the follicular phase, but that more recent studies rather suggest similar ovarian dynamics as in cows (and sheep and cattle).

In [GGG+04], the ovarian dynamics between mares and women were compared and the results indicated many similarities in their follicular function. [AP95] uses knowledge from the follicular waves in bovine to study similar wave-patterns in humans. This is a promising approach also for the models presented in this thesis.

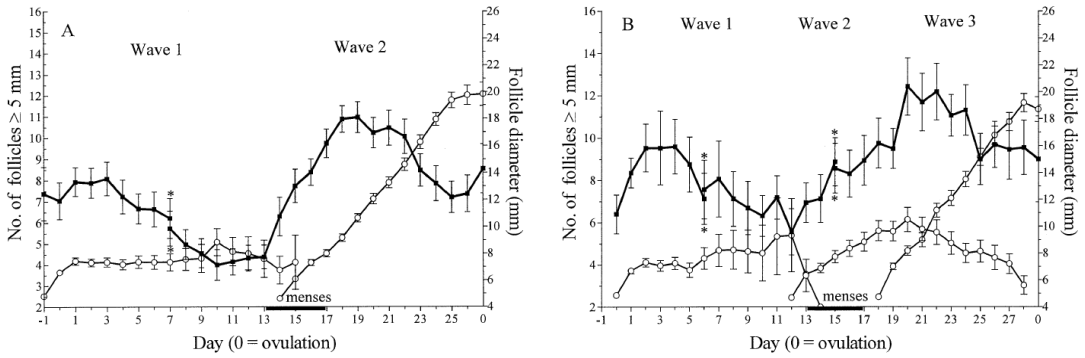

Figure 3.8: Development of the diameter of the largest follicle of each wave (∘), together with the number of follicles ≥ 5 mm (■) for women exhibiting (A) two waves (n=34) and (B) three waves (n=16) during one interovulatory interval (Source: [BAP03]).

In [BAP03], a clinical study with fifty healthy women was performed that investigated the follicular phenomenon in women. The study showed an existence of several follicular waves in all women. In particular, a large part of the patients had two waves, a smaller part three waves per cycle. An example of the results is illustrated in Figure 3.8. These findings suggest that the model for follicular waves developed in Section 2.4 may be useful for an improved model of the human menstrual cycle, where waves of folliculogenesis replace the currently used approach of successive follicular stages.

From the current point of view, a model for the human menstrual cycle that takes into account different follicular wave patterns would be closer to reality. An improved model that would map the experimental findings from [BAP03] would thus be promising to even better capture the mechanisms behind the menstrual cycle, and thus would help to make predictions with this model even more reliable.

Chapter 4

Analysis of the Numerical Bovine Model

This chapter focuses on properties of the ODE model for the bovine estrous cycle. In particular, it investigates the stability of the model via a standard Floquet-multiplier approach. Also, a new procedure is presented to detect different follicular wave patterns for different parameterizations of this model. A method to calculate robustness regions for parameters in which normal P4 profiles are obtained is performed. Finally, a reduction technique is applied that uses the qualitative structure of the model to derive a smaller model that generates the same output for some components.

The methods in this chapter are only applied to the bovine model, but could also be used for the human model. Due to the similar structure of the human model, comparable results are expected.

4.1 Stability

A well-known but nevertheless remarkable characteristic of biological and in particular endocrinological systems is their stability. In most cases, even after large and long environmental changes, the functioning of the system comes back to original. The ability to recover after illnesses, treatments or other perturbations of normal functioning is an important characteristic to have in mind when modeling biological systems.

A numerical model is called stable, if small perturbations do not disturb the overall behavior of the solution. In the continuous case with its infinite possible states, there are several possibilities to explore the stability of the system.

A first hint for the stability of the model is depicted in Figure 4.1. Therein, a flow of the two-dimensional phase space of estradiol versus progesterone is depicted. Initial values for the two variables E2 and P4 are chosen along a grid in the phase space. The initial values for the other variables in the models are kept fixed. Wherever the initial values

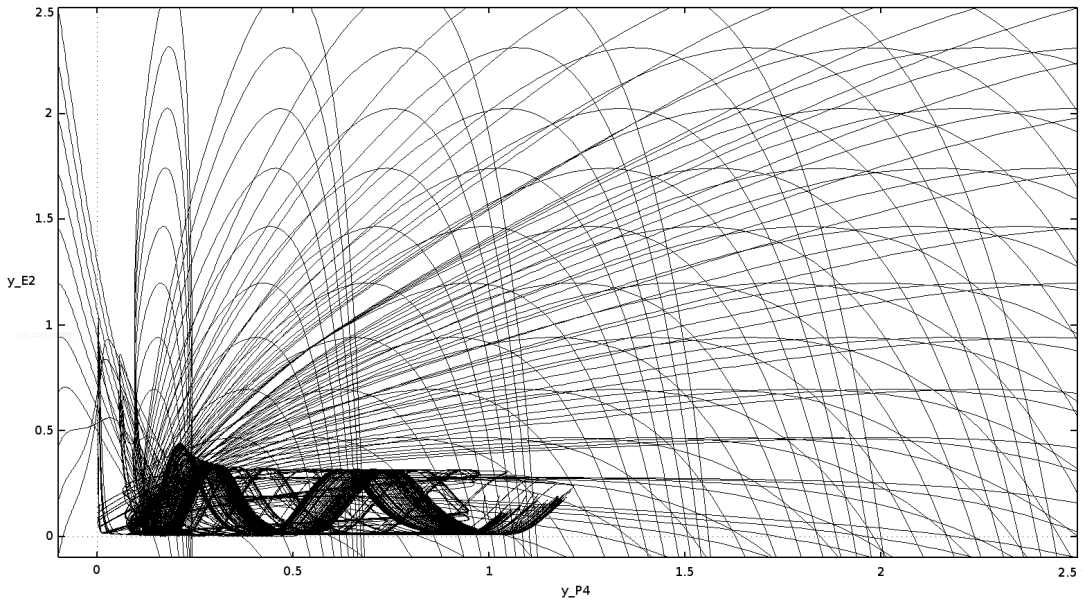

Figure 4.1: A flow for the two-dimensional phase space of y_{E2} versus y_{P4}, generated with XPPAUT [Erm]

for P4 and E2 are chosen, the simulation converges to the same limit cycle. This suggests that even relatively large perturbations of the system do not disturb its long-term behavior.

The evolution of such perturbations of the initial values of a system of ODEs can be described by the Wronskian matrix [Deu84]. It is obtained by solving a variational equation calculated from the right hand side of the ODE system. This provides an analytical tool to investigate model stability.

The Wronskian matrix is obtained as the solution of the variational equation

$$\frac{dW}{dt}(t) = f_y(y(t)) \cdot W(t), \quad W(0) = Id,$$

for the ODE system $y' = f(y)$. Let T be the period length of the solution of the ODE system, and let the solution be disturbed at time $t = 0$. The Wronskian W evaluated at time $t = T$ tells how this disturbance has impacted the solution after one period, $\delta y_T = W(T) \cdot \delta y_0$. If the perturbation has become smaller, $|\delta y_T| < |\delta y_0|$, i.e. closer to the real limit cycle, the system is locally stable.

Thus, with the columns of the Wronskian denoted as $W_i(t)$,

$$W(T) = [W_1(T), W_2(T), \ldots, W_n(T)],$$

the Wronskian matrix is obtained by numerically solving the system

$$\begin{pmatrix} y' \\ W_1'(T) \\ \vdots \\ W_n'(T) \end{pmatrix} = \begin{pmatrix} f(y) & & & \\ & f_y(y(T)) & & \\ & & \ddots & \\ & & & f_y(y(T)) \end{pmatrix} \cdot \begin{pmatrix} 1 \\ W_1(T) \\ \vdots \\ W_n(T) \end{pmatrix} . \qquad (*)$$

The eigenvalues of the Wronskian are called *Floquet multipliers* of the system. If the Floquet multipliers are all in the unit circle, the system is stable, see e.g. [Deu84].

The nonzero entries of the Jacobian with respect to the variables, $f_y(y(T))$, as well as the Wronskian matrix of the system of the bovine estrous cycle can be found in the Appendix.

The numerically computed eigenvalues of the Wronskian matrix are calculated as

$$\begin{pmatrix} 5.7839 \cdot 10^{-1} \\ -3.1083 \cdot 10^{-1} \\ -7.4904 \cdot 10^{-3} \\ -9.2361 \cdot 10^{-4} \\ 1.0751 \cdot 10^{-5} \\ 5.5680 \cdot 10^{-7} \\ -5.1326 \cdot 10^{-10} \\ 1.1917 \cdot 10^{-10} \\ 8.8229 \cdot 10^{-14} + 6.9451 \cdot 10^{-12i} \\ 8.8229 \cdot 10^{-14} - 6.9451 \cdot 10^{-12i} \\ 6.0748 \cdot 10^{-12} \\ -2.1544 \cdot 10^{-12} \\ 2.8519 \cdot 10^{-13} \\ -1.2054 \cdot 10^{-13} \\ 1.4909 \cdot 10^{-27} \end{pmatrix}$$

All eigenvalues are within the unit circle, thus, the model for the bovine estrous cycle is locally stable.

Note that the stability is only shown for the current set of parameters, and locally for a subset of possible initial values. In Chapter 5, a parameter-independent discrete model for the bovine estrous cycle is derived, and stability is investigated globally.

4.2 Follicular Wave Patterns

Ovulation takes place once in every cycle at the end of a follicular growth and maturation process. In bovine, an estrous cycle includes several, normally two or three, wave-like

patterns of follicle development [For94]. In each wave, several follicles from the pool of primordial follicles start to grow and compete to become the dominant follicle. One after another, they all undergo atresia. In the last wave, the dominant follicle does not undergo atresia but continues to grow and ovulates. The number of follicular waves that occur per cycle will be discussed and analyzed in this section.

There are several reasons to study the difference in hormone patterns between two- and three-wave cows. For example, [BGK04] found that cows with two follicle waves during the estrous cycle produce more milk than those with three waves. Another motivation to study this difference is to investigate the relation of the number of waves and fertility.

Biological Evidence

The number of follicular waves per cycle differs between cows. According to [BGK04, WIR+04], most cows have two or three waves, i.e. one or two anovulatory waves plus the ovulatory wave in each cycle. Some cows may have only one or even four follicular waves per cycle, and often the number of waves differs from cycle to cycle.

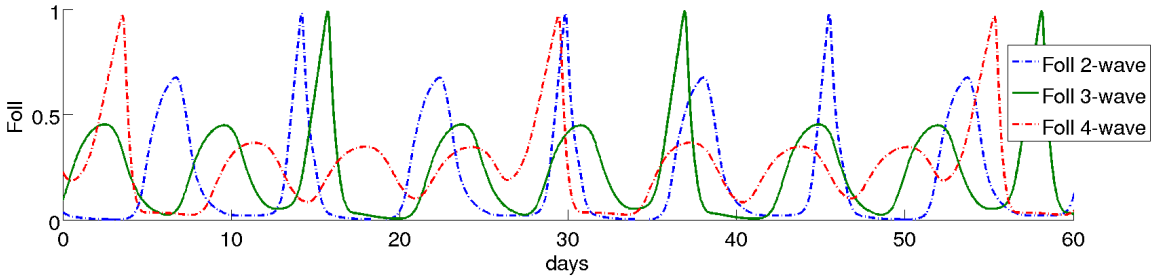

Figure 4.2: Follicular function with different parameterizations of the model. Varying certain parameters, a simulation output with two, three, or four follicular waves per cycle can be generated.

Two-wave cows, i.e. cows with usually two follicular waves per cycle, have a shorter cycle than three-wave cows. Since in a long time span, a two-wave cow ovulates more often, one can derive that, at a randomly chosen time point, a herd of two-wave cows probably includes more cows that are at the stage around ovulation. Therefore, one could assume that two-wave cows have higher fertility rates compared to three-wave cows. However, reality is more complex. While some studies show no difference regarding fertility rates [BGK04, CAŞD05], other studies report better fertility in three-wave cycles compared to two-wave cycles [TTB+02], and it has been suggested that the older and larger ovulatory follicles in cycles with two waves contain oocytes of less quality than cycles with three waves [RB96].

The reason for this could be as follows: The follicle that is dominant at the moment of CL regression ovulates. Therefore, the number of follicular waves in a cycle is largely affected by the interplay of follicle growth rate and the time point of CL regression. Thus, it is influenced by the timing of two major rhythm drivers of the cycle, follicle growth under control of FSH, and CL regression under control of $PGF_{2\alpha}$. When the CL is regressed at the moment that a prolonged dominant follicle is present, the oocyte could be of inferior quality [RB96].

The factors that regulate the number of waves in bovine are not fully explored, though experimental effort has been made to search for endocrine mechanisms that could be responsible for controlling these factors. [WIR+04] did not find any difference in number of waves between cows and heifers. Also, breed or age do not affect the number of waves per cycle [AJSM08]. However, some findings on differences between two- and three-wave cows have been reported. [JSMA09] observed that CL regression occurs 2.5 days earlier in two-wave compared to three-wave cows. The onset of luteolysis thus might play an important role. [BGK04] found that ovulatory follicles in two-wave cycles have a lower growth rate compared to the ovulatory follicles in three-wave cycles. [PRGM03] observed that cows with three-wave cycles had lower FSH and Inhibin blood concentrations at non-ovulatory waves compared to two-wave cows. [MTA+06] found that immunization against Inhibin A increased the number of waves per cycle. Summarizing, three biological mechanisms are found that have been reported to influence the number of waves: the time of CL regression, the growth rate of the follicles, and low Inhibin and FSH concentrations.

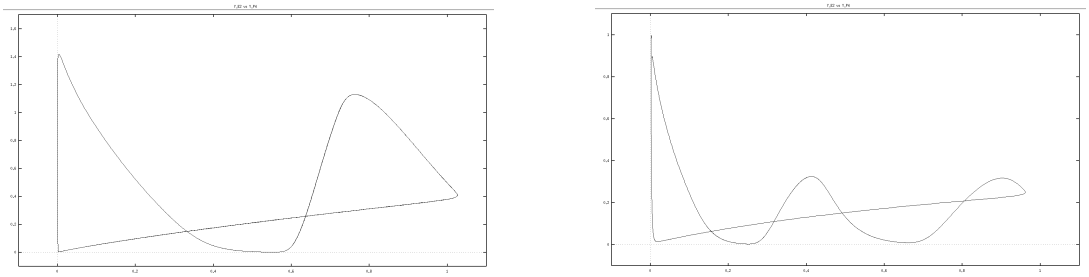

(a) Two-wave cycle

(b) Three-wave cycle

Figure 4.3: Two-dimensional view on the phase space. By changing one parameter, a different rhythm of the limit cycle can be enforced

Ten parameters of the bovine model that can directly be associated with these described biological mechanisms have been tested for inducing a change in wave number in [BRm+11]. Their values are varied, sometimes in combination with each other, and for certain parameters, a change in wave number is obtained.

Fourier Analysis to Explore Different Wave Patterns

A systematic approach to analyze how parameter changes lead to different wave patterns can be taken with the help of Fourier analysis. Even without having biological evidence, this allows to detect the responsible model parameters that control the type of periodicity of the solution. The aim of the analysis described in the following is to calculate the number of waves per cycle while one parameter varies. All parameters are varied individually, and the development of the wave number is shown. Later, two parameters are varied at a time. Visual detection of changes in the number of waves may lead to new insights.

From the simulations it is clear that, in the bovine model, mainly two types of components exist. The variables that are associated with luteal development, i.e. the corpus luteum itself, progesterone, or the substances involved in luteolysis, peak once every cycle. The variables that are associated with follicular development, i.e. the follicles and the hormones produced by them, have several waves per cycle. For substances as GnRH, LH, or OT it is not clear which one is more dominant, but they represent the bridge between the CL and the follicles and play a role in the change of the model behavior regarding the number of waves in the simulation. Decisive is that the number of waves per cycle can be counted by comparing the one-peak variables with the several-wave variables.

For the following analysis, we take the variable describing the follicles, y_{Foll}, as representative for the several-wave-variables, and y_{CL} as representative for the one-peak variables. In the following, the *rhythm* of a variable denotes the time interval between two maxima. The rhythm of the one-peak variables is the cycle length, while the rhythm of the several-wave-variables can be calculated through spectral analysis. To compare the two rhythms via the calculation of their Fourier coefficients, first the precise cycle length is needed.

To obtain the precise cycle length, the code PERIOD, presented in [Deu84], is used. As the algorithm used in PERIOD is sensitive to starting values, a good first approximation of the cycle length is needed. A rough approximation by hand is not good enough. Thus, the Fourier transformation of the simulation of the variable y_{CL} is used for improvement. The maximum coefficient of the Fourier transformation is then taken as the starting value for the length of the period. With this starting value, PERIOD uses NLSCON to iteratively optimize the initial values of the ODE system to obtain a precise periodic solution.

Knowing the true period length T and initial values of the system, a Fourier analysis is now performed on the several-wave-variable y_{Foll},

$$y_{\text{Foll}}(t) = \sum_k c_k \exp(ik\pi t/T).$$

This delivers the contribution of the most dominant, lowest frequent components of this variable to the total value of y_{Foll}, and therefore the contribution of the components that have one, two, three, or four oscillations to the course of y_{Foll}.

This approach is performed with different parameter values. Possibly, the component having the most dominant oscillation changes. For example, it changes from the two-wave component having the highest contribution to the three-wave component being the most dominant oscillation of y_{Foll}, indicating a change from a two-wave to a three-wave cycle pattern of the whole system. Two examples of such changes are depicted in Figure 4.4. Varying one parameter at a time and performing the Fourier analysis simultaneously, leads also to a varying period length.

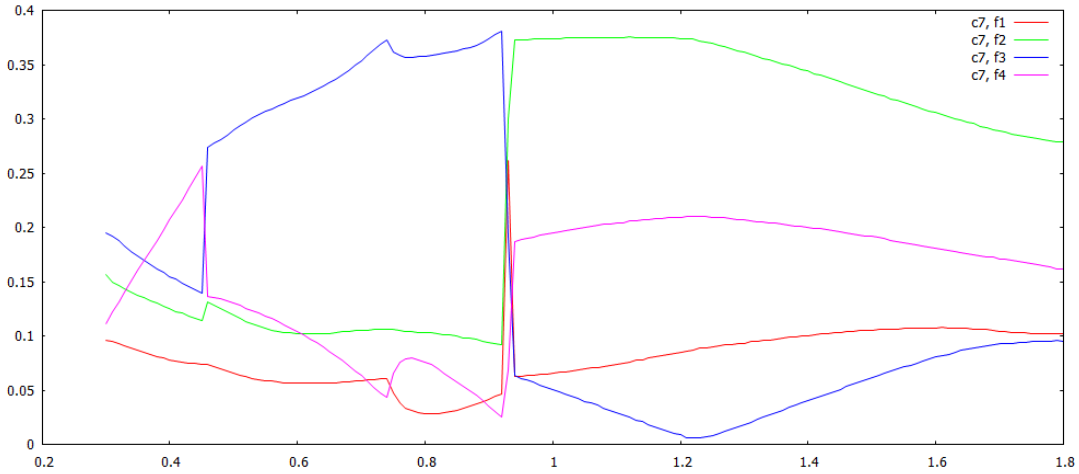

(a) Variation of $m_{\text{FSH}}^{\text{Foll}}$

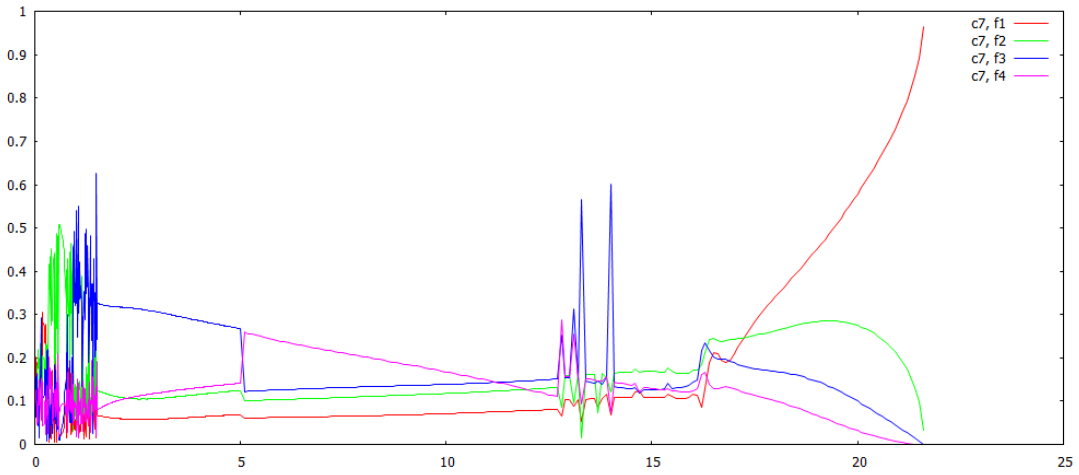

(b) Variation of c_{FSH}

Figure 4.4: The contribution of the first Fourier coefficients $f1$, $f2$, $f3$, and $f4$ (the most dominant oscillations) to y_{Foll} as function of single parameters. A change of the order of the lines indicates a change in wave numbers in the simulation in this parameter region.

Table 4.1: Parameters and their regions controlling the number of waves per cycle if one parameter is varied at a time. The fixed values of the remaining parameters can be found in the Appendix.

par	range one-wave	range two-wave	range three-wave	range four-wave
c_{FSH}	.	.	1.5 - 5.0	5.0 - 10.7
b_{FSH}	.	.	0.55 - 1.7	1.7 - 24.0
$m_{\mathrm{E2}}^{\mathrm{LH}}$	.	5.5 - 30.0	0 - 5.5	.
$m_{\mathrm{FSH}}^{\mathrm{Foll}}$	.	0.92 - 1.8	0.45 - 0.92	0.36 - 0.45
$T_{\mathrm{Enz}}^{\mathrm{PGF}}$	.	.	0.91 - 1.8	1.8 - 2.8
$T_{\mathrm{OT}}^{\mathrm{PGF}}$	.	.	0 - 2.4	2.4 - 7.7
c_{PGF}	.	.	0 - 4.5	4.5 - 24.0
SF	0.58 - 5.0	0.3 - 0.51	0.15 - 0.3	0.045 - 0.15
$m_{\mathrm{CL}}^{\mathrm{P4}}$	.	5.0 - 15.7	1.62 - 5.0	0.72 - 1.62
c_{Enz}	.	.	1.8 - 3.9	3.9 - 5.7
$m_{\mathrm{E2}}^{\mathrm{OT}}$	.	.	1.0 - 20.0	0.22 - 1.0
c_{OT}	.	.	0 - 1.4	1.4 - 5.5

For all 60 parameters, this spectral analysis is performed and the results are visually checked. For the value of p_{orig} identified in Chapter 2, the here investigated range of values is $[0.1 \cdot p_{orig}, 10 \cdot p_{orig}]$. Within this range, for 12 parameters, there is a change in wave numbers. These parameters, together with their investigated regions of interest, are depicted in Table 4.1. For the rest of the parameters, there is no change in the order of the oscillatory components in the observed range of values.

In biology, one expects the number of waves to depend not necessarily on only a single parameter, but eventually on a combination of multiple parameter changes. Extension of the above described analysis technique into higher dimensions, thus varying several parameters at a time and investigating the order of the oscillation components of the simulation, is not difficult. Visual evaluation of the results, however, needs more careful consideration because evaluation of all graphs even for only two dimensions would be too time-consuming. Thus, a systematic approach has been chosen that takes into account sensitivities with respect to the cycle length.

In the one-dimensional case, it has been observed that a change in the order of the oscillatory components comes along with an abrupt change in the cycle length at the value of the parameter, which corresponds to a step-like shape of the period-length-curve. This is reasonable, since this change of order results from the interplay between the wave variables (e.g. follicles) and the peak-variable (e.g. $\mathrm{PGF}_{2\alpha}$).

A sensitivity analysis of the cycle length L with respect to the parameters, dL/dp, ob-

Table 4.2: The 10 most sensitive parameters w.r.t the period

par	upper bound	lower bound	change in period length
$m_{\mathrm{CL}}^{\mathrm{CL}}$	0.03530	0.00035	-52.733803991115
$T_{\mathrm{Inh}}^{\mathrm{FSH}}$	0.11800	0.00118	-24.257181177979
$m_{\mathrm{Foll}}^{\mathrm{Foll}}$	0.22000	0.00220	-10.970023704650
$m_{\mathrm{P4}}^{\mathrm{Foll}}$	1.10000	0.01100	-6.787401610235
$m_{\mathrm{FSH}}^{\mathrm{Foll}}$	0.56200	0.00562	6.663947390851
$m_{\mathrm{LH}}^{\mathrm{Ovul}}$	0.20000	0.00200	-5.874556420251
$T_{\mathrm{P4}}^{\mathrm{LH}}$	0.02690	0.00027	-4.207062858462
b_{FSH}	0.94800	0.00948	-2.638375776888
$m_{\mathrm{E2}}^{\mathrm{FSH}}$	0.39600	0.00396	-2.450479865804
$T_{\mathrm{E2}}^{\mathrm{G,2}}$	0.64800	0.00648	2.411158103445

Table 4.3: Parameter combinations and their sensitivities w.r.t the period

sens. rank	par1	par2	change in period length
1	$m_{\mathrm{FSH}}^{\mathrm{Foll}}$	$m_{\mathrm{P4}}^{\mathrm{Foll}}$	0.0112112802
2	$T_{\mathrm{Inh}}^{\mathrm{FSH}}$	$m_{\mathrm{P4}}^{\mathrm{Foll}}$	0.0103284892
3	$m_{\mathrm{P4}}^{\mathrm{Foll}}$	$c_{\mathrm{Foll}}^{\mathrm{Inh}}$	0.0103283604
4	b_{FSH}	$m_{\mathrm{P4}}^{\mathrm{Foll}}$	0.0099673220
5	$m_{\mathrm{Foll}}^{\mathrm{Foll}}$	$m_{\mathrm{P4}}^{\mathrm{Foll}}$	0.0098795470
6	$m_{\mathrm{P4}}^{\mathrm{Foll}}$	$m_{\mathrm{CL}}^{\mathrm{CL}}$	0.0093276451
7	c_{FSH}	$m_{\mathrm{P4}}^{\mathrm{Foll}}$	0.0092558397
59	$T_{\mathrm{Inh}}^{\mathrm{FSH}}$	$m_{\mathrm{FSH}}^{\mathrm{Foll}}$	0.0066074858
60	$m_{\mathrm{FSH}}^{\mathrm{Foll}}$	$c_{\mathrm{Foll}}^{\mathrm{Inh}}$	0.0066073571
61	b_{FSH}	$m_{\mathrm{FSH}}^{\mathrm{Foll}}$	0.0062463187
63	$T_{\mathrm{Inh}}^{\mathrm{FSH}}$	$c_{\mathrm{Foll}}^{\mathrm{Inh}}$	0.0057245661
66	$T_{\mathrm{Inh}}^{\mathrm{FSH}}$	b_{FSH}	0.0053635276

tained through numerical differentiation, can give a hint to which parameters might lead to a change in the order of the components. Since the cycle length is quite sensitive to these parameters locally, their changes may lead to a step in the cycle length at some point. The sensitivity of the cycle-length to the parameters is not a global information, but a hint to which parameters to examine further. In the one-dimensional case, all parameters have been evaluated visually, and the sensitivity analysis yields that of the 12 parameters that can by themselves control the number of waves, 6 are among the eight most sensitive.

In the two-dimensional case it is therefore convenient, instead of visually checking all $60 \cdot 59/2 = 1741$ possible combinations, to restrict the examination to the most sensitive, in order to find at least some combinations that lead to a change in the number of waves. It is assumed that a parameter that is itself very sensitive is also sensitive in any combination. It can be observed that in the 58 most sensitive combinations, $m_{\mathrm{P4}}^{\mathrm{Foll}}$ is always one of the two parameters in the combination. To also check different parameter combinations, besides the seven most sensitive combinations, also the five most sensitive combinations without $m_{\mathrm{P4}}^{\mathrm{Foll}}$ have been checked visually. The corresponding sensitivities with respect to the period length are given in Table 4.3. Two examples of the development of the Fourier fractions are illustrated in Figure 4.5. Among all 12 of the checked combinations, there is a change in order of the most dominant fraction, thus a change of waves depending on the values of the parameters.

Summarizing, for the 12 parameters depicted in Table 4.1, a change of the number of waves per cycle can be obtained by changing the value of a single parameter. These 12 parameters have been identified by visually checking the developments of the contributions of the first four Fourier coefficients. The ranges for the parameter values that lead to a particular wave pattern have been determined. Regarding the simultaneous change of two parameter values, the sensitivity analysis with respect to the cycle length gives good suggestions which parameter combinations can provoke a change in wave patterns.

In contrast to [BRm$^+$11], which used biological knowledge to find parameters that regulate the wave patterns, the here presented approach represents a more systematic approach that finds such parameters based on mathematical properties of the simulation output. This extends the previous findings in [BRm$^+$11], and it gives a more reliable set of candidates that experimental effort can be focused on.

As another systematic approach to analyze the model, parameter regions can be explored with regard to other cycle characteristics. This will be the subject of the next section.

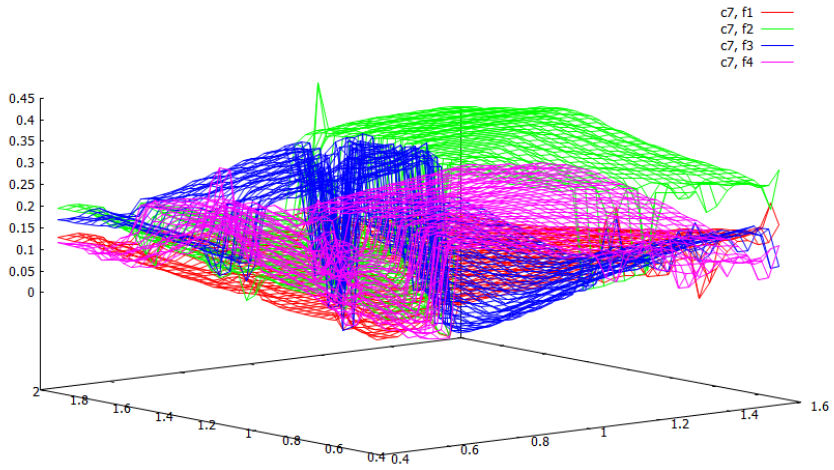

(a) $m_{\mathrm{FSH}}^{\mathrm{Foll}}$ and $m_{\mathrm{P4}}^{\mathrm{Foll}}$

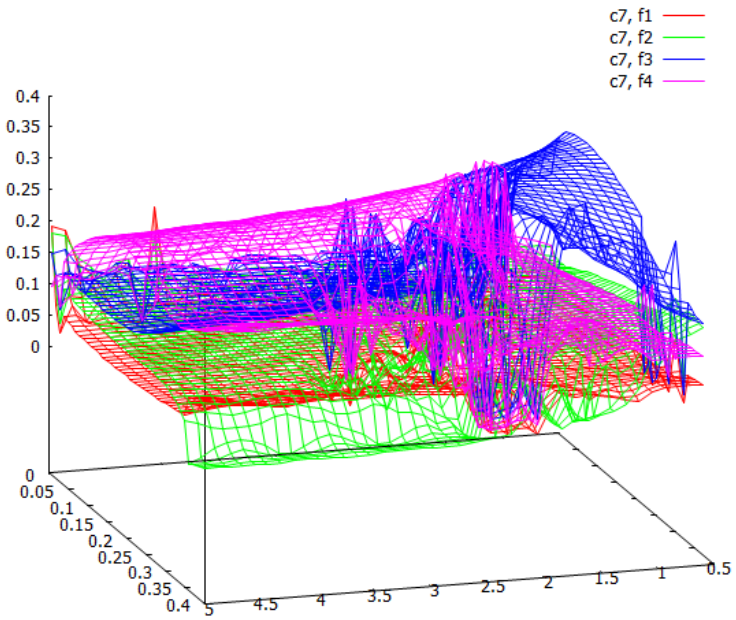

(b) $T_{\mathrm{Inh}}^{\mathrm{FSH}}$ and b_{FSH}

Figure 4.5: Two examples of the fraction of the first four Fourier coefficients (the most dominant oscillations) to y_{Foll} as a function of two parameters. A change of the order of the lines indicates a change in wave numbers in the simulation in this parameter region.

4.3 Parameter Robustness Regions

In the ODE model for the bovine estrous cycle, several factors may perturb the periodic behavior of a normal cycle. Such factors are likely the effect of simultaneous changes in multiple parameters, which could be mapped to biological mechanisms in a real cow. In this section, a method for parameter perturbation is presented that finds parameter configurations which correspond to certain pathological situations. In particular, *robustness regions*, in which a normal cycle takes place, are defined and with this method detected. Due to the way they are defined, outside of the robustness regions, the occurrence of cystic ovaries, coherent with atypical P4 levels, is suggested. In this section, the idea of the procedure and the most important results are presented, for more details see [BAM+12].

Cystic ovaries, or persistent corpora lutea, are an important cause of reproductive failure in dairy cows [Gar97]. They develop when the dominant follicle or the CL fails to regress and maintains steroidogenesis. Several metabolic and endocrine factors are known to increase the risk of the formation of cystic ovaries, but the exact pathogenesis is unclear. Detection of parameter regions involved in the formation of cystic ovaries could help to understand which biological mechanisms play a role.

Deduced from [DLW98], an estrous cycle is considered *normal* when P4 levels are lower between 0.15 and 2.00 (on the relative scale) for 9-19 days in the luteal phase and below 0.15 for less than 12 days in the inter-luteal interval. This is illustrated in Figure 4.6.

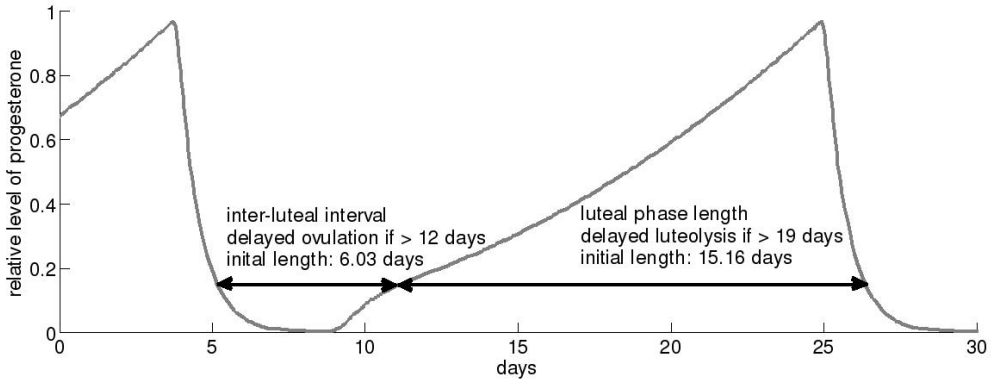

Figure 4.6: Illustration of the *normal* luteal phase analyzed in the model. The figure shows the P4 (progesterone) levels obtained with the initial parameterization (Source: [BAM+12]).

For the determination of the robustness regions in the ODE model, a simulation of the bovine estrous cycle is considered as *normal* if

- all parameters are positive,
- $y_{\mathrm{P4}} < 2$,
- the length of the luteal phase length is 9-19 days (no delayed luteolysis),
- the inter-luteal interval has a maximum length of 12 days (no delayed ovulation).

In a certain region in the 60-dimensional space around the initial parameter values, the system still shows fulfills the criteria for a normal cycle. This region is referred to as the *robustness region.*

In [AMGV10], a method is developed to estimate parameter robustness regions for models with oscillatory behavior. This method is especially designed to be efficient for systems with a large number of parameters. The number of simulations scales linearly and not exponentially with the number of parameters. Using the criteria from above, this approach was adjusted and applied to find an approximation of the robustness region for a normal estrous cycle. The adjusted method is described in [BAM$^+$12]. First, the gradient vector representing the sensitivity of luteal phase length to changes in each parameter value is calculated. This gradient vector represents the direction in which the luteal phase length changes most. This vector is taken as the first direction in which the nominal parameter set is perturbed. Next, the other perturbation directions are constructed such that they are perpendicular to each other and also to the first perturbation direction.

Starting from the initial values of the 60 model parameters, denoted as *nominal set* k_0, all parameter values are perturbed along the perpendicular directions to detect where along these directions the model behavior shows a qualitative transition. As the current model contains 60 parameters, the nominal parameter set is perturbed in 60 positive and 60 negative directions. The perturbation along a certain direction is stopped when one of the parameters approached zero, when P4 levels became too high, or when the P4 profiles met the definition for delayed ovulation or delayed luteolysis.

An example of a lower dimensional robustness region is shown in Figure 4.7. A two-dimensional robustness analysis is carried out in the plane spanned by these two most sensitive parameters, $m_{\mathrm{CL}}^{\mathrm{CL}}$, and $m_{\mathrm{P4}}^{\mathrm{OT}}$ in the system. The cross section of the robustness region within this plane is presented in Figure 4.7. This cross section, colored in gray, is obtained by sampling the parameter space ($m_{\mathrm{CL}}^{\mathrm{CL}}$, $m_{\mathrm{P4}}^{\mathrm{OT}}$) meanwhile fixing the other parameters at their nominal value. For all points in the gray region the model predicts a normal cycle. Obviously, the nominal parameter set k_0 lies inside the robustness region.

After estimating the first two-dimensional robustness region, the analysis is continued such that the following perturbations are each perpendicular to each other. All perturbations

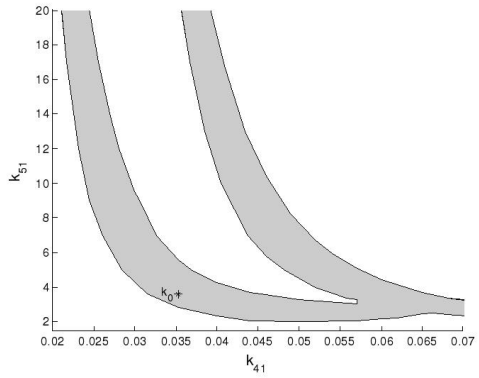

Figure 4.7: The cross section of the robustness region of the model in the 2-dimensional ($m_{\mathrm{CL}}^{\mathrm{CL}}$, $m_{\mathrm{P4}}^{\mathrm{OT}}$) plane (gray area). The nominal parameter set k_0 is marked by '$*$'. A normal cycle is obtained when ($m_{\mathrm{CL}}^{\mathrm{CL}}$, $m_{\mathrm{P4}}^{\mathrm{OT}}$) take values in the gray area, keeping the other parameters fixed at nominal values (Source: [BAM$^+$12]).

are started from the nominal set k_0, and all direction vectors are normalized. For each perturbation direction, the maximal variations are calculated, both in positive and negative directions, in which the system still leads to a normal simulation, according to the definition above.

Perturbation along two specific vectors was found to cause non-robustness of the system immediately: for these directions, a very small perturbation in negative direction resulted in delayed luteolysis, and in positive direction in delayed ovulation. In one direction, parameters $m_{\mathrm{CL}}^{\mathrm{CL}}$, $c_{\mathrm{CL}}^{\mathrm{P4}}$, $m_{\mathrm{P4}}^{\mathrm{OT}}$, and $T_{\mathrm{P4}}^{\mathrm{OT}}$ can be further perturbed than others. In the other direction, parameters c_{G}^{1} and $m_{\mathrm{CL}}^{\mathrm{CL}}$ can be disturbed the most. This suggests that these parameters strongly determine the occurrence of P4 patterns that are associated with delayed ovulation and delayed luteolysis.

The described method can help to generate hypotheses regarding the mechanisms and predisposing factors involved in the development of cystic ovaries. The simulation results suggest that mechanisms regulating CL functioning, luteolytic signals, and GnRH synthesis are likely involved in the development of cystic ovaries. This represents another systematic approach that could be used to focus experimental effort, or to indicate mechanisms for further investigation.

4.4 Model Reduction

The last section of this chapter deals with the reduction of the bovine ODE model. Combined with a method that explores the parameter space, structure-based reduction steps

are performed. The bovine model of 15 odes and 60 parameters is reduced to a model of 10 odes and 38 parameters.

Nowadays, the simulation of large ODE systems usually does not present large difficulties. However, model reduction can lead to interesting insights regarding the underlying dynamics of the modeled phenomenon. Biological models are often based on a variety of assumptions, and it is up to the modeler which mechanisms to include and which not. Whether the mechanisms that constitute to the model are the right ones is validated with the help of measurements, thus by checking the output of the model. Whether the chosen mechanisms are unique, or whether there exist other mechanisms that lead to the same model behavior, can usually not be proven. Model reduction techniques aim at finding simpler models that result in the same validated model output. They can help to decide which components are essential for the predictive power of the model.

A lot of model reduction techniques are based on quasi steady state assumptions. For models where all variables are periodic, such methods cannot be used. In [AGM12], a method is proposed that reduces an ODE system based on its logical structure. After applying this method, additional structure-based ideas are presented in this section.

The method in [AGM12] is based on the exploration of the *admissible parameter region*. A certain model output is specified that needs to be captured by the model. More specifically, time series for y_{LH}, y_{FSH}, y_{P4}, y_{E2}, and y_{Inh}, that are taken from the simulation of BovCycle, need to be reproduced with a certain tolerance while varying the parameter values. The admissible region is the subspace of the parameter space, in which this output is only changed within certain tolerance ϵ. If the admissible region includes zero for some parameters, these parameters are set to zero in the reduction procedure.

Let p denote the current vector of parameter values. Then, the admissible region is the set of all parameter values $\tilde{p} = [\tilde{p}_1, ..., \tilde{p}_q]$ for which the distance of the two solutions is small,

$$\frac{1}{n\ m\ n_D} \sum_{l=1}^{n_D} \sum_{j=1}^{n} \sum_{i=1}^{m} \left(\frac{y_j^l(t_i, \tilde{p}) - y_j^l(ti, p)}{y_j^l(t_i)} \right)^2 < \epsilon$$

m being the number of time points, n the dimension of the unreduced ODE system, and n_D the number of different data sets that are available [AGM12].

To determine the admissible region for BovCycle, first single parameters are set to zero. It is tested whether the simulation output can be obtained by adjusting the other parameters. This is performed for all parameters, in the order suggested by the sensitivity analysis. It turned out that, for 10 out of 60 parameters, the deviation at 50 time points of the specified substances is about 3 % in average. These parameters are

- within the function $H^-_{\mathrm{P4\&E2},G}$ the parameters $m^{\mathrm{G}}_{\mathrm{P4\&E2}}$, $T^{\mathrm{G}}_{\mathrm{E2}}$, $T^{\mathrm{G}}_{\mathrm{P4}}$,

- within $H^+_{\mathrm{P4,FSH}}$ the parameters $m^{\mathrm{FSH}}_{\mathrm{P4}}$ and $T^{\mathrm{FSH}}_{\mathrm{P4}}$,
- within $H^+_{\mathrm{G,FSH}}$ the parameters $m^{\mathrm{FSH}}_{\mathrm{G}}$ and $T^{\mathrm{FSH}}_{\mathrm{G}}$,
- within $H^+_{\mathrm{E2,LH}}$ the parameters $m^{\mathrm{LH}}_{\mathrm{E2}}$ and $T^{\mathrm{LH}}_{\mathrm{E2}}$, and
- within $H^+_{\mathrm{P4,Enz}}$ the parameter $T^{\mathrm{Enz}}_{\mathrm{P4}}$.

This does not automatically lead to a reduction of equations as described in [Boe12]. Instead, the following steps can been taken.

Among the parameters that can be set to zero are thus some scaling factors for Hill functions. It follows that the Hill functions $H^-_{\mathrm{P4\&E2},G}$, $H^+_{\mathrm{P4,FSH}}$, $H^+_{\mathrm{G,FSH}}$, and $H^+_{\mathrm{E2,LH}}$ can be omitted in the model. With $T^{\mathrm{Enz}}_{\mathrm{P4}} := 0$, the function $H^+_{\mathrm{P4,Enz}}$ can be replaced by its scaling factor $m^{\mathrm{Enz}}_{\mathrm{P4}}$. All of the 10 parameters can thus be omitted.

Besides removing the above functions and parameters from the model, further reduction can be performed by exploiting the structure of the model.

Most of the reduction can be obtained for substances that occur in two compartments simultaneously, namely for GnRH, LH, and FSH. For GnRH, the compartments hypothalamus and pituitary can be lumped, i.e. merged, together. This means that the processes for this substance can be described in one ODE instead of two. For LH and FSH, the compartments pituitary and blood can be lumped together, and the ODE describing their development is interpreted as blood levels. The lumping has been performed by integrating the first compartment into the second via multiplication and scaling. More precisely, the ODEs are modified as follows,

$$\left.\begin{array}{rcl} \frac{d}{dt}y_i(t) & = & Syn_i(t) - Rel_i(t) \\ \frac{d}{dt}y_j(t) & = & Rel_i(t) - c_j \cdot y_j(t) \end{array}\right\} \rightarrow \left\{\begin{array}{l} \text{set } \frac{d}{dt}\widetilde{y_j}(t) := Syn_i(t) \cdot Rel_i(t) - c_j \cdot y_j(t), \\ \text{delete } y_i \text{ and adapt growth rates.} \end{array}\right.$$

Also, the threshold that restricts GnRH synthesis in the hypothalamus, $\mathrm{G}^{\max}_{Hypo}$ is never reached in the simulation. Therefore, the term restricting GnRH synthesis can be omitted, and Syn_{G} can be replaced by the constant synthesis rate $c_{\mathrm{G},1}$. After lumping GnRH in the hypothalamus and in the pituitary, the three parameters $c_{\mathrm{G},1}$, $m^{\mathrm{G}}_{\mathrm{E2}}$, and $m^{\mathrm{G},2}_{\mathrm{P4}}$ can be replaced by one parameter, namely their product, which is denoted as $m^{\mathrm{G}}_{\mathrm{P4,E2}}$. The Hill function $H^-\mathrm{P4\&E2}, G$ was already omitted above, thus it follows that y_{G} can be modeled with one ODE instead of two, and four parameters instead of ten,

$$\frac{d}{dt}y_{\mathrm{G}}(t) = m^{\mathrm{G}}_{\mathrm{P4,E2}} \cdot h^-(y_{\mathrm{P4}}(t); T^{\mathrm{G}}_{\mathrm{P4}}, 2) \cdot h^+(y_{\mathrm{E2}}(t); T^{\mathrm{G}}_{\mathrm{E2}}, 5) - c_{\mathrm{G}} \cdot y_{\mathrm{G}}(t).$$

After lumping FSH in the pituitary and in the blood, and omitting the Hill functions $H^+_{\mathrm{P4,FSH}}$ and $H^+_{\mathrm{G,FSH}}$ as suggested above, leaves the product of $H^-_{\mathrm{E2,FSH}}$ and $H^-_{\mathrm{Inh,FSH}}$ as

growth term for y_{FSH}. The effect of the basal release parameter b_{FSH} can be included through scaling of the Hill functions. As y_{E2} and y_{Inh} have similar profiles, and the threshold for the effect of y_{E2} is low compared to the threshold for y_{Inh}, $H^{-}_{\mathrm{E2,FSH}}$ can be omitted. In total, one instead of two ODEs, and three instead of nine parameters are sufficient to describe the development of FSH,

$$\frac{d}{dt}y_{\mathrm{FSH}}(t) = m^{\mathrm{FSH}}_{\mathrm{Inh}} \cdot h^{-}(y_{\mathrm{Inh}}(t); T^{\mathrm{FSH}}_{\mathrm{Inh}}, 5) - c_{\mathrm{FSH}} \cdot y_{\mathrm{FSH}}(t).$$

Lumping LH in the pituitary and in the blood together saves another ODE. As suggested above, the Hill function $H^{+}_{\mathrm{E2,LH}}$ is omitted. Also, the parameter for the basal LH release is so low ($b_{\mathrm{LH}} = 0.0141$) that its effect does not play a significant role. Due to the multiplication of synthesis and release term during lumping, the scaling factors of the Hill functions, $m^{\mathrm{LH}}_{\mathrm{P4}}$ and $m^{\mathrm{LH}}_{\mathrm{G}}$ can be replaced by their product, $m^{\mathrm{LH}}_{\mathrm{G,P4}}$. Thus four parameters could be deleted from the model, and LH is described by

$$\frac{d}{dt}y_{\mathrm{LH}}(t) = m^{\mathrm{LH}}_{\mathrm{G,P4}} \cdot h^{-}(y_{\mathrm{P4}}(t); T^{\mathrm{LH}}_{\mathrm{P4}}, 2) \cdot h^{+}(y_{\mathrm{G}}(t); T^{\mathrm{LH}}_{\mathrm{G}}, 2) - c_{\mathrm{LH}} \cdot y_{\mathrm{LH}}(t).$$

Until here, via the described steps, the model for the bovine estrous cycle has been reduced by three ODEs and 17 parameters.

The processes controlling the rise of $\mathrm{PGF}_{2\alpha}$ can be simplified, as the three involved variables y_{Enz}, y_{OT}, and y_{PGF} are only regulated by the two variables y_{P4} and y_{E2}. Since the function $H^{+}_{\mathrm{P4,Enz}}$ was replaced by its scaling factor $m^{\mathrm{Enz}}_{\mathrm{P4}}$, the variable y_{Enz} is constant. Therefore, its occurrence in the right hand sides of other variables can be replaced by a parameter, and the equation for y_{Enz} can be deleted from the model. Also, y_{OT} is just an upstream of y_{PGF}, thus it is possible to merge these substances as well. In total, two ODEs and six parameters can be saved, and the ODE describing the development of $\mathrm{PGF}_{2\alpha}$ becomes

$$\frac{d}{dt}y_{\mathrm{PGF}}(t) = h^{+}(y_{\mathrm{E2}}(t); T^{\mathrm{PGF}}_{\mathrm{E2}}, 2) \cdot h^{+}(y_{\mathrm{P4}}(t); T^{\mathrm{PGF}}_{\mathrm{P4}}, 5) - c_{\mathrm{PGF}} \cdot y_{\mathrm{PGF}}(t).$$

The rest of the model is not essentially changed. The Hill exponent for the influence of y_{CL} on y_{IOF} is lowered from ten to five,

$$\frac{d}{dt}y_{\mathrm{IOF}}(t) = m^{\mathrm{IOF}}_{\mathrm{PGF,CL}} \cdot h^{+}_{\mathrm{PGF,IOF}}(y_{\mathrm{PGF}}(t); T^{\mathrm{IOF}}_{\mathrm{PGF}}, 5) \cdot h^{+}_{\mathrm{CL,IOF}}(y_{\mathrm{CL}}(t); T^{\mathrm{IOF}}_{\mathrm{CL}}, 5) - c_{\mathrm{IOF}} \cdot y_{\mathrm{IOF}}(t),$$

the quadratic dependencies of the steroid hormones on the CL and the follicles is replaced by a linear relationship,

$$\begin{aligned}
\frac{d}{dt}y_{\mathrm{P4}}(t) &= k^{\mathrm{P4}}_{\mathrm{CL}} \cdot y_{\mathrm{CL}}(t) - c_{\mathrm{P4}} \cdot y_{\mathrm{P4}}(t),\\
\frac{d}{dt}y_{\mathrm{E2}}(t) &= k^{\mathrm{E2}}_{\mathrm{Foll}} \cdot y_{\mathrm{Foll}}(t) - c_{\mathrm{E2}} \cdot y_{\mathrm{E2}}(t),\\
\frac{d}{dt}y_{\mathrm{Inh}}(t) &= k^{\mathrm{Inh}}_{\mathrm{Foll}} \cdot y_{\mathrm{Foll}}(t) - c_{\mathrm{Inh}} \cdot y_{\mathrm{Inh}}(t),
\end{aligned}$$

and the equation for the follicles is simplified to

$$\frac{d}{dt}y_{\text{Foll}}(t) = m_{\text{FSH}}^{\text{Foll}} \cdot h^+(y_{\text{FSH}}(t); T_{\text{FSH}}^{\text{Foll}}, 2) \cdot (1 + h^+(y_{\text{Foll}}(t); T_{\text{Foll}}^{\text{Foll}}, 2)) \\ - (m_{\text{P4}}^{\text{Foll}} \cdot h^+(y_{\text{P4}}(t); T_{\text{P4}}^{\text{Foll}}, 5) + m_{\text{LH}}^{\text{Ovul}} \cdot h^+(y_{\text{LH}}(t); T_{\text{LH}}^{\text{Ovul}}, 2) \cdot y_{\text{Foll}}(t).$$

The parameter $T_{\text{Foll}}^{\text{Foll}}$ is introduced as threshold above which there is a positive effect of the follicles on themselves. This replaces the more complex formulation of a rising FSH sensitivity of the larger follicles.

The only equation that is not changed in the reduced model is the ODE for the corpus luteum, it stays

$$\frac{d}{dt}y_{\text{CL}}(t) = \text{SF} \cdot m_{\text{LH}}^{\text{Ovul}} \cdot h^+(y_{\text{LH}}(t); T_{\text{LH}}^{\text{Ovul}}, 2) \cdot y_{\text{Foll}}(t) \\ + m_{\text{CL}}^{\text{CL}} \cdot h^+(y_{\text{CL}}(t); T_{\text{CL}}^{\text{CL}}, 2) - m_{\text{IOF}}^{\text{CL}} \cdot h^+(y_{\text{IOF}}(t); T_{\text{IOF}}^{\text{CL}}, 5) \cdot y_{\text{CL}}(t).$$

In total, the reduced system consists of 10 ODEs and only 38 parameters.

The flowchart for the reduced model is shown in Figure 4.8. In comparison with the original flowchart in Figure 2.10, several substances and mechanisms have been omitted. In particular, the changes compared to the model in Chapter 2 are

- the variables occurring in two compartments have been merged,
- GnRH synthesis is not restricted by a maximum level anymore,
- E2 has only one effect on GnRH,
- P4 also has only one effect on GnRH,
- there is no basal FSH,
- there is no direct influence of E2 on FSH, only via GnRH,
- there is no influence of P4 on FSH,
- there is no direct influence of E2 on LH, only via GnRH,
- there is no basal LH,
- the quadratic dependencies of Foll and CL on the steroid hormones P4, E2 and Inh have been replaced by linear relationships,
- the variable for the enzymes has been omitted,

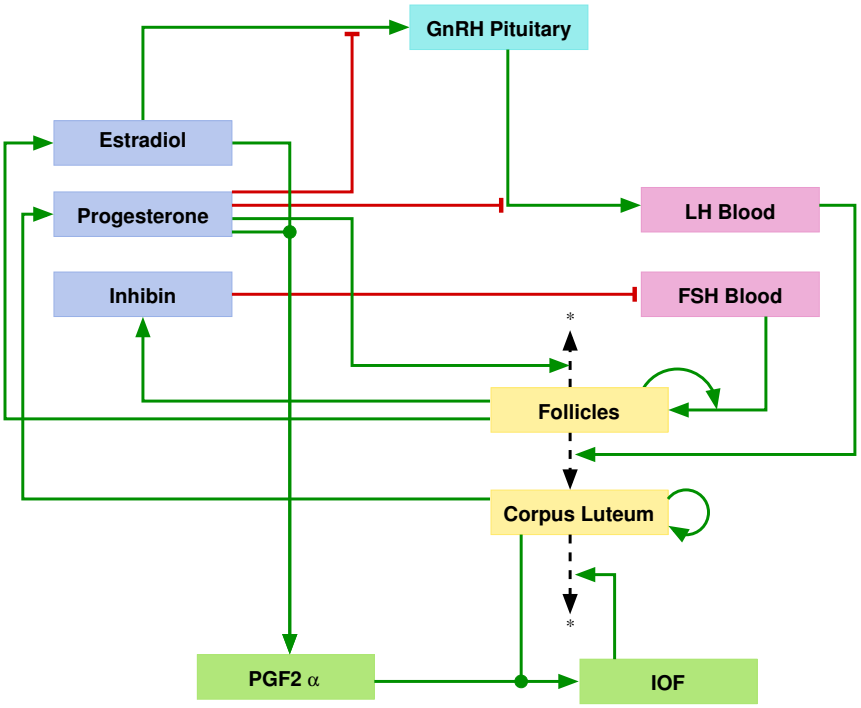

Figure 4.8: Interaction graph of the reduced model. A green pointed arrow marks a stimulatory effect, a red stump arrow an inhibitory influence. A black dashed arrow means a transition, and '$*$' marks a degraded substance. The substances GnRH in the hypothalamus, LH in the pituitary, FSH in the pituitary, Oxytocin, and the Enzymes could be omitted in the model.

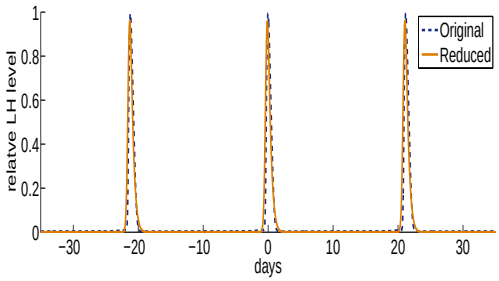

(a) LH

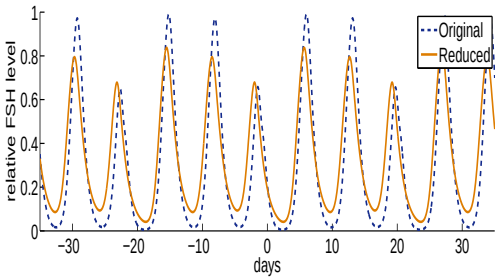

(b) FSH

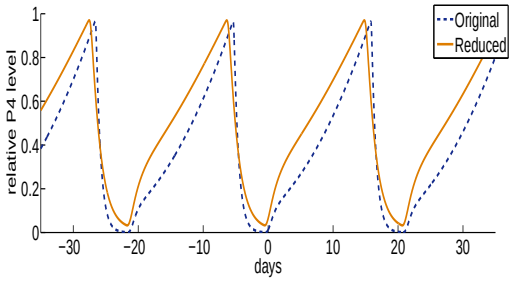

(c) P4

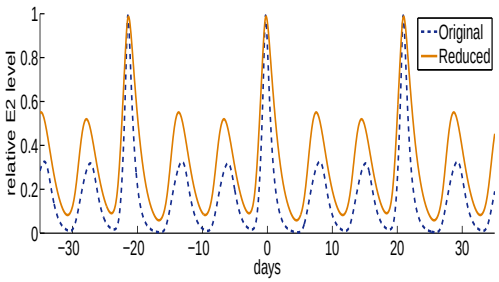

(d) E2

Figure 4.9: Simulation with the original and the reduced bovine model. The blue dashed lines show the course of the hormones as simulated with the original model of 15 ODEs, the orange solid lines show simulations with the reduced model of 10 ODEs

- the variable for oxytocin has been omitted.

In the Appendix, the reduced model for the bovine estrous cycle can be found in Table A.7, together with a list of parameter values (Table A.8) and initial values (Table A.9), that have been used for the simulation depicted in Figure 4.9.

Simulations with the reduced model for a normal cycle show no great difference to the unreduced model for all components. For the variables y_{FSH}, y_{LH}, y_{P4}, and y_{E2}, simulations of both the unreduced and the reduced model are depicted in Figure 4.9. It is remarkable that the system of highly nonlinear ODEs could be reduced by 30% of the equations, and 36.7% of the parameters, while keeping the simulation output for the remaining variables close to the original one.

However, a risk of model reduction is that some effects that can be captured with the original model could no longer be reproduced. The reduced model for the bovine estrous cycle is not able to equally well reproduce the results from the synchronization protocols in Section 2.3. Hence, there are good reasons to use the unreduced model for further applications, but to keep in mind the reduced version for complementary investigations.

Chapter 5

Discrete Modeling of the Bovine Estrous Cycle

Recall that the hormonal cycle is a result of a large feedback loop, whose self-regulation is the result of the complex interactions between multiple components. In this chapter, the regulatory concepts, which generate the periodic changes of the components, are used to develop different discrete modeling approaches.

Quantitative information about numerical parameters, i.e. rate constants or thresholds, is often not available, but information in literature about qualitative behavior is frequent. Therefore, it is convenient to look at qualitative models to describe a biological phenomenon. Already the models developed in the previous chapters are based on qualitative, i.e. regulatory, mechanisms. To get quantitative output and to fit the simulation to measurements, differential equation models were chosen. The numerical parameter values were estimated such that the model simulation best fits the given data points. Although very detailed predictions can be made with these models about the development of certain substances or rate constants, one has to keep in mind that the simulations are performed with a model on a very high abstraction level. Many mechanisms have been left out in the modeling process, and whether or not one has identified and mapped the entire key mechanisms can only be assumed. Also, the identified numerical parameter values are not necessarily unique. Another restriction of the ODE models is that the derived dynamical properties only hold locally for the current set of parameters.

In this chapter, different discrete modeling approaches are used, one partly discrete and another one discrete in both time and space. The dynamical behavior of both model types is illustrated in the *state transition graph* (STG), which consists of all possible states of the system, connected by their transitions. A simulation trajectory of a discrete model is a sequence of states in the STG. Recognition of biological phenomena in the STG is often possible, as we will see in the subsequent sections. How the simulation runs through the states is defined differently in the different model types that will be treated in this chapter.

A particular question of interest regards the global stability of the bovine model with respect to perturbations of variables. For the continuous model, local stability has been investigated in Chapter 4. It has been observed numerically that even for large perturbations of initial values, the simulation always converges to the same limit cycle. A proof of local stability via the computation of the Floquet multipliers has been performed in Section 4.1. Extending this local property to the global behavior of the model is not possible due to the continuous and thus infinitely large phase space. However, proving such a dynamical property globally would be of great interest. In the discrete case, stability can be analyzed via the state transition graph. The dynamical properties of this graph are analyzed in Section 5.2. For a discrete counterpart of the reduced bovine model, stability will be shown in Section 5.4.

In the continuous model, the range of the variables is an interval of real numbers, and the simulation can thus take any value within this uncountable set. In this chapter, this level of detail is not intended, and it is concentrated on the underlying mechanisms of the qualitative periodic behavior. In a discrete model, the variable space is finite and can thus be analyzed easier. It is possible to investigate the whole state space, which is difficult in the continuous model. Besides a global stability analysis, this investigation includes the search for other dynamical properties, e.g. alternative fixed points or attractors. As both the discrete model and its continuous counterpart are based on the same principles it is assumed that these properties also hold for the continuous model.

The continuous and the discrete models are based on the same principles, and all biological information one puts into the models is the same. It is thus important to keep in mind that, when deriving discrete models from the continuous one, no biological information is lost. The models represent different possibilities to describe the same biological phenomenon. The expectation is thus that results regarding the dynamical properties can be transferred to each other.

This chapter focuses on the model of the bovine estrous cycle, but, of course, techniques could be transferred to the human model. A piecewise-affine differential equation model is derived as a first discretization step in Section 5.1. Qualitative simulation leads to a state space that is still too large to explore, thus, a purely discrete model of the estrous cycle is derived and analyzed in Section 5.2.

5.1 Piecewise Affine Differential Equations

Piecewise affine differential equations (PADE), often also referred to as *piecewise-linear models*, have been well studied in mathematical biology [Jon02]. In PADE models, variable behavior is described piecewise via ordinary differential equations, where regulations

Table 5.1: Comparison of the different model types

	ODE	PADE	discrete
variable notation	y_S	X_S	x_S
dynamics	phase space in $\mathbb{R}^n$	domains in phase space	expression level vector
regulations	Hill functions	step functions	interactions
parameters	kinetic parameters	parameter ordering	logical parameters

are incorporated as step functions. Whether a regulation of a variable on another is active is threshold-dependent only.

A logical analysis for qualitative properties of quantitative biochemical networks has been developed by Glass and Kauffmann [GK73]. [MPO95] extended their work and proposed a class of piecewise differential equations to model these dynamics. The basic idea is that the piecewise affine differential equations are only valid locally between thresholds. The thresholds partition the phase space into *domains*, in which the model has different dynamical behavior. In the notation of Snoussi [Sno89], the system of piecewise linear differential equations is of the form

$$\frac{dX_i(t)}{dt} = F_i(X) - c_i X_i, \quad i = 1, 2, ..., n,$$

where $c_i \in \mathbb{R}^*_+$ and each F_i is a positive combination of sums and products of Heaviside functions given for all $X \in \mathbb{R}$ by

$$S^+(X_i, T_i^j) = \begin{cases} 1 & \text{if } X_i \geq T_i^j, \\ 0 & \text{if } X_i < T_i^j. \end{cases}$$

where T_i^j are the thresholds for the activation of influences.

In each domain, the corresponding ODE reduces to an uncoupled, linear differential equation. For a qualitative simulation trajectory of a PADE model it is only decisive between which thresholds T_i^j the variables X_i are, i.e. in which domains the variables are. The simulation is then a sequence of domains, which here will be each represented by the stationary points of a variable X_i. The stationary points are calculated from the combinations of growth and clearance rates that correspond to the linear coefficients in the function F_i above. The procedure will be described in more detail in the following. The resulting finite state graph can be analyzed with methods from discrete math and graph theory.

Recall that the ODE model BovCycle has been constructed based on qualitative information, i.e. it mainly consists of regulatory mechanisms. Therefore, its transformation into a PADE model is mostly straightforward, and the numerical parameter values identified in Chapter 2 can be used. Hill functions in the ODE model are directly transformed into the

step functions S_i.

According to the formalism of Glass and Kauffmann, the parameters in a PADE model are computed as fractions of growth and clearance rates, m_i and c_i. The number of parameters for a variable X_i in the PADE model depends on the number of predecessors of X_i, i.e. the number of regulating variables of X_i that are specified in the function $F_i(X)$ defined above. Depending on how many predecessors X_j of X_i are below or above their thresholds T_i^j for their action on X_i, i.e. depending on whether this predecessor is on or off, the variable X_i has different growth rates. For a PADE variable X_i, where the growth of the corresponding ODE variable y_i is regulated by the variables y_j^1, y_j^2 etc. and the clearance rate constant is c_i in the ODE model, the parameters have the form m_j^1/c_i, m_j^2/c_i, $(m_j^1 + m_j^2)/c_i$, etc.

There are mechanisms regulating the growth term of a variable in the ODE model in Chapter 2 that are not modeled via Hill functions, but instead with a direct proportional relationship. This regulation is converted to the PADE model as if it were originally a Hill function. As the simulations for all variables in the ODE model are on a relative scale, i.e. all simulations are between zero and one, the maximum level is set to be one, and the threshold as 0.5.

For example, the equation (B2) in the ODE model

$$\frac{d}{dt}y_{\mathrm{G}}(t) = \Big(m_{\mathrm{P4\&E2}}\left(1 - h^+(y_{\mathrm{P4}}(t); T_{\mathrm{P4}}^{\mathrm{G},1}, 2)h^+(y_{\mathrm{E2}}(t); T_{\mathrm{E2}}^{\mathrm{G},1}, 2)\right) + m_{\mathrm{P4}}^{\mathrm{G},2}h^-(y_{\mathrm{P4}}(t); T_{\mathrm{P4}}^{\mathrm{G},2}, 2)\Big) \cdot y_{\mathrm{Gh}}(t) \cdot m_{\mathrm{E2}}^{\mathrm{G}} \cdot h^+(y_{\mathrm{E2}}(t); T_{\mathrm{E2}}^{\mathrm{G},2}, 2) - c_{\mathrm{G},2} \cdot y_{\mathrm{G}}(t)$$

transforms to the PADE formulation as follows

$$\begin{aligned}\frac{d}{dt}X_{\mathrm{G}}(t) = {} & m_{\mathrm{P4\&E2}}m_{\mathrm{E2}}^{\mathrm{G}} \cdot (1 - S^+(X_{\mathrm{P4}}(t), T_{\mathrm{P4}}^{\mathrm{G},1}) \cdot S^+(X_{\mathrm{Gh}}(t), 0.5) \cdot S^+(X_{\mathrm{E2}}(t), T_{\mathrm{E2}}^{\mathrm{G},1})) \\ & + m_{\mathrm{P4}}^{\mathrm{G},2}m_{\mathrm{E2}}^{\mathrm{G}} \cdot S^-(X_{\mathrm{P4}}(t), T_{\mathrm{P4}}^{\mathrm{G},2}) \cdot S^+(X_{\mathrm{Gh}}(t), 0.5) \cdot S^+(X_{\mathrm{E2}}(t), T_{\mathrm{E2}}^{\mathrm{G},1})) \\ & - c_{\mathrm{G},2} \cdot X_{\mathrm{G}}(t).\end{aligned}$$

X_{G} has three incoming regulations, X_{Gh}, X_{P4} and X_{E2}. It can grow with the rates $m_{\mathrm{P4\&E2}}m_{\mathrm{E2}}^{\mathrm{G}}$, $m_{\mathrm{P4}}^{\mathrm{G},2}m_{\mathrm{E2}}^{\mathrm{G}}$, and $(m_{\mathrm{P4\&E2}}m_{\mathrm{E2}}^{\mathrm{G}} + m_{\mathrm{P4}}^{\mathrm{G},2}m_{\mathrm{E2}}^{\mathrm{G}})$. The clearance does not depend on other variables, therefore, X_{G} has three different stationary points, $m_{\mathrm{P4\&E2}}m_{\mathrm{E2}}^{\mathrm{G}}/c_{\mathrm{G},2}$, $m_{\mathrm{P4}}^{\mathrm{G},2}m_{\mathrm{E2}}^{\mathrm{G}}/c_{\mathrm{G},2}$, and $(m_{\mathrm{P4\&E2}}m_{\mathrm{E2}}^{\mathrm{G}} + m_{\mathrm{P4}}^{\mathrm{G},2}m_{\mathrm{E2}}^{\mathrm{G}})/c_{\mathrm{G},2}$. As GnRH acts in the model as a regulator of two other variables, it has two activation thresholds, $T_{\mathrm{G}}^{\mathrm{FSH}}$ and $T_{\mathrm{G}}^{\mathrm{LH}}$. For the qualitative simulation of the PADE model it is crucial to order thresholds and stationary points. This can be done with the identified parameter values from the ODE model.

In the following, some more examples for the transformations from ODE to PADE models are given. Equation (B4) for FSH

$$\frac{d}{dt}y_{\mathrm{FSH}}(t) = \big(b_{\mathrm{FSH}} + H^+_{\mathrm{P4,FSH}}(y_{\mathrm{P4}}(t)) + H^-_{\mathrm{E2,FSH}}(y_{\mathrm{E2}}(t) + H^+_{\mathrm{G,FSH}}(y_{\mathrm{G}}(t)\big) \cdot y_{\mathrm{FSHp}}(t) - c_{\mathrm{FSH}} \cdot y_{\mathrm{FSH}}(t)$$

transforms to

$$\begin{aligned}\frac{d}{dt}X_{\mathrm{FSH}}(t) = {} & b_{\mathrm{FSH}} \cdot S^{+}(X_{\mathrm{FSHp}}(t), T_{\mathrm{FSHp}}) \\ & + m_{\mathrm{P4}}^{\mathrm{FSH}} \cdot S^{+}(X_{\mathrm{P4}}(t), T_{\mathrm{P4}}^{\mathrm{FSH}}) \cdot S^{+}(X_{\mathrm{FSHp}}(t), T_{\mathrm{FSHp}}) \\ & + m_{\mathrm{E2}}^{\mathrm{FSH}} \cdot S^{-}(X_{\mathrm{E2}}(t), T_{\mathrm{E2}}^{\mathrm{FSH}}) \cdot S^{+}(X_{\mathrm{FSHp}}(t), T_{\mathrm{FSHp}}) \\ & + m_{\mathrm{G}}^{\mathrm{FSH}} \cdot S^{+}(X_{\mathrm{G}}(t), T_{\mathrm{G}}^{\mathrm{FSH}}) \cdot S^{+}(X_{\mathrm{FSHp}}(t), T_{\mathrm{FSHp}}) \\ & - c_{\mathrm{FSH}} \cdot X_{\mathrm{FSH}}(t)\end{aligned}$$

with the seven stationary points $\frac{b_{\mathrm{FSH}}}{c_{\mathrm{FSH}}}$, $\frac{b_{\mathrm{FSH}}+m_{\mathrm{P4}}^{\mathrm{FSH}}}{c_{\mathrm{FSH}}}$, $\frac{b_{\mathrm{FSH}}+m_{\mathrm{E2}}^{\mathrm{FSH}}}{c_{\mathrm{FSH}}}$, $\frac{b_{\mathrm{FSH}}+m_{\mathrm{G}}^{\mathrm{FSH}}}{c_{\mathrm{FSH}}}$, $\frac{b_{\mathrm{FSH}}+m_{\mathrm{P4}}^{\mathrm{FSH}}+m_{\mathrm{E2}}^{\mathrm{FSH}}}{c_{\mathrm{FSH}}}$, $\frac{b_{\mathrm{FSH}}+m_{\mathrm{P4}}^{\mathrm{FSH}}+m_{\mathrm{G}}^{\mathrm{FSH}}}{c_{\mathrm{FSH}}}$, $\frac{b_{\mathrm{FSH}}+m_{\mathrm{E2}}^{\mathrm{FSH}}+m_{\mathrm{G}}^{\mathrm{FSH}}}{c_{\mathrm{FSH}}}$, $\frac{b_{\mathrm{FSH}}+m_{\mathrm{P4}}^{\mathrm{FSH}}+m_{\mathrm{E2}}^{\mathrm{FSH}}+m_{\mathrm{G}}^{\mathrm{FSH}}}{c_{\mathrm{FSH}}}$, and one activation threshold $T_{\mathrm{FSH}}^{\mathrm{Foll}}$.

Equation (B6) in the ODE model

$$\frac{d}{dt}y_{\mathrm{LH}}(t) = \left(b_{\mathrm{LH}} + m_{\mathrm{G}}^{\mathrm{LH}} \cdot h^{+}(y_{\mathrm{G}}(t), T_{\mathrm{G}}^{\mathrm{LH}}, n_{\mathrm{G}}^{\mathrm{LH}})\right) \cdot y_{\mathrm{LHp}}(t) - c_{\mathrm{LH}} \cdot y_{\mathrm{LH}}(t)$$

transforms to the PADE formulation as follows

$$\frac{d}{dt}X_{\mathrm{LH}}(t) = b_{\mathrm{LH}} \cdot S^{+}(X_{\mathrm{LHp}}, T_{\mathrm{LHp}}) + m_{\mathrm{G}}^{\mathrm{LH}} \cdot S^{+}(X_{\mathrm{G}}, T_{\mathrm{G}}^{\mathrm{LH}}) \cdot S^{+}(X_{\mathrm{LHp}}, T_{\mathrm{LHp}}) - c_{\mathrm{LH}} \cdot X_{\mathrm{LH}}(t).$$

The stationary points for X_{LH} are $b_{\mathrm{LH}}/c_{\mathrm{LH}}$, $(b_{\mathrm{LH}} + m_{\mathrm{G}}^{\mathrm{LH}})/c_{\mathrm{LH}}$, and there is one activation threshold $T_{\mathrm{LH}}^{\mathrm{Ovul}}$.

The equation (B7) for the follicles,

$$\begin{aligned}\frac{d}{dt}y_{\mathrm{Foll}}(t) = {} & m_{\mathrm{FSH}}^{\mathrm{Foll}} \cdot h^{+}\left(y_{\mathrm{FSH}}(t), T_{\mathrm{FSH}}^{\mathrm{Foll}} \cdot h^{+}(y_{\mathrm{Foll}}(t), T_{\mathrm{Foll}}^{\mathrm{Foll}}, n_{\mathrm{Foll}}^{\mathrm{Foll}}), n_{\mathrm{FSH}}^{\mathrm{Foll}}\right) \\ & - \left(m_{\mathrm{P4}}^{\mathrm{Foll}} \cdot h^{+}(y_{\mathrm{P4}}(t), T_{\mathrm{P4}}^{\mathrm{Foll}}, n_{\mathrm{P4}}^{\mathrm{Foll}}) + m_{\mathrm{LH}}^{\mathrm{Ovul}} \cdot h^{+}(y_{\mathrm{LH}}(t), T_{\mathrm{LH}}^{\mathrm{Ovul}}, n_{\mathrm{LH}}^{\mathrm{Ovul}})\right) \cdot y_{\mathrm{Foll}}(t),\end{aligned}$$

has been simplified and converted to

$$\begin{aligned}\frac{d}{dt}X_{\mathrm{Foll}}(t) = {} & 0.5 \cdot m_{\mathrm{FSH}}^{\mathrm{Foll}} \cdot S^{+}(X_{\mathrm{FSH}}(t), T_{\mathrm{FSH}}^{\mathrm{Foll}}) \\ & + 0.5 \cdot m_{\mathrm{FSH}}^{\mathrm{Foll}} \cdot S^{+}(X_{\mathrm{FSH}}(t), T_{\mathrm{FSH}}^{\mathrm{Foll}}) \cdot S^{+}(X_{\mathrm{Foll}}(t), T_{\mathrm{Foll}}^{\mathrm{Foll}}) \\ & - \left(m_{\mathrm{P4}}^{\mathrm{Foll}} \cdot S^{+}(X_{\mathrm{P4}}(t), T_{\mathrm{P4}}^{\mathrm{Foll}}) + m_{\mathrm{LH}}^{\mathrm{Foll}} \cdot S^{+}(X_{\mathrm{LH}}(t), T_{\mathrm{LH}}^{\mathrm{Foll}})\right) \cdot X_{\mathrm{Foll}}(t).\end{aligned}$$

The stationary points are are $0.5m_{\mathrm{FSH}}^{\mathrm{Foll}}/m_{\mathrm{P4}}^{\mathrm{Foll}}$, $0.5m_{\mathrm{FSH}}^{\mathrm{Foll}}/m_{\mathrm{LH}}^{\mathrm{Foll}}$, $0.5m_{\mathrm{FSH}}^{\mathrm{Foll}}/(m_{\mathrm{LH}}^{\mathrm{Foll}} + m_{\mathrm{P4}}^{\mathrm{Foll}})$, $m_{\mathrm{FSH}}^{\mathrm{Foll}}/m_{\mathrm{P4}}^{\mathrm{Foll}}$, $m_{\mathrm{FSH}}^{\mathrm{Foll}}/m_{\mathrm{LH}}^{\mathrm{Foll}}$, and $m_{\mathrm{FSH}}^{\mathrm{Foll}}/(m_{\mathrm{LH}}^{\mathrm{Foll}} + m_{\mathrm{P4}}^{\mathrm{Foll}})$, and the activation thresholds $T_{\mathrm{Foll}}^{\mathrm{Foll}}$, $T_{\mathrm{Foll}}^{\mathrm{E2}}$, and $T_{\mathrm{Foll}}^{\mathrm{Inh}}$. Additionally, $\tilde{T}_{\mathrm{Foll}}^{\mathrm{Ovul}} = 0.5$ is introduced for the regulation of X_{CL}.

Similarly, the equation (B8) describing the development of the CL is in the ODE model

$$\begin{aligned}\frac{d}{dt}y_{\mathrm{CL}}(t) = \mathrm{SF}\cdot m_{\mathrm{LH}}^{\mathrm{CL}}\cdot h^{+}(y_{\mathrm{LH}}(t),T_{\mathrm{LH}}^{\mathrm{CL}},n_{\mathrm{LH}}^{\mathrm{CL}})\cdot y_{\mathrm{Foll}}(t)\\ + m_{\mathrm{CL}}^{\mathrm{CL}}\cdot h^{+}(y_{\mathrm{CL}}(t),T_{\mathrm{CL}}^{\mathrm{CL}},n_{\mathrm{CL}}^{\mathrm{CL}})\\ - m_{\mathrm{IOF}}^{\mathrm{CL}}\cdot h^{+}(y_{\mathrm{IOF}}(t),T_{\mathrm{IOF}}^{\mathrm{CL}},n_{\mathrm{IOF}}^{\mathrm{CL}})\cdot y_{\mathrm{CL}}(t),\end{aligned}$$

converts in the PADE formulation to

$$\begin{aligned}\frac{d}{dt}X_{\mathrm{CL}}(t) = \mathrm{SF}\cdot m_{\mathrm{LH}}^{\mathrm{Ovul}}\cdot S^{+}(X_{\mathrm{LH}}(t),T_{\mathrm{LH}}^{\mathrm{Ovul}})\cdot S^{+}(X_{\mathrm{Foll}}(t),0.5)\\ + m_{\mathrm{CL}}^{\mathrm{CL}}\cdot S^{+}(X_{\mathrm{CL}}(t),T_{\mathrm{CL}}^{\mathrm{CL}})\\ - m_{\mathrm{IOF}}^{\mathrm{CL}}\cdot S^{+}(X_{\mathrm{IOF}}(t),T_{\mathrm{IOF}}^{\mathrm{CL}})\cdot X_{\mathrm{CL}}(t),\end{aligned}$$

with the stationary points $\mathrm{SF}\cdot m_{\mathrm{LH}}^{\mathrm{Ovul}}/m_{\mathrm{IOF}}^{\mathrm{CL}}$, $m_{\mathrm{CL}}^{\mathrm{CL}}/m_{\mathrm{IOF}}^{\mathrm{CL}}$, $(\mathrm{SF}\cdot m_{\mathrm{LH}}^{\mathrm{Ovul}}+m_{\mathrm{CL}}^{\mathrm{CL}})/m_{\mathrm{IOF}}^{\mathrm{CL}}$, and the activation thresholds $T_{\mathrm{CL}}^{\mathrm{CL}}$, $T_{\mathrm{CL}}^{\mathrm{P4}}$, $T_{\mathrm{CL}}^{\mathrm{IOF}}$, and $\tilde{T}_{\mathrm{CL}}^{\mathrm{OT}} := 0.5$.

The conversion for the rest of the variables is straightforward:

$$\begin{aligned}\frac{d}{dt}X_{\mathrm{P4}} &= m_{\mathrm{CL}}^{\mathrm{P4}}\cdot S^{+}(X_{\mathrm{CL}}(t),T_{\mathrm{CL}}^{\mathrm{P4}}) - c_{\mathrm{P4}}\cdot X_{\mathrm{P4}}(t)\\ \frac{d}{dt}X_{\mathrm{E2}} &= m_{\mathrm{Foll}}^{\mathrm{E2}}\cdot S^{+}(X_{\mathrm{Foll}}(t),T_{\mathrm{Foll}}^{\mathrm{E2}}) - c_{\mathrm{E2}}\cdot X_{\mathrm{E2}}(t)\\ \frac{d}{dt}X_{\mathrm{Inh}} &= m_{\mathrm{Foll}}^{\mathrm{Inh}}\cdot S^{+}(X_{\mathrm{Foll}}(t),T_{\mathrm{Foll}}^{\mathrm{Inh}}) - c_{\mathrm{Inh}}\cdot X_{\mathrm{Inh}}(t)\\ \frac{d}{dt}X_{\mathrm{Enz}} &= m_{\mathrm{P4}}^{\mathrm{Enz}}\cdot S^{+}(X_{\mathrm{P4}}(t),T_{\mathrm{P4}}^{\mathrm{Enz}}) - c_{\mathrm{Enz}}\cdot X_{\mathrm{Enz}}(t)\\ \frac{d}{dt}X_{\mathrm{IOF}} &= m_{\mathrm{PGF}}^{\mathrm{IOF}}\cdot S^{+}(X_{\mathrm{PGF}}(t),T_{\mathrm{PGF}}^{\mathrm{IOF}})\cdot S^{+}(X_{\mathrm{CL}}(t),T_{\mathrm{CL}}^{\mathrm{IOF}}) - c_{\mathrm{IOF}}\cdot X_{\mathrm{IOF}}(t)\\ \frac{d}{dt}X_{\mathrm{OT}} &= m_{\mathrm{E2}}^{\mathrm{OT}}\cdot S^{+}(X_{\mathrm{E2}}(t),T_{\mathrm{E2}}^{\mathrm{OT}})\cdot S^{+}(X_{\mathrm{CL}}(t),\tilde{T}_{\mathrm{CL}}^{\mathrm{OT}}) - c_{\mathrm{OT}}\cdot X_{\mathrm{OT}}(t)\\ \frac{d}{dt}X_{\mathrm{PGF}} &= m_{\mathrm{OT}}^{\mathrm{PGF}}\cdot S^{+}(X_{\mathrm{OT}}(t),T_{\mathrm{OT}}^{\mathrm{PGF}})\cdot S^{+}(X_{\mathrm{Enz}}(t),T_{\mathrm{Enz}}^{\mathrm{PGF}}) - c_{\mathrm{PGF}}\cdot X_{\mathrm{PGF}}(t)\end{aligned}$$

For the simulation, the thresholds for each variable need to be ordered. In the notation of [Sno89], the mapping $\pi_i(j)$ gives the number of the position of the threshold T_i^j within the ascending ordered thresholds of X_i. The *interaction graph* is defined as the directed graph (X, E), which consists of nodes $X = \{X_1 = X_{\mathrm{GnRHH}}, \ldots, X_{15} = X_{\mathrm{PGF}}\}$, and edges $(i, j, w_{ij}) \in E$. For specification of the edges, i indicates the activating substance, j the substance that is being regulated and $|w_{ij}| = \pi_i(j)$. The sign of w_{ij} depends on whether the interaction is stimulatory $(+)$ or inhibitory $(-)$.

An circuit in the interaction graph is *negative*, if the number of negative, i.e. inhibitory, edges is odd.

On the way during the translation of an ODE model into a PADE formulation, theoretical results can be used to derive parameter constraints for the continuous model, which is described in the following. Prerequisite for periodic behavior can be derived for simpler PADE systems. The corresponding theorem has been stated in [Sno89].

Theorem ([Sno89])**.** *Given an n-dimensional system of piecewise linear equations*

$$\frac{dX_i(t)}{dt} = m_i S^{\alpha_i}(X_{i-1}, T^i_{i-1}) - c_i X_i, \quad i = 1, 2, ...N, N > 1,$$

for which the interaction graph is a negative circuit m_i, c_i, T_i are strictly positive, $\alpha_i \in \{+, -\}$ and indices are taken modulo N, then it holds: If for all i, $m_i/c_i > T_i^{i+1}$, then, for $N \geq 3$, there is an asymptotically stable limit cycle.

A necessary condition for the parameters to result in a periodic solution is thus

$$\frac{m_i}{c_i} > T_i^j,$$

where m_i are the coefficients of the step functions, c_i the clearance constants, and T_i^j the thresholds of the step functions where X_i is the source variable, and X^j the regulated substance.

Transforming this theorem to more complex networks, where variables have more than one predecessor and more than one successor, like the system of ODEs in BovCycle, would be of great interest. Derived parameter constraints could be used in the parameter identification algorithm for the continuous model. This way, the parameter space can be reduced by not considering non-periodic solutions. Intuitively, in the more complex setting, a necessary condition for periodic behavior is that, for all variables in a PADE model, the above inequality has to be fulfilled for at least one quotient and one activation threshold. Whenever a variables has several predecessors, several quotients are associated with its development, as explained above. Now, for every variable one claims that the maximum of the corresponding quotients is larger or equal to the minimum of all its activation thresholds. Until now, there is no proof of such a condition, thus the following results need to be taken with caution. However, so far the constraints yield good results in practical computations.

The following inequalities are assumed to be necessary in order to have periodic behavior

in BovCycle

$$\frac{m_{\mathrm{P4\&E2}} m^{\mathrm{G}}_{\mathrm{E2}} + m^{\mathrm{G},2}_{\mathrm{P4}} m^{\mathrm{G}}_{\mathrm{E2}}}{c_{\mathrm{G},2}} > \min(T^{\mathrm{FSH}}_{\mathrm{G}}, T^{\mathrm{LH}}_{\mathrm{G}})$$

$$\frac{b_{\mathrm{FSH}} + m^{\mathrm{FSH}}_{\mathrm{P4}} + m^{\mathrm{FSH}}_{\mathrm{E2}} + m^{\mathrm{FSH}}_{\mathrm{G}}}{c_{\mathrm{FSH}}} > T^{\mathrm{Foll}}_{\mathrm{FSH}}$$

$$\frac{(b_{\mathrm{LH}} + m^{\mathrm{LH}}_{\mathrm{G}})}{c_{\mathrm{LH}}} > T^{\mathrm{Ovul}}_{\mathrm{LH}}$$

$$\max(\frac{m^{\mathrm{Foll}}_{\mathrm{FSH}}}{m^{\mathrm{Foll}}_{\mathrm{P4}}}, \frac{m^{\mathrm{Foll}}_{\mathrm{FSH}}}{m^{\mathrm{Foll}}_{\mathrm{LH}}}) > \min(T^{\mathrm{Foll}}_{\mathrm{Foll}}, T^{\mathrm{E2}}_{\mathrm{Foll}}, T^{\mathrm{Inh}}_{\mathrm{Foll}}, \tilde{T}^{\mathrm{Ovul}}_{\mathrm{Foll}})$$

$$\frac{(\mathrm{SF} \cdot m^{\mathrm{Ovul}}_{\mathrm{LH}} + m^{\mathrm{CL}}_{\mathrm{CL}})}{m^{\mathrm{CL}}_{\mathrm{IOF}}} > \min(T^{\mathrm{CL}}_{\mathrm{CL}}, T^{\mathrm{P4}}_{\mathrm{CL}}, T^{\mathrm{IOF}}_{\mathrm{CL}}, \tilde{T}^{\mathrm{OT}}_{\mathrm{CL}})$$

$$\frac{m^{\mathrm{P4}}_{\mathrm{CL}}}{c_{\mathrm{P4}}} > \min(T^{\mathrm{G},1}_{\mathrm{P4}}, T^{\mathrm{G},2}_{\mathrm{P4}}, T^{\mathrm{FSH}}_{\mathrm{P4}}, T^{\mathrm{LH}}_{\mathrm{P4}}, T^{\mathrm{Foll}}_{\mathrm{P4}}, T^{\mathrm{Enz}}_{\mathrm{P4}})$$

$$\frac{m^{\mathrm{E2}}_{\mathrm{Foll}}}{c_{\mathrm{E2}}} > \min(T^{\mathrm{G},1}_{\mathrm{E2}}, T^{\mathrm{G},2}_{\mathrm{E2}}, T^{\mathrm{FSH}}_{\mathrm{E2}}, T^{\mathrm{LH}}_{\mathrm{E2}}, T^{\mathrm{OT}}_{\mathrm{E2}})$$

$$\frac{m^{\mathrm{Inh}}_{\mathrm{Foll}}}{c_{\mathrm{Inh}}} > T^{\mathrm{FSH}}_{\mathrm{Inh}}$$

$$\frac{m^{\mathrm{Enz}}_{\mathrm{P4}}}{c_{\mathrm{Enz}}} > T^{\mathrm{PGF}}_{\mathrm{Enz}}$$

$$\frac{m^{\mathrm{OT}}_{\mathrm{E2}}}{c_{\mathrm{OT}}} > T^{\mathrm{PGF}}_{\mathrm{OT}}$$

$$\frac{m^{\mathrm{IOF}}_{\mathrm{PGF\&CL}}}{c_{\mathrm{IOF}}} > T^{\mathrm{CL}}_{\mathrm{IOF}}$$

$$\frac{m^{\mathrm{PGF}}_{\mathrm{Enz\&OT}}}{c_{\mathrm{PGF}}} > T^{\mathrm{CL}}_{\mathrm{PGF}}$$

The simulation of the PADE model for BovCycle is performed with the software Genetic Network Analyzer (GNA) presented in [JGHP03]. This tool is based on a qualitative simulation method, which uses qualitative relations in form of parameter inequalities, in contrast to the specified numerical parameter values in quantitative simulation tools. In order to obtain a PADE description in GNA for the bovine estrous cycle, the parameter values of the validated ODE model are used to derive the parameter ordering, i.e. the qualitative constraints in the PADE model, as described above. Besides the qualitative simulation of a model, i.e. the derivation of the state transition graph, several analysis tools are implemented in GNA, e.g. attractor search or model-checking for the automated verification of dynamical properties.

For the implementation of the bovine model in GNA, basic degradation rates have to be specified for the variables whose decay is regulated only by other substances, X_{Foll} and

X_{CL}, in order to avoid the case of no degradation.

For the model of the bovine estrous cycle, simulations with the PADE model still lead to a state graph that is too large to analyze in straightforward manner. However, PADE models are in principle a practical tool to analyze systems based on regulatory networks. A different discretization procedure which only considers regulatory information is presented and focused on in the rest of this chapter.

5.2 A Purely Discrete Model

Purely discrete, i.e. discrete in time and state space, models for biological systems have been used extensively [Jon02]. In [Tho73], a formalism has been developed that will be used in the following. Roughly, a logical model consists of a regulatory graph, where substances are depicted as nodes, and interactions between them are shown in arcs. The simulation with a purely discrete model is a sequence of vectors representing discrete states of the system.

In the ODE models treated in the previous chapters, interactions between biological substances were modeled as regulatory (stimulatory or inhibitory) mechanisms. As the action of the substances is assumed to be threshold dependent, the substances can be modeled as discrete variables as will be explained. Starting with the validated continuous model, interactions between the variables are derived from the signs of the coefficients of the Jacobian of the ODE model.

The simplest way to develop a discrete model is to use boolean formalization as in [Tho73], where variables are considered to be either on or off. As soon as variables have more than one influence on other variables, a multilevel logical approach is better suited, where variables can take more than two values. A formalism for such models has also been introduced by Thomas [Tho91]. This framework has been used by several other researchers. In particular, a software called GINsim has been developed that is based on this formalism and that will be used in this Chapter to analyze the bovine model developed in Chapter 2 and 3. Before going into the details of transferring a particular ODE model, the formalism for multilevel logical models will be introduced.

According to [CRMT03], a regulatory graph consists of

- a finite set of elements $X = \{x_{S_1}, \ldots, x_{S_n}\}$,
- a set of positive integers for each of the elements $\{m_1, ..., m_n\}$, representing the *maximum expression level* of each element, i.e. the maximum possible value it can take. The integer m_i is thus the number of different actions the variable x_{S_i} takes

on other variables or itself. In the boolean case, the set $\{m_1, ..., m_n\}$ would consist of only ones,

- an *influence graph* $(X, \mathcal{T})$ consisting of vertices (variables) $x_{S_i} \in X$ which are connected by labeled arcs (interactions) $T_{ij} \in \mathcal{T}$. The *label* (A, q) that is assigned to each arc specifies the interaction. A is an integer interval which indicates the values for which the source variable is *functional*, i.e. active, on this arc, and the sign of interaction q indicating whether this influence is an activation/stimulation or an inhibition.

Every interaction $T_{ij} \in \mathcal{T}$ is described by a quadruple $T_{ij} = (x_{S_i}, x_{S_j}, A(T_{ij}), q(T_{ij}))$, i.e. by its source x_{S_i}, its target x_{S_j}, and its label $(A(T_{ij}), q(T_{ij}))$. The interval $A(T_{ij}) = [a_{\min}(T_{ij}), a_{\max}(T_{ij})]$, with $a_{\min} > 0$, $a_{\max}(T_{ij} \leq m_i$, indicates the expression levels of x_{S_i} on this interaction. These expression levels could also be a set of disjoint intervals, if different signs of the interaction are assumed depending on the value of the source variable. $q(T_{ij})$ denotes the sign of the interaction, i.e. whether it is inhibitory or stimulatory.

To explicitly describe the interactions, *logical functions* are used. Let $\mathcal{I}_j$ denote the set of all incoming, thus all active, interactions into x_{S_j}. A logical function K_j maps any subset of incoming interactions $I \subset \mathcal{I}_j$ to an expression level of x_{S_j}. The expression level $K_j(I)$, $0 \leq K_j(I) \leq m_j$, is called *logical parameter* of the model. $K_j(\emptyset)$ can be greater than zero if $\mathcal{I}_j$ contains inhibiting interactions, which lead to an increase of the expression level if not functional.

A subset of the incoming interactions I of a variable is called *admissible* if it does not contain interactions having the same source. Therefore, all information of an interaction must be stored in the label, and different actions are described via the label consisting eventually of several disjoint intervals. If I_j is not an admissible subset of the incoming interactions for x_{S_j}, then $K_j(I_j) = 0$. In the following, every state will be provided with an admissible set of active interactions, thus, not-admissible sets will not play a role.

This formalism is now used to derive a discrete model of the bovine estrous cycle. The state transition graph, which consists of all possible trajectories of the simulation, thus all possible states connected by their transitions, follows directly from the regulatory graph. For the bovine model, this will be presented in the following sections.

5.2.1 BovCycle in Discrete Time and Space

In this Section, the development of a purely discrete model for the bovine estrous cycle is described in detail, followed by an analysis of the model with the software GINsim. The continuous model developed in Chapter 2 is discretized using a multilevel logical formalism.

Each real-valued variable y_{S_i}, $i = 1, ..., 15$ of the ODE model is now represented by a discrete counterpart x_{S_i}, which is depicted as vertex in an influence graph. According to the formalism of Thomas, the regulatory graph for BovCycle consists of the finite set of elements

$$\begin{aligned} X &= (x_{S_i})_{i=1,...,15} \\ &= (x_{\mathrm{GnRHH}}, x_{\mathrm{GnRH}}, x_{\mathrm{FSHP}}, x_{\mathrm{FSH}}, x_{\mathrm{LHP}}, x_{\mathrm{LH}}, x_{\mathrm{Fol}}, x_{\mathrm{PGF}}, x_{\mathrm{CL}}, x_{\mathrm{P4}}, x_{\mathrm{E2}}, x_{\mathrm{Inh}}, x_{\mathrm{Enz}}, x_{\mathrm{OT}}, x_{\mathrm{IOF}}), \end{aligned}$$

a set of maximum expression levels $(m_i)_{i=1,...,15}$, and a label-oriented influence graph $(X, \mathcal{T})$.

The labels $(A(T_{ij}), q(T_{ij}))$ for the transitions $T_{ij} \subset \mathcal{T}$ in the influence graph, in particular the intervals $A(T_{ij})$, mostly follow directly from the the maximum expression levels, which will be derived in the next subsection. Prior to the maximum expression levels, the set of interactions $\mathcal{T} = \{T_{ij}, T_{ij} = (x_{S_i}, x_{S_j})\}$ is derived, together with the signs $q(T_{ij})$ of the interactions.

Thus, according to the preceding definition, the discrete version of BovCycle also requires

- an influence graph, consisting of variables and transitions,
- a maximum expression level for each variable,
- a label for each transition,
- a set of logical parameters specifying the interactions.

These parts of the model will be derived in the following.

Derivation of the Influence Graph

An influence graph is derived for the ODE system from its Jacobian matrix with respect to the variables. According to the definition in [FS08] the influence graph associated to a reaction model is the graph having as vertices the substances, and as edge-set the following two kinds of edges:

$$\left\{ A \text{ activates } B \mid \frac{\delta y'_B}{y_A} > 0 \text{ in some point} \right\}$$
$$\left\{ A \text{ inhibits } B \mid \frac{\delta y'_B}{y_A} < 0 \text{ in some point} \right\}$$

The signs of the Jacobian define the type of interaction between the two discrete variables x_{S_i} an x_{S_j}. This directly gives the values for the $q(T_{ij})$, and indirectly the set $\mathcal{T} = \{T_{ij}, q(T_{ij}) \neq 0)\}$. The nonzero entries of the Jacobian matrix with respect to the variables for the derived ODE system for the bovine cycle can be found in the Appendix.

Based on this matrix, the - not yet fully labeled - influence graph can be derived. Since the ODE system is nonlinear, the entries in the Jacobian still depend on multiple variables. Thus, several considerations have to be made in order to determine the signs of the matrix entries. In BovCycle, all variables are normalized such they that take values on a relative scale. Therefore, they are always between zero and one. In particular, all variables are positive. The signs of the Jacobian can be calculated as will be described in the following.

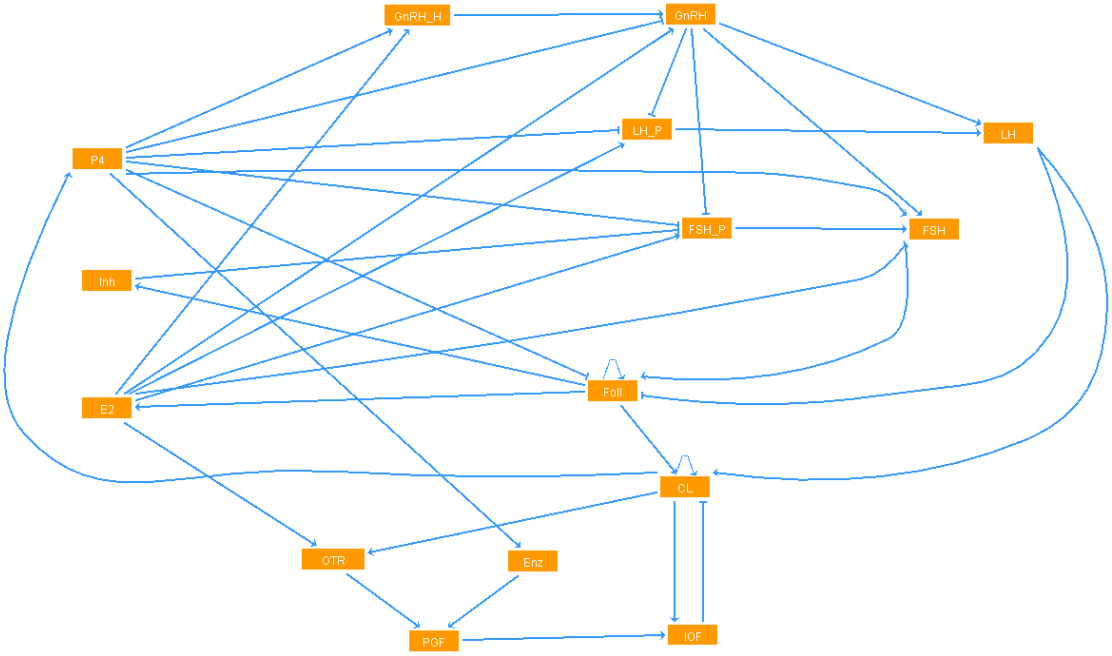

Figure 5.1: Influence graph derived from the Jacobian, leaving out the negative self-influences due to exponential decay

Most of the entries in the Jacobian $J_{y_{S_i},y_{S_j}}$, $i,j = 1,\ldots,n$, are zero, indicating no influence between the two substances S_i and S_j. If nonzero, the entries in the Jacobian of the bovine model are mostly sums and products of either only positive or only negative terms, therefore the translation to the discrete model is straightforward, as can be explained in an example.

The first column of the Jacobian, which represents the influence of GnRH in the hypothalamus on other substances, only has nonzero entries in the first two lines. Transferring this to the discrete formalism, y_{GnRHH} only has two targets: itself and y_{GnRH}.

$$J_{1,1} = J_{y_{GnRHH},y_{GnRHH}} = \frac{-0.17\left(y_{p4}^2+0.082\right)\left(y_{p4}^2+2.3\right)y_{e2}^2 - 0.021\left(y_{p4}^2+0.12\right)\left(y_{p4}^2+0.12\right)}{\left(y_{e2}^2+0.0094\right)\left(y_{p4}^2+0.064\right)\left(y_{p4}^2+0.12\right)}.$$

All summands of $J_{1,1}$ have a negative sign, thus $J_{1,1} < 0$, and the self-influence of y_{GnRHH} is negative. In contrast,

$$J_{1,2} = J_{y_{\mathrm{GnRH}},y_{\mathrm{GnRHH}}} = \frac{0.99y_{\mathrm{E2}}^5\left(\left(0.37y_{\mathrm{P4}}^2+0.031\right)y_{\mathrm{E2}}^2+0.019\left(y_{\mathrm{P4}}^2+0.12\right)^2\right)}{\left(y_{\mathrm{E2}}^2+0.0094\right)\left(y_{\mathrm{E2}}^5+0.11\right)\left(y_{P4}^2+0.064\right)\left(y_{\mathrm{P4}}^2+0.12\right)},$$

only consists of summands with a positive sign, thus $J_{1,1} > 0$, and y_{GnRHH} has an activating effect on y_{GnRH}. The rest of the matrix entries can be analyzed in the same way, as long as all summands have the same sign.

In some cases however, a sum of positive and negative terms occurs in the Jacobian, which requires a closer look. These entries are $J_{1,10}$ (influence of y_{P4} on y_{GnRHH}), $J_{2,10}$ (influence of y_{P4} on y_{GnRH}), $J_{2,11}$ (influence of y_{E2} on y_{GnRH}), $J_{7,7}$ (self-influence of the follicles), $J_{9,9}$ (self-influence of the CL). For the first three of these, it can be numerically observed that for any value of y_{P4} and y_{E2}, the sign never changes. It holds $J_{1,10} = \frac{\delta y'_{\mathrm{GnRHH}}}{\delta y_{\mathrm{P4}}} > 0$, $J_{2,10} = \frac{\delta y'_{\mathrm{GnRH}}}{\delta y_{\mathrm{P4}}} < 0$, and $J_{2,11} = \frac{\delta y'_{\mathrm{GnRH}}}{\delta y_{\mathrm{E2}}} > 0$ for all $y_{\mathrm{P4}}, y_{\mathrm{E2}} \in [0,1]$.

The sign of the other two entries of the Jacobian with alternating summand signs, $J_{7,7} = J_{y_{\mathrm{Fol}},y_{\mathrm{Fol}}}$ and $J_{9,9} = J_{y_{\mathrm{CL}},y_{\mathrm{CL}}}$, changes depending on the values of the influencing variables. Considering $y_{\mathrm{P4}}, y_{\mathrm{LH}}, y_{\mathrm{Fol}}, y_{\mathrm{FSH}}, y_{\mathrm{IOF}}, y_{\mathrm{CL}} \in [0,1]$, it can be observed numerically that

$$J_{7,7} = -\frac{1.1y_{\mathrm{P4}}^5}{y_{\mathrm{P4}}^5+0.000032} - \frac{3.5y_{\mathrm{LH}}^2}{y_{\mathrm{LH}}^2+0.029} + \frac{0.0017y_{\mathrm{Fol}}y_{\mathrm{FSH}}^2}{\left(y_{\mathrm{Fol}}^2+0.048\right)^3\left(y_{\mathrm{FSH}}^2+\frac{0.00076}{\left(y_{\mathrm{Fol}}^2+0.048\right)^2}\right)^2} \in [-4.5, 68.53],$$

and

$$J_{9,9} = -\frac{41.y_{iof}^5}{y_{\mathrm{IOF}}^5+4.0} + \frac{0.071y_{\mathrm{CL}}}{y_{\mathrm{CL}}^2+0.010} - \frac{0.071y_{\mathrm{CL}}^3}{\left(y_{\mathrm{CL}}^2+0.010\right)^2} \in [-8.2, 0.2303].$$

These two mechanisms, the self-influence of the follicles and the corpus luteum, can be either positive or negative, depending on the values of the influencing substances.

The first two summands in $J_{7,7}$ are in $[-4.5, 0]$ and thus account for the negative effect in the self-influence of the Follicles. The third summand is in $[0, 68.53]$, and is thus responsible for the positive feedback. Whenever the third summand is larger than the sum of the first two, there is a stimulatory effect.

In $J_{9,9}$, the summand depending on y_{IOF} is in $[-8.2, 0]$, thus responsible for the negative influence in CL, while the two summands depending on y_{CL} only are in $[0, 0.2302]$ and account for the positive effect of CL on itself.

Summarizing, the signs in the Jacobian are

$$sign(J) = \begin{pmatrix}
- & 0 & 0 & 0 & 0 & 0 & 0 & 0 & 0 & + & + & 0 & 0 & 0 & 0 \\
+ & - & 0 & 0 & 0 & 0 & 0 & 0 & 0 & - & + & 0 & 0 & 0 & 0 \\
0 & - & - & 0 & 0 & 0 & 0 & 0 & 0 & - & + & - & 0 & 0 & 0 \\
0 & + & + & - & 0 & 0 & 0 & 0 & 0 & + & - & 0 & 0 & 0 & 0 \\
0 & - & 0 & 0 & - & 0 & 0 & 0 & 0 & - & + & 0 & 0 & 0 & 0 \\
0 & + & 0 & 0 & + & - & 0 & 0 & 0 & 0 & 0 & 0 & 0 & 0 & 0 \\
0 & 0 & 0 & + & 0 & - & +/- & 0 & 0 & - & 0 & 0 & 0 & 0 & 0 \\
0 & 0 & 0 & 0 & 0 & 0 & 0 & - & 0 & 0 & 0 & 0 & + & + & 0 \\
0 & 0 & 0 & 0 & 0 & + & + & 0 & +/- & 0 & 0 & 0 & 0 & 0 & - \\
0 & 0 & 0 & 0 & 0 & 0 & 0 & 0 & + & - & 0 & 0 & 0 & 0 & 0 \\
0 & 0 & 0 & 0 & 0 & 0 & + & 0 & 0 & 0 & - & 0 & 0 & 0 & 0 \\
0 & 0 & 0 & 0 & 0 & 0 & + & 0 & 0 & 0 & 0 & - & 0 & 0 & 0 \\
0 & 0 & 0 & 0 & 0 & 0 & 0 & 0 & 0 & + & 0 & 0 & - & 0 & 0 \\
0 & 0 & 0 & 0 & 0 & 0 & 0 & 0 & + & 0 & + & 0 & 0 & - & 0 \\
0 & 0 & 0 & 0 & 0 & 0 & 0 & + & + & 0 & 0 & 0 & 0 & 0 & -
\end{pmatrix}$$

The diagonal part of this matrix consists of mostly negative signs, indicating a negative self-influence of the corresponding variables. This is due to the assumed exponential decay of each variable. In the discrete model, this effect can be included as a reset to zero in case of no influence, which allows to leave out these negative self-destroyance properties. The resulting interactions are displayed in Figure 5.1.

Derivation of Maximum Expression Levels and Labels

In many discrete modeling approaches, variables take as many discrete values as they have influences on other variables. A variable with four successors has five possible values, indicating the different levels of action. In the piecewise affine approach presented in Section 5.1, the change of a variable from one value to another follows from a piecewise defined differential equation attached to this variable. In a purely discrete model, all changes occur only due to the regulatory mechanisms. Here, it could occur that obtaining as many values for a variable as it has successors is not straightforward to realize. If a variable has fewer incoming regulations than required actions, a self-influence of this variable might become necessary. For example, x_{E2} is influencing four other variables, but is itself only preceded by x_{Fol}, which may have a different number of possible values. To make x_{E2} four-valued, the influence of x_{Fol} would have to be remodeled. To avoid a jump from the expression level $x_{\mathrm{E2}} = 0$ to $x_{\mathrm{E2}} = 4$, a possibility to get four different values is to include several positive self-influences of x_{E2}. However, at which values to start the self-stimulation and where to include the influence of the follicles is not straightforward and not considered in this thesis.

To keep this difficulty as small as possible, and on the way simplify the discrete model, it is desirable to have many variables binary valued. The number of values that a variable

can take is decided individually as follows.

Most of the variables are assumed to be in an *on* or an *off* state. For example, when GnRH is *on*, it promotes the release of the gonadotropins, when LH is *on* it promotes ovulation. Every FSH wave corresponds to an *on*-state and promotes the growth of the follicles. For variables with one target only, it is convenient to take a binary variable in the discrete model, indicating whether the corresponding substance is active or not. Thus, for x_{GnRHH}, x_{LHP}, x_{FSHP}, x_{LH}, x_{FSH}, x_{OT}, x_{Enz}, x_{PGF}, x_{IOF}, and x_{Inh} binary valued variables are chosen.

The remaining variables having more than one target are x_{GnRH}, x_{E2}, x_{P4}, x_{CL}, and x_{Fol}. In the continuous model, GnRH influences FSH release before it affects LH release in the sense that the parameter that represents the threshold for the FSH stimulation is lower. However, both the maximum stimulatory influence and the Hill exponent are higher in the LH influence. Since it is not clear from literature which action of GnRH, LH or FSH release, requires higher or lower GnRH levels, we assume that this is the same and take x_{GnRH} as binary.

x_{E2} has four successors in the influence graph. Arguing with the biological background, the influence of estradiol on the three-wave appearing FSH release can be considered as the same for all waves. Regarding the influence of estradiol on GnRH and LH, which peak only once a cycle, this can interpreted as being due to P4. For these both successors, E2 and P4 are taking action together, and their effect is opposed. P4 is inhibitory whenever there is a stimulatory effect of E2, such that the different profile of the peak-like hormones and E2 does not require a certain E2 behavior to account for it, but can be achieved by the combination of E2 and P4 influences. Regarding the E2 influence on OT, the argument is similar: while OT is not automatically high when E2 is, it requires both E2 and a high CL to react. Which of the successors reacts to which levels of estradiol is not clear, thus E2 is taken as binary valued.

The variable x_{P4} even has five successors, but is nevertheless taken as binary valued in the discrete model, due to the same reasons as x_{E2}. Since it is not clear in which sequence the successors of x_{P4} are affected by its value, the possibly different order is neglected, and it is assumed that x_{P4} is either *on* or *off*.

For x_{CL} and x_{Fol}, the order of influences cannot be neglected, since they themselves belong to their successors. These two variables are the only ones in the model containing a positive self-influence, which can only be achieved after having reached a non-off state. Therefore, these two variables are taken as three-valued.

The preceding discussion can also be approached via the Jacobian matrix and its signs, i.e. the influence graph. Whenever the sign of an entry of the Jacobian is always positive or negative, respectively, the influencing variable is sufficient to be binary, as its action is either *off*, or it is positive or negative, respectively.

The entry in the Jacobian for y_{CL} is only depending on two variables, y_{IOF} and y_{CL}. One can observe in a 3d-plot that depending on y_{CL}, for any value of y_{IOF}, the value of y_{CL} is first increasing, reaches its maximum shortly afterwards, and then declines due to the decay term to its original low value. Therefore, we take y_{CL} three valued, and assume a negative self-influence for low values ($y_{\mathrm{CL}} = 0$), a positive effect for medium values ($y_{\mathrm{CL}} = 0$), and a negative effect for high values ($y_{\mathrm{CL}} = 0$) which will only become active in presence of IOF.

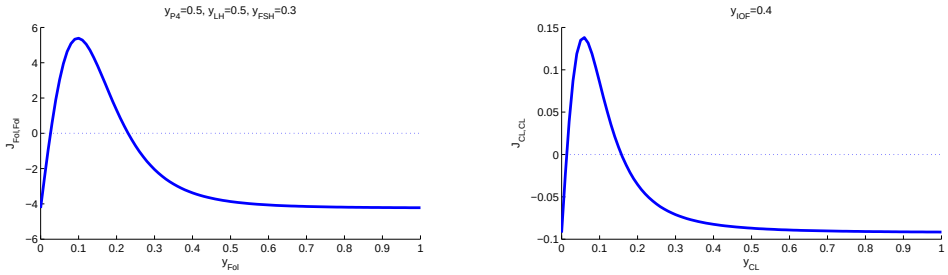

(a) $J_{7,7} = J_{\mathrm{Fol,Fol}}$ (b) $J_{9,9} = J_{\mathrm{CL,CL}}$

Figure 5.2: Development of the self-influence of the y_{Fol} and y_{CL} in the ODE model, depending on the current value. As the entries of the Jacobian are alternating negative and positive for fixed values of the other influencing substances, these two variables are chosen to be three-valued in the discrete model.

Summarizing, all variables in the discrete model except x_{CL} and x_{Fol} are modeled as binary. Thus, the maximum expression levels are $m_1 = m_{\mathrm{GnRHH}} = 1$, $m_2 = m_{\mathrm{GnRH}} = 1$, $m_3 = m_{\mathrm{FSHP}} = 1$, $m_4 = m_{\mathrm{FSH}} = 1$, $m_5 = m_{\mathrm{LHP}} = 1$, $m_6 = m_{\mathrm{LH}} = 1$, $m_7 = m_{\mathrm{Fol}} = 2$, $m_8 = m_{\mathrm{PGF}} = 1$, $m_9 = m_{\mathrm{CL}} = 2$, $m_{10} = m_{\mathrm{P4}} = 1$, $m_{11} = m_{\mathrm{E2}} = 1$, $m_{12} = m_{\mathrm{Inh}} = 1$, $m_{13} = m_{\mathrm{Enz}} = 1$, $m_{14} = m_{\mathrm{OT}} = 1$, $m_{15} = m_{\mathrm{IOF}} = 1$.

The labels $(A(T_{ij}), q(T_{ij}))$ for the above derived influence graph are now straightforward to determine. The signs of the interactions $q(T_{ij})$ are already depicted in the influence graph. As most of the variables are binary, the interval $A(T_{ij})$ for which an interaction can be functional is usually [1], as the influence a binary variable takes on its successors is either *on* or *off*, and 0 does not activate an interaction. Thus, the maximum expression levels are 1. For the non-binary variables x_{Foll} and x_{CL}, it has to be decided at which level they act on their targets. It is assumed that the expression level $x_{\mathrm{Foll}} = 1$ is needed to start further follicular growth, and that only at higher levels, $x_{\mathrm{Foll}} = 2$, the follicles become functional and produce steroids. Thus $A(T_{7,7}) = [1]$, $A(T_{7,11}) = [2]$,$A(T_{7,12}) = [2]$. Further, it is assumed that $x_{\mathrm{CL}} = 1$ already activates progesterone production, while higher CL levels are needed to activate variables involved in luteolysis, i.e. not until the level $x_{\mathrm{CL}} = 2$, the CL impacts x_{OT} and x_{IOF}. It follows that $A(T_{9,9}) = [1]$, $A(T_{9,10}) = [1]$, $A(T_{9,14}) = [2]$, $A(T_{9,15}) = [2]$.

Interplay of the Mechanisms - Derivation of the Logical Parameters

For every substance $x_{S_j}, j = 1, ..., 15$, the logical function K_j associates an integer $K_j(I)$ to any admissible subset I of I_j. These logical parameters $K_j(I)$ will be derived in this subsection.

For the variables with only one predecessor (x_{P4}, x_{E2}, x_{Inh}, and x_{Enz}), i.e. only one incoming arc, regulation is obvious and can be directly derived from the above signs of the Jacobian. In contrast, whenever a variable has more than one predecessor, specifications need to be made about how the incoming actions function together to regulate this variable. The right hand sides of the corresponding ODEs are considered in order to derive the concurrence of the regulations in the discrete model. In particular, one can decide whether the incoming regulatory mechanisms are merged with *AND* or *OR*. The Hill functions in the right hand sides of the ODEs can easily be used to derive the regulation of the corresponding discrete variable. An increasing Hill function stands for activation, a decreasing Hill function for inhibition. If a variable affects another variable directly and not via a Hill function, e.g. in case of proportional release into another compartment, this effect is taken as an activation.

If only the rise and not the decay of a continuous variable is regulated by other variables, the discrete interplay of these variables is straightforward: If the Hill functions or direct effects are multiplied, in the discrete model this is translated to an *AND*-relation, while a summation of effects is taken as an *OR*-relation.

The rise of the continuous counterparts for the variables x_{PGF}, x_{OT}, and x_{IOF} is modeled via products of two increasing Hill functions. Therefore, the incoming regulations in the discrete model both need to be active to result in a stimulation of the variables. The development of the variables x_{GnRH}, x_{FSH}, and x_{LH} can be derived via the combination of *AND*- and *OR*-relations, as the rise of the corresponding continuous variables is modeled via sums and products of Hill functions or direct effects.

If both rise and decay of a variable are regulated by other substances, which is the case for x_{GnRHH}, x_{FSHP}, x_{LHP}, x_{Foll}, and x_{CL}, the interplay of the incoming mechanisms is not as straightforward. For a start, examine only the binary variables x_{GnRHH}, x_{FSHP}, and x_{LHP}. A translation scheme from the numerical to the discrete model is derived in the following.

Recall that in an ODE model, Hill functions represent smooth switches. In the discrete model, the switches are sharp. In the boolean case, one neglects the different maximum levels of the Hill functions, and takes the switches as either *on* or *off*. This is represented by variables which are either one or zero. Assume that an ODE has the form

$$y'(t) = a - b \cdot y(t),$$

where a and b are either one or zero, representing the original Hill functions as being *on* or *off*, respectively. Since the expression level of a discrete variable x is not explicitly time-dependent, the value of $y(t)$ as $t \to \infty$ is considered.

For $b \neq 0$, the solution of the above ODE

$$y(t) = \frac{a}{b} + \exp(-b \cdot t) \cdot C_{y_0} \qquad \overset{t\to\infty}{\longrightarrow} \qquad \frac{a}{b},$$

where C_{y_0} is a constant. The limit of $y(t)$ thus depends on the relation of the constants a and b. For $a = 0$, $y(t) \to 0$.

For $b = 0$, the solution of the ODE

$$y(t) = a \cdot t + C_{y_0} \quad \overset{t\to\infty}{\longrightarrow} \begin{cases} \infty, & a \neq 0 \\ C_{y_0}, & a = 0. \end{cases}$$

The four cases for the boolean variables a and b are considered to derive the value of $y(t)$, and subsequently the value of the corresponding discrete variable x. If $a = 1$ and $b = 1$, $y(t) \to 1$. If $a = 0$ and $b = 1$. $y(t) \to 0$. For $a = 1$ and $b = 0$, $y(t) \to \infty$, which in the boolean case is set to $\infty =: 1$. Finally, for $a = 0$ and $b = 0$, $y(t) = C_{y_0}$, which is set to $C_{y_0} := 0$, assuming that the variable rather decays than growths.

The translation scheme is thus

$$y'_C = H^+(y_A) - H^+(y_B) \cdot y_C \rightsquigarrow \begin{cases} x_C = 1, & \text{if } x_A = 1 \wedge x_B = 1 \\ x_C = 1, & \text{if } x_A = 1 \wedge x_B = 0 \\ x_C = 0, & \text{if } x_A = 0 \wedge x_B = 1 \\ x_C = 0, & \text{if } x_A = 0 \wedge x_B = 0 \end{cases}$$

The expression level of the variable x_C is thus mainly controlled by the variables regulating the rise term. For GnRH, FSH, and FSH, the rise term thus controls the value of the variable in the first compartment. The release term, in contrast, controls the substance in the succeeding compartment.

A basal level $K_j(\emptyset)$ is defined for each variable x_{s_j}, representing the level it takes when all incoming mechanisms are *off*. As an exponential decay with a constant decay rate is included for many variables in the ODE model, the basal level of most of the variables is set to zero. Exceptions are the variables that have a decreasing Hill function in the control of their rise. For these variables, a constant growth term is assumed that is inhibited via the Hill function. The variables only decay when the growth inhibiting substance is *on*. When the inhibiting substance is *off*, the resulting variable rises, thus the basal level is set to the maximum level. In the Bovine model, the variables with an inhibiting control on their rise are x_{GnRHH}, x_{FSHP}, and x_{LHP}. The basal level for these three variables is set to one.

The growth term of y_{GnRH} constitutes of a multiplication of several mechanisms, the GnRH release, activation of GnRH, and of E2. Since the release is only *on* if $x_{\mathrm{P4}} = 0 \wedge x_{\mathrm{E2}} = 1$, the only case where $x_{\mathrm{GnRH}} = 1$ is when $x_{\mathrm{P4}} = 0 \wedge x_{\mathrm{E2}} = 1 \wedge x_{\mathrm{GnRHH}} = 1$. The basal value, i.e. the value that is obtained if none of the incoming regulations is active, $x_{\mathrm{P4}} = 0 \wedge x_{\mathrm{E2}} = 0 \wedge x_{\mathrm{GnRHH}} = 0$, is thus $x_{\mathrm{GnRH}} = 0$.

The variable x_{LHP} is regulated by x_{E2}, x_{P4}, and x_{GnRH}. The right hand side of the ODE is translated as

$$
\begin{aligned}
y'_{\mathrm{LHP}} =& H^+(y_{\mathrm{E2}}) + H^-(y_{\mathrm{P4}}) - H^+(y_{\mathrm{GnRH}}) \cdot y_{\mathrm{LHP}} \\
\rightsquigarrow & \begin{cases}
x_{\mathrm{LHP}} = 1, & \text{if } (x_{\mathrm{E2}} = 1 \vee x_{\mathrm{P4}} = 0) \wedge x_{\mathrm{GnRH}} = 1 \\
x_{\mathrm{LHP}} = 1, & \text{if } (x_{\mathrm{E2}} = 1 \vee x_{\mathrm{P4}} = 0) \wedge x_{\mathrm{GnRH}} = 0 \\
x_{\mathrm{LHP}} = 0, & \text{if } \underbrace{\neg(x_{\mathrm{E2}} = 1 \vee x_{\mathrm{P4}} = 0)}_{x_{\mathrm{E2}}=0 \wedge x_{\mathrm{P4}}=1} \wedge x_{\mathrm{GnRH}} = 1 \\
x_{\mathrm{LHP}} = 0, & \text{if } x_{\mathrm{E2}} = 0 \wedge x_{\mathrm{P4}} = 1 \wedge x_{\mathrm{GnRH}} = 0.
\end{cases}
\end{aligned}
$$

The only situations that lead to $x_{\mathrm{LHP}} = 1$ is thus when either $x_{\mathrm{E2}} = 1 \wedge x_{\mathrm{P4}} = 1 \wedge x_{\mathrm{GnRH}} = 0$ or $x_{\mathrm{E2}} = 1 \wedge x_{\mathrm{P4}} = 0 \wedge x_{\mathrm{GnRH}} = 0$. The basal value, i.e. the value that x_{LHP} gets if $x_{\mathrm{E2}} = 0 \wedge x_{\mathrm{P4}} = 0 \wedge x_{\mathrm{GnRHH}} = 0$, is thus $x_{\mathrm{LHP}} = 1$.

The interplay of the mechanisms that control x_{LH} is straightforward, as its rise is only controlled by x_{LHP} and x_{GnRH}. Due to the basal release, GnRH is not needed to switch on x_{LH}. The two cases $x_{\mathrm{LHP}} = 1 \wedge x_{\mathrm{GnRH}} = 0$ and $x_{\mathrm{LHP}} = 1 \wedge x_{\mathrm{GnRH}} = 1$ lead to $x_{\mathrm{LH}} = 1$, its basal value is $x_{\mathrm{LH}} = 0$.

The variable y_{FSHP} in the continuous model is derived from the interplay of x_{Inh}, x_{P4}, x_{E2}, and x_{GnRH}, and the right hand side of the ODE is translated as

$$
\begin{aligned}
y'_{\mathrm{FSP}} =& H^-(y_{\mathrm{Inh}}) - (H^+(y_{\mathrm{P4}}) + H^-(y_{\mathrm{E2}}) + y_{\mathrm{GnRH}}) \\
\rightsquigarrow & \begin{cases}
x_{\mathrm{FSHP}} = 1, & \text{if } x_{\mathrm{Inh}} = 0 \wedge (x_{\mathrm{P4}} = 1 \vee x_{\mathrm{E2}} = 0 \vee x_{\mathrm{GnRH}} = 1) \\
x_{\mathrm{FSHP}} = 1, & \text{if } x_{\mathrm{Inh}} = 0 \wedge x_{\mathrm{P4}} = 0 \wedge x_{\mathrm{E2}} = 1 \wedge x_{\mathrm{GnRH}} = 0 \\
x_{\mathrm{FSHP}} = 0, & \text{if } x_{\mathrm{Inh}} = 1 \wedge (x_{\mathrm{P4}} = 1 \vee x_{\mathrm{E2}} = 0 \vee x_{\mathrm{GnRH}} = 1) \\
x_{\mathrm{FSHP}} = 0, & \text{if } x_{\mathrm{Inh}} = 1 \wedge x_{\mathrm{P4}} = 0 \wedge x_{\mathrm{E2}} = 1 \wedge x_{\mathrm{GnRH}} = 0.
\end{cases}
\end{aligned}
$$

The basal value is thus $K_3(\emptyset) = K_{\mathrm{FSHP}}(\emptyset) = 1$, which is obtained in the first of the above cases. Furthermore, the variable x_{FSHP} is activated whenever x_{Inh} is *off*.

Regulation of x_{FSH} is again straightforward, its basal value is $K_4(\emptyset) = K_{\mathrm{FSH}}(\emptyset) = 0$, and it is activated if either only x_{FSHP} is *on* (due to the basal release term), or if $x_{\mathrm{FSHP}} = 1 \wedge x_{\mathrm{P4}} = 1$, $x_{\mathrm{FSHP}} = 1 \wedge x_{\mathrm{GnRH}} = 1$, or $x_{\mathrm{FSHP}} = 1 \wedge x_{\mathrm{P4}} = 1 \wedge x_{\mathrm{GnRH}} = 1$. Its basal value is thus $x_{\mathrm{FSH}} = 0$.

x_{Fol} is getting activated by x_{FSH}, and grows further to the expression level $x_{\mathrm{Fol}} = 2$ even without the help of x_{FSH} (growing sensitivity of the follicles to FSH). This is in contrast to the continuous model, where for any growth of the follicles, FSH is needed in eventually very little amounts. The choice to neglect the need for FSH at a certain stage of follicular development has been made to guarantee the development of the follicles to a final stage. Only if the follicles have reached this final stage ($x_{\mathrm{Fol}} = 2$), P4 can promote atresia, or LH promotes ovulation, and thus its decay to $x_{\mathrm{Fol}} = 0$. All combinations need to be specified in the software, such that the overall interplay of the mechanisms is, written with logical parameters:

$I \subset \mathcal{I}_{\mathrm{Fol}}$	$K_{\mathrm{Fol}}(I)$
$x_{\mathrm{FSH}} = 1$	1
$x_{\mathrm{FSH}} = 1 \wedge x_{\mathrm{P4}} = 1$	1
$x_{\mathrm{FSH}} = 1 \wedge x_{\mathrm{LH}} = 1$	1
$x_{\mathrm{Fol}} = 1 \wedge x_{\mathrm{FSH}} = 1$	2
$x_{\mathrm{Fol}} = 1 \wedge x_{\mathrm{FSH}} = 1 \wedge x_{\mathrm{P4}} = 1$	2
$x_{\mathrm{Fol}} = 1 \wedge x_{\mathrm{FSH}} = 1 \wedge x_{\mathrm{LH}} = 1$	2
$x_{\mathrm{Fol}} = 1$	2
$x_{\mathrm{Fol}} = 2$	2
$x_{\mathrm{Fol}} = 2 \wedge x_{\mathrm{FSH}} = 1$	2
$x_{\mathrm{Fol}} = 2 \wedge x_{\mathrm{FSH}} = 1 \wedge x_{\mathrm{P4}} = 1$	2
$x_{\mathrm{Fol}} = 2 \wedge x_{\mathrm{FSH}} = 1 \wedge x_{\mathrm{LH}} = 1$	2
all other interactions	0

Note that in presence of FSH, both $x_{\mathrm{P4}} = 1$ and $x_{\mathrm{LH}} = 1$ do not indicate the decay of the follicles. Only if both active, $x_{\mathrm{P4}} = 1 \wedge x_{\mathrm{LH}} = 1$, the follicles decline even though $x_{\mathrm{FSH}} = 1$.

The variable x_{CL} rises from zero at ovulation, thus if LH levels are high and follicles ready for ovulation, $x_{\mathrm{LH}} = 1 \wedge x_{\mathrm{Fol}} = 2$. It stays at the same expression level as long as $x_{\mathrm{LH}} = 1$, in order to admit the decline of LH before any further self-growth. If solely $x_{\mathrm{CL}} = 1$, this self-growth leads to a rise to $x_{\mathrm{CL}} = 2$. $x_{\mathrm{IOF}} = 1$ promotes the decay of $x_{\mathrm{CL}} = 2$ to zero. The logical parameters leading to the different expression levels of x_{CL} are thus

$I \subset \mathcal{I}_{\mathrm{CL}}$	$K_{\mathrm{CL}}(I)$
$x_{\mathrm{LH}} = 1 \wedge x_{\mathrm{Fol}} = 2$	1
$x_{\mathrm{LH}} = 1 \wedge x_{\mathrm{CL}} = 1$	1
$x_{\mathrm{LH}} = 1 \wedge x_{\mathrm{CL}} = 1 \wedge x_{\mathrm{Fol}} = 2$	1
$x_{\mathrm{CL}} = 1$	2
$x_{\mathrm{CL}} = 1 \wedge x_{\mathrm{Fol}} = 2$	2
$x_{\mathrm{CL}} = 2$	2
$x_{\mathrm{CL}} = 2 \wedge x_{\mathrm{Fol}} = 2$	2
$x_{\mathrm{CL}} = 2 \wedge x_{\mathrm{LH}} = 1$	2
$x_{\mathrm{CL}} = 2 \wedge x_{\mathrm{LH}} = 1 \wedge x_{\mathrm{Fol}} = 2$	2
all other interactions	0

This completes the derivation of the discrete model. Simulation of the model corresponds to computing the state transition graph, which consists of all states, connected by all possible transition between them. In the following, simulations are often started from a particular initial state. The graph that is calculated with the simulation is thus a subgraph of the STG, comprising all states and transitions that are reachable from the particular initial state. This graph is called *reachability graph*

Different update strategies can be chosen for the simulation, e.g. asynchronous update, where only one step after another is performed, leading to a change of one variable in each step. Time is not explicitly included in the simulation. Even for small models, asynchronous update eventually leads to a very complex STG. Note that the dynamics of the discrete model with asynchronous update is non-deterministic in the way that, usually, from the current state of the simulation, several transitions are possible.

Choosing a synchronous update implies the update of all possible changes based on the current variable set within the next step. This usually omits several states and leads to a smaller and thus better arranged STG. Another possibility to perform the update is to define priority classes of variables that are updated before others. Within these priority classes, synchronous or asynchronous update can be chosen. It is important to keep in mind that the steady states are the same for all update strategies.

Validation of the Derived Discrete Model

To check whether the discrete model captures the right behavior, i.e. the behavior of the numerical model, the output of the ODE simulation is translated to a sequence of discrete stages, and the results are compared via *model checking*. Model checking is a technique to verify certain properties of a finite system with the help of temporal logic. Typically, it is tested whether a model (the finite system) can verify a logical formula (describing the property). Here, it is tested whether the discrete model can run through the sequence of states from the ODE simulation, provided that asynchronous update is chosen.

What is needed for the model checking procedure is a time series that potentially corresponds to an output of the above described model. The time series thus comprises a sequence of states of 13 binary and two three-valued variables. To derive this sequence of states, the output of the ODE model derived in Section 2 is used. For simplification, the simulation with the parameterization for a two-wave cow is used. An approximation of the continuous solution is thus available as a time series of real-valued variables.

For the translation of the real-valued time series into a binary and three-valued one, thresholds are chosen for the continuous variables y_{S_i}. With these thresholds, discrete values can be derived for all continuous variables that depend on whether they are above or below these values. For the binary variables, one thresholds is needed, while for the three-valued variables, x_{Fol} and x_{CL}, two thresholds are needed. In the following, these thresholds are called *translation thresholds*. Thus, for the system of 15 ODEs, 17 thresholds are needed.

The parameters from the ODE model that represent biological thresholds are used. Furthermore, translation thresholds are derived as follows:

- Whenever a substance acts on exactly one other substance via a Hill function, the threshold of the Hill function is used as translation threshold.

- When a substance is influencing several others in the ODE model via Hill functions, the mean value of the Hill thresholds is taken as translation threshold.

- When a substance is influencing other variables directly, not via Hill functions, the mean of the numerical simulation for this substance is taken as translation threshold.

- Due to the smoothness of the switches in the numerical model, for the simulation of the ODE model, the threshold does not need to be fully reached in order to already have an impact the succeeding variable. Therefore, the mean of the threshold and the numerical solution is calculated and taken as final translation threshold for the real-valued variables.

The output of the continuous simulation, a time series of real-valued variables, can now be compared with the thresholds to derive a time series of boolean or three-valued variables, depending on whether the simulation is below or above the thresholds. After elimination of double entries, this result can be compared to the state transition graph of the above derived model.

With model checking, it can be tested whether it is possible for the discrete model to run through the generated sequence of states. The software NuSMV has been used, which is a symbolic model checker for the verification of finite state systems [CCGR00]. The result is:

For the discretized model, there is a trajectory that runs through the specified time series derived from the ODE model. This validates the above derived discretization.

5.3 Analysis of the Discrete Dynamics

A remarkable property of the ODE system of the bovine estrous cycle is its stability with respect to different starting values or perturbations of the variables, as well as its large parameter range that results in the same limit cycle. For the continuous case, the proof of local stability as in Section 4.1 cannot be extended to show global stability. For the discrete model, however, such kind of behavior can be analyzed globally.

Stability for discrete event dynamical systems has been discussed in [Sob91]. Given a set of states E, a state x of a discrete system is called E-stable, if all trajectories go through E in a finite number of transitions, and then visit E infinitely often. A set of states is stable if all elements are stable. Here, due to the chosen asynchronous update strategy, proving stability for the derived model is not possible due to the multiple state transitions which lead to several cycles in the STG. The simulation trajectory could stay in these cycles for infinitely many steps, and does not necessarily go through other states. However, the ability of the system to visit E in a finite number of transition can be analyzed.

The above derived model description for the bovine estrous cycle is implemented in GINsim, described in [NBF+09]. GINsim is a simulation software for qualitative modeling and analysis of regulatory models. It is based on the multilevel logical formalism introduced in [Tho91], which was used above to derive the discrete model formulation. In GINsim, besides the simulation with a regulatory model, i.e. the computation of its state transition graph, several analysis tools for the model dynamics are included: computation of the strongly connected components (SCC) graph, i.e. the subgraph of states that are each reachable from another, as well as path finding to search for particular state transitions. With the simulation of a model, GINsim computes the number of steady states, which is of great interest here.

Another tool that GINsim comprises is the investigation of circuit functionality, a property derived from the structure of the regulatory concepts. After the calculation of the number of circuits in the model, the circuit functionality analysis provides information in the interaction graph about whether these circuits are positive, negative, or functional. With this information, the combination of interactions responsible for periodic behavior can be found. Due to the high number of circuits in the bovine model, this analysis is omitted here.

GINsim has been used in a variety of work. [NBF+09] describes an introduction to logical

modelling with GINsim. [ST+03] develops a model which describes the paths between cells, taking into consideration a dozen molecular components. Depending on the initial state, different steady states are reached. Disturbances are analyzed and a feedback circuit analysis is performed. Such an analysis is also promising for the hormonal cycle models.

In [AJOK09], a four-variable model is analyzed with a logical approach, and *logical bifurcation diagrams* are derived. It is shown that the essential dynamics of this small model can be captured by the balance between positive and negative circuits of the regulatory network. Different dynamical properties are associated with the different circuits, positive circuits lead to multistationarity, and negative circuits result in homeostasis and oscillations. The model is finally translated into an ODE model, preserving the dynamical properties. An interesting - and possibly similar to BovCycle - property is that two oscillatory regimen have been observed in this small model.

In Figure 5.3, the reachability graph computed with synchronous update for the bovine model is depicted. Starting in a state that is part of the time series derived above, after a certain number of steps, the simulation reaches a limit cycle. Examining the states in this limit cycle, one can observe that some variables oscillate and some stay constant. This implies that synchronous update does not capture the dynamics of the continuous model for the bovine estrous cycle, where all variables are oscillatory.

Starting the simulation with asynchronous update from a particular initial state that is taken from the automated time series derived in the previous subsection, namely from

$$\begin{aligned}\widehat{x} = \{&x_{\mathrm{GnRHH}} = 0, x_{\mathrm{GnRH}} = 1, x_{\mathrm{FSHP}} = 1, x_{\mathrm{FSH}} = 1, x_{\mathrm{LHP}} = 1, x_{\mathrm{LH}} = 0, x_{\mathrm{Foll}} = 2,\\ &x_{\mathrm{PGF}} = 0, x_{\mathrm{CL}} = 0, x_{\mathrm{P4}} = 0, x_{\mathrm{E2}} = 1, x_{\mathrm{Inh}} = 1, x_{\mathrm{Enz}} = 0, x_{\mathrm{OT}} = 0, x_{\mathrm{IOF}} = 0\},\end{aligned}$$

leads to a reachability graph of 68864 nodes. If no initial state is specified, all possible states are taken as starting point for the simulation, and the resulting STG consists of 73728 nodes. Note that the reachability graph for any initial state is always a subgraph of the STG. An important result of the simulation is:

No fixed points are detected.

For all combinations of values for the variables, i.e. any disturbances of the variables, the simulation thus never reaches a steady state.

The reachability graph for the initial state $\widehat{x}$ is too large to visualize, but computation of the corresponding SCC graph gives more information about the dynamics. The SCC graph for the reachability graph that is computed with GINsim starting from the initial state above, consists of only one component. This means that within the 68864 nodes, all nodes are reachable from another, and they are together an attractor of the model.

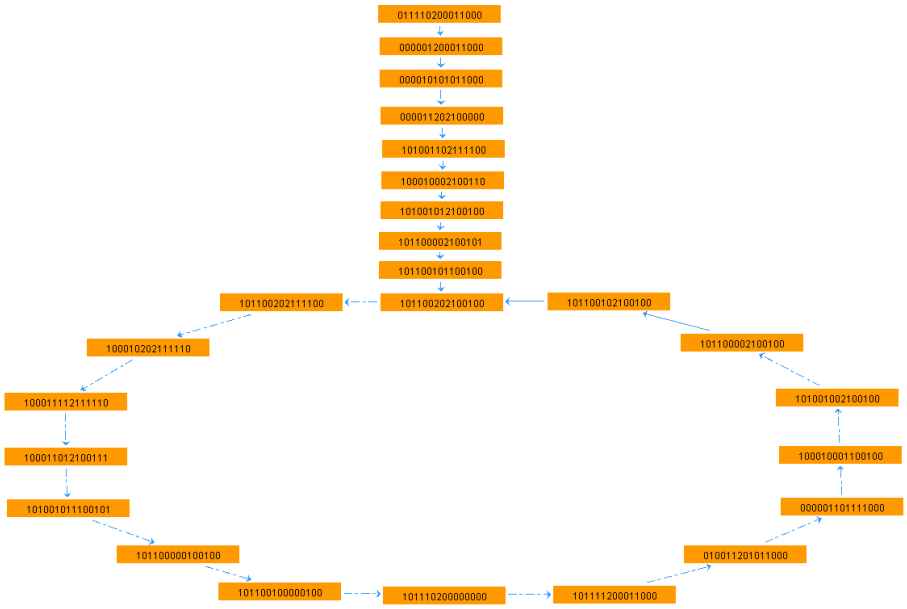

Figure 5.3: Reachability graph calculated with synchronous update for the discrete unreduced bovine model. Starting from the initial state $\widehat{x} = \{(x_{\mathrm{GnRHH}}, x_{\mathrm{GnRH}}, x_{\mathrm{FSHP}}, x_{\mathrm{FSH}}, x_{\mathrm{LHP}}, x_{\mathrm{LH}}, x_{\mathrm{Foll}}, x_{\mathrm{PGF}}, x_{\mathrm{CL}}, x_{\mathrm{P4}}, x_{\mathrm{E2}}, x_{\mathrm{Inh}}, x_{\mathrm{Enz}}, x_{\mathrm{OT}}, x_{\mathrm{IOF}}) = (0, 1, 1, 1, 1, 0, 2, 0, 0, 0, 1, 1, 0, 0, 0)\}$, a cyclical attractor is reached within several steps. Some variables are oscillatory, but others stay constant throughout this simulation trajectory.

The test whether there is another initial state that leads to another attractor can be performed with NuSMV. For this, the state $\widehat{x}$ is taken, it is tested whether the computational tree logic (CTL) formula $AG(EF(\widehat{x}))$ (all globally: exists finally: $\widehat{x}$) is fulfilled for all possible states. This is tested for all possible initial states. The answer is yes, i.e. starting from every state, along any possible outgoing path, $\widehat{x}$ is reached. This implies that there is exactly one attractor, and $\widehat{x}$ lies in this attractor.

Summarizing:

The time series calculated from the simulation with the ODE model with a two-wave parameterization lies in the only attractor of the discrete model.

A Modified Version of the Model

Recall that cows have different number of follicular waves per cycle, as discussed in Section 4.2. It has been shown that the model from above is able to simulate the behavior of a two-wave cow. For a three-wave cow, it is probable that the regulations in the model are different during the first and the second follicular wave. Therefore, mechanisms need to be adjusted. Recall that the model has to capture the effect that the second follicular wave, as the first one, undergoes regression, and the ovulation then takes place in the third wave. Looking at the simulation output for a three-wave cow of the continuous model, a difference between the levels of the variables during the second and the third follicular wave is that y_{Enz}, and as consequence y_{PGF} and y_{IOF} are not yet high enough to cause luteolysis. Thus, the corpus luteum still produces progesterone which represses the follicles. After luteolysis, progesterone decreases and the dominant follicle can continue to grow until ovulation.

Translating the activation levels to the discrete model, it follows that x_{P4} has to perform two different different actions, and thus gets two different action levels. As soon as it rises, it suppresses x_{GnRH} and x_{LH}, but only after the first wave it starts to activate x_{Enz}, which, together with x_{OT} and via x_{PGF} and x_{IOF} cause luteolysis after the second follicular wave.

The model from above is modified in two points: the variable x_{P4} is not binary anymore, but instead three-valued. It is directly regulated by the three-valued x_{CL}, and has the described two action levels. Also, since the follicles only act when their level is $x_{\mathrm{Foll}} = 2$, the intermediate step $x_{\mathrm{Foll}} = 1$ is not necessary, and in the modified version of the model the variable is modeled as binary.

As with the former version of the model, to validate the discrete model, a time series is generated from the output of the continuous model, now with the parameterization that leads to a three-wave cow. The threshold $T_{\mathrm{P4}}^{\mathrm{Enz}}$ is used as extra threshold for y_{P4} to get a three-valued sequence of states for x_{P4}. For the follicles, $T_{\mathrm{Foll}}^{\mathrm{FSH}}$ is used as only threshold to

generate a sequence of states for the now binary variable x_{Foll}. With NuSMV it is confirmed that the new model version can generate the new time series.

Running the modified version of the model starting from a particular initial state leads to a reachability graph of 70912 nodes, and its SCC graph again consists of only one component. Thus, there is one attractor. If the initial state is not specified, the derived STG consists of 73728 nodes, but the corresponding SCC graph consist of 1609 nodes, i.e. not all states are reachable from another. The important result in both cases is:

The modified model has no fixed points for any possible initial state.

As above, to test whether there is another attractor for any initial state, i.e. for any perturbation of variables, a particular state from the derived time series is taken,

$$\begin{aligned}\widehat{x}^{mod} = \{&x_{\text{GnRHH}} = 0, x_{\text{GnRH}} = 1, x_{\text{FSHP}} = 0, x_{\text{FSH}} = 0, x_{\text{LHP}} = 1, x_{\text{LH}} = 1, x_{\text{Foll}} = 1,\\ &x_{\text{PGF}} = 0, x_{\text{CL}} = 0, x_{\text{P4}} = 0, x_{\text{E2}} = 1, x_{\text{Inh}} = 1, x_{\text{Enz}} = 0, x_{\text{OT}} = 0, x_{\text{IOF}} = 0\}.\end{aligned}$$

With NuSMV the CTL formula $AG(EF(\widehat{x}^{mod}))$ (all globally: exists finally: $\widehat{x}^{mod}$) is checked. Again, the answer is yes. Thus, there is exactly one attractor, and $\widehat{x}^{mod}$ lies in this attractor.

Summarizing:

The time series calculated from the simulation with the ODE model with a three-wave parameterization lies in the unique attractor of the modified discrete model.

Hence, the above derived discretization of BovCycle has been validated, in the sense that the model is able to generate the appropriate sequence of states. Also, for all starting values there is the same attractor, and the time series lies within this unique attractor.

Since the simulation with the discrete model is non-deterministic, it is not known whether every possible trajectory necessarily runs through the specified sequence of states, and whether it inevitably leads to a cyclical solution. However, as the generated sequence of states is cyclical, i.e., oscillatory in all components, it is now known that the attractor includes trajectories that are cyclical in all components.

Due to the non-deterministic simulation, a proof of global stability in the sense of [Sob91] is not possible. However, the potential to show stable behavior is given, since for both versions of the discrete model, no steady states are ever reached with the simulation. Also, any perturbation of the simulation always ends up in the only attractor of the model. One can conclude:

The system is designed for oscillatory behavior. Also, any perturbation can potentially find back to the observed behavior.

To learn more about the model and the generated trajectories, the derived discrete model is reduced to its core components to explore the STG even better.

5.4 Model Reduction

It could be possible that the stability of the cycle models might come from a certain coupling of the underlying regulatory mechanisms. To better understand the oscillation of the system, to look into the core structure of the model, reduction of the model dimension can be performed. Specific model reduction techniques lead to a smaller model with less variables which still displays the essential dynamical properties. In particular, the limit cycles observed in the STG of a reduced model can be related to limit cycles in the original STG, and the underlying key dynamics can be identified. The reduction procedure for the discrete model is described in the following.

Most model reduction techniques are based on steady-state assumptions or mass conservation laws. Neither of these prerequisites are fulfilled in our models, thus these techniques are not applicable here.

The STG of the above derived model for the bovine estrous cycle, calculated with asynchronous update, is too large to visualize. Therefore, it seems reasonable to have a look at a discrete version of the reduced ODE model derived in Section 4.4. This model consists of 10 ODEs, and discretization happens according to the same principles as above. The simulation is here started from the initial state $\widehat{x}^a = \{x_{\mathrm{G}} = 1, x_{\mathrm{FSH}} = 1, x_{\mathrm{LH}} = 0, x_{\mathrm{Foll}} = 2, x_{\mathrm{PGF}} = 0, x_{\mathrm{CL}} = 0, x_{\mathrm{P4}} = 0, x_{\mathrm{E2}} = 1, x_{\mathrm{Inh}} = 1, x_{\mathrm{IOF}} = 0\}$. The reachability graph for $\widehat{x}^a$ with asynchronous update still has 2176 nodes, no stable states, and the SCC graph still consists of one component. The SCC could either represent a cyclical attractor, or the simulation could lead to chaotic behavior.

To make a next reduction step, the regulatory mechanisms of the graph are examined. The variables that have only one predecessor are omitted, and the arcs are modified in the way that the incoming arc is redirected to all successors of the eliminated variable. For the bovine model, this leads to an elimination of x_{P4}, x_{E2} and x_{Inh}. The new influence graph is depicted in Figure 5.4(b). The new reachability graph, starting from $\widehat{x}^b = \{x_{\mathrm{G}} = 1, x_{\mathrm{FSH}} = 1, x_{\mathrm{LH}} = 0, x_{\mathrm{Foll}} = 2, x_{\mathrm{PGF}} = 0, x_{\mathrm{CL}} = 0, x_{\mathrm{IOF}} = 0\}$ contains 216 nodes, there are still no steady states, and its SCC graph has exactly one component.

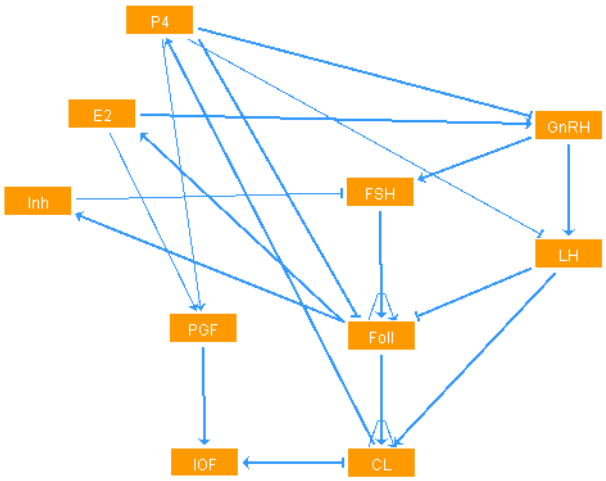

(a) Step 1: Discretization of reduced ODE model derived in Section 4.4

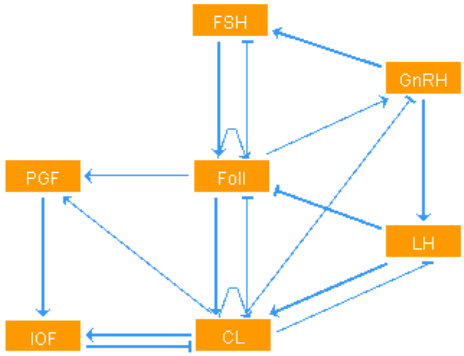

(b) Step 2: Elimination of variables that have only one incoming arc

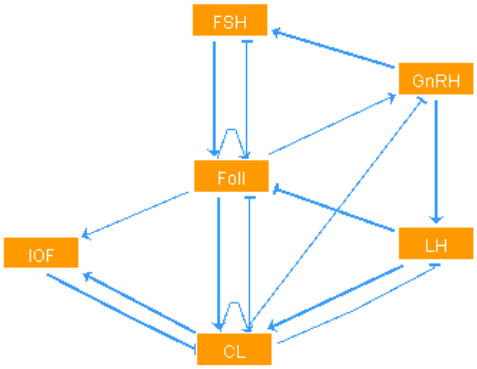

(c) Step 3: Elimination of variables with only one outgoing arc without direct feedback

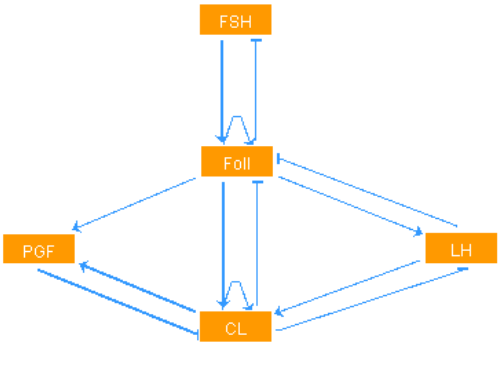

(d) Step 4: Elimination of variables not involved in any direct feedback

Figure 5.4: Influence graphs throughout the different steps of the discrete reduction

The next reduction step eliminates x_{PGF}, the only variable that has a single target without direct feedback mechanism. The interplay of the predecessors of x_{PGF}, $x_{\mathrm{Fol}} = 2$ and $x_{\mathrm{CL}} = 1$, is now redirected to its target, x_{IOF}, see Figure 5.4(c). As x_{IOF} is already influenced by $x_{\mathrm{CL}} = 2$, and an *AND*-relation was between x_{PGF} and $x_{\mathrm{CL}} = 2$, x_{IOF} is now activated if $x_{\mathrm{Fol}} = 2 \wedge x_{\mathrm{CL}} = 2$. The resulting reachability graph with asynchronous update, starting from $\widehat{x}^c = \{x_{\mathrm{G}} = 1, x_{\mathrm{FSH}} = 1, x_{\mathrm{LH}} = 0, x_{\mathrm{Foll}} = 2, x_{\mathrm{PGF}} = 0, x_{\mathrm{CL}} = 0, x_{\mathrm{IOF}} = 0\}$ consists of 108 nodes, and there is still exactly one strongly connected component, which implies that there is exactly one cyclical attractor.

Since 108 nodes are still difficult to interpret, another reduction step is performed. In the continuous simulation, y_{GnRH} and y_{LH} have a similar pattern, thus merging the two discrete counterparts is reasonable. In the discrete model, x_{GnRH} is the only remaining variable without direct feedback with any of its successors or predecessors. Therefore, this variable is omitted. The regulation of x_{LH} by x_{GnRH} is now performed by the predecessors of x_{GnRH}, $x_{\mathrm{Foll}} = 2$ and $x_{\mathrm{CL}} = 1$. The only activating arc of x_{LH}, $x_{\mathrm{GnRH}} = 1$ is replaced by the arc $x_{\mathrm{Foll}} = 2$. The other regulation that x_{GnRH} performs, is the activation of x_{FSH}. However, since the basal level of x_{FSH} is one, the variable also becomes one in case that none of the regulators are active, i.e. in case of $x_{\mathrm{GnRH}} = 0$. Therefore it is evident that activation of x_{FSH} by x_{GnRH} is omittable. After this reduction step, the resulting reachability graph with asynchronous update, starting from $\widehat{x}^d = \{x_{\mathrm{FSH}} = 1, x_{\mathrm{LH}} = 0, x_{\mathrm{Foll}} = 2, x_{\mathrm{PGF}} = 0, x_{\mathrm{CL}} = 0, x_{\mathrm{PGF}} = 0\}$ consists of 54 nodes, no steady states, and its SCC graph contains exactly one component which consists of 10 different states, the cyclical attractor.

Having performed this reduction step, the reduced model now contains five variables. Paths in the STG can now more easily be interpreted. Keeping in mind the simulation of the ODE model, and looking at the 54 nodes within the reachability graph and its transitions, certain similarities can be detected in the sequence of events or states. In contrast, certain succession of states in the STG can be identified as not in line with the continuous simulation. To get the discrete simulation more in line with the continuous one, priority classes are defined in order to restrict the asynchronous simulation.

Priority classes are subsets of the variables assigned with a ranking. The simulation with priority classes updates the variables in higher ranked priority class before the others, which allows to force or to prevent certain transitions in the STG. Analysis of the asynchronous STG and comparison with the continuous model output leads to the definition of three priority classes:

1. x_{Foll}, x_{CL}
2. x_{LH}
3. x_{FSH}, x_{PGF}

The simulation with these priority classes, starting from $(x_{\text{FSH}}, x_{\text{LH}}, x_{\text{Foll}}, x_{\text{CL}}, x_{\text{PGF}}) = (1, 1, 2, 0, 0)$ leads to a reachability graph with 27 nodes, which is visualized in Figure 5.5. In the figure, each state corresponds to a value which the vector $(x_{\text{FSH}}, x_{\text{LH}}, x_{\text{Foll}}, x_{\text{CL}}, x_{\text{PGF}})$ takes. For example, the state $(1, 1, 2, 0, 0)$ in the upper part of the figure corresponds to the situation around ovulation: LH and FSH are at a high level, the Follicles are at their highest level, i.e. ready for ovulation. The next step in the graph is the rise of the CL, which in the graph corresponds to the state $(1, 1, 2, 1, 0)$. In this manner, the state transition graph can be related to the known biological behavior. It can be observed that there is one large limit cycle where different paths can be taken. At five states in the reachability graph, two possibilities to pursue the simulation exist.

From the state $(0, 1, 0, 1, 0)$, where FSH is high ($x_{\text{FSH}} = 1$) in the beginning of the luteal phase ($x_{\text{CL}} = 1$), there are two ways to proceed. Either the CL first reaches higher levels before the follicles start to grow, or first the follicles start growing. In the latter case, there are again two ways to proceed further, either the follicles first continue to rise, or the CL reaches higher levels before that. In all of the cases, after three transitions, both the CL and the follicles have reached their maximum levels, the simulation is in the state $(0, 1, 2, 2, 0)$.

It can also be observed in the reachability graph that there are two subcycles. The one on the left side in Figure 5.5 corresponds to the follicular waves, while the cycle on the right side in the figure can not be observed in a normal, healthy cow. In the left cycle, at the state $(x_{\text{FSH}}, x_{\text{LH}}, x_{\text{Foll}}, x_{\text{CL}}, x_{\text{IOF}}) = (0, 1, 2, 2, 0)$, either FSH decays followed by a decline of the follicular wave, or PGF rises followed by luteolysis and ovulation. If the decline of the follicles occurs, the simulation gets back to the point where FSH starts to rise again $(0, 1, 0, 2, 0)$, followed by a rise of the follicles to their maximum.

The right part of Figure 5.5 describes everything that happens between luteolysis and ovulation. In a healthy cow, after the decay of the corpus luteum, PGF declines and LH rises. This corresponds to the outer path of the figure. In the reachability graph, after the rise of LH, there is the possibility that FSH and the follicles decay, and LH declines again. Whether this corresponds to a pathological situation in reality, i.e. whenever LH peaks happen without ovulation, still needs to be explored.

The described reduction steps can also be applied to the modified version of the discrete model, where x_{P4} is three-valued, and x_{Foll} binary. Recall that this model was derived because it is expected that certain mechanisms differ from the first follicular wave to the second. With this model, after the first step the reachability graph computed with asynchronous update has 1952 nodes, after the second step 184, after the third 72, and after the fourth reduction step 36 nodes. As above, in every reduced model the SCC of the reachability graph has one component. Thus, the reduced models are all capable to describe the desired cyclical behavior for the bovine estrous cycle.

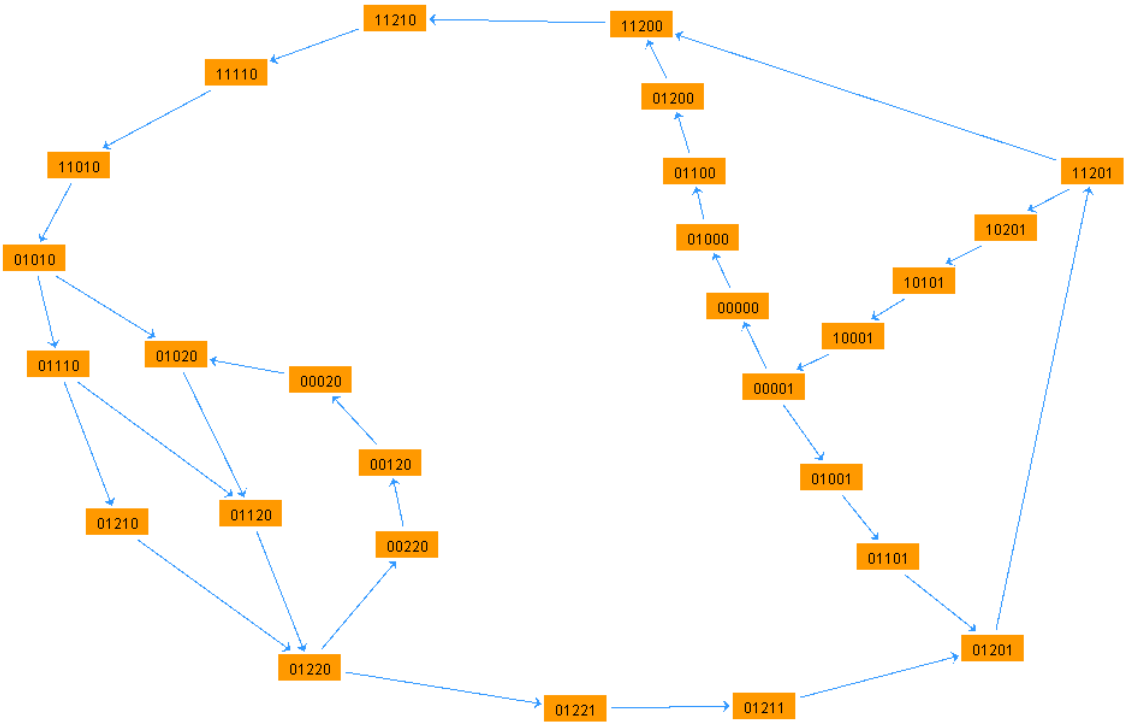

Figure 5.5: Reachability graph calculated with priority classes from the reduced model depicted Figure 5.4(d), starting from the initial state $(x_{\mathrm{FSH}}, x_{\mathrm{LH}}, x_{\mathrm{Foll}}, x_{\mathrm{CL}}, x_{\mathrm{IOF}}) = (1, 1, 2, 0, 0)$, which represents ovulation. On the left part of the graph, follicular waves can be observed, and on the right the state transitions between luteolysis and ovulation.

Using the same priority classes as above, the modified version of the model leads to a reachability graph that is very similar to the one from the original version that is depicted in Figure 5.5. The expectation that the three-valued X_{P4} makes a difference in the simulation of the wave patterns is not met. Instead, almost the same two subcycles are detected, one representing the follicular waves, and one between luteolysis and ovulation.

A further reduction can simplify this model and the simulation even more. As x_{FSH} in the described models only influences x_{Foll}, this variable can be eliminated and replaced by a self-influence of Foll. Considering all variables as binary leads to the model and state transition graph that are illustrated in Figure 5.6.

The sequence of events in the reachability graph in Figure 5.6 is as follows: Starting from ovulation at the initial state $\{x_{\mathrm{LH}} = 1, x_{\mathrm{Foll}} = 1, x_{\mathrm{CL}} = 0, x_{\mathrm{PGF}} = 0\}$, there are two possibilities to proceed, but both lead to a decay of the follicles and a rise of the CL within the next two transitions. Next, LH levels fall, and the next follicular wave rises. While the CL is still high, follicles can grow and directly undergo atresia for several times. This can be observed in the direct transitions between the states $\{x_{\mathrm{LH}} = 0, x_{\mathrm{Foll}} = 0, x_{\mathrm{CL}} = 1, x_{\mathrm{PGF}} = 0\}$ and $\{x_{\mathrm{LH}} = 0, x_{\mathrm{Foll}} = 1, x_{\mathrm{CL}} = 1, x_{\mathrm{PGF}} = 0\}$ at the lower part of Figure 5.6. While follicles are high, the simulation can proceed when PGF is rising. This is followed by two events, the decay of the CL and the decay of the follicles. The order of these two events is exchangeable. Now, only PGF levels are high, but they fall to zero in the next step. As all variables are zero, the follicles start to grow again, followed by a rise of LH, and the next ovulation.

Theoretically, a trajectory could rest in a subcycle forever. To avoid this and be able to use each trajectory as a time series for a real cow, a modification of the modeling approach is needed. For example, a memory effect might be included, or a probabilistic approach could be chosen for the state transitions. This might be of interest for future modeling questions.

One conclusion of this section is that also the reduced versions of the model are designed for oscillatory behavior, and they each have only one attractor. This is a hint to global stability. The system is able to compensate even large perturbations.

Moreover, as the reduced models still capture the essential dynamics of the bovine estrous cycle, one can conclude that some of its key variables and mechanisms have been identified. The variables are x_{LH}, x_{FSH}, x_{Foll}, x_{CL}, and x_{PGF}. Among the key mechanisms are several direct negative feedback loops, namely between x_{FSH} and x_{Foll}, x_{PGF} and x_{CL}, x_{LH} and x_{Foll}, x_{LH} and x_{CL}, x_{Foll} and x_{CL}. It is expected that any larger model of the bovine estrous cycle should map these core dynamics.

Derived as an additional representation for ODE models, the discrete counterparts contribute to a better understanding of the system. The core variables and mechanisms of the

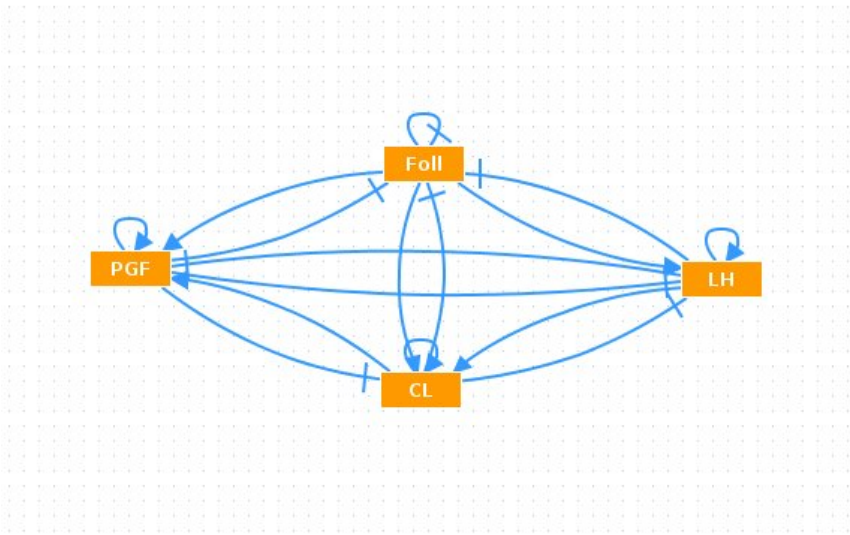

(a) Influence graph

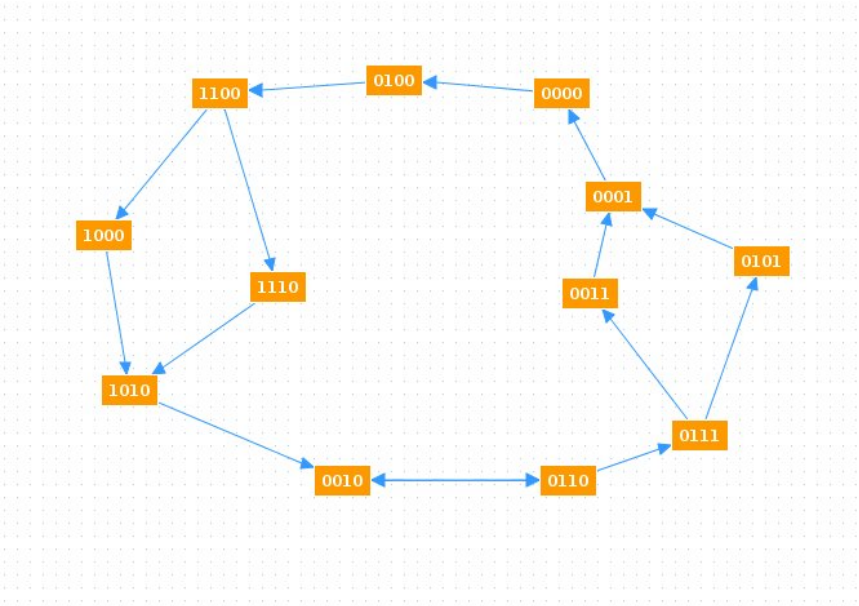

(b) State transition graph

Figure 5.6: Influence graph and reachability graph of a binary model for the bovine estrous cycle, computed with asynchronous update, starting from the initial state $(x_{\mathrm{LH}}, x_{\mathrm{Foll}}, x_{\mathrm{CL}}, x_{\mathrm{PGF}}) = (1, 1, 0, 0)$. In the graph, the key events of the bovine estrous cycle can be observed, and the order of the events (state transitions) maps the order of the biological changes remarkably well. The direct transitions corresponding to follicular waves can be observed in the lower part of this graph, between the states $(0, 0, 1, 0)$ and $(0, 1, 1, 0)$.

discrete model also represent the core relations in the continuous model. It is expected that the dynamical results can be transferred to the continuous setting, and that also therein, only one global attractor exists which the system reaches even after large perturbations.

Conclusion

With this thesis, a detailed step towards reliable and predictive modeling of hormonal networks has been taken.

A contribution to the use of mathematical models in animal sciences has been made with the development of a differential equation model for the bovine estrous cycle. For this, a whole body approach was presented, where the interplay of mechanisms in different parts of the organism results in estrus regulation. The developed fully coupled feedback model was compared in detail with an existing differential equation model of the human menstrual cycle.

To validate these two continuous models, simulations were compared with time courses of measurements, and also the response of the systems to drug administration was studied. Exemplarily for the bovine model, continuous analysis tools were applied to investigate stability, cycle patterns, and robustness with respect to parameter perturbations. The model was significantly reduced while still capturing the essential output.

Supplementary, to take a look at alternative modeling approaches, appropriate discrete models were derived, exemplarily, for the bovine estrous cycle. In the discrete setting, parameter constraints for the continuous model were calculated from a piecewise affine version of the model, and stability was analyzed globally for a purely discrete model. In addition, reduced models were presented that preserve the key dynamical characteristics.

The new models in this thesis improve the understanding of the biological mechanisms behind the hormonal cycle. Their predictive ability has been shown via the simulation of external influences, and their mapping of biological stability allows for advanced applications. Such models can assist research in drug development, and in the design of new therapeutic strategies regarding fertility.

Appendix

Here, after a list of used abbreviations and notations, the nonzero entries of the Jacobian for BovCycle are given. Also the Wronskian matrix is provided. Afterwards, three ODE models are provided, GynCycle, BovCycle, and a reduced version of BovCycle, together with parameters and initial values.

List of used Abbreviations

GnRH	Gonadotropin releasing hormone
LH	Luteinizing Hormone
FSH	Follicle stimulating hormone
E2	Estradiol
P4	Progesterone
Inh	Inhibin
PGF2α	Prostaglandin F2α
OT	Oxytocin
CL	Corpus luteum
Foll	Follicular function
Enz	Enzymes
IOF	Intra-ovarian factors
Syn	Synthesis
Rel	Release
Hyp	Hypothalamus
Pit	Pituitary

The Jacobian for the model of the bovine estrous cycle

$$
\begin{aligned}
\mathrm{J}(1,1) &= \frac{-0.17\left(y_{\mathrm{P4}}^2+0.082\right)\left(y_{\mathrm{P4}}^2+2.3\right)y_{\mathrm{E2}}^2-0.021\left(y_{\mathrm{P4}}^2+0.12\right)\left(y_{\mathrm{P4}}^2+0.12\right)}{\left(y_{\mathrm{E2}}^2+0.0094\right)\left(y_{\mathrm{P4}}^2+0.064\right)\left(y_{\mathrm{P4}}^2+0.12\right)} \\
\mathrm{J}(1,10) &= y_{\mathrm{Gh}}y_{\mathrm{P4}}\left(\frac{0.24}{\left(y_{\mathrm{P4}}^2+0.064\right)^2}+\frac{0.5}{\left(y_{\mathrm{P4}}^2+0.12\right)^2}-\frac{0.0048}{\left(y_{\mathrm{P4}}^2+0.12\right)^2\left(y_{\mathrm{E2}}^2+0.0095\right)}\right) \\
\mathrm{J}(1,11) &= \frac{0.039y_{\mathrm{E2}}y_{\mathrm{Gh}}y_{\mathrm{P4}}^2}{\left(y_{\mathrm{E2}}^2+0.0095\right)^2\left(y_{\mathrm{P4}}^2+0.12\right)} \\
\mathrm{J}(2,1) &= \frac{0.99y_{\mathrm{E2}}^5\left(\left(0.372y_{\mathrm{P4}}^2+0.03\right)y_{\mathrm{E2}}^2+0.019\left(y_{\mathrm{P4}}^2+0.12\right)\left(y_{\mathrm{P4}}^2+0.12\right)\right)}{\left(y_{\mathrm{E2}}^2+0.0095\right)\left(y_{\mathrm{E2}}^5+0.11\right)\left(y_{\mathrm{P4}}^2+0.063\right)\left(y_{\mathrm{P4}}^2+0.12\right)} \\
\mathrm{J}(2,2) &= -1.63 \\
\mathrm{J}(2,10) &= \frac{0.99y_{\mathrm{E2}}^5y_{\mathrm{Gh}}y_{\mathrm{P4}}\left(-\frac{0.24}{\left(y_{\mathrm{P4}}^2+0.064\right)^2}-\frac{0.5}{\left(y_{\mathrm{P4}}^2+0.12\right)^2}+\frac{0.0048}{\left(y_{\mathrm{P4}}^2+0.123\right)^2\left(y_{\mathrm{E2}}^2+0.0095\right)}\right)}{y_{\mathrm{E2}}^5+0.114} \\
\mathrm{J}(2,11) &= \frac{y_{\mathrm{E2}}^4y_{\mathrm{Gh}}\left(-0.038y_{\mathrm{P4}}^2\left(y_{\mathrm{P4}}^2+0.064\right)y_{\mathrm{E2}}^7+\left(0.21y_{\mathrm{P4}}^2+0.017\right)y_{\mathrm{E2}}^4+0.0066\left(y_{\mathrm{P4}}^2+0.086\right)\left(y_{\mathrm{P4}}^2+0.58\right)y_{\mathrm{E2}}^2+0.0001\left(y_{\mathrm{P4}}^2+0.12\right)\left(y_{\mathrm{P4}}^2+0.12\right)\right)}{\left(y_{\mathrm{E2}}^2+0.0095\right)^2\left(y_{\mathrm{E2}}^5+0.11\right)^2\left(y_{\mathrm{P4}}^4+0.186y_{\mathrm{P4}}^2+0.0078\right)} \\
\mathrm{J}(3,2) &= -\frac{0.087y_{\mathrm{FSHp}}}{\left(y_{\mathrm{G}}+0.07\right)^2} \\
\mathrm{J}(3,3) &= -\frac{0.293y_{\mathrm{P4}}^2}{y_{\mathrm{P4}}^2+0.023}-\frac{0.039}{y_{\mathrm{E2}}^2+0.097}-\frac{1.23y_{\mathrm{G}}}{y_{\mathrm{G}}+0.07}-0.95 \\
\mathrm{J}(3,10) &= -\frac{0.014y_{\mathrm{FSHp}}y_{\mathrm{P4}}}{\left(y_{\mathrm{P4}}^2+0.023104\right)^2} \\
\mathrm{J}(3,11) &= \frac{0.077y_{\mathrm{E2}}y_{\mathrm{FSHp}}}{\left(y_{\mathrm{E2}}^2+0.097344\right)^2} \\
\mathrm{J}(3,12) &= -\frac{0.00048y_{\mathrm{Inh}}^4}{\left(y_{\mathrm{Inh}}^5+0.0000228776\right)^2} \\
\mathrm{J}(4,2) &= \frac{0.087y_{\mathrm{FSHp}}}{\left(y_{\mathrm{G}}+0.0708\right)^2} \\
\mathrm{J}(4,3) &= \frac{0.29y_{\mathrm{P4}}^2}{y_{\mathrm{P4}}^2+0.023}+\frac{0.039}{y_{\mathrm{E2}}^2+0.097}+\frac{1.23y_{\mathrm{G}}}{y_{\mathrm{G}}+0.07}+0.95 \\
\mathrm{J}(4,4) &= -2.73 \\
\mathrm{J}(4,10) &= \frac{0.014y_{\mathrm{FSHp}}y_{\mathrm{P4}}}{\left(y_{\mathrm{P4}}^2+0.023\right)^2} \\
\mathrm{J}(4,11) &= -\frac{0.077y_{\mathrm{E2}}y_{\mathrm{FSHp}}}{\left(y_{\mathrm{E2}}^2+0.097\right)^2} \\
\mathrm{J}(5,2) &= -\frac{1.74y_{\mathrm{G}}^4y_{\mathrm{LHp}}}{\left(y_{\mathrm{G}}^5+0.16\right)^2} \\
\mathrm{J}(5,5) &= -\frac{2.22y_{\mathrm{G}}^5}{y_{\mathrm{G}}^5+0.16}-0.014 \\
\mathrm{J}(5,10) &= -\frac{0.0039y_{\mathrm{P4}}}{\left(y_{\mathrm{P4}}^2+0.00072\right)^2} \\
\mathrm{J}(5,11) &= \frac{0.044y_{\mathrm{E2}}}{\left(y_{\mathrm{E2}}^2+0.059\right)^2} \\
\mathrm{J}(6,2) &= \frac{1.74y_{\mathrm{G}}^4y_{\mathrm{LHp}}}{\left(y_{\mathrm{G}}^5+0.16\right)^2}
\end{aligned}
$$

$$
\begin{aligned}
\mathrm{J}(6,5) &= \frac{2.22y_{\mathrm{G}}^5}{y_{\mathrm{G}}^5+0.16}+0.014\\
\mathrm{J}(6,6) &= -12\\
\mathrm{J}(7,4) &= \frac{0.00086\left(y_{\mathrm{Foll}}^2+0.048\right)^2 y_{\mathrm{FSH}}}{\left(\left(y_{\mathrm{Foll}}^4+0.097y_{\mathrm{Foll}}^2+0.0023\right)y_{\mathrm{FSH}}^2+0.00076\right)^2}\\
\mathrm{J}(7,6) &= -\frac{0.2y_{\mathrm{Foll}}y_{\mathrm{LH}}}{\left(y_{\mathrm{LH}}^2+0.029241\right)^2}\\
\mathrm{J}(7,7) &= -\frac{1.1y_{\mathrm{P4}}^5}{y_{\mathrm{P4}}^5+0.000032}-\frac{3.49y_{\mathrm{LH}}^2}{y_{\mathrm{LH}}^2+0.029}+\frac{0.0017y_{\mathrm{Foll}}y_{\mathrm{FSH}}^2}{\left(y_{\mathrm{Foll}}^2+0.048\right)^3\left(y_{\mathrm{FSH}}^2+\frac{0.00076}{\left(y_{\mathrm{Foll}}^2+0.048\right)^2}\right)^2}\\
\mathrm{J}(7,10) &= -\frac{0.00017y_{\mathrm{Foll}}y_{\mathrm{P4}}^4}{\left(y_{\mathrm{P4}}^5+0.000032\right)^2}\\
\mathrm{J}(8,8) &= -1.23\\
\mathrm{J}(8,13) &= \frac{1611.83y_{\mathrm{Enz}}^4y_{\mathrm{OT}}^2}{\left(y_{\mathrm{Enz}}^5+5.98\right)^2\left(y_{\mathrm{OT}}^2+1.18\right)}\\
\mathrm{J}(8,14) &= \frac{127.397y_{\mathrm{Enz}}^5y_{\mathrm{OT}}}{\left(y_{\mathrm{Enz}}^5+5.98\right)\left(y_{\mathrm{OT}}^2+1.18\right)^2}\\
\mathrm{J}(9,6) &= \frac{0.04y_{\mathrm{Foll}}y_{\mathrm{LH}}}{\left(y_{\mathrm{LH}}^2+0.029241\right)^2}\\
\mathrm{J}(9,7) &= \frac{0.7y_{\mathrm{LH}}^2}{y_{\mathrm{LH}}^2+0.029241}\\
\mathrm{J}(9,9) &= -\frac{41.39y_{\mathrm{IOF}}^5}{y_{\mathrm{IOF}}^5+4.0075}+\frac{0.071y_{\mathrm{CL}}}{y_{\mathrm{CL}}^2+0.01}-\frac{0.071y_{\mathrm{CL}}^3}{\left(y_{\mathrm{CL}}^2+0.01\right)^2}\\
\mathrm{J}(9,15) &= -\frac{829.35y_{\mathrm{CL}}y_{\mathrm{IOF}}^4}{\left(y_{\mathrm{IOF}}^5+4.0075\right)^2}\\
\mathrm{J}(10,9) &= 4.5y_{\mathrm{CL}}\\
\mathrm{J}(10,10) &= -1.41\\
\mathrm{J}(11,7) &= 4.38y_{\mathrm{Foll}}\\
\mathrm{J}(11,11) &= -1.23\\
\mathrm{J}(12,7) &= 2.82y_{\mathrm{Foll}}\\
\mathrm{J}(12,12) &= -0.475\\
\mathrm{J}(13,10) &= \frac{4.85y_{\mathrm{P4}}^4}{\left(y_{\mathrm{P4}}^5+0.27\right)^2}\\
\mathrm{J}(13,13) &= -2.98\\
\mathrm{J}(14,9) &= \frac{3.18y_{\mathrm{CL}}y_{\mathrm{E2}}^2}{y_{\mathrm{E2}}^2+0.02}\\
\mathrm{J}(14,11) &= \frac{0.065y_{\mathrm{CL}}^2y_{\mathrm{E2}}}{\left(y_{\mathrm{E2}}^2+0.02\right)^2}\\
\mathrm{J}(14,14) &= -0.64
\end{aligned}
$$

$$\begin{aligned}
\mathrm{J}(15,8) &= \frac{536.22\,y_{\mathrm{CL}}^{10}\,y_{\mathrm{PGF}}^{4}}{\left(y_{\mathrm{CL}}^{10}+0.006\right)\left(y_{\mathrm{PGF}}^{5}+2.7\right)^{2}} \\
\mathrm{J}(15,9) &= \frac{2.4\,y_{\mathrm{CL}}^{9}\,y_{\mathrm{PGF}}^{5}}{\left(y_{\mathrm{CL}}^{10}+0.006\right)^{2}\left(y_{\mathrm{PGF}}^{5}+2.7\right)} \\
\mathrm{J}(15,15) &= -0.33
\end{aligned}$$

The Wronskian matrix of the ODE model for the bovine estrous cycle

$$W = \begin{pmatrix}
0.0027 & 0.0055 & -0.0007 & 0.0000 & 0.0017 & 0.0030 & -0.0056 \\
-0.0189 & -0.0347 & -0.0589 & -0.0662 & -0.0320 & -0.0432 & -0.3401 \\
-0.0037 & -0.0046 & -0.0089 & -0.0093 & -0.0024 & -0.0031 & -0.0587 \\
-0.0066 & -0.0069 & -0.0205 & -0.0212 & -0.0044 & -0.0052 & -0.1364 \\
-0.4576 & -0.8704 & 0.4645 & 0.3866 & -0.0476 & -0.1947 & 2.6424 \\
-0.0818 & -0.1546 & 0.0321 & 0.0156 & -0.0278 & -0.0574 & 0.1786 \\
-0.0065 & -0.0101 & -0.0165 & -0.0182 & -0.0071 & -0.0096 & -0.1022 \\
-0.0000 & 0.0002 & -0.0009 & -0.0009 & -0.0000 & 0.0000 & -0.0060 \\
0.0046 & 0.0110 & -0.0074 & -0.0060 & 0.0023 & 0.0050 & -0.0502 \\
0.0045 & 0.0096 & -0.0019 & -0.0007 & 0.0028 & 0.0051 & -0.0146 \\
-0.0169 & -0.0313 & -0.0273 & -0.0324 & -0.0185 & -0.0268 & -0.1590 \\
-0.0038 & -0.0073 & -0.0261 & -0.0285 & -0.0126 & -0.0162 & -0.1486 \\
0.0000 & 0.0000 & -0.0000 & -0.0000 & 0.0000 & 0.0000 & -0.0000 \\
0.0042 & 0.0120 & -0.0129 & -0.0113 & 0.0021 & 0.0053 & -0.0875 \\
-0.0007 & 0.0074 & -0.0307 & -0.0295 & -0.0015 & 0.0011 & -0.2050
\end{pmatrix}$$

$$\begin{pmatrix}
0.0000 & 0.1802 & -0.0339 & 0.0104 & -0.0979 & 0.0000 & 0.0000 & -0.0053 \\
-0.0000 & -4.7801 & 0.7586 & -0.1438 & 1.5115 & -0.0000 & -0.0000 & 0.1425 \\
-0.0000 & -0.5153 & 0.0560 & -0.0204 & 0.1260 & -0.0000 & -0.0000 & 0.0151 \\
-0.0000 & -1.0636 & 0.1080 & -0.0398 & 0.2283 & -0.0000 & -0.0000 & 0.0312 \\
0.0000 & 0.4587 & -0.2404 & -1.1965 & 6.1877 & 0.0000 & 0.0000 & -0.0316 \\
-0.0000 & -3.0289 & 0.4531 & -0.2752 & 1.9155 & -0.0000 & -0.0000 & 0.0876 \\
-0.0000 & -1.1962 & 0.1671 & -0.0413 & 0.3512 & -0.0000 & -0.0000 & 0.0354 \\
-0.0000 & -0.0279 & 0.0017 & -0.0006 & 0.0009 & -0.0000 & -0.0000 & 0.0008 \\
0.0000 & 0.0881 & -0.0386 & 0.0131 & -0.1477 & 0.0000 & 0.0000 & -0.0025 \\
0.0000 & 0.2800 & -0.0553 & 0.0171 & -0.1642 & 0.0000 & 0.0000 & -0.0082 \\
-0.0000 & -2.6904 & 0.4218 & -0.0977 & 0.9313 & -0.0000 & -0.0000 & 0.0799 \\
-0.0000 & -1.9018 & 0.3094 & -0.0473 & 0.5652 & -0.0000 & -0.0000 & 0.0569 \\
0.0000 & 0.0000 & -0.0000 & 0.0000 & -0.0000 & 0.0000 & 0.0000 & -0.0000 \\
0.0000 & -0.0872 & -0.0293 & 0.0082 & -0.1402 & 0.0000 & 0.0000 & 0.0025 \\
-0.0000 & -0.9802 & 0.0622 & -0.0235 & 0.0437 & -0.0000 & -0.0000 & 0.0282
\end{pmatrix}$$

ODEs and parameters for GynCycle

Table A.1: The model of the human menstrual cycle. It consists of 33 ODEs and 114 parameters.

$freq(t)$	$=$	$H^{-}_{\mathrm{P4},freq}(y_{\mathrm{P4}}(t)) \cdot (1 + H^{+}_{\mathrm{E2},freq}(y_{\mathrm{E2}}(t)))$	
$mass(t)$	$=$	$H^{+}_{E2,mass}(y_{\mathrm{E2}}(t))$	
$\frac{d}{dt}y_{\mathrm{G}}(t)$	$=$	$k_G \cdot mass(t) \cdot freq(t) - k^{G}_{on} \cdot y_{\mathrm{G}}(t) \cdot y_{\mathrm{RG}}(t)$	
		$+k^{G}_{off} \cdot y_{(\text{G-RG})}(t) - k^{G}_{degr} \cdot y_{\mathrm{G}}(t)$	(H1)
$\frac{d}{dt}y_{\mathrm{RG}}(t)$	$=$	$k^{G}_{off} \cdot y_{(\text{G-RG})}(t) - k^{G}_{on} \cdot y_{\mathrm{G}}(t) \cdot y_{\mathrm{RG}}(t)$	
		$-k^{\mathrm{RG}}_{inter} \cdot y_{\mathrm{RG}}(t) + k^{\mathrm{RG}}_{recy} \cdot y_{\mathrm{RG}^*}(t)$	(H2)
$\frac{d}{dt}y_{\mathrm{RG}^*}(t)$	$=$	$k^{(\text{G-RG})}_{diss} \cdot y_{(\text{G-RG})^*}(t) + k^{\mathrm{RG}}_{inter} \cdot y_{\mathrm{RG}}(t)$	
		$-k^{\mathrm{RG}}_{recy} \cdot y_{\mathrm{RG}^*}(t) + k^{\mathrm{RG}}_{syn} - k^{\mathrm{RG}}_{degr} \cdot y_{\mathrm{RG}^*}(t)$	(H3)
$\frac{d}{dt}y_{(\text{G-RG})}(t)$	$=$	$k^{G}_{on} \cdot y_{\mathrm{G}}(t) \cdot y_{\mathrm{RG}}(t) - k^{G}_{off} \cdot y_{(\text{G-RG})}(t)$	
		$-k^{(\text{G-RG})}_{inact} \cdot y_{(\text{G-RG})}(t) + k^{(\text{G-RG})}_{act} \cdot y_{(\text{G-RG})^*}(t)$	(H4)
$\frac{d}{dt}y_{(\text{G-RG})^*}(t)$	$=$	$k^{(\text{G-RG})}_{inact} \cdot y_{(\text{G-RG})}(t) - k^{(\text{G-RG})}_{act} \cdot y_{(\text{G-RG})^*}(t)$	
		$-k^{\mathrm{RG}}_{degr} \cdot y_{(\text{G-RG})^*} - k^{\mathrm{RG}}_{diss} \cdot y_{\mathrm{RG}^*}(t)$	(H5)
$Syn_{\mathrm{LH}}(t)$	$=$	$\left(b^{\mathrm{LH}}_{Syn} + H^{+}_{\mathrm{E2,LH}}(y_{\mathrm{E2}}(t)\right) \cdot H^{-}_{\mathrm{P4,LH}}(y_{\mathrm{P4}}(t))$	
$Rel_{\mathrm{LH}}(t)$	$=$	$\left(b^{\mathrm{LH}}_{Rel} + H^{+}_{(\text{G-RG}),\mathrm{LH}}\left(y_{(\text{G-RG})}(t) + y_{(\text{Ago-RG})}(t)\right)\right) \cdot y_{\mathrm{LHp}}(t)$	
$\frac{d}{dt}y_{\mathrm{LHp}}(t)$	$=$	$Syn_{\mathrm{LH}}(t) - Rel_{\mathrm{LH}}(t)$	(H6)
$\frac{d}{dt}y_{\mathrm{LH}}(t)$	$=$	$\frac{1}{V_{\mathrm{blood}}} \cdot Rel_{\mathrm{LH}}(t) - \left(k^{\mathrm{LH}}_{on} \cdot y_{\mathrm{RL}}(t) + cl_{\mathrm{LH}}\right) \cdot y_{\mathrm{LH}}(t)$	(H7)
$Syn_{\mathrm{FSH}}(t)$	$=$	$\frac{1}{1+\left(\frac{y_{\mathrm{IhAe}}(t)}{T_{\mathrm{IhAe}}}\right)^{n_{\mathrm{IhAe}}}+\left(\frac{y_{\mathrm{IhB}}(t)}{T_{\mathrm{IhB}}}\right)^{n_{\mathrm{IhB}}}} \cdot H^{-}_{freq,\mathrm{P4}}(freq(t))$	
$Rel_{\mathrm{FSH}}(t)$	$=$	$\left(b_{\mathrm{FSH}_{Rel}} + H^{+}_{(\text{G-RG}),\mathrm{FSH}}(y_{(\text{G-RG})}(t) + y_{(\text{Ago-RG})}(t))\right) \cdot y_{\mathrm{FSHp}}(t)$	
$\frac{d}{dt}y_{\mathrm{FSHp}}(t)$	$=$	$Syn_{\mathrm{FSH}}(t) - Rel_{\mathrm{FSH}}(t)$	(H8)
$\frac{d}{dt}y_{\mathrm{FSH}}(t)$	$=$	$\frac{1}{V_{\mathrm{blood}}} \cdot Rel_{\mathrm{FSH}}(t) - \left(k^{\mathrm{FSH}}_{on} \cdot y_{\mathrm{RF}}(t) + cl_{\mathrm{FSH}}\right) \cdot y_{\mathrm{FSH}}(t)$	(H9)
$\frac{d}{dt}y_{\mathrm{RL}}(t)$	$=$	$k^{\mathrm{LH}}_{recy} \cdot y_{\mathrm{RLdes}}(t) - k^{\mathrm{LH}}_{on} \cdot y_{\mathrm{LH}}(t) \cdot y_{\mathrm{RL}}(t)$	(H10)
$\frac{d}{dt}y_{(\text{LH-RL})}(t)$	$=$	$k^{\mathrm{LH}}_{on} \cdot y_{\mathrm{LH}}(t) \cdot y_{\mathrm{RL}}(t) - k^{\mathrm{LH}}_{des} \cdot y_{(\text{LH-RL})}(t)$	(H11)
$\frac{d}{dt}y_{\mathrm{RLdes}}(t)$	$=$	$k^{\mathrm{LH}}_{des} \cdot y_{(\text{LH-RL})}(t) - k^{\mathrm{LH}}_{recy}(t) \cdot y_{\mathrm{RLdes}}(t)$	(H12)
$\frac{d}{dt}y_{\mathrm{RF}}(t)$	$=$	$k^{\mathrm{FSH}}_{recy} \cdot y_{\mathrm{RFdes}}(t) - k^{\mathrm{FSH}}_{on} \cdot y_{\mathrm{FSH}}(t) \cdot y_{\mathrm{RF}}(t)$	(H13)
$\frac{d}{dt}y_{(\text{FSH-RF})}(t)$	$=$	$k^{\mathrm{FSH}}_{on} \cdot y_{\mathrm{FSH}}(t) \cdot y_{\mathrm{RF}}(t) - k^{\mathrm{FSH}}_{des} \cdot y_{(\text{FSH-RF})}(t)$	(H14)
$\frac{d}{dt}y_{\mathrm{RFdes}}(t)$	$=$	$k^{\mathrm{FSH}}_{des} \cdot y_{(\text{FSH-RF})}(t) - k^{\mathrm{FSH}}_{recy} \cdot y_{\mathrm{RFdes}}(t)$	(H15)
$\frac{d}{dt}y_{\mathrm{s}}(t)$	$=$	$H^{+}_{\mathrm{FSH,s}}\left(y_{(\text{FSH-RF})}(t)\right) - H^{+}_{\mathrm{P4,s}}\left(y_{\mathrm{P4}}(t)\right) \cdot y_{\mathrm{s}}(t)$	(H16)

Continued on next page...

Table A.1 – *continued from previous page*

$$\frac{d}{dt}y_{\mathrm{AF1}}(t) = H^{+}_{\mathrm{FSH,AF1}}\left(y_{(\mathrm{FSH\text{-}RF})}(t)\right) - k^{\mathrm{AF2}}_{\mathrm{AF1}} \cdot y_{(\mathrm{FSH\text{-}RF})}(t) \cdot y_{\mathrm{AF1}}(t) \quad \text{(H17)}$$

$$\frac{d}{dt}y_{\mathrm{AF2}}(t) = k^{\mathrm{AF2}}_{\mathrm{AF1}} \cdot y_{(\mathrm{FSH\text{-}RF})}(t) \cdot y_{\mathrm{AF1}}(t) - k^{\mathrm{AF3}}_{\mathrm{AF2}} \cdot \left(\frac{y_{(\mathrm{LH\text{-}RL})}(t)}{\mathrm{SF}_{(\mathrm{LH\text{-}RL})}}\right)^{n^{\mathrm{AF3}}_{\mathrm{AF2}}} \cdot y_{\mathrm{s}}(t) \cdot y_{\mathrm{AF2}}(t) \quad \text{(H18)}$$

$$\begin{aligned}\frac{d}{dt}y_{\mathrm{AF3}}(t) = {} & k^{\mathrm{AF3}}_{\mathrm{AF2}} \cdot \left(\frac{y_{(\mathrm{LH\text{-}RL})}(t)}{\mathrm{SF}_{(\mathrm{LH\text{-}RL})}}\right)^{n^{\mathrm{AF3}}_{\mathrm{AF2}}} \cdot y_{\mathrm{s}}(t) \cdot y_{\mathrm{AF2}}(t) \\ & + k^{\mathrm{AF3}}_{\mathrm{AF3}} \cdot y_{(\mathrm{FSH\text{-}RF})}(t) \cdot y_{\mathrm{AF3}}(t) \cdot \left(1 - \frac{y_{\mathrm{AF3}}(t)}{\mathrm{AF}_{\max}}\right) \\ & - k^{\mathrm{AF4}}_{\mathrm{AF3}} \cdot \left(\frac{y_{(\mathrm{LH\text{-}RL})}(t)}{\mathrm{SF}_{(\mathrm{LH\text{-}RL})}}\right)^{n^{\mathrm{AF4}}_{\mathrm{AF3}}} \cdot y_{\mathrm{s}}(t) \cdot y_{\mathrm{AF3}}(t) \end{aligned} \quad \text{(H19)}$$

$$\begin{aligned}\frac{d}{dt}y_{\mathrm{AF4}}(t) = {} & k^{\mathrm{AF4}}_{\mathrm{AF3}} \cdot \left(\frac{y_{(\mathrm{LH\text{-}RL})}(t)}{\mathrm{SF}_{(\mathrm{LH\text{-}RL})}}\right)^{n^{\mathrm{AF4}}_{\mathrm{AF3}}} \cdot y_{\mathrm{s}}(t) \cdot y_{\mathrm{AF3}}(t) \\ & + k^{\mathrm{AF4}}_{\mathrm{AF4}} \cdot \left(\frac{y_{(\mathrm{LH\text{-}RL})}(t)}{\mathrm{SF}_{(\mathrm{LH\text{-}RL})}}\right)^{n_{\mathrm{AF4}}} \cdot y_{\mathrm{AF4}}(t) \cdot \left(1 - \frac{y_{\mathrm{AF4}}(t)}{\mathrm{AF}_{\max}}\right) \\ & - k^{\mathrm{PrF}}_{\mathrm{AF4}} \cdot \left(\frac{y_{(\mathrm{LH\text{-}RL})}(t)}{\mathrm{SF}_{(\mathrm{LH\text{-}RL})}}\right) \cdot y_{\mathrm{s}}(t) \cdot y_{\mathrm{AF4}}(t) \end{aligned} \quad \text{(H20)}$$

$$\begin{aligned}\frac{d}{dt}y_{\mathrm{PrF}}(t) = {} & k^{\mathrm{PrF}}_{\mathrm{AF4}} \cdot \left(\frac{y_{(\mathrm{LH\text{-}RL})}(t)}{\mathrm{SF}_{(\mathrm{LH\text{-}RL})}}\right) \cdot y_{\mathrm{s}}(t) \cdot y_{\mathrm{AF4}}(t) \\ & - k^{\mathrm{PrF}}_{cl} \cdot \left(\frac{y_{(\mathrm{LH\text{-}RL})}(t)}{\mathrm{SF}_{(\mathrm{LH\text{-}RL})}}\right)^{n^{\mathrm{OvF}}_{\mathrm{PrF}}} \cdot y_{\mathrm{s}}(t) \cdot y_{\mathrm{PrF}}(t) \end{aligned} \quad \text{(H21)}$$

$$\frac{d}{dt}y_{\mathrm{OvF}}(t) = k^{\mathrm{OvF}} \cdot \left(\frac{y_{(\mathrm{LH\text{-}RL})}(t)}{\mathrm{SF}_{(\mathrm{LH\text{-}RL})}}\right)^{n^{\mathrm{OvF}}_{\mathrm{PrF}}} \cdot y_{\mathrm{s}}(t) \cdot H^{+}_{\mathrm{PrF,OvF}}(y_{\mathrm{PrF}}(t)) - k^{\mathrm{OvF}}_{cl} \cdot y_{\mathrm{OvF}}(t) \quad \text{(H22)}$$

$$\frac{d}{dt}y_{\mathrm{Sc1}}(t) = H^{+}_{\mathrm{OvF,Sc1}}\left(y_{\mathrm{OvF}}(t)\right) - k^{\mathrm{Sc2}}_{\mathrm{Sc1}} \cdot y_{\mathrm{Sc1}}(t) \quad \text{(H23)}$$

$$\frac{d}{dt}y_{\mathrm{Sc2}}(t) = k^{\mathrm{Sc2}}_{\mathrm{Sc1}} \cdot y_{\mathrm{Sc1}}(t) - k^{\mathrm{Lut1}}_{\mathrm{Sc2}} \cdot y_{\mathrm{Sc2}}(t) \quad \text{(H24)}$$

$$\begin{aligned}\frac{d}{dt}y_{\mathrm{Lut1}}(t) = {} & k^{\mathrm{Lut1}}_{\mathrm{Sc2}} \cdot y_{\mathrm{Sc2}}(t) \\ & - k^{\mathrm{Lut2}}_{\mathrm{Lut1}} \cdot \left(1 + H^{+}_{(\mathrm{G\text{-}RG}),\mathrm{Lut}}\left(y_{(\mathrm{G\text{-}RG})}(t) + y_{(\mathrm{Ago\text{-}RG})}(t)\right)\right) \cdot y_{\mathrm{Lut1}}(t) \end{aligned} \quad \text{(H25)}$$

$$\begin{aligned}\frac{d}{dt}y_{\mathrm{Lut2}}(t) = {} & k^{\mathrm{Lut2}}_{\mathrm{Lut1}} \cdot \left(1 + H^{+}_{(\mathrm{G\text{-}RG}),\mathrm{Lut}}\left(y_{(\mathrm{G\text{-}RG})}(t) + y_{(\mathrm{Ago\text{-}RG})}(t)\right)\right) \cdot y_{\mathrm{Lut1}}(t) \\ & - k^{\mathrm{Lut3}}_{\mathrm{Lut2}} \cdot \left(1 + H^{+}_{(\mathrm{G\text{-}RG}),\mathrm{Lut}}\left(y_{(\mathrm{G\text{-}RG})}(t) + y_{(\mathrm{Ago\text{-}RG})}(t)\right)\right) \cdot y_{\mathrm{Lut2}}(t) \end{aligned} \quad \text{(H26)}$$

$$\begin{aligned}\frac{d}{dt}y_{\mathrm{Lut3}}(t) = {} & k^{\mathrm{Lut3}}_{\mathrm{Lut2}}\left(1 + H^{+}_{(\mathrm{G\text{-}RG}),\mathrm{Lut}}\left(y_{(\mathrm{G\text{-}RG})}(t) + y_{(\mathrm{Ago\text{-}RG})}(t)\right)\right) \cdot y_{\mathrm{Lut2}}(t) \\ & - k^{\mathrm{Lut4}}_{\mathrm{Lut3}} \cdot \left(1 + H^{+}_{(\mathrm{G\text{-}RG}),\mathrm{Lut}}\left(y_{(\mathrm{G\text{-}RG})}(t) + y_{(\mathrm{Ago\text{-}RG})}(t)\right)\right) \cdot y_{\mathrm{Lut3}}(t) \end{aligned} \quad \text{(H27)}$$

$$\begin{aligned}\frac{d}{dt}y_{\mathrm{Lut4}}(t) = {} & k^{\mathrm{Lut4}}_{\mathrm{Lut3}}\left(1 + H^{+}_{(\mathrm{G\text{-}RG}),\mathrm{Lut}}\left(y_{(\mathrm{G\text{-}RG})}(t) + y_{(\mathrm{Ago\text{-}RG})}(t)\right)\right) \cdot y_{\mathrm{Lut3}}(t) \\ & - k^{\mathrm{Lut4}}_{cl} \cdot \left(1 + H^{+}_{(\mathrm{G\text{-}RG}),\mathrm{Lut}}\left(y_{(\mathrm{G\text{-}RG})}(t) + y_{(\mathrm{Ago\text{-}RG})}(t)\right)\right) \cdot y_{\mathrm{Lut4}}(t) \end{aligned} \quad \text{(H28)}$$

$$\begin{aligned}\frac{d}{dt}y_{\mathrm{E2}}(t) = {} & b_{\mathrm{E2}} + k^{\mathrm{E2}}_{\mathrm{AF2}} \cdot y_{\mathrm{AF2}}(t) + k^{\mathrm{E2}}_{\mathrm{AF3}} \cdot y_{\mathrm{LH}}(t) \cdot y_{\mathrm{AF3}}(t) \\ & + k^{\mathrm{E2}}_{\mathrm{AF4}} \cdot y_{\mathrm{AF4}}(t) + k^{\mathrm{E2}}_{\mathrm{PrF}} \cdot y_{\mathrm{LH}}(t) \cdot y_{\mathrm{PrF}} \\ & + k^{\mathrm{E2}}_{\mathrm{Lut1}} \cdot y_{\mathrm{Lut1}}(t) + k^{\mathrm{E2}}_{\mathrm{Lut4}} \cdot y_{\mathrm{Lut4}}(t) - k^{\mathrm{E2}}_{cl} \cdot y_{\mathrm{E2}}(t) \end{aligned} \quad \text{(H29)}$$

$$\frac{d}{dt}y_{\mathrm{P4}}(t) = b_{\mathrm{P4}} + k^{\mathrm{P4}}_{\mathrm{Lut4}} \cdot y_{\mathrm{Lut4}}(t) - k^{\mathrm{P4}}_{cl} \cdot y_{\mathrm{P4}}(t) \quad \text{(H30)}$$

$$\begin{aligned}\frac{d}{dt}y_{\mathrm{IhA}}(t) = {} & b_{\mathrm{IhA}} + k^{\mathrm{IhA}}_{\mathrm{PrF}} \cdot y_{\mathrm{PrF}}(t) + k^{\mathrm{IhA}}_{\mathrm{Sc1}} \cdot y_{\mathrm{Sc1}}(t) + k^{\mathrm{IhA}}_{\mathrm{Lut1}} \cdot y_{\mathrm{Lut1}}(t) + k^{\mathrm{IhA}}_{\mathrm{Lut2}} \cdot y_{\mathrm{Lut2}}(t) \\ & + k^{\mathrm{IhA}}_{\mathrm{Lut3}} \cdot y_{\mathrm{Lut3}}(t) + k^{\mathrm{IhA}}_{\mathrm{Lut4}} \cdot y_{\mathrm{Lut4}}(t) - k^{\mathrm{IhA}} \cdot y_{\mathrm{IhA}}(t) \end{aligned} \quad \text{(H31)}$$

$$\frac{d}{dt}y_{\mathrm{IhAe}}(t) = k^{\mathrm{IhA}} \cdot y_{\mathrm{IhA}}(t) - k^{\mathrm{IhAe}}_{cl} \cdot y_{\mathrm{IhAe}}(t) \quad \text{(H32)}$$

$$\frac{d}{dt}y_{\mathrm{IhB}}(t) = b_{\mathrm{IhB}}(t) + k^{\mathrm{IhB}}_{\mathrm{AF2}} \cdot y_{\mathrm{AF2}}(t) + k^{\mathrm{IhB}}_{\mathrm{Sc2}} \cdot y_{\mathrm{Sc2}}(t) - k^{\mathrm{IhB}}_{cl} \cdot y_{\mathrm{IhB}}(t) \quad \text{(H33)}$$

Table A.2: Parameter values for the full human model(d=days). (More details about the parameter identifiability can be found in [RmD+12].

No.	Symbol	value	unit
1*	b^{LH}_{Syn}	7309.92	IU/d
2	$k^{\mathrm{LH}}_{\mathrm{E2}}$	7309.92	IU/d
3	$T^{\mathrm{LH}}_{\mathrm{E2}}$	192.2	pg/mL
4	$n^{\mathrm{LH}}_{\mathrm{E2}}$	10	–
5	$T^{\mathrm{LH}}_{\mathrm{P4}}$	2.371	ng/mL
6	$n^{\mathrm{LH}}_{\mathrm{P4}}$	1	–
7*	b^{LH}_{Rel}	0.00476	1/d
8*	$k^{\mathrm{LH}}_{\mathrm{(G\text{-}RG)}}$	0.1904	1/d
9	$T^{\mathrm{LH}}_{\mathrm{(G\text{-}RG)}}$	0.0003	nmol/L
10	$n^{\mathrm{LH}}_{\mathrm{(G\text{-}RG)}}$	5	–
11	V_{blood}	6.589	L
12	k^{LH}_{on}	2.143	L/(d·IU)
13	k^{LH}_{cl}	74.851	1/d
14	k^{LH}_{recy}	68.949	1/d
15	k^{LH}_{des}	183.36	1/d
16	T^{FSH}_{freq}	12.8	1/d
17	n^{FSH}_{freq}	5	–
18	$k^{\mathrm{FSH}}_{\mathrm{Inh}}$	2.213e+4	IU/d
19	T_{InhA}	95.81	IU/mL
20	T_{InhB}	70	pg/mL
21	n_{InhA}	5	–
22	n_{InhB}	2	–
23	b^{FSH}_{Rel}	0.057	1/d
24	$k^{\mathrm{FSH}}_{\mathrm{(G\text{-}RG)}}$	0.272	1/d
25	$T^{\mathrm{FSH}}_{\mathrm{(G\text{-}RG)}}$	0.0003	nmol/L
26	$n^{\mathrm{FSH}}_{\mathrm{(G\text{-}RG)}}$	2	–
27	k^{FSH}_{on}	3.529	L/(d·IU)
28	k^{FSH}_{cl}	114.25	1/d
29	k^{FSH}_{recy}	61.029	1/d
30	k^{FSH}_{des}	138.3	1/d
31	T^{s}_{FSH}	3	IU/L

Continued on next page...

Table A.2 – *continued from previous page*

No.	Symbol	value	unit
32	n^{s}_{FSH}	5	–
33	T^{s}_{P4}	1.235	ng/mL
34	n^{s}_{P4}	5	–
35	k^{s}	0.219	1/d
36	k^{s}_{cl}	1.343	1/d
37	$n^{\mathrm{AF1}}_{\mathrm{(FSH\text{-}RF)}}$	5	–
38	$T^{\mathrm{AF1}}_{\mathrm{(FSH\text{-}RF)}}$	0.608	IU/L
39	k^{AF1}	3.662	[PrA1]/d
40	$k^{\mathrm{AF2}}_{\mathrm{AF1}}$	1.221	L/(d·IU)
41	$\mathrm{SF}_{\mathrm{(LH\text{-}RL)}}$	2.726	IU/L
42	$k^{\mathrm{AF3}}_{\mathrm{AF2}}$	4.882	1/d
43	$n^{\mathrm{AF3}}_{\mathrm{AF2}}$	3.689	–
44	$k^{\mathrm{AF3}}_{\mathrm{AF3}}$	0.122	L/(d·IU)
45	$SeF_{\max}$	10	[SeF1]
46	$k^{\mathrm{AF4}}_{\mathrm{AF3}}$	122.06	1/d
47	$n^{\mathrm{AF4}}_{\mathrm{AF3}}$	5	–
48	$k^{\mathrm{AF4}}_{\mathrm{AF4}}$	12.206	1/d
49	n^{AF4}	2	–
50	$k^{\mathrm{PrF}}_{\mathrm{AF4}}$	332.75	1/d
51	k^{PrF}_{cl}	122.06	1/d
52	n^{OvF}	6	–
53	k^{OvF}	7.984	1/d
54	$T^{\mathrm{OvF}}_{\mathrm{PrF}}$	3	[PrF]
55	$n^{\mathrm{OvF}}_{\mathrm{PrF}}$	10	–
56	k^{OvF}_{cl}	12.206	1/d
57	k^{Sc1}	1.208	1/d
58	$T^{\mathrm{Sc1}}_{\mathrm{OvF}}$	0.02	[OvF]
59	$n^{\mathrm{Sc1}}_{\mathrm{OvF}}$	10	–
60	$k^{\mathrm{Sc2}}_{\mathrm{Sc1}}$	1.221	1/d
61	$k^{\mathrm{Lut1}}_{\mathrm{Sc2}}$	0.958	1/d
62	$k^{\mathrm{Lut2}}_{\mathrm{Lut1}}$	0.925	1/d
63	$k^{\mathrm{Lut3}}_{\mathrm{Lut2}}$	0.7567	1/d
64	$k^{\mathrm{Lut4}}_{\mathrm{Lut3}}$	0.610	1/d
65	k^{Lut4}_{cl}	0.543	1/d
66	$m^{\mathrm{Lut}}_{\mathrm{(G\text{-}RG)}}$	20	–
67	$T^{\mathrm{Lut}}_{\mathrm{(G\text{-}RG)}}$	0.0008	nmol/L
68	$n^{\mathrm{Lut}}_{\mathrm{(G\text{-}RG)}}$	5	–
69	b^{E2}	51.558	$\frac{\mathrm{pg/mL}}{\mathrm{d}}$

Continued on next page...

Table A.2 – *continued from previous page*

No.	Symbol	value	unit
70	$k^{\mathrm{E2}}_{\mathrm{AF2}}$	2.0945	$\frac{\mathrm{pg/mL}}{[\mathrm{AF2}]\cdot\mathrm{d}}$
71	$k^{\mathrm{E2}}_{\mathrm{AF3}}$	9.28	$\frac{\mathrm{pg/mL}}{[\mathrm{AF3}]\cdot[\mathrm{LH}]\cdot\mathrm{d}}$
72	$k^{\mathrm{E2}}_{\mathrm{AF4}}$	6960.53	$\frac{\mathrm{pg/mL}}{[\mathrm{AF4}]\cdot\mathrm{d}}$
73	$k^{\mathrm{E2}}_{\mathrm{PrF}}$	0.972	$\frac{\mathrm{pg/mL}}{[\mathrm{PrF}]\cdot[\mathrm{LH}]\cdot\mathrm{d}}$
74	$k^{\mathrm{E2}}_{\mathrm{Lut1}}$	1713.71	$\frac{\mathrm{pg/mL}}{[\mathrm{Lut1}]\cdot\mathrm{d}}$
75	$k^{\mathrm{E2}}_{\mathrm{Lut4}}$	8675.14	$\frac{\mathrm{pg/mL}}{[\mathrm{Lut4}]\cdot\mathrm{d}}$
76	k^{E2}_{cl}	5.235	1/d
77	b^{P4}	0.943	$\frac{\mathrm{ng/mL}}{\mathrm{d}}$
78	$k^{\mathrm{P4}}_{\mathrm{Lut4}}$	761.64	$\frac{\mathrm{ng/mL}}{[\mathrm{Lut4}]\cdot\mathrm{d}}$
79	k^{P4}_{cl}	5.13	1/d
80	b^{InhA}	1.445	$\frac{\mathrm{IU/mL}}{\mathrm{d}}$
81	k^{InhA}_{PrF}	2.285	$\frac{\mathrm{IU/mL}}{[\mathrm{PrF}]\cdot\mathrm{d}}$
82	k^{InhA}_{Sc1}	60	$\frac{\mathrm{pg/mL}}{[Sc1]\cdot\mathrm{d}}$
83	k^{InhA}_{Lut1}	180	$\frac{\mathrm{pg/mL}}{[\mathrm{Lut1}]\cdot\mathrm{d}}$
84	k^{InhA}_{Lut2}	28.211	$\frac{\mathrm{IU/mL}}{[\mathrm{Lut2}]\cdot\mathrm{d}}$
85	k^{InhA}_{Lut3}	216.85	$\frac{\mathrm{IU/mL}}{[\mathrm{Lut3}]\cdot\mathrm{d}}$
86	k^{InhA}_{Lut4}	114.25	$\frac{\mathrm{IU/mL}}{[\mathrm{Lut4}]\cdot\mathrm{d}}$
87	k^{InhA}	4.287	1/d
88	$k^{InhA_e}_{cl}$	0.199	1/d
89	b^{InhB}	89.493	$\frac{\mathrm{pg/mL}}{\mathrm{d}}$
90	k^{InhB}_{AF2}	447.47	$\frac{\mathrm{pg/mL}}{[\mathrm{AF2}]\cdot\mathrm{d}}$
91	k^{InhB}_{Sc2}	134240.2	$\frac{\mathrm{pg/mL}}{[\mathrm{AF3}]\cdot\mathrm{d}}$
92	k^{InhB}_{cl}	172.45	1/d
93	f_0	16	1/d
94	T^{freq}_{P4}	1.2	ng/mL
95	n^{freq}_{P4}	2	–
96	m^{freq}_{E2}	1	–
97	T^{freq}_{E2}	220	pg/mL
98	n^{freq}_{E2}	10	–
99	a_0	5.593e-3	nmol
100	$T^{mass,1}_{\mathrm{E2}}$	220	pg/mL
101	$n^{mass,1}_{\mathrm{E2}}$	2	–
102	$T^{mass,2}_{\mathrm{E2}}$	9.6	pg/mL
103	$n^{mass,2}_{\mathrm{E2}}$	1	–
104	k^{G}_{degr}	0.447	1/d
105	k^{G}_{on}	322.18	$\frac{\mathrm{L}}{\mathrm{d}\cdot\mathrm{nmol}}$
106	k^{G}_{off}	644.35	1/d
107	$k^{(\mathrm{G\text{-}RG})*}_{degr}$	0.00895	1/d

Continued on next page...

Table A.2 – *continued from previous page*

No.	Symbol	value	unit
108	$k^{(\mathrm{G\text{-}RG})*}_{diss}$	32.218	1/d
109	k^{RG}_{inter}	3.222	1/d
110	k^{RG}_{recy}	32.218	1/d
111	k^{RG}_{degr}	0.0895	1/d
112	$k^{(\mathrm{G\text{-}RG})}_{inact}$	32.218	1/d
113	$k^{(\mathrm{G\text{-}RG})}_{act}$	3.222	1/d
114	k^{RG}_{syn}	8.949e-5	$\frac{\mathrm{nmol}}{\mathrm{L}\cdot\mathrm{d}}$

Table A.3: Initial values

No.	component	value	unit
1	y_{LHp}	3.141e+5	IU
2	y_{LH}	3.487	IU/L
3	y_{RL}	8.157	IU/L
4	$y_{(\mathrm{LH\text{-}RL})}$	0.332	IU/L
5	y_{RLdes}	0.882	IU/L
6	y_{FSHp}	6.928e+4	IU
7	y_{FSH}	6.286	IU/L
8	y_{RF}	5.141	IU/L
9	$y_{(\mathrm{FSH\text{-}RF})}$	1.030	IU/L
10	y_{RFdes}	2.330	IU/L
11	y_{s}	0.417	–
12	y_{AF1}	2.811	uFoll
13	y_{AF2}	27.64	uFoll
14	y_{AF3}	0.801	uFoll
15	y_{AF4}	6.345e-5	uFoll
16	y_{PrF}	0.336	uFoll
17	y_{OvF}	1.313e-16	uFoll
18	y_{Sc1}	1.433e-10	uFoll
19	y_{Sc2}	7.278e-8	uFoll
20	y_{Lut1}	1.293e-6	uFoll
21	y_{Lut2}	3.093e-5	uFoll
22	y_{Lut3}	4.853e-4	uFoll
23	y_{Lut4}	3.103e-3	uFoll
24	y_{E2}	30.94	pg/mL

Continued on next page...

Table A.3 – *continued from previous page*

No.	component	value	unit
25	y_{P4}	0.688	ng/mL
26	y_{IhA}	0.637	IhA
27	y_{IhB}	72.17	IhB
28	y_{IhAe}	52.43	uIhA
29	y_{G}	1.976e-2	nmol/L
30	y_{RG}	9.121e-3	nmol/L
31	$y_{\mathrm{RG*}}$	9.893e-4	nmol/L
32	$y_{\mathrm{(G\text{-}RG)}}$	8.618e-5	nmol/L
33	$y_{\mathrm{(G\text{-}RG)*}}$	7.768e-5	nmol/L
34	$y_{\mathrm{Ago,D}}$	0	μg
35	$y_{\mathrm{Ago,C}}$	0	μg/L=ng/mL
36	$y_{\mathrm{(Ago\text{-}RG)}}$	0	nmol/L
37	$y_{\mathrm{(Ago\text{-}RG)*}}$	0	nmol/L
38	$y_{\mathrm{Ant,D}}$	0	μg
39	$y_{\mathrm{Ant,C}}$	0	μg/L=ng/mL
40	$y_{\mathrm{Ant,P}}$	0	μg/L=ng/mL
41	$y_{\mathrm{(Ant\text{-}RG)}}$	0	nmol/L

ODEs and parameters for BovCycle

Table A.4: The ODE model of the bovine estrous cycle. It consists of 15 ODEs and 45 parameters.

$Syn_{\mathrm{G}}(t)$	$=$	$c_{\mathrm{G},1} \cdot \left(1 - \frac{y_{\mathrm{Gh}}(t)}{\mathrm{G}^{\max}_{Hypo}}\right)$	
$Rel_{\mathrm{G}}(t)$	$=$	$\left(H^{-}_{\mathrm{P4\&E2,G}}(y_{\mathrm{P4}}(t), y_{\mathrm{E2}}(t)) + H^{-}_{\mathrm{P4,G}}(y_{\mathrm{P4}}(t))\right) \cdot y_{\mathrm{Gh}}(t)$	
$\frac{d}{dt} y_{\mathrm{Gh}}(t)$	$=$	$Syn_{\mathrm{G}}(t) - Rel_{\mathrm{G}}(t)$	(B1)
$\frac{d}{dt} y_{\mathrm{G}}(t)$	$=$	$Rel_{\mathrm{G}}(t) \cdot H^{+}_{\mathrm{E2,G}}(y_{\mathrm{E2}}(t)) - c_{\mathrm{G},2} \cdot y_{\mathrm{G}}(t)$	(B2)
$Syn_{\mathrm{FSH}}(t)$	$=$	$H^{-}_{\mathrm{Inh,FSH}}(y_{\mathrm{Inh}}(t))$	
$Rel_{\mathrm{FSH}}(t)$	$=$	$\left(b_{\mathrm{FSH}} + H^{+}_{\mathrm{P4,FSH}}(y_{\mathrm{P4}}(t)) + H^{-}_{\mathrm{E2,FSH}}(y_{\mathrm{E2}}(t)) + H^{+}_{\mathrm{G,FSH}}(y_{\mathrm{G}}(t))\right) \cdot y_{\mathrm{FSHp}}(t)$	
$\frac{d}{dt} y_{\mathrm{FSHp}}(t)$	$=$	$Syn_{\mathrm{FSH}}(t) - Rel_{\mathrm{FSH}}(t)$	(B3)
$\frac{d}{dt} y_{\mathrm{FSH}}(t)$	$=$	$Rel_{\mathrm{FSH}}(t) - c_{\mathrm{FSH}} \cdot y_{\mathrm{FSH}}(t)$	(B4)
$Syn_{\mathrm{LH}}(t)$	$=$	$H^{+}_{\mathrm{E2,LH}}(y_{\mathrm{E2}}(t)) + H^{-}_{\mathrm{P4,LH}}(y_{\mathrm{P4}}(t))$	
$Rel_{\mathrm{LH}}(t)$	$=$	$\left(b_{\mathrm{LH}} + H^{+}_{\mathrm{G,LH}}(y_{\mathrm{G}}(t))\right) \cdot y_{\mathrm{LHp}}(t)$	
$\frac{d}{dt} y_{\mathrm{LHp}}(t)$	$=$	$Syn_{\mathrm{LH}}(t) - Rel_{\mathrm{LH}}(t)$	(B5)
$\frac{d}{dt} y_{\mathrm{LH}}(t)$	$=$	$Rel_{\mathrm{LH}}(t) - c_{\mathrm{LH}} \cdot y_{\mathrm{LH}}(t),$	(B6)
$\frac{d}{dt} y_{\mathrm{Foll}}(t)$	$=$	$\widetilde{H^{+}}_{\mathrm{FSH,Foll}}\left(y_{\mathrm{FSH}}(t)\right) - \left(H^{+}_{\mathrm{P4,Foll}}(y_{\mathrm{P4}}(t)) + H^{+}_{\mathrm{LH,Foll}}(y_{\mathrm{LH}}(t))\right) \cdot y_{\mathrm{Foll}}(t)$	(B7)
		$\widetilde{H^{+}}_{\mathrm{FSH,Foll}}\left(y_{\mathrm{FSH}}(t)\right) := m^{\mathrm{Foll}}_{\mathrm{FSH}} \cdot h^{+}\left(y_{\mathrm{FSH}}(t), T^{\mathrm{Foll}}_{\mathrm{FSH}} \cdot h^{+}(y_{\mathrm{Foll}}(t), T^{\mathrm{Foll}}_{\mathrm{Foll}}, n^{\mathrm{Foll}}_{\mathrm{Foll}}), n^{\mathrm{Foll}}_{\mathrm{FSH}}\right)$	
$\frac{d}{dt} y_{\mathrm{CL}}(t)$	$=$	$\mathrm{SF} \cdot H^{+}_{\mathrm{LH,CL}}(y_{\mathrm{LH}}(t)) \cdot y_{\mathrm{Foll}}(t) + H^{+}_{\mathrm{CL,CL}}(y_{\mathrm{CL}}(t)) - H^{+}_{\mathrm{IOF,CL}}(y_{\mathrm{IOF}}(t)) \cdot y_{\mathrm{CL}}(t)$	(B8)
$\frac{d}{dt} y_{\mathrm{P4}}(t)$	$=$	$c^{\mathrm{P4}}_{\mathrm{CL}} \cdot y_{\mathrm{CL}}(t)^2 - c_{\mathrm{P4}} \cdot y_{\mathrm{P4}}(t)$	(B9)
$\frac{d}{dt} y_{\mathrm{E2}}(t)$	$=$	$c^{\mathrm{E2}}_{\mathrm{Foll}} \cdot y_{\mathrm{Foll}}(t)^2 - c_{\mathrm{E2}} \cdot y_{\mathrm{E2}}(t)$	(B10)
$\frac{d}{dt} y_{\mathrm{Inh}}(t)$	$=$	$c^{\mathrm{Inh}}_{\mathrm{Foll}} \cdot y_{\mathrm{Foll}}(t)^2 - c_{\mathrm{Inh}} \cdot y_{\mathrm{Inh}}(t)$	(B11)
$\frac{d}{dt} y_{\mathrm{Enz}}(t)$	$=$	$H^{+}_{\mathrm{P4,Enz}}(y_{\mathrm{P4}}(t)) - c_{\mathrm{Enz}} \cdot y_{\mathrm{Enz}}(t)$	(B12)
$\frac{d}{dt} y_{\mathrm{OT}}(t)$	$=$	$H^{+}_{\mathrm{E2,OT}}(y_{\mathrm{E2}}(t)) \cdot y_{\mathrm{CL}}(t)^2 - c_{\mathrm{OT}} \cdot y_{\mathrm{OT}}(t)$	(B13)
$\frac{d}{dt} y_{\mathrm{PGF}}(t)$	$=$	$H^{+}_{\mathrm{Enz\&OT,PGF}}(y_{\mathrm{Enz}}(t), y_{\mathrm{OT}}(t)) - c_{\mathrm{PGF}} \cdot y_{\mathrm{PGF}}(t)$	(B14)
$\frac{d}{dt} y_{\mathrm{IOF}}(t)$	$=$	$H^{+}_{\mathrm{PGF\&CL,IOF}}(y_{\mathrm{PGF}}(t), y_{\mathrm{CL}}(t)) - c_{\mathrm{IOF}} \cdot y_{\mathrm{IOF}}(t)$	(B15)

Table A.5: Parameter values for the original BovCycle. Hill exponents have been set fixed as $n_{\mathrm{E2}}^{\mathrm{G,2}} = n_{\mathrm{Inh}}^{\mathrm{FSH}} = n_{\mathrm{G}}^{\mathrm{LH}} = n_{\mathrm{P4}}^{\mathrm{Foll}} = n_{\mathrm{Enz}}^{\mathrm{PGF}} = n_{\mathrm{IOF}}^{\mathrm{CL}} = n_{\mathrm{P4}}^{\mathrm{Enz}} = n_{\mathrm{PGF}}^{\mathrm{IOF}} = 5$, $n_{\mathrm{CL}}^{\mathrm{IOF}} = 10$, $n_{\mathrm{G}}^{\mathrm{FSH}} = 1$, and the rest of the Hill exponents are set to 2.

No.	Symbol	Value	Unit
1	$\mathrm{G}_{Hypo}^{\max}$	16	$[\mathrm{GnRH_{Hypo}}]$
2	$c_{\mathrm{G},1}$	2.75	$\frac{[\mathrm{GnRH_{Hypo}}]}{[\mathrm{t}]}$
3	$m_{P_4\&E_2}$	2.05	$1/[t]$
4	$T_{E_2}^{\mathrm{G},1}$	0.0972	[E2]
5	$T_{P_4}^{\mathrm{G},1}$	0.35	[P4]
6	$m_{P_4}^{\mathrm{G},2}$	1.91	1/[t]
7	$T_{P_4}^{\mathrm{G},2}$	0.252	[P4]
8	$m_{E_2}^{\mathrm{G},2}$	0.99	$\frac{[\mathrm{GnRH_{Pit}}]}{[\mathrm{GnRH_{Hypo}}]}$
9	$T_{E_2}^{\mathrm{G},2}$	0.648	[E2]
10	$c_{\mathrm{G},2}$	1.63	1/[t]
11	$m_{\mathrm{Inh}}^{\mathrm{FSH}}$	4.21	[FSH]/[t]
12	$T_{\mathrm{Inh}}^{\mathrm{FSH}}$	0.118	[Inh]
13	b_{FSH}	0.948	1/[t]
14	$m_{P_4}^{\mathrm{FSH}}$	0.293	1/[t]
15	$T_{P_4}^{FSH}$	0.152	[P4]
16	$m_{E_2}^{\mathrm{FSH}}$	0.396	1/[t]
17	$T_{E_2}^{\mathrm{FSH}}$	0.312	[E2]
18	$m_{\mathrm{G}}^{\mathrm{FSH}}$	1.23	1/[t]
19	$T_{\mathrm{G}}^{\mathrm{FSH}}$	0.0708	$[\mathrm{GnRH_{Pit}}]$
20	c_{FSH}	2.73	1/[t]
21	$m_{E_2}^{\mathrm{LH}}$	0.376	[LH]/[t]
22	$T_{E_2}^{\mathrm{LH}}$	0.243	[E2]
23	$m_{P_4}^{\mathrm{LH}}$	2.71	[LH]/[t]
24	$T_{P_4}^{\mathrm{LH}}$	0.0269	[P4]
25	b_{LH}	0.0141	1/[t]
26	$m_{\mathrm{G}}^{\mathrm{LH}}$	2.22	1/[t]
27	$T_{\mathrm{G}}^{\mathrm{LH}}$	0.69	$[\mathrm{GnRH_{Pit}}]$
28	c_{LH}	12.0	1/[t]
29	$m_{\mathrm{FSH}}^{\mathrm{Foll}}$	0.562	[Foll]/[t]

Continued on next column...

Table A.5 – *continued from previous column*

No.	Symbol	Value	Unit
30	$T_{\mathrm{FSH}}^{\mathrm{Foll}}$	0.57	[FSH]
31	$T_{\mathrm{Foll}}^{\mathrm{FSH}}$	0.22	[Foll]
32	$m_{P_4}^{\mathrm{Foll}}$	1.1	1/[t]
33	$T_{P_4}^{\mathrm{Foll}}$	0.126	[P4]
34	m_{LH}^{Ovul}	3.49	1/[t]
35	T_{LH}^{Ovul}	0.171	[LH]
36	SF	0.2	[CL]/[t]
37	$m_{\mathrm{CL}}^{\mathrm{CL}}$	0.0353	[CL]/[t]
38	$T_{\mathrm{CL}}^{\mathrm{CL}}$	0.1	[CL]
39	$m_{\mathrm{IOF}}^{\mathrm{CL}}$	41.39	1/[t]
40	$T_{\mathrm{IOF}}^{\mathrm{CL}}$	1.32	[IOF]
41	$c_{\mathrm{CL}}^{\mathrm{P4}}$	2.25	$\frac{[\mathrm{P4}]/[\mathrm{CL}]^2}{[\mathrm{t}]}$
42	c_{P4}	1.41	1/[t]
43	$c_{\mathrm{Foll}}^{\mathrm{E2}}$	2.19	$\frac{[\mathrm{E2}]/[\mathrm{Foll}]^2}{[\mathrm{t}]}$
44	c_{E2}	1.23	1/[t]
45	$c_{\mathrm{Foll}}^{\mathrm{Inh}}$	1.41	$\frac{[\mathrm{Inh}]/[\mathrm{Foll}]^2}{[\mathrm{t}]}$
46	c_{Inh}	0.475	1/[t]
47	$m_{\mathrm{P4}}^{\mathrm{Enz}}$	3.58	[Enz]/[t]
48	$T_{\mathrm{P4}}^{\mathrm{Enz}}$	0.77	[P4]
49	c_{Enz}	2.98	1/[t]
50	$m_{\mathrm{E2}}^{\mathrm{OT}}$	1.59	$\frac{[\mathrm{OT}]/[\mathrm{CL}]^2}{[\mathrm{t}]}$
51	$T_{\mathrm{E2}}^{\mathrm{OT}}$	0.143	[E2]
52	c_{OT}	0.644	1/[t]
53	$m_{\mathrm{PGF\&CL}}^{\mathrm{IOF}}$	39.68	[IOF]/[t]
54	$T_{\mathrm{PGF}}^{\mathrm{IOF}}$	1.22	[PGF]
55	$T_{\mathrm{CL}}^{\mathrm{IOF}}$	0.6	[CL]
56	c_{IOF}	0.298	1/[t]
57	$m_{\mathrm{Enz\&OT}}^{\mathrm{PGF}}$	53.91	[PGF]/[t]
58	$T_{\mathrm{Enz}}^{\mathrm{PGF}}$	1.43	[Enz]
59	$T_{\mathrm{OT}}^{\mathrm{PGF}}$	1.087	[OT]
60	c_{PGF}	1.23	1/[t]
	D	3.7	[PGF]
	β	100	1/[t]
	$c_{PGF_{syn}}$	5.5	1/[t]

Table A.6: Initial values for the full bovine model

No.	Symbol	Value
1	y_{Gh}	0.667
2	y_{G}	0.551
3	y_{FSHp}	0.316
4	y_{FSH}	0.395
5	y_{LHp}	4.563
6	y_{LH}	0.642
7	y_{Foll}	0.796
8	y_{CL}	0.0651
9	y_{P4}	0.004
10	y_{E2}	0.89
11	y_{Inh}	0.826
12	y_{Enz}	0
13	y_{OT}	0.183
14	y_{PGF}	0.00506
15	y_{IOF}	0.253

ODEs and parameters for the reduced version of BovCycle

Table A.7: Reduced model for the bovine estrous cycle. It consists of 10 ODEs and 38 parameters.

$$\frac{d}{dt}y_{\mathrm{G}}(t) = H^{-}_{\mathrm{P4,G}}\left(y_{\mathrm{P4}}(t)\right) \cdot H^{+}_{\mathrm{E2,G}}\left(y_{\mathrm{E2}}(t)\right) - c_{\mathrm{G}} \cdot y_{\mathrm{G}}(t) \quad \text{(BR1)}$$

$$\frac{d}{dt}y_{\mathrm{FSH}}(t) = H^{-}_{\mathrm{Inh,FSH}}(y_{\mathrm{Inh}}(t)) - c_{\mathrm{FSH}} \cdot y_{\mathrm{FSH}}(t) \quad \text{(BR2)}$$

$$\frac{d}{dt}y_{\mathrm{LH}}(t) = H^{-}_{\mathrm{P4,LH}}(y_{\mathrm{P4}}(t)) \cdot H^{+}_{\mathrm{G,LH}}\left(y_{\mathrm{G}}(t)\right) - c_{\mathrm{LH}} \cdot y_{\mathrm{LH}}(t) \quad \text{(BR3)}$$

$$\begin{aligned}\frac{d}{dt}y_{\mathrm{Foll}}(t) = {} & H^{+}_{\mathrm{FSH,Foll}}\left(y_{\mathrm{FSH}}(t)\right) \cdot \Big(1 + H^{+}_{\mathrm{Foll,Foll}}\left(y_{\mathrm{Foll}}(t)\right)\Big) \\ & - \Big(H^{+}_{\mathrm{P4,Foll}}(y_{\mathrm{P4}}(t)) + H^{+}_{\mathrm{LH,Ovul}}(y_{\mathrm{LH}}(t))\Big) \cdot y_{\mathrm{Foll}}(t)\end{aligned} \quad \text{(BR4)}$$

$$\frac{d}{dt}y_{\mathrm{CL}}(t) = H^{+}_{\mathrm{LH,Ovul}}\left(y_{\mathrm{LH}}(t)\right) \cdot y_{\mathrm{Foll}}(t) + H^{+}_{\mathrm{CL,CL}}\left(y_{\mathrm{CL}}(t)\right) - H^{+}_{\mathrm{IOF,CL}}\left(y_{\mathrm{IOF}}(t)\right) \cdot y_{\mathrm{CL}}(t) \quad \text{(BR5)}$$

$$\frac{d}{dt}y_{\mathrm{P4}}(t) = k^{\mathrm{P4}}_{\mathrm{CL}} \cdot y_{\mathrm{CL}}(t) - c_{\mathrm{P4}} \cdot y_{\mathrm{P4}}(t) \quad \text{(BR6)}$$

$$\frac{d}{dt}y_{\mathrm{E2}}(t) = k^{\mathrm{E2}}_{\mathrm{Foll}} \cdot y_{\mathrm{Foll}}(t) - c_{\mathrm{E2}} \cdot y_{\mathrm{E2}}(t) \quad \text{(BR7)}$$

$$\frac{d}{dt}y_{\mathrm{Inh}}(t) = k^{\mathrm{Inh}}_{\mathrm{Foll}} \cdot y_{\mathrm{Foll}}(t) - c_{\mathrm{Inh}} \cdot y_{\mathrm{Inh}}(t) \quad \text{(BR8)}$$

$$\frac{d}{dt}y_{\mathrm{PGF}}(t) = H^{+}_{\mathrm{E2,PGF}}(y_{\mathrm{E2}}(t)) \cdot H^{+}_{\mathrm{P4,PGF}} - c_{\mathrm{PGF}} \cdot y_{\mathrm{PGF}}(t) \quad \text{(BR9)}$$

$$\frac{d}{dt}y_{\mathrm{IOF}}(t) = H^{+}_{\mathrm{PGF,IOF}}(y_{\mathrm{PGF}}(t)) \cdot H^{+}_{\mathrm{CL,IOF}}(y_{\mathrm{CL}}(t)) - c_{\mathrm{IOF}} \cdot y_{\mathrm{IOF}}(t) \quad \text{(BR10)}$$

Table A.8: Parameter values for the reduced bovine model. Hill exponents have been set fixed as $n_{\mathrm{E2}}^{\mathrm{GnRH}} = n_{\mathrm{Inh}}^{\mathrm{FSH}} = n_{\mathrm{P4}}^{\mathrm{Foll}} = n_{\mathrm{IOF}}^{\mathrm{CL}} = n_{\mathrm{P4}}^{\mathrm{PGF}} = n_{\mathrm{PGF}}^{\mathrm{IOF}} = n_{\mathrm{CL}}^{\mathrm{IOF}} = 5$, the rest of the Hill exponents are set to 2.

No.	Symbol	Value	Unit
1	$m_{\mathrm{E2,P4}}^{\mathrm{G}}$	6.212	[GnRH]/[t]
2	$T_{\mathrm{P4}}^{\mathrm{G}}$	0.274	[P4]
3	$T_{\mathrm{E2}}^{\mathrm{G}}$	1.104	[E2]
4	cl_{G}	1.664	1/[t]
5	$m_{\mathrm{Inh}}^{\mathrm{FSH}}$	1.207	[FSH]/[t]
6	$T_{\mathrm{Inh}}^{\mathrm{FSH}}$	0.155	[Inh]
7	cl_{FSH}	0.761	1/[t]
8	$m_{\mathrm{G},P4}^{\mathrm{LH}}$	39.983	[LH]/[t]
9	$T_{\mathrm{P4}}^{\mathrm{LH}}$	0.0547	[P4]
10	$T_{\mathrm{G}}^{\mathrm{LH}}$	0.717	[GnRH]
11	clLH	12.253	1/[t]
12	$m_{\mathrm{FSH}}^{\mathrm{Foll}}$	0.351	[Foll]/[t]
13	$T_{\mathrm{FSH}}^{\mathrm{Foll}}$	0.669	[FSH]
14	$m_{\mathrm{Foll}}^{\mathrm{Foll}}$	3.927	-
15	$T_{\mathrm{Foll}}^{\mathrm{Foll}}$	0.277	[Foll]
16	$m_{\mathrm{P4}}^{\mathrm{Foll}}$	1.075	1/[t]
17	$T_{\mathrm{P4}}^{\mathrm{Foll}}$	0.126	[P4]
18	$m_{\mathrm{LH}}^{\mathrm{Foll}}$	2.313	[1/[t]
19	$T_{\mathrm{LH}}^{\mathrm{Foll}}$	0.555	[LH]
20	$\mathrm{SF}_{\mathrm{CL}}$	0.253	[CL]
21	$m_{\mathrm{CL}}^{\mathrm{CL}}$	0.0506	[CL]/[t]
22	$T_{\mathrm{CL}}^{\mathrm{CL}}$	0.251	[CL]
23	$m_{\mathrm{IOF}}^{\mathrm{CL}}$	10.25	1/[t]
24	$T_{\mathrm{IOF}}^{\mathrm{CL}}$	1.087	[IOF]
25	$k_{\mathrm{CL}}^{\mathrm{P4}}$	0.969	[P4]/[t]
26	cl_{P4}	0.725	1/[t]
27	$k_{\mathrm{Foll}}^{\mathrm{E2}}$	1.402	[E2]/[t]
28	cl_{E2}	0.98	1/[t]
29	$k_{\mathrm{Foll}}^{\mathrm{Inh}}$	0.652	[Inh]/[t]
30	cl_{Inh}	0.501	1/[t]
31	$m_{\mathrm{E2}}^{\mathrm{PGF}}$	1.844	[PGF]/[t]
32	$T_{\mathrm{E2}}^{\mathrm{PGF}}$	0.217	[E2]
33	$T_{\mathrm{P4}}^{\mathrm{PGF}}$	0.979	[P4]
34	cl_{PGF}	0.484	1/[t]
35	$m_{\mathrm{PGF,CL}}^{\mathrm{IOF}}$	17.527	[IOF]/[t]
36	$T_{\mathrm{PGF}}^{\mathrm{IOF}}$	1.346	[PGF]
37	$T_{\mathrm{CL}}^{\mathrm{IOF}}$	0.511	[CL]
38	cl_{IOF}	0.292	1/[t]

Continued on next column...

Table A.8 – *continued from previous column*

Table A.9: Initial values for the reduced bovine model

No.	Symbol	Value
1	y_{G}	0.0027
2	y_{FSH}	0.5706
3	y_{LH}	0.0000
4	y_{Foll}	0.6131
5	y_{CL}	0.0098
6	y_{P4}	0.0504
7	y_{E2}	0.3650
8	y_{Inh}	0.2603
9	y_{PGF}	0.1418
10	y_{IOF}	0.2630

Bibliography

[AJOK09] W. Abou-Jaoudé, D. A. Ouattara, and M. Kaufman. From structure to dynamics: Frequency tuning in the p53–Mdm2 network: I. Logical approach. *Journal of Theoretical Biology*, 258(4):561–577, 2009.

[Aco07] T. J. Acosta. Studies of follicular vascularity associated with follicle selection and ovulation in cattle. *Journal of Reproduction and Development*, 53(1):39–44, 2007.

[AOK+00] T. J. Acosta, T. Ozawa, S. Kobayashi, K. Hayashi, M. Ohtani, W. D. Kraetzl, K. Sato, D. Schams, and A. Miyamoto. Periovulatory changes in the local release of vasoactive peptides, prostaglandin F2α, and steroid hormones from bovine mature follicles in vivo. *Biology of Reproduction*, 63(5):1253–1261, 2000.

[AJSM08] G. P. Adams, R. Jaiswal, J. Singh, and P. Malhi. Progress in understanding ovarian follicular dynamics in cattle. *Theriogenology*, 69(1):72–80, 2008.

[AMG92] G. P. Adams, R. L. Matteri, and O. J. Ginther. Effect of progesterone on ovarian follicles, emergence of follicular waves and circulating follicle-stimulating hormone in heifers. *Journal of Reproduction and Fertility*, 96(2):627–640, 1992.

[AP95] G. P. Adams and R. A. Pierson. Bovine model for study of ovarian follicular dynamics in humans. *Theriogenology*, 43(1):113–120, 1995.

[AGM12] M. Apri, M. de Gee, and J. Molenaar. Complexity reduction preserving dynamical behavior of biochemical networks. *Journal of Theoretical Biology*, 304:16–26, 2012.

[AMGV10] M. Apri, J. Molenaar, M. de Gee, and G. van Voorn. Efficient estimation of the robustness region of biological models with oscillatory behavior. *PLoS ONE*, 5(4):e9865, 2010.

[AGF+09] R. R. Araujo, O. J. Ginther, J. C. Ferreira, M.M. Palhão, M.A. Beg, and M.C. Wiltbank. Role of follicular estradiol-17beta in timing of luteolysis in heifers. *Biology of Reproduction*, 81(2):426–437, 2009.

[AGBF96] E. Asselin, A. K. Goff, H. Bergeron, and M. A. Fortier. Influence of sex steroids on the production of prostaglandins F2α and E2 and response to oxytocin in cultured ephithelial and stromal cells of the bovine endometrium. *Biology of Reproduction*, 54(2):371–379, 1996.

[BAP03] A. R. Baerwald, G. P. Adams, and R. A. Pierson. A new model for ovarian follicular development during the human menstrual cycle. *Fertility and Sterility*, 80(1):116–122, 2003.

[Bal95] R.L. Baldwin. *Modeling ruminant digestion and metabolism.* Chapman & Hall, London, 1995.

[BG98] B. Bao and H. A. Garverick. Expression of steroidogenic enzyme and gonadotropin receptor genes in bovine follicles during ovarian follicular waves: A review. *Journal of Animal Science*, 76(7):1903–1921, 1998.

[BBKG02] M. A. Beg, D. R. Bergfelt, K. Kot, and O. J. Ginther. Follicle selection in cattle: Dynamics of follicular fluid factors during development of follicle dominance. *Biology of Reproduction*, 66(1):120–126, 2002.

[BKC+96] E. G. M. Bergfeld, F. N. Kojima, A. S. Cupp, M. E. Wehrman, K. E. Peters, V. Mariscal, T. Sanchez, and J. E. Kinder. Changing dose of progesterone results in sudden changes in frequency of luteinizing hormone pulses and secretion of 17β-estradiol in bovine females. *Biology of Reproduction*, 54(3):546–553, 1996.

[BGF+01] E. C. L. Bleach, R. G. Glencross, S. A. Feist, N. P. Groome, and P. G. Knight. Plasma inhibin A in heifers: Relationship with follicle dynamics, gonadotropins, and steroids during the estrous cycle and after treatment with bovine follicular fluid. *Biology of Reproduction*, 64(3):743–752, 2001.

[BGK04] E. C. L. Bleach, R. G. Glencross, and P. G. Knight. Association between ovarian follicle development and pregnancy rates in dairy cows undergoing spontaneous oestrous cycles. *Reproduction*, 127(5):621–629, 2004.

[Boc81] H. G. Bock. Numerical treatment of inverse problems in chemical reaction kinetics. In K. H. Ebert, P. Deuflhard, and W. Jäger, editors, *Modelling of Chemical Reaction Systems*, volume 18 of *Springer Series in Chemical Physics*, pages 102–125. Springer Berlin Heidelberg, 1981.

[Boc87] H. G. Bock. *Randwertproblemmethoden zur Parameteridentifizierung in Systemen nichtlinearer Differentialgleichungen.* Number 183 in Bonner Mathematische Schriften. Math.-Naturwiss. Fakultät der Universität Bonn, 1987.

[Boe12] H. M. T. Boer. *All in good time : dynamics of the bovine estrous cycle investigated with a mathematical model.* PhD thesis, Wageningen University, 2012.

[BAM+12] H. M. T. Boer, M. Apri, J. Molenaar, C. Stötzel, R. F. Veerkamp, and H. Woelders. Candidate mechanisms underlying atypical progesterone profiles as deduced from parameter perturbations in a mathematical model of the bovine estrous cycle. *Journal of Dairy Science*, 95(7):3837–3851, 2012.

[BmR+10] H. M. T. Boer, C. Stötzel, S. Röblitz, P. Deuflhard, R. F. Veerkamp, and H. Woelders. A simple mathematical model of the bovine estrous cycle: follicle development and endocrine interactions. ZIB-Report 10-06, Konrad-Zuse-Zentrum für Informationstechnik Berlin, 2010.

[BmR+11] H. M. T. Boer, C. Stötzel, S. Röblitz, P. Deuflhard, R. F. Veerkamp, and H. Woelders. A simple mathematical model of the bovine estrous cycle: follicle development and endocrine interactions. *Journal of Theoretical Biology*, 278:20–31, 2011.

[BRm+11] H. M. T. Boer, S. Röblitz, C. Stötzel, R. F. Veerkamp, B. Kemp, and H. Woelders. Mechanisms regulating follicle wave patterns in the bovine estrous cycle investigated with a mathematical model. *Journal of Dairy Science*, 94(12):5987–6000, 2011.

[BVBW10] H. M. T. Boer, R. F. Veerkamp, B. Beerda, and H. Woelders. Estrous behavior in dairy cows: identification of underlying mechanisms and gene functions. *Animal*, 4:446–453, 2010.

[CAŞD05] H. A. Celik, İ Aydın, S. Şendag, and D. A. Dinc. Number of follicular waves and their effect on pregnancy rate in the cow. *Reproduction in Domestic Animals*, 40(2):87–92, 2005.

[CBB02] N. Chabbert-Buffet and P. Bouchard. The normal human menstrual cycle. *Reviews in Endocrine and Metabolic Disorders*, 3(3):173–183, 2002.

[CRMT03] C. Chaouiya, E. Remy, B. Mossé, and D. Thieffry. Qualitative analysis of regulatory graphs: a computational tool based on a discrete formal framework. *Positive Systems*, pages 830–832, 2003.

[CTK+75] J. R. Chenault, W. W. Thatcher, P. S. Kalra, R. M. Abrams, and C. J. Wilcox. Transitory changes in plasma progestins, estradiol, and luteinizing hormone approaching ovulation in the bovine. *Journal of Dairy Science*, 58:709–717, 1975.

[CM10] C. A. Christian and S. M. Moenter. The neurobiology of preovulatory and estradiol-induced gonadotropin-releasing hormone surges. *Endocrine Reviews*, 31(4):544–577, 2010.

[CCGR00] A. Cimatti, E. Clarke, F. Giunchiglia, and M. Roveri. NuSMV: a new symbolic model checker. *International Journal on Software Tools for Technology Transfer*, 2(4):410–425, 2000.

[CSS03] L. H. Clark, P. M. Schlosser, and J. F. Selgrade. Multiple stable periodic solutions in a model for hormonal control of the menstrual cycle. *Bulletin of Mathematical Biology*, 65(1):157–173, 2003.

[CF07] F. Clément and J. P. Francoise. Mathematical modeling of the GnRH pulse and surge generator. *SIAM Journal on Applied Dynamical Systems*, 6(2):441–456, 2007.

[CMS+01] F. Clément, D. Monniaux, J. Stark, K. Hardy, J. C. Thalabard, S. Franks, and D. Claude. Mathematical model of FSH-induced cAMP production in ovarian follicles. *American Journal of Physiology-Endocrinology And Metabolism*, 281(1):E35–E53, 2001.

[CMTC02] F. Clément, D. Monniaux, J.-C. Thalabard, and D. Claude. Contribution of a mathematical modelling approach to the understanding of the ovarian function. *Comptes Rendus Biologies*, 325(4):473–485, 2002.

[CLEB12] S. B. Cummins, P. Lonergan, A. C. O. Evans, and S. T. Butler. Genetic merit for fertility traits in holstein cows: Ii. ovarian follicular and corpus luteum dynamics, reproductive hormones, and estrus behavior. *Journal of Dairy Science*, 95(7):3698–3710, 2012.

[DLW98] A. O. Darwash, G. E. Lamming, and J. A. Woolliams. Identifying heritable endocrine parameters associated with fertility in postpartum dairy cows. *Interbull Bulletin*, (18):40, 1998.

[Dat06] KEGG PATHWAY Database. http://www.genome.jp/kegg/pathway.html, 2006.

[DGS02] H. Derendorf, T. Gramatté, and H. G. Schäfer. *Pharmakokinetik: Einführung in die Theorie und Relevanz für die Arzneimitteltherapie*. 2. Auflage. Wissenschaftliche Verlagsgesellschaft, 2002.

[Deu84] P. Deuflhard. Computation of periodic solutions of nonlinear ODEs. *BIT Numerical Mathematics*, 24(4):456–466, 1984.

[Deu11] P. Deuflhard. *Newton methods for nonlinear problems: affine invariance and adaptive algorithms*, volume 35 of *Series in Computational Mathematics*. Springer-Verlag, Berlin Heidelberg, 2011.

[DB02] P. Deuflhard and F. Bornemann. *Scientific computing with ordinary differential equations*, volume 42 of *Texts in Applied Mathematics*. Springer, New York, 2002.

[DRm10] P. Deuflhard, S. Röblitz, and C. Stötzel. Mathematical Systems Biology at Zuse Institute Berlin (ZIB). *BioTOPics, Journal of Biotechnology in Berlin-Brandenburg*, 39:12–13, 2010.

[DMT+86] T. Díaz, M. Manzo, J. Trocóniz, N. Benacchio, and O. Verde. Plasma progesterone levels during the estrous cycle of Holstein and Brahman cows, Carora type and cross-bred heifers. *Theriogenology*, 26:419–432, 1986.

[DBTW86] S.J. Dieleman, M.M. Bevers, H.T.M. van Tol, and A.H. Willemse. Peripheral plasma concentrations of oestradiol, progesterone, cortisol, LH and prolactin during the oestrous cycle in the cow, with emphasis on the peri-oestrous period. *Animal Reproduction Science*, 10:275–292, 1986.

[DB85] S.J. Dieleman and D.M. Blankenstein. Progesterone-synthesizing ability of preovulatory follicles of cows relative to the peak of LH. *Journal of Reproduction and Fertility*, 75:609–615, 1985.

[DRWD13] T. Dierkes, S. Röblitz, M. Wade, and P. Deuflhard. Parameter identification in large kinetic networks with BioPARKIN. *CoRR*, arXiv:1303.4928, March 2013.

[DNBF92] J. Dijkstra, H. D. Neal, D. E. Beever, and J. France. Simulation of nutrient digestion, absorption and outflow in the rumen: model description. *The Journal of Nutrition*, 122(11):2239, 1992.

[EH73] S. E. Echternkamp and W. Hansel. Concurrent changes in bovine plasma hormone levels prior to and during the first postpartum estrous cycle. *Journal of Animal Science*, 37:1362–1370, 1973.

[ENOD99] R. Ehrig, U. Nowak, L. Oeverdieck, and P. Deuflhard. Advanced extrapolation methods for large scale differential algebraic problems. *Lecture Notes in Computational Science and Engineering*, 8:233–244, 1999.

[Erm] Bard Ermentrout. Xppaut: X-windows phase plane plus auto. http://www.math.pitt.edu/ bard/xpp/xpp.html.

[EKWF97] A. C. O. Evans, C. M. Komar, S. A. Wandji, and J. E. Fortune. Changes in androgen secretion and luteinizing hormone pulse amplitude are associated with the recruitment and growth of ovarian follicles during the luteal phase of the bovine estrous cycle. *Biology of Reproduction*, 57:394–401, 1997.

[EDGK94] N. P. Evans, G. E. Dahl, B. H. Glover, and F. J. Karsch. Central regulation of pulsatile gonadotropin-releasing hormone (GnRH) secretion by estradiol during the period leading up to the preovulatory GnRH surge in the ewe. *Endocrinology*, 134(4):1806–1811, 1994.

[FS08] F. Fages and S. Soliman. From reaction models to influence graphs and back: a theorem. *Formal Methods in Systems Biology*, pages 90–102, 2008.

[FJO+02] B. C. Fauser, D. de Jong, F. Olivennes, H. Wramsby, C. Tay, J. Itskovitz-Eldor, and H. G. van Hooren. Endocrine profiles after triggering of final oocyte maturation with GnRH agonist after cotreatment with the GnRH antagonist ganirelix during ovarian hyperstimulation for in vitro fertilization. *Journal of C ical Endocrinology & Metabolism*, 87(2):709–715, 2002.

[For94] J. E. Fortune. Ovarian follicular growth and development in mammals. *Biology of Reproduction*, 50:225–232, 1994.

[Gar97] H. A. Garverick. Ovarian follicular cysts in dairy cows. *Journal of Dairy Science*, 80(5):995–1004, 1997.

[GAP+09] O. J. Ginther, R. R. Araujo, M. P. Palhao, B. L. Rodrigues, and M. A. Beg. Necessity of sequential pulses of prostaglandin F2alpha for complete physiologic luteolysis in cattle. *Biology of Reproduction*, 80(4):641–648, 2009.

[GBB+01] O. J. Ginther, M. A. Beg, D. R. Bergfelt, F. X. Donadeu, and K. Kot. Follicle selection in monovular species. *Biology of Reproduction*, 65(3):638–647, 2001.

[GBBK02] O. J. Ginther, D. R. Bergfelt, M. A. Beg, and K. Kot. Role of low circulating FSH concentrations in controlling the interval to emergence of the subsequent follicular wave in cattle. *Reproduction*, 124:475–482, 2002.

[GGG+04] O. J. Ginther, E. L. Gastal, M. O. Gastal, D. R. Bergfelt, A. R. Baerwald, and R. A. Pierson. Comparative study of the dynamics of follicular waves in mares and women. *Biology of Reproduction*, 71(4):1195–1201, 2004.

[GK73] L. Glass and S. A. Kauffman. The logical analysis of continuous, non-linear biochemical control networks. *Journal of Theoretical Biology*, 39(1):103–129, 1973.

[GEBP81] R. G. Glencross, R. J. Esslemont, M. J. Bryant, and G. S. Pope. Relationships between the incidence of pre-ovulatory behaviour and the concentrations of oestradiol-17β and progesterone in bovine plasma. *Applied Animal Ethology*, 7:141–148, 1981.

[GKHP+07] C. Glidewell-Kenney, L. A. Hurley, L. Pfaff, J. Weiss, J. E. Levine, and J. L. Jameson. Nonclassical estrogen receptor α signaling mediates negative feedback in the female mouse reproductive axis. *Proceedings of the National Academy of Sciences*, 104:8173–8177, 2007.

[Goo88] R. L. Goodman. *The physiology of reproduction*, volume 2. Raven Press, Ltd, New York, 1988. Neuroendocrine control of the ovine estrous cycle.

[GIO+96] N. P. Groome, P. J. Illingworth, M. O'Brien, R. Pai, F. E. Rodger, J. P. Mather, and A. S. McNeilly. Measurement of dimeric inhibin B throughout the human menstrual cycle. *Journal of Clinical Endocrinology and Metabolism*, 81(4):1401–1405, 1996.

[GH01] N. Guglielmi and E. Hairer. Implementing Radau IIA methods for stiff delay differential equations. *Computing*, 67(1):1–12, 2001.

[Hal09] J. E. Hall. Neuroendocrine control of the menstrual cycle. *Yen and Jaffe's reproductive endocrinology: Physiology, pathophysiology, and clinical management*, 6:139–154, 2009.

[Har01] L. A. Harris. *Differential equation models for the hormonal regulation of the menstrual cycle.* PhD thesis, North Carolina State University, 2001.

[HHBC98] F. Hayes, J. E. Hall, P. A. Boepple, and Jr. W. F. Crowly. Differential control of gonadotropin secretion in the human: Endocrine role of inhibin. *Journal of Clinical Endocrinology and Metabolism*, 83:1835–1841, 1998.

[HKM98] K. Heinze, R. W. Keener, and A. R. Midgley. A mathematical model of luteinizing hormone release from ovine pituitary cells in perifusion. *American Journal of Physiology - Endocrinology And Metabolism*, 275(6):1061–1071, 1998.

[HH74] J. E. Hixon and W. Hansel. Evidence for preferential transfer of prostaglandin F2α to the ovarian artery following intrauterine administration in cattle. *Biology of Reproduction*, 11(5):543–552, 1974.

[IMA+00] J. J. Ireland, M. Mihm, E. Austin, M. G. Diskin, and J. F. Roche. Historical perspective of turnover of dominant follicles during the bovine estrous cycle: Key concepts, studies, advancements, and terms. *Journal of Dairy Science*, 83:1648–1658, 2000.

[JSMA09] R. S. Jaiswal, J. Singh, L. Marshall, and G. P. Adams. Repeatability of 2-wave and 3-wave patterns of ovarian follicular development during the bovine estrous cycle. *Theriogenology*, 72(1):81–90, 2009.

[Joh07] M. H. Johnson. *Essential Reproduction.* Sixth Edition. Wiley-Blackwell, 2007.

[JL06] R. E. Jones and K. H. Lopez. *Human Reproductive Biology.* Academic Press, 2006.

[Jon02] H. de Jong. Modeling and simulation of genetic regulatory systems: a literature review. *Journal of Computational Biology*, 9(1):67–103, 2002.

[JGHP03] H. de Jong, J. Geiselmann, C. Hernandez, and M. Page. Genetic network analyzer: qualitative simulation of genetic regulatory networks. *Bioinformatics*, 19(3):336–344, 2003.

[KDWF76] L. N. Kanchev, H. Dobson, W. R. Ward, and R. J. Fitzpatrick. Concentration of steroids in bovine peripheral plasma during the oestrous cycle and the effect of betamethasone treatment. *Journal of Reproduction and Fertility*, 48(2):341–345, 1976.

[KKW+95] H. Kaneko, H. Kishi, G. Watanabe, K. Taya, S. Sasamoto, and H. Yoshihisa. Changes in plasma concentrations of immunoreactive inhibin, estradiol and FSH associated with follicular waves during the estrous cycle of the cow. *Journal of Reproduction and Development*, 41(4):311–320, 1995.

[KBG90] J. P. Kastelic, D. R. Bergfelt, and O. J. Ginther. Relationship between ultrasonic assessment of the corpus luteum and plasma progesterone concentration in heifers. *Theriogenology*, 33(6):1269–1278, 1990.

[KV98] D. M. Keenan and J. D. Veldhuis. A biomathematical model of time-delayed feedback in the human male hypothalamic-pituitary-leydig cell axis. *American Journal of Physiology - Endocrinology and Metabolism*, 275(1):E157–E176, 1998.

[KSM+99] J. Kotwica, D. Skarzynski, G. Miszkiel, P. Melin, and K. Okuda. Oxytocin modulates the pulsatile secretion of prostaglandin F2α in initiated luteolysis in cattle. *Research in Veterinary Science*, 66(1):1–5, 1999.

[KW82] J. Kotwica and G. L. Williams. Relationship of plasma testosterone concentrations to pituitary-ovarian hormone secretion during the bovine estrous cycle and the effects of testosterone propionate administered during luteal regression. *Biology of Reproduction*, 27(4):790–801, 1982.

[KKKH09] B. F. Krippendorff, K. Kuester, C. Kloft, and W. Huisinga. Nonlinear pharmacokinetics of therapeutic proteins resulting from receptor mediated endocytosis. *Journal of pharmacokinetics and pharmacodynamics*, 36(3):239–260, 2009.

[Kro03] R. Kroker. Beeinflussung der Uterusfunktion. In W. Löscher, F. R. Ungemach, and R. Kroker, editors, *Pharmakotherapie bei Haus- und Nutztieren*, pages 168–171. Parey Buchverlag, 6 edition, 2003.

[LPRC05] E. A. Lane, V. Padmanabhan, J. F. Roche, and M. A. Crowe. Alterations in the ability of the bovine pituitary gland to secrete gonadotropins in vitro during the first follicle-stimulating hormone increase of the estrous cycle and in response to exogenous steroids. *Domestic Animal Endocrinology*, 28(2):190–201, 2005.

[LS88] C. C. Lin and L. A. Segel. *Mathematics applied to deterministic problems in the natural sciences*, volume 1 of *Classics in Applied Mathematics*. Society for Industrial and Applied Mathematics, 1988.

[ML95] G. E. Mann and G. E Lamming. Progesterone inhibition of the development of the luteolytic signal in cows. *Journal of Reproduction and Fertility*, 104:1–5, 1995.

[MS13] A. Margolskee and J. F. Selgrade. A lifelong model for the female reproductive cycle with an antimüllerian hormone treatment to delay menopause. *Journal of Theoretical Biology*, 326:21–35, 2013.

[MS11] A. Margolskee and J.F. Selgrade. Dynamics and bifurcation of a model for hormonal control of the menstrual cycle with inhibin delay. *Mathematical Biosciences*, 2011.

[MFD+13] O. Martin, N. C. Friggens, J. Dupont, P. Salvetti, S. Freret, C. Rame, S. Elis, J. Gatien, C. Disenhaus, and F. Blanc. Data-derived reference profiles with corepresentation of progesterone, estradiol, LH, and FSH dynamics during the bovine estrous cycle. *Theriogenology*, 79(2):331–343, 2013.

[MS07] O. Martin and D. Sauvant. Dynamic model of the lactating dairy cow metabolism. *Animal*, 1(08):1143–1166, 2007.

[MCL99] J. A. McCracken, E. E. Custer, and J. C. Lamsa. Luteolysis: A neuroendocrine-mediated event. *Physiological Reviews*, 79:263–323, 1999.

[MCD+90] R. I. McLachlan, N. L. Cohen, K. D. Dahl, W. J. Bremner, and M. R. Soules. Serum inhibin levels during the periovulatory interval in normal women: Relationships with sex steroid and gonadotrophin levels. *Clinical Endocrinology*, 32(1):39–48, 1990.

[MTA+06] M. S. Medan, T. Takedomi, Y. Aoyagi, M. Konishi, S. Yazawa, G. Watanabe, and K. Taya. The effect of active immunization against inhibin on gonadotropin secretions and follicular dynamics during the estrous cycle in cows. *Journal of Reprodtion and Development*, 52:107–113, 2006.

[MRKB09] S. Meier, J. R. Roche, E. S. Kolver, and R. C. Boston. A compartmental model desribing changes in progesterone concentrations during the estrous cycle. *Journal of Dairy Research*, 76:249–256, 2009.

[MPO95] T. Mestl, E. Plahte, and S. W. Omholt. A mathematical framework for describing and analysing gene regulatory networks. *Journal of Theoretical Biology*, 176(2):291–300, 1995.

[MSS09] A. Miyamoto, K. Shirasuna, and K. Sasahara. Local regulation of corpus luteum development and regression in the cow: Impact of angiogenic and vasoactive factors. *Domestic Animal Endocrinology*, 37(3):159–169, 2009.

[MBA+86] S. E. Monroe, Z. Blumenfeld, J. L. Anderyko, E. Schriock, M. R. Henzl, and R. B. Jaffe. Dose-dependent inhibition of pituitary-ovarian function during administration of a gonadotropin-releasing hormone agonistic analog (nafarelin). *Journal of Clinical Endocrinology & Metabolism*, 63(6):1334–1341, 1986.

[MHM+85] S. E. Monroe, M. R. Henzl, M. C. Martin, E. Schriock, V. Lewis, C. Nerenberg, and R. B. Jaffe. Ablation of folliculogenesis in women by a single dose of gonadotropin-releasing hormone agonist: significance of time in cycle. *Fertility and Sterility*, 43(3):361–368, 1985.

[mPHR12] C. Stötzel, J. Plöntzke, W. Heuwieser, and S. Röblitz. Advances in modeling of the bovine estrous cycle: Synchronization with pgf2α. *Theriogenology*, 78(7):1415–1428, 2012.

[NBF+09] A. Naldi, D. Berenguier, A. Fauré, F. Lopez, D. Thieffry, and C. Chaouiya. Logical modelling of regulatory networks with ginsim 2.3. *Biosystems*, 97(2):134, 2009.

[NJS+00] G.D. Niswender, J.L. Juengel, P.J. Silva, M.K. Rollyson, and E.W. McIntush. Mechanisms controlling the function and life span of the corpus luteum. *Physiological Reviews*, 80(1):1–29, 2000.

[NW00] U. Nowak and L. Weimann. NLSCON, Nonlinear Least Squares with nonlinear equality CONstraints. http://www.zib.de/de/numerik/software/codelib/nonlin.html, 1993–2000.

[PRGM03] K. I. Parker, D. M. Robertson, N. P. Groome, and K. L. Macmillan. Plasma concentrations of inhibin A and follicle-stimulating hormone differ between cows with two or three waves of ovarian follicular development in a single estrous cycle. *Biology of Reproduction*, 68:822–828, 2003.

[Pas08] R. D. Pasteur. *A Multiple-Inhibin Model of the Human Menstrual Cycle*. PhD thesis, North Carolina State University, 2008.

[PM05] A.J. Pawson and A.S. McNeilly. The pituitary effects of GnRH. *Animal Reproduction Science*, 88:75–94, 2005.

[Per04] G. Perry. The bovine estrous cycle. South Dakota State University - Cooperative Extension Service, http://agbiopubs.sdstate.edu/articles/FS921A.pdf, 2004.

[PCK+91] R. C. Perry, L. R. Corah, G. H. Kiracofe, J. S. Stevenson, and W. E. Beal. Endocrine changes and ultrasonography of ovaries in suckled beef cows during resumption of postpartum estrous cycles. *Journal of Animal Science*, 69:2548–2555, 1991.

[Poy95] N. L. Poyser. The control of prostaglandin production by the endometrium in relation to luteolysis and menstruation. *Prostaglandins, Leukotrienes and Essential Fatty Acids*, 53:147–195, 1995.

[POK+12] S. R. Pring, M. Owen, J. R. King, K. D. Sinclair, R. Webb, A. P. F. Flint, and P. C. Garnsworthy. A mathematical model of the bovine oestrous cycle: simulating outcomes of dietary and pharmacological interventions. *Journal of Theoretical Biology*, 313:115–126, 2012.

[RPM+98] S. Ramaswamy, C. R. Pohl, A. S. McNeilly, S. J. Winters, and T. M. Plant. The time course of follicle-stimulating hormone suppression by recombinant human inhibin a in the adult male rhesus monkey (macaca mulatta). *Endocrinology*, 139(8):3409–3415, 1998.

[RPP+03] N. L. Rasgon, L. Pumphrey, P. Prolo, S. Elman, A. B. Negrao, J. Licinio, and A. Garfinkel. Emergent oscillations in a mathematical model of the human menstrual cycle. *CNS spectrums*, 8:805–814, 2003.

[RKF+01] M. J. Rathbone, J. E. Kinder, K. Fike, F. Kojima, D. Clopton, C. R. Ogle, and C. R. Bunt. Recent advances in bovine reproductive endocrinology and physiology and their impact on drug delivery system design for the control of the estrous cycle in cattle. *Advanced Drug Delivery Reviews*, 50(3):277–320, 2001.

[Rei09] I. Reinecke. *Mathematical modeling and simulation of the female menstrual cycle*. PhD thesis, Freie Universität Berlin, 2009.

[RD07] I. Reinecke and P. Deuflhard. A complex mathematical model of the human menstrual cycle. *Journal of Theoretical Biology*, 247:303–330, 2007.

[RB96] I. Revah and W. R. Butler. Prolonged dominance of follicles and reduced viability of bovine oocytes. *Journal of reproduction and fertility*, 106(1):39–47, 1996.

[RmD+12] S. Röblitz, C. Stötzel, P. Deuflhard, H. M. Jones, D. O. Azulay, P. van der Graaf, and S. W. Martin. A mathematical model of the human menstrual cycle for the administration of GnRH analogues. *Journal of Theoretical Biology*, 321:8–27, 2012.

[RIR10] R. J. Rodgers and H. F. Irving-Rodgers. Morphological classification of bovine ovarian follicles. *Reproduction*, 139(2):309–318, 2010.

[ST+03] Lucas Sanchez, Denis Thieffry, et al. Segmenting the fly embryo: a logical analysis of the pair-rule cross-regulatory module. *Journal of Theoretical Biology*, 224(4):517, 2003.

[SGF+09] R. M. dos Santos, M. D. Goissis, D. A. Fantini, C. M. Bertan, J. L. M. Vasconcelos, and M. Binelli. Elevated progesterone concentrations enhance prostaglandin F2α synthesis in dairy cows. *Animal Reproduction Science*, 114:62–71, 2009.

[SKBR88] J.D. Savio, L. Keenan, M.P. Boland, and J.F. Roche. Pattern of growth of dominant follicles during the oestrous cycle of heifers. *Journal of Reprodction and Fertility*, 83:663–671, 1988.

[SSW84] E. Schallenberger, B. Schams, D. Bullermann, and D. L. Walters. Pulsatile secretion of gonadotrophins, ovarian steroids and ovarian oxytocin during prostaglandin-induced regression of the corpus luteum in the cow. *Journal of Reproduction and Fertility*, 71(2):493–501, 1984.

[SMEN04] M. Schlegel, W. Marquardt, R. Ehrig, and U. Nowak. Sensitivity analysis of linearly-implicit differential–algebraic systems by one-step extrapolation. *Applied Numerical Mathematics*, 48(1):83–102, 2004.

[SS00] P. M. Schlosser and J. F. Selgrade. A model of gonadotropin regulation during the menstrual cycle in women: Qualitative features. *Environmental Health Perspectives*, pages 873–881, 2000.

[SJA+00] A. Sehested, A. Juul, A. M. Andersson, J. H. Petersen, T. K. Jensen, J. Müller, and N. E. Skakkebaek. Serum inhibin A and inhibin B in healthey prepubertal, pubertal, and adolescent girls and adult women: Relation to age, stage of puberty, menstrual cycle, follicle-stimulating hormone, luteinizing hormone, and estradiol levels. *Journal of Clinical Endocrinology and Metabolism*, 85(4):1634–1640, 2000.

[SS99] J. F. Selgrade and P. M. Schlosser. A model for the production of ovarian hormones during the menstrual cycle. *Fields Institute Communications*, 21:429–446, 1999.

[SLM+91] W. J. Silvia, G. S. Lewis, J. A. McCracken, W. W. Thatcher, and L. Wilson Jr. Hormonal regulation of uterine secretion of prostaglandin f2α during luteolysis in ruminants. *Biology of reproduction*, 45(5):655–663, 1991.

[SFDO08] D. J. Skarzynski, G. Ferreira-Dias, and K. Okuda. Regulation of luteal function and corpus luteum regression in cows: hormonal control, immune mechanisms and intercellular communication. *Reproduction in Domestic Animals*, 43:57–65, 2008.

[SJO01] D. J. Skarzynski, J. J. Jaroszewski, and K. Okuda. Luteotropic mechanisms in the bovine corpus luteum: Role of oxytocin, prostaglandin F2α, progesterone and noradrenaline. *Journal of Reproduction and Development*, 47:125–137, 2001.

[Sno89] E. H. Snoussi. Qualitative dynamics of piecewise-linear differential equations: A discrete mapping approach. *Dynamics and Stability of Systems*, 4(3-4):565–583, 1989.

[Sob91] Tarek M Sobh. Discrete event dynamic systems: An overview. *Technical Reports (CIS)*, page 388, 1991.

[SPP+00] T. K. Soboleva, A. J. Peterson, A. B. Pleasants, K. P. McNatty, and F. M. Rhodes. A model of follicular development and ovulation in sheep and cattle. *Animal Reproduction Science*, 58:45–57, 2000.

[SEM69] G. H. Stabenfeldt, L. L. Ewing, and L. E. McDonald. Peripheral plasma progesterone levels during the bovine oestrous cycle. *Jopurnal of Reproduction and Fertility*, 19:433–442, 1969.

[SLHS75] J. N. Stellflug, T. M. Louis, H. D. Hafs, and B. E. Seguin. Luteolysis, estrus and ovulation, and blood prostaglandin F after intramuscular administration of 15, 30 or 60 mg prostaglanding F2α. *Prostaglandins*, 9(4):609–615, 1975.

[SDS+08] J. L. Stevenson, J. C. Dalton, J. E. Santos, R. Sartori, A. Ahmadzadeh, and R. C. Chebel. Effect of synchronization protocols on follicular development and estradiol and progesterone concentrations of dairy heifers. *Journal of Dairy Science*, 91(8):3045–3056, 2008.

[SJO72] R. S. Swerdloff, H. S. Jacobs, and W. D. Odell. Synergistic role of progestogens in estrogen induction of lh and fsh surge. *Endocrinology*, 90(6):1529, 1972.

[TR91] C. Taylor and R. Rajamahendran. Follicular dynamics and corpus luteum growth and function in pregnant versus nonpregnant cows. *Journal of Dairy Science*, 74:115–123, 1991.

[Tho73] R. Thomas. Boolean formalization of genetic control circuits. *Journal of Theoretical Biology*, 42(3):563–585, 1973.

[Tho91] R. Thomas. Regulatory networks seen as asynchronous automata: a logical description. *Journal of Theoretical Biology*, 153(1):1–23, 1991.

[TAS+07] C. W. Tornøe, H. Agersø, T. Senderovitz, H. A. Nielsen, H. Madsen, M. O. Karlsson, and E. N. Jonsson. Population pharmacokinetic/pharmacodynamic (pk/pd) modelling of the hypothalamic–pituitary–gonadal axis following

treatment with gnrh analogues. *British journal of clinical pharmacology*, 63(6):648–664, 2007.

[TTB+02] D. H. Townson, P. C. W. Tsang, W. R. Butler, M. Frajblat, L. C. Griel, C. J. Johnson, R. A. Milvae, G. M. Niksic, and J. L. Pate. Relationship of fertility to ovarian follicular waves before breeding in dairy cows. *Journal of Animal Science*, 80(4):1053–1058, 2002.

[TK84] T.R. Troxel and D.J. Kesler. The effect of progestin and GnRH treatments on ovarian function and reproductive hormone secretions of anestrous postpartum suckled beef cows. *Theriogenology*, 21:699–711, 1984.

[VWB+97] J. Vizcarra, R.P. Wettemann, T.D. Braden, A.M. Turzillo, and T.M. Nett. Effect of gonadotropin-releasing hormone (GnRH) pulse frequency on serum and pituitary concentrations of luteinizing hormone and follicle-stimulating hormone, GnRH receptors, and messenger ribonucleic acid for gonadotropin subunits in cows. *Endocrinology*, 139:594–601, 1997.

[VF93] A. K. Voss and J. E. Fortune. Estradiol-17beta has a biphasic effect on oxytocin secretion by bovine granulosa cells. *Biology of Reproduction*, 48(6):1404–1409, 1993.

[Wei97] J. N. Weiss. The Hill equation revisited: uses and misuses. *The FASEB Journal*, 11(11):835–841, 1997.

[Wis87] T. Wise. Biochemical analysis of bovine follicular fluid: albumin, total protein, lysosomal enzymes, ions, steroids and ascorbic acid content in relation to follicular size, rank, atresia classification and day of estrous cycle. *Journal of Animal Science*, 64:1153–1169, 1987.

[WTPB+11] H. Woelders, M .F. W. Te Pas, A. Bannink, R. F. Veerkamp, and M. A. Smits. Systems biology in animal sciences. *Animal*, 5(7):1036, 2011.

[WIR+04] D. Wolfenson, G. Inbar, Z. Roth, M. Kaim, A. Bloch, and R. Braw-Tal. Follicular dynamics and concentrations of steroids and gonadotropins in lactating cows and nulliparous heifers. *Theriogenology*, 62(6):1042–1055, 2004.

[XLSG98] C. W. Xiao, J. M. Liu, J. Sirois, and A. K. Goff. Regulation of cyclooxygenase-2 and prostaglandin F synthase gene expression by steroid hormones and interferon-τ in bovine endometrial cells. *Endocrinology*, 139(5):2293–2299, 1998.

[ZWG03] M. L. Zeeman, W. Weckesser, and D. Gokhman. Resonance in the menstrual cycle: a new model of the LH surge. *Reproductive biomedicine online*, 7(3):295–300, 2003.

Danksagung

Die vorliegende Dissertation habe ich im Laufe meiner Tätigkeit als Wissenschaftliche Mitarbeiterin am Zuse-Institut Berlin (ZIB), innerhalb des Projektes *Mathematische Systembiologie* des DFG Forschungszentrums MATHEON - Mathematics for key technologies - erstellt. Die hervorragenden Forschungsbedingungen an diesen Einrichtungen haben sehr zum Gelingen dieser Arbeit beigetragen.

Mein Dank gilt zuallererst meinem Doktorvater Prof. Peter Deuflhard für die Möglichkeit, an einem so spannenden Thema zwischen Mathematik und Biologie zu forschen, sowie für die kontinuierliche Unterstützung, für die Ermöglichung mehrerer interdisziplinärer Kooperationen, und das große entgegengebrachte Vertrauen in meine Arbeit. Besonders bedanken möchte ich mich außerdem bei meiner Arbeitsgruppenleiterin Susanna Röblitz, die mit unerschöpflicher Energie und Enthusiasmus stets mit Rat und Tat zur Seite stand.

I would like to thank the veterinary scientists Marike Boer and Henri Woelders from Wageningen University, whose idea to develop a mathematical model for the bovine estrous cycle has led to such a fruitful collaboration. I have very much enjoyed our interdisciplinary work. I thank Mochamad Apri for his initial help with the model reduction. I would further like to thank Hannah Jones, Piet van der Graaf, David Azulay, and Steven Martin from Pfizer for the cooperation on GynCycle, and especially for the opportunity to look inside the daily life of pharmaceutical research. I am also thankful to the graduate program PharMetrX for the inspiring courses.

Weiterhin möchte ich mich bei der Gruppe Diskrete Mathematik an der FU Berlin bedanken für die Einführung in diskrete Methoden und die zugehörigen Softwaretools. Bei Hannes Klarner möchte ich mich bedanken für die mehrmalige Umsetzung des Model Checkings, und bei Shahrad Jamshidi für die interessante Zusammenarbeit bei den PADE-Modellen. Insbesondere gilt mein Dank Heike Siebert für die Koordination und Lenkung der Ansätze und für die zahlreichen nützlichen Tipps.

Allen ehemaligen und aktuellen Kollegen aus der Arbeitsgruppe Mathematische Systembiologie und der eng befreundeten Arbeitsgruppen am ZIB sei an dieser Stelle gedankt für das nette Arbeitsklima, in dem man stets jeden um Rat fragen konnte. Dank gilt Marcus Weber, ohne den ich gar nicht am ZIB gelandet wäre. Bei Thomas Dierkes möchte ich mich insbesondere bedanken für die vielen hilfreichen Diskussionen zur Numerischen Mathematik. Rainald Ehrig gilt mein Dank für die Hilfe bei der Fourier-Analyse und bei sämtlichen Fortran-Fragen. Bei Juli Plöntzke möchte ich mich für den frischen Wind bei der Erweiterung des Kuhmodells bedanken. Für die POEM-Umgebung von Uli Nowak, die ich während meiner Arbeit sehr viel genutzt habe, bin ich ebenfalls äusserst dankbar.

Zu guter Letzt möchte ich meiner besseren Hälfte Sebastian Wiedemann danken, für das gelegentliche Krisenmanagement und all die Geduld und Unterstützung.

Zusammenfassung

Die vorliegenden Dissertation beschäftigt sich mit der mathematischen Modellierung von endokrinologischen Netzwerken, die dem weiblichen Hormonzyklus zu Grunde liegen. Diese Netzwerke bestehen aus einer Vielzahl von biologischen Mechanismen in unterschiedlichen Teilen des Organismus. Ihr Zusammenspiel führt zu periodischen Veränderungen verschiedener Substanzen, die für die Reproduktion notwendig sind.

In jedem Zyklus werden Hormone aus der Hypothalamus-Hypophysen-Gonaden-Achse in die Blutbahn ausgeschüttet. So werden sie im ganzen Körper verteilt und steuern verschiedene Prozesse. Ihre wichtigste Aufgabe für die Reproduktion ist die Regulierung von Vorgängen in den Ovarien, wo sich Follikel und Gelbkörper entwickeln. Diese produzieren Steroide, die ebenfalls ins Blut abgegeben werden. Von dort aus beeinflussen sie wiederum die Prozesse in der Hypothalamus-Hypophysen-Gonaden-Achse. Aus dieser komplexen Rückkopplung ensteht der Hormonzyklus.

Für die Modellierung dieser Vorgänge ist ein hohes Abstraktionslevel notwendig, welches durch verschiedene Modellierungsansätze realisiert werden kann. In dieser Arbeit wurden einige dieser Ansätze realisiert. Erster Schritt bei allen Ansätzen ist die Darstellung der wichtigsten beteiligten Mechnismen in einem Flussdiagramm. Dieses kann im nächsten Schritt mit Hilfe von Hill-Funktionen als ein System von gewöhnlichen Differentialgleichungen, als stückweise definiertes affines Modell, oder direkt als rein regulatorisches Modell implementiert werden.

Mit Hilfe dieses Vorgehens wurde ein Differentialgleichungsmodell für den Hormonzyklus von Kühen von Grund auf entwickelt. Dieses wurde mit einem weiterentwickelten Modell des weiblichen Zyklus beim Menschen verglichen. Beide Modelle wurden validiert, indem sowohl Simulationen mit Messwerten einzelner Substanzen verglichen, als auch externe Einflüsse wie Medikamentengabe studiert wurden. Am Beispiel des Zyklus der Kuh wurden kontinuiertliche Analyse-Verfahren benutzt, um Stabilität, follikulare Wellenmuster, und Robustheit bezüglich Parameterstörungen zu untersuchen. Weiterhin wurde das Modell für den Kuhzyklus erheblich reduziert, wobei die wichtigsten Simulationsergebnisse erhalten blieben.

Um einen Blick auf alternative Modellansätze zu werfen, wurden entsprechende diskrete Modelle abgeleitet, exemplarisch für das Modell des Kuhzyklus. Aus einer stückweise affinen Version des Modells wurden Parameterbedingungen für das kontinuierliche Modell berechnet. Die Stabilität wurde global für ein rein diskretes Modell analysiert. Darüber hinaus wurden auch stark reduzierte diskrete Modelle hergeleitet, welche die wichtigsten dynamischen Eigenschaften des ursprünglichen Modells beibehalten.